EPR INVESTIGATION OF FREE RADICALS IN EXCISED AND ATTACHED LEAVES SUBJECTED TO OZONE AND SULPHUR DIOXIDE AIR POLLUTION

by

MANIVALDE VAARTNOU

B.A., The University of British Columbia, 1972

M.Sc., The University of British Columbia, 1980

A THESIS SUBMITTED IN PARTIAL FULFILMENT OF

THE REQUIREMENTS FOR THE DEGREE OF

DOCTOR OF PHILOSOPHY

in

THE FACULTY OF GRADUATE STUDIES

(Department of Plant Science)

We accept this thesis as conforming

to the required standard

THE UNIVERSITY OF BRITISH COLUMBIA

In presenting this thesis in partial fulfilment of the requirements for an advanced degree at the University of British Columbia, I agree that the Library shall make it freely available for reference and study. I further agree that permission for extensive copying of this thesis for scholarly purposes may be granted by the head of my department or by his or her representatives. It is understood that copying or publication of this thesis for financial gain shall not be allowed without my written permission.

Department of Plant Science

The University of British Columbia
Vancouver, Canada

Date October 3, 1988

ABSTRACT

The X-band EPR spectrometry system was modified to allow for the in situ monitoring of free radical changes in attached, intact plant leaves, which were caused by stress factors such as exposure to excessive photon flux density, ozone or sulphur dioxide. This was done through use of the dewar insert of the variable temperature accessory as a guide, the construction of 'T' shaped cellulose acetate holders to which leaves could be attached with adhesive tape, and modification of the gas flow system used for controlled temperature studies.

Kinetic studies of free radical formation were possible with leaves which had minimal underlying Fe^{++} and Mn^{++} signals. In leaves with large underlying signals a Varian software program was used to subtract overlapping signals from each other, thereby revealing the free-radical signal changes which occurred under different light regimes and stress conditions. Preliminary investigation disclosed the formation of a new signal upon prolonged exposure to far-red light and the effect of oxygen depletion upon photosynthetic Signals I and II.

Leaves subject to high photon flux density reveal an unreported free-radical signal, which decays upon exposure to microwave radiation; and concomitant damage to Photosystems I

and II. Upon elimination of this signal leaves return to the undamaged state or reveal permanent damage to either photosystem, depending upon the degree of damage.

Kentucky bluegrass and perennial ryegrass leaves subject to low levels of ozone (up to 80ppb) for periods of 8 hours show no changes in free-radical signal formation. At intermediate levels of ozone (80-250ppb) a new free-radical signal was formed within 3 hours of fumigation, Signal II was decreased and Signal I decayed. These changes were reversible if fumigation was terminated. At fumigation levels exceeding 250ppb a different new irreversible free-radical signal was formed in darkness within 1.5 hours of fumigation.

Radish, Kentucky bluegrass and perennial ryegrass leaves subject to high levels of sulphur dioxide (10-500ppm) reveal the formation of Signal I upon irradiation with broad-band white or 650nm light, thereby indicating an interruption of normal electron flow from PSII to PSI. Damage to the oxygen-evolving complex and reaction centre of PSII is also revealed through changes in Signal II and the Mn^{++} signal. These changes in the normal EPR signals are dose-dependent. Leaves subject to low levels of sulphur dioxide (600-2000ppb) reveal the disappearance of Signal I after 3 hours of fumigation and the formation of a

new free-radical signal with parameters similar to the sulphur trioxide free-radical signal. These latter changes are partially reversible upon termination of fumigation.

After prolonged exposure to either ozone or sulphur dioxide, a free-radical signal with parameters similar to the superoxide anion free-radical signal is formed in plant leaves.

TABLE OF CONTENTS

TABLE OF CONTENTS (Continued)

TABLE OF CONTENTS (Continued)

LIST OF TABLES

LIST OF FIGURES

LIST OF FIGURES (Continued)

LIST OF FIGURES (Continued)

LIST OF FIGURES (Continued)

LIST OF FIGURES (Continued)

LIST OF FIGURES (Continued)

ABBREVIATIONS

BPN	N-t-butyl-*α*-phenylnitrone
DCMU	3-(3,4-dichlorophenyl)-1,1-dimethyl urea
DMPO	5,5-dimethyl-pyrroline-N-oxide
DPPH	1,1-diphenyl-2-picryl-hydrazyl
EDU	N-(2-(2-oxo-1-imidazolidinyl)-ethyl)-N'-phenyl urea ("ethylene diurea")
FAD	Flavin adenine dinucleotide
kDa	kiloDalton
MDA	Malondialdehyde
NADP	Nicotinamide adenine dinucleotide phosphate
OEC	Oxygen-evolving complex
PBN	4-pyridyl-1-oxide-N-tert-butyl-nitrone
PFD	Photon flux density
PSI	Photosystem I
PSII	Photosystem II
PUFA	Polyunsaturated fatty acid
SOD	Superoxide dismutase
TEMPO	2,2,6,6-tetramethyl-1-piperidine-N-oxyl
TIRON	1,2-dihydroxybenzene-3,5-disulphonate

ACKNOWLEDGEMENTS

This thesis is dedicated to:

Kitty Furball Vaartnou

because she is a lot of fun, has a mind of her own and could easily play both roles in "A Tale of Two Kitties".

I would like to thank my wife Valorie and daughter Christie for both support and tolerance over an unusually extended period of time, and thank Val for printing the many drafts of this thesis.

I would also like to acknowledge the contribution of my research supervisor, Dr. V.C. Runeckles: financial support through his N.R.C. graduate assistantships; extensive useful editorial help with the manuscript; and advice and encouragement throughout the course of the research.

In addition, the support of the others in my immediate family was appreciated: Parents Dr. Herman and Mrs. Hella Vaartnou, brothers Peter and Erik, and sisters-in-law Cindy and Linda.

Last, but not least, the Cecil crowd of 1967-74 - scattered from Kamloops to Montreal to Tucson to Kuala Lumpur - the memories remain: Ken, Gord, Eric, Susan, Bob, Robin H., Robin E., Barb, Bruce, Maureen, Joanne, Russ, Willie, Brock, Dunc and Steve.

1.0 INTRODUCTION

Plants, in their natural environment, are subject to numerous stresses which may either retard or terminate their growth and development. Many stressful conditions, such as exposure to excessive radiation or a shortage of water, may occur naturally, but some stresses, such as exposure to elevated levels of gaseous air pollutants, are largely due to the activity of man (Levitt, 1980).

Plants respond to such stresses in various ways. Overall growth may be affected, and characteristic symptoms may develop in response to different stresses. In many instances, necrosis of cells and tissues may occur. However, such responses are the ultimate manifestation of various actions occurring at the biochemical level within the cells of the plant, which lead to disruptions of normal metabolic processes.

In the case of air pollutants, such as ozone and sulphur dioxide, the reductions in plant growth which they cause have been, at least in part, attributed to reductions in photosynthesis (Black and Unsworth, 1979; Koziol and Jordan, 1978; Sisson et al. 1981). One suggested cause of this reduction is the impairment of the photosynthetic electron transport chain through the formation of detrimental free radicals (Tanaka and Sugahara, 1980; Sakaki et al. 1983).

Electron paramagnetic resonance (EPR) spectroscopy, a brief description of which is presented in Appendix A, allows the study of free radicals, i.e. chemical species which contain unpaired electrons. EPR has been found to be useful for the study of metabolic electron transport chains because some of the components of such chains have unpaired electrons in either their oxidized or reduced state.

The natural formation of free radicals in photosynthesizing chloroplasts has been known since the pioneering EPR studies of Commoner et al. (1956, 1957). Subsequent investigations by numerous workers have shown that one free-radical signal (Signal I) observed in isolated chloroplasts illuminated by far-red light (700-730nm) is associated with Photosystem I (PSI) (Beinart et al. 1962; Malkin, 1982). A second signal (Signal II) is increased by illumination over a wide range of wave lengths less than 700nm and has been been associated with oxidation-reduction reactions in the water-splitting process of Photosystem II (PSII) (Babcock and Sauer, 1973a). Plant leaves also reveal a six peak Mn^{++} signal, the intensity of which varies greatly among species and with plant leaf age (Mishra et al. 1971; McCain et al. 1984). Signal II is superimposed on the fourth peak from the low field end of this Mn^{++} signal, while Signal I is superimposed on Signal II. In addition, a broad sloping signal attributed to Fe^{++} (Treharne and Eyster, 1962; Treharne et al. 1964) underlies the Mn^{++} signal (Appendix C).

Independent of possible direct effects on photosynthetic processes, air pollutants have been hypothesized as giving rise to deleterious free radicals which are generally disruptive to the normal functioning of cell membranes (Mudd, 1973,1982). Free radicals are also hypothesized as providing the basis for senescence in plant tissues (Leshem, 1981). In particular, formation of toxic oxygen-based species such as the superoxide (O_2^-) and hydroxyl ($OH^\cdot$) free radicals has been proposed as the primary cause of injury. However, this has not been demonstrated in intact leaves, nor has it been conclusively established in studies using chloroplast or subchloroplast preparations under ambient conditions. Nevertheless, free radicals have been causally implicated in plant senescence (Chia et al. 1981, 1982; McRae and Thompson, 1983; Thompson et al. 1987), and premature senescence is a symptom frequently associated with the exposure of plants to air pollutants.

Although the pollutant-induced production of the superoxide and other free radicals has been proposed as the primary cause of the general impairment of membrane functions throughout the cell following pollutant uptake, Lee and Bennett (1982) suggested that such adverse affects were minimized in the presence of the superoxide disproportionating enzyme, superoxide dismutase (SOD). However, Chanway and Runeckles (1984a, 1984b) and McKersie et al. (1982) were unable to confirm the proposed role of SOD in reducing the harmful effects of ozone.

The superoxide anion radical has been detected in rapid flow enzyme systems (Palmer et al. 1964; Bray et al. 1964; Knowles et al. 1969). Detection of the superoxide (Harbour and Bolton, 1975; McRae and Thompson, 1983) and hydroxyl (Harbour and Bolton, 1978) free radicals has also been demonstrated by the use of spin-trapping EPR techniques with chloroplast and other subcellular preparations. However, few studies have been conducted on the changes in formation of EPR free-radical signals resulting from exposure to ozone or sulphur dioxide (Rowlands et al. 1970; Shimazaki et al. 1984b). Furthermore, they all used excised tissues or chloroplast preparations after plants had been exposed to the air pollutants for various time periods rather than observing the signals during fumigation. Such approaches preclude making observations on the dynamics of free radical formation during exposure to gaseous pollutants. Also, effects observed in excised leaves or chloroplast preparations are not necessarily indicative of effects occurring in intact, normally functioning, attached leaves.

The first objective of the present study was therefore to develop a method permitting the observation of EPR signals in whole, attached leaves, at room temperature. The second objective was to observe the changes in the photosynthetic signals occurring when leaves were fumigated with ozone or sulphur dioxide. A third objective was to observe the

appearance of new signals during or subsequent to fumigation, and to determine how these changes reflected the initial stages of plant response.

Although the overall objective was to investigate free radical changes induced by exposure to gaseous air pollutants, it was also necessary to investigate the various factors which influence EPR spectroscopy of intact tissues, such as photoinhibition and oxygen toxicity effects, in order to obtain a clear understanding of the potential and limitations of studying intact tissue.

2.0 LITERATURE REVIEW

2.1 Free Radicals and Oxygen Toxicity

Free radicals are molecules or atoms which contain unpaired electrons. They may be positively or negatively charged, or may be neutral. Most free radicals are highly reactive because of their unstable electronic configuration. This reactivity may cause deleterious effects in biological systems, such as a loss of membrane fluidity or inactivation of numerous enzymes. Also, because free radicals contain an unpaired electron they create another free radical when they react with a non-radical. Thus, they have the potential to initiate a chain reaction and greatly increase the damage caused by the initiating radical. In recent years, the involvement of oxygen-based free radicals in biological systems has been proposed as a likely factor contributing to stress-related injury suffered by plants (Pryor, 1976).

Oxygen toxicity is usually not ascribed to molecular oxygen, but to the reactive species derived from it. Molecular oxygen (dioxygen) is relatively unreactive because of the spin restriction of its two unpaired electrons. In its ground state, molecular oxygen has two unpaired electrons of the same spin which occupy distinct orbitals of equal energy. These unpaired electrons constitute a spin restriction to covalent bonding

since one of the spins must be inverted before O_2 can react with a reductant (Allen and Hill, 1978). This inversion requires energy as well as time, and as the time for a spin inversion (10^{-8} s) is long in comparison to the lifetime of a molecular collision (10^{-12} s), the probability of oxygen being involved in many reactions is low (Allen and Hill, 1978). The spin restriction can be overcome if sufficient energy is supplied to the ground state O_2 to form either of two species of the excited singlet state oxygen in which the spins are occupying either separate orbitals ($^1\Sigma g$) or the same orbital ($^1\Delta g$). These can return to the ground state either through radiation of excess energy or by energy transfer to another molecule. Of these species, ($^1\Sigma g$) is rapidly quenched and does not engage in significant chemistry (Rabinowitch and Fridovich, 1983). ($^1\Delta g$) is more stable and is involved in dye-sensitized oxidations called photodynamic effects. Photodynamic effects can be an important aspect of oxygen toxicity (Nilsson and Kearns, 1973). Green plants, which are naturally exposed to intense light and oxygen, contain the photosensitizer, chlorophyll.

The spin restriction can also be overcome by a one electron transfer to O_2. This energetically favourable reaction results in formation of the superoxide radical (O_2^-) (Samuel and Steckel, 1974). The univalent reduction occurs in both abiotic and biological oxidations.

The superoxide radical (O_2^-) and another oxygen-based free radical, the hydroxyl radical (OH·), are most frequently cited as having detrimental effects on biological systems. Superoxide has been known to induce lipid peroxidation (Kellogg and Fridovich, 1975), injure membranes (Goldberg and Stern, 1976; Kellogg and Fridovich, 1977), inactivate viruses (Lavelle et al. 1973) and cause the death of cells (Michelson and Buckingham, 1974). Molecules susceptible to superoxide attack include proteins, nucleic acids, polyunsaturated fatty acids (PUFA) and carbohydrates (Leshem, 1981). Plant senescence and fruit ripening are thought to be processes associated with increased free radical formation, in particular, the formation of free radicals derived from oxygen (Frenkel, 1978; Halliwell, 1981; Rabinowitch and Sklan, 1981; Buchvarov and Gantcheff, 1984). Accelerated spoilage of cut flowers (Leshem, 1981), wounding (Thompson et al. 1987), aging (Priestley et al. 1980) and sunscald (Rabinowitch and Sklan, 1980) may also involve free radical activity.

Numerous oxidative enzymes are known to generate the superoxide radical in biological systems. This occurs in reactions involving oxygen which are mediated by chloroplast and mitochondrial membranes. Some examples of such enzymes include xanthine oxidase, aldehyde oxidase, dihydroorotic dioxygenase, indoleamine dioxygenase and 2-nitropropane dioxygenase (Palmer et al. 1964; Bray et al. 1964; Knowles et al. 1969; Fridovich,

1981). Superoxide may also be formed through photooxidative processes. These reactions are mediated by photosensitizers such as riboflavin, porphyrins and anthroquinones. These chemicals pass excitation energy absorbed from light to oxygen with the resultant formation of high energy singlet oxygen or superoxide via univalent oxygen reduction (Ballou et al. 1969).

EPR spin trapping was used to demonstrate the presence of the superoxide radical in young chloroplast suspensions exposed to elevated levels of oxygen (Harbour and Bolton, 1975) and in aged chloroplast suspensions (McRae and Thompson, 1983). Superoxide production has also been shown in mitochondria (Rich and Bonner, 1978), microsomes (Kuthan et al. 1982) and nuclei (Patton et al. 1980).

Photosynthetic electron flow may also cause the formation of the superoxide radical. Asada et al. (1976), presented evidence using superoxide dismutase (SOD), a scavenger of superoxide, which suggested that superoxide is produced in illuminated chloroplasts. SOD was also shown to inhibit the photoreduction of cytochrome c by spinach chloroplast suspensions, thereby implicating the activity of the superoxide radical in this photoreduction (Nelson et al. 1972). Oxygen can be reduced to H_2O_2 by illuminated chloroplasts (Mehler, 1951). The reaction probably involves the superoxide radical as an intermediate:

$O_2^- + O_2^- + 2H^+$ yields $H_2O_2 + O_2$

(Harbour and Bolton, 1975; Glidewell and Raven, 1975)

Enzymatic processes such as the breakdown of xanthine to uric acid in purine catabolism also produce superoxide. The oxidative nature of respiration itself results in superoxide production even though the major enzyme which utilizes oxygen, cytochrome oxidase, reduces tetravalent oxygen to water without the release of any toxic intermediate (Fridovich, 1978). Lipoxygenase activity can also produce superoxide and PUFA can become converted to free radicals via H^+ abstraction during this process (Leshem, 1981).

Ozone has been implicated in initiating free radical producing reactions, especially in membrane fatty acids (Pryor, 1976). The reactive ozone molecule is capable of reacting with numerous organic molecules. These include alkanes, alkenes, aldehydes and amines (Pryor, 1976). Frequently this interaction can result in free radical formation. There is also potential for the formation of various free radicals when ozone dissolves in water. The prominent product of this reaction is probably the hydroxyl radical (Weiss, 1935), but within biological systems there has been no detailed analysis of the products as yet (Heath, 1975).

The most likely source of superoxide in injured tissues is

lipid peroxidation of membrane PUFA (Tomlinson and Rich, 1970; Pauls and Thompson, 1981a, 1981b). Even under normal metabolic circumstances, the danger of initiating peroxidation of the closely associated hydrophobic tails via H^+ abstraction and free radical production is always present. Due to the reactivity of ozone, only a few molecules exposed to a portion of the hydrophobic membrane could initiate peroxidative processes. However, Mudd (1982) cautions that the peroxidation may, in some instances, be confused with ozone-induced ozonolysis, as the most readily measured product, malondialdehyde (MDA), is a product of both reactions.

Toxic free radical formation has been proposed as a primary event in the sequence through which ozone may cause detrimental changes to the photosynthetic process (Sakaki et al. 1983). Free radical-induced membrane impairment is often cited as the reason for photosynthetic reduction (Mudd, 1973, 1982). The degree of impairment has been correlated to the level of superoxide dismutase (SOD) present in the leaves (Lee and Bennett, 1982), but this was not confirmed by subsequent investigators (McKersie et al. 1982; Chanway and Runeckles, 1984a, 1984b). These diverse results are probably attributable to inherent differences in plant material and experimental conditions. Sakaki et al. (1983) found that levels of SOD in spinach chloroplast suspensions from leaves previously fumigated with 0.5ppm O_3 were decreased 50 per cent by 4 hours of

fumigation. However, there was no change in SOD levels when spinach leaves were fumigated with 0.1 or 0.2ppm O_3 for 24 hours, but there was a 50 per cent reduction when leaves were fumigated with 0.3ppm O_3 for 24 hours. Thus, the effects on SOD seem to be exposure dependent. At the lower fumigation levels, MDA levels increased even though SOD, chlorophyll a, chlorophyll b, L-ascorbate and dehydro-L-ascorbate levels remained unchanged (Sakaki et al. 1983). This supports the contention that increases in MDA levels are a function of ozonolysis, not lipid peroxidation (Mudd, 1982).

It has been suggested that molecular oxygen may also act as the terminal acceptor of Photosystem I in higher plants (Leshem et al. 1981; Foster and Hess, 1982). While this is strictly a hypothesis at the present time, the univalent reduction would result in the production of superoxide. The presence of the superoxide thus created would partially explain the presence of the majority of SOD activity in the chloroplasts of plants (Asada et al. 1973; Kono et al. 1979; Foster and Edwards, 1980). Mudd et al. (1974) also point out that potential superoxide production could occur through cleavage of the nicotinamide ring of NADP(H).

Superoxide generated in aqueous media is unstable, particularly with decreasing pH, whereas in an aprotic medium such as the interior of the hydrocarbon bilayer in biomembranes,

its lifetime is longer (Allen and Hill, 1978).

Superoxide can spontaneously dismutate to form H_2O_2 as shown below:

$2O_2^- + 2H^+$ yields $H_2O_2 + O_2$

This is the reaction that is also catalyzed by the enzyme, superoxide dismutase.

Despite the proliferation of reports which attribute damage to biological systems to the activity of the superoxide radical, other studies suggest that at least some of this damage may be caused by the more toxic hydroxyl radical (Leshem, 1981). Fridovich (1978) showed that addition of superoxide dismutase (SOD) or catalase inhibited the production of ethylene from methional (CH_3-S-CH_2-CH_2-CHO) exposed to an enzymatic source of both superoxide and H_2O_2. However, the addition of ethanol or benzoate, both of which scavenge the hydroxyl radical selectively, while remaining unreactive to superoxide or H_2O_2, also inhibited the production of ethylene. This supports the contention that the hydroxyl radical is the active agent since superoxide and H_2O_2 can combine to form the hydroxyl radical, through iron catalysis of the Haber-Weiss reaction shown below:

$H_2O_2 + O_2^-$ yields $OH^\cdot + OH^\cdot + O_2$

(Leshem, 1981)

Another alternative for the formation of the hydroxyl radical is the Fenton reaction in which H_2O_2 reacts with divalent ferrous iron to form the hydroxyl radical, a hydroxyl ion and a trivalent ferric ion:

$$H_2O_2 + Fe^{+2} \text{ yields } OH^- + OH^{\cdot} + Fe^{+3}$$

Once formed, the hydroxyl radical is extremely reactive and attacks numerous target molecules indiscriminately. Thus, there are no specific scavengers for this radical within plants as they would be required at unrealistically high concentrations. It appears that organisms defend themselves against the effects of the hydroxyl radical through various antioxidants which prevent the formation of the precursors to the hydroxyl radical. Specifically, catalases and peroxidases scavenge H_2O_2 (Asada et al. 1975), while superoxide dismutases scavenge O_2^- (Kono and Fridovich, 1982).

2.2 Photoinhibition

Injury to the photosynthetic apparatus of plants induced by exposure to excessive light has been documented for many years (Emerson, 1936; Rabinowitch, 1945; Kok, 1956). The intensity of light needed to induce photoinhibition varies from full sunlight (2000μmol $m^{-2}s^{-1}$) to a little as 50μmol $m^{-2}s^{-1}$ for algae grown at low photon flux density (PFD) (Whitelam and Codd, 1983). Damage to the photosynthetic process can be caused by

exposure to light in the ultraviolet wavelength (Caldwell, 1981), by excessive light in the visible part of the spectrum (Kok, 1956; Critchley, 1981) or by interaction of light in these spectra (Warner and Caldwell, 1983). Herein, only damage which occurs through excessive exposure to visible light is discussed. Thus, photoinhibition is defined as the reduction in photosynthetic capacity, which is not dependent upon changes in pigment concentration, but which is induced by exposure to excessive intensities of visible light in the 400-700nm region. This inhibition is not caused by CO_2 limitations.

The terms photooxidation, photoinactivation, photolability, solarization and photodynamic reactions have also been applied to events that lead to the reduction of photosynthetic capacity which occurs through exposure to strong light (Powles, 1984).

Photoxidation is usually used to describe the photodestruction of photosynthetic pigments by strong light. This is usually evident as the bleaching of pigments and is both light and oxygen dependent. In this case prolonged treatment results in the death of the cell or organism. Photooxidation of pigments occcurs after initial photoinhibition (Myers and Burr, 1940; Kok et al. 1965; Satoh, 1970a), with a distinct time lag between the two processes. The start of photooxidation usually occurs after photoinhibition has reached a maximum (Sironval and Kandler, 1958).

Evidence of photoinhibition has been shown in both aquatic and land plants. Land plants can be classified as either shade or sun plants. In addition to growth in their natural environment, sun plants can generally grow in conditions of lower photon flux density (Bjorkman, 1973,1981). The reverse often does not hold true for shade plants, because of susceptibility to photoinhibition. For instance, Bjorkman and Holmgren (1963) and Bjorkman (1968) showed that populations of Solidago virgaurea from open habitats were able to grow in the sun but were also able to survive and grow, though at slower rates, when held under conditions of lower light intensity. In contrast, populations originating from low light intensity habitats grew well under low PFD but had minimal growth at higher light intensities. In these studies some photooxidative bleaching occurred on the exposed parts of leaves but was not responsible for the initial inhibition of photosynthesis. The photoinhibition was evident as a decline in light-saturated photosynthesis and photon yield.

Plants have different mechanisms for dissipating the excessive light energy. At the biophysical level, plants have the potential for the spillover of excitation energy from PSII to PSI. At the metabolic level, the maintenance of minimal photosynthetic carbon metabolism can minimize photoinhibition, while at the morphological level, leaf movement in response to high PFD can prevent photoinhibition (Powles, 1984).

Different species adjust in differing ways to exposure to intense light. Some species, such as Fragaria virginiana, which is not exclusively a shade plant, also show lower light-saturated photosynthetic capacity and photon yield when grown in conditions of full sunlight. Sun plants, grown originally at low PFD, exhibit the same characteristics if moved suddenly to a higher PFD environment (Bunce et al. 1977; Powles and Critchley, 1980; Powles and Thorne, 1981; Powles and Bjorkman, 1983). Plants which experience this initial photoinhibition may respond by increasing their photosynthetic capacity at the higher PFD (Prenzel and Lichtenthaler, 1982) or may suffer photooxidative bleaching and cell death (Louwerse and Zweerde, 1977).

The mechanism through which exposure to excessive light causes a decline and disruption in the photosynthetic process is poorly understood. Early experiments with dilute suspensions of algal cells led to the conclusion that intense light "inhibited the primary photochemical process, thereby causing a reduction in the capacity for efficiently passing on light quanta and a concomitant diminuation of light-saturated photosynthesis" (Kok, 1956). Subsequent experimentation with shade plants indicated that PSII was impaired when shade plants were grown at a higher PFD. PSI was also damaged, but to a lesser extent (Bjorkman, 1968). Similar effects were shown in studies where sun plants were initially grown in shade and then exposed to a PFD comparable to full sunlight. Chloroplast thylakoids isolated

from these leaves showed some degree of inhibition of light-saturated, uncoupled electron transport capacity (Powles and Critchley, 1980; Powles and Bjorkman, 1983), depending upon length of exposure time (Critchley, 1981). Again, there was less inhibition of PSI activity and photophosphorylation was not inhibited by the higher PFD (Critchley, 1981).

Studies of PSII fluorescence at 77K also indicated damage to PSII. Photoinhibition was shown as an inhibition of light-saturated photosynthesis, photon yield and PSII electron transport. Fluorescence kinetics of the exposed upper leaf surface at 77K revealed time and PFD-dependent inhibition of PSII maximal fluorescence (F_{max}) with minimal changes in the initial fluorescence (F_o). Little change in F_{max} occurred on the self-shaded lower surfaces of leaves. F_{max} could not be restored by the addition of donors which bypass the water-splitting reaction; thereby suggesting that the inactivation of PSII occurred through an effect on the reaction centre complex (Powles and Bjorkman, 1983).

Photoinhibition is not oxygen-dependent, as similar results were obtained when the oxygen partial pressure was at atmospheric levels or close to zero (Belay and Fogg, 1978; Belay, 1981). However, photoinhibition at moderate PFD levels also occurs in the absence of CO_2. Results from experiments conducted under a high PFD without CO_2 were similar to those

obtained in the presence of CO_2 and a high PFD (Powles et al. 1979; Powles and Critchley, 1980). Photoinhibition through exposure to high PFD is increased through the synergistic action of stress from low temperature (Fork et al. 1980; Baker et al. 1983), high temperature (Ludlow and Borkman, 1983) and water deficit (Gauhl, 1979).

The precise mechanisms through which excessive PFD causes damage to Photosystems I and II, respectively, are unknown at the present time but clearly differ. PSII electron transport and primary photochemistry inhibition occur identically in the presence or absence of oxygen. This suggests that the generation of oxygen radicals is unlikely to be the cause of the photoinhibition. Kyle et al. (1984) suggested that photo-inhibitory damage in Chlamydomonas reinhardii was due to the loss of the 32 kiloDalton (kDa) herbicide-binding polypeptide, which is also the polypeptide carrying the the secondary electron acceptor quinone (QB). However, Cleland and Critchley (1985) found that photoinhibition under similar conditions was not accompanied by the loss of the 32 kDa protein. They conclude that the reduction in F_{max} occurs because of the generation of a very efficient fluorescence quencher during photoinhibition. They suggest that the quencher may be a modified form of QA, caused either by attack by a hydroxyl radical with subsequent hydroxylation or by interaction of the quinone with thiol groups on the polypeptide. They suggest that

the loss of the 32 kDa protein is a result, not a cause of photoinhibition. Some support is available for their hypothesis as Den Haan et al. (1973) found an unidentified quencher (T) which was generated in a light flash and disappeared in a dark reaction of the order of 10μs. Such a quencher may have a longer life during a photoinhibitory episode.

In contrast, the photoinhibition of PSI electron transport requires the presence of oxygen (Powles and Bjorkman, 1983) and electron transport from PSII (Satoh, 1970b). The site of PSI inhibition has been shown to be very close to the PSI reaction centre (Satoh, 1970c) and the oxygen requirement suggests that toxic oxygen compounds may be involved in PSI photoinhibition.

Recovery from photoinhibition has received little attention to date but is a very slow process in relation to the speed of onset of photoinhibition (Powles, 1984).

2.3 Photosynthetic Electron Transport

Photosynthetic electron transport in green plants entails the absorption of light energy by a large array of light-harvesting pigments, and subsequent transfer of this energy by resonance to the reaction centres of two different photosystems, Photosystems I and II (PSI and PSII). There it is converted into chemical energy. The photosystems act through a series of

oxidation-reduction reactions in the non-cyclic transfer of electrons from H_2O to $NADP^+$. In the light, PSII generates a strong oxidant capable of oxidizing water, and, concomitantly, a weak reductant, while PSI generates a strong reductant capable of reducing $NADP^+$, and, concomitantly, a weak oxidant (Malkin, 1982). Hill and Bendall (1960) proposed the Z scheme (Figure 1) which places the components of the electron transport chain according to their redox potentials and establishes a basis for energetic considerations. The vectorial charge separation in the reaction centres and the vectorial transport of protons provide the electrochemical gradient across the thylakoid membrane which drives the synthesis of ATP, as first suggested by Mitchell (1961).

Lateral mobility of the integral protein complexes in the thylakoid membrane first proposed in the fluid-mosaic model of Singer and Nicholson (1972) has been confirmed in the 1980's. There is an extreme lateral heterogeneity in the distribution of PSII and PSI in appressed grana and stroma-exposed thylakoid membranes, respectively (Andersson and Anderson, 1980). The mobile electron carriers, plastoquinone and plastocyanin, which respectively receive electrons from PSII and donate electrons to PSI, are thought to link the photosystems by moving laterally through the plane of the thylakoid membranes between the granal

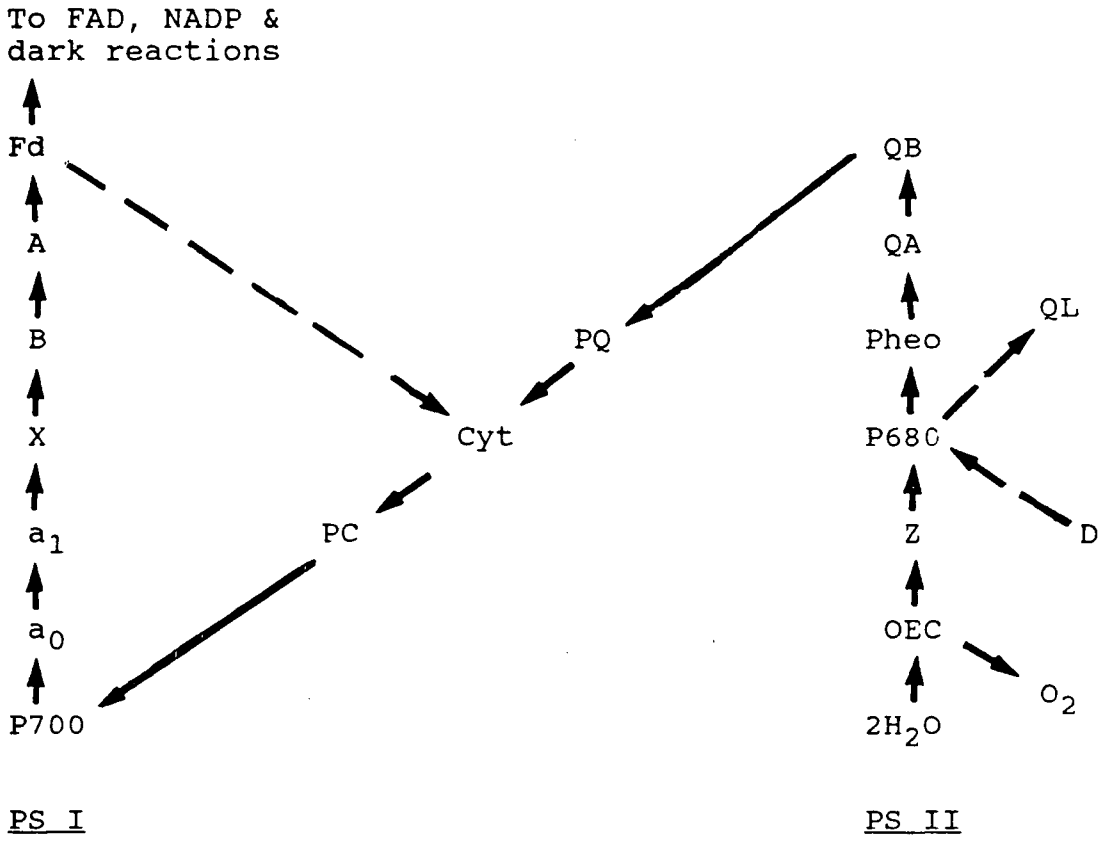

Figure 1. Current concept of the Z scheme first proposed by Hill and Bendall (1960). OEC=Oxygen-evolving complex; Z=the immediate electron donor to P680; D=an auxiliary electron donor to P680; P680=photosystem II reaction centre chlorophyll *a*; Pheo=pheophytin; QL=unidentified component which may be an electron acceptor; QA=iron-plastoquinone electron acceptor; QB=second iron-plastoquinone electron acceptor; PQ=plastoquinone; cyt=cytochrome b_6-*f* complex; PC=plastocyanin; P700=photosystem I reaction centre chlorophyll *a*; a_0 and a_1=unidentified early electron acceptors; X=a possible iron-sulphur electron acceptor; B and A=iron-sulphur centres; Fd=Ferredoxin; FAD=Flavin adenine dinucleotide; NADP=Nicotinamide adenine dinucleotide phosphate.

Combined from Govindjee *et al*. (1985), Haehnel (1984) and Malkin (1982).

and stromal regions (Ford and Barber, 1983).

The greater part of the electron transport chain from H_2O to NADP+ is organized into three membrane-spanning complexes. These are the PSII complex, the cytochrome $\underline{b}_6$-$\underline{f}$ complex, and the PSI complex. Each contains several extrinsic and intrinsic polypeptides. These complexes do not interact directly but are linked by small electron carriers. Plastoquinone links the PSII complex with the cytochrome $\underline{b}_6$-$\underline{f}$ complex and plastocyanin links the cytochrome $\underline{b}_6$-$\underline{f}$ complex with the PSI complex. Ferredoxin mediates the electron transfer from PSI to the membrane-bound ferredoxin-$NADP^+$ reductase and possibly to the cytochrome $\underline{b}_6$-$\underline{f}$ complex in cyclic electron transport (Haehnel, 1984).

2.3.1 Photosystem II

Photosystem II is a chlorophyll-containing protein complex involved in light-induced oxygen evolution and plastoquinone reduction. The scheme is outlined below:

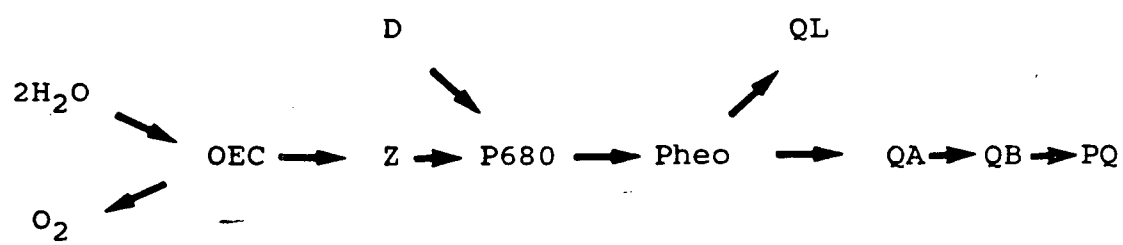

where OEC is the oxygen evolving complex; P680 is a chlorophyll $\underline{a}$ molecule which is the primary electron donor, D and Z are

electron donors; Pheo is pheophytin a; QA and QB are iron-plastosemiquinone electron acceptors; QL is postulated to be another electron acceptor; and PQ is plastoquinone.

A quantum absorbed in the antenna pigments is transferred to the reaction centre and induces an electron transfer from the primary donor P680 to the intermediate acceptor, pheophytin a, (Pheo) within a few hundred picoseconds. The following electron transfer from Pheo to QA is likely to be the electrogenic step (van Gorkum et al. 1983) in the charge separation of PSII from the inside to the outside of the thylakoid membrane. Electron transfer from QA^-, which has been identified as a plasto-semiquinone-Fe^{+2} complex (Nugent et al. 1981a), involves a two electron gate mechanism (Bouges-Bocquet, 1977). The secondary acceptor (QB) is also a plastoquinone molecule which is not exchanged with another plastoquinone molecule of the pool (PQ) until it is fully reduced. The mechanism is as follows:

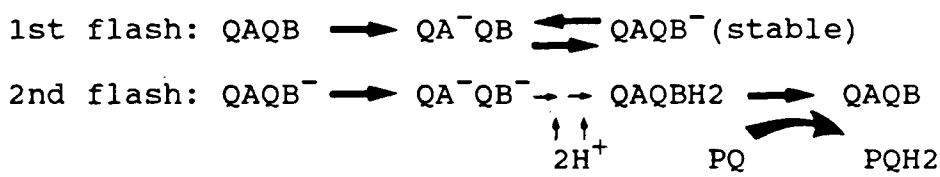

One relevant aspect of PSII is the location of the inhibition site of 3-(3,4-dichlorophenyl)-1,1-dimethylurea (DCMU) and atrazine-type inhibitors of PSII. Binding by these inhibitor herbicides is competitive with the binding of plastoquinone to the QB site (Velthuys and Amesz, 1974; Crofts

and Wraight, 1983) and results in a block in the electron transport chain. The function of the postulated acceptor QL is not known at present (Eckert and Renger, 1980).

Electron transfer from the donor Z to $P680^+$ can be followed by EPR measurements of the rapidly reversible Signal II_{vf}, attributed to Z^+. Simultaneous measurements at room temperature of the EPR signal of Z^+ and the decay of $P680^+$ in Tris-treated thylakoids provided evidence that Z is the immediate donor to $P680^+$ (Babcock and Sauer, 1983b). The donor D is represented by EPR Signal II_{u+s}. This species is only marginally understood as yet, but appears to be a secondary donor on a side chain (Boussac and Etienne, 1982a, 1982b).

Once oscillations were found in the oxygen yield after short saturating flashes (Joliot et al. 1969), Kok et al. (1970) formulated the kinetic S-state-scheme for oxygen evolution. On excitation of its associated PSII reaction centre complex, each individual oxygen-evolving complex goes through a sequence of increasing oxidation states from S_0 to S_4. After the enzyme reaches the S_4 state, it releases oxygen and returns to the S_0 state. The light-induced transitions from S_0 to S_1 and from S_2 to S_3 result in the release of one proton, and the transition from S_3 to S_0 via S_4 results in the release of two protons (Bowes and Crofts, 1978; Forster et al. 1981). Proton release from S_0 to S_1 but not from S_1 to S_2 was

confirmed by Rutherford et al. (1984b).

Manganese is also involved in the mechanism of oxygen evolution (Cheniae and Martin, 1970). Treatment-induced release of Mn from the membrane shows the presence of at least three different pools of Mn in chloroplasts. Weakly bound Mn, not involved in oxygen evolution, can be removed by incubation with divalent ions or EDTA (Yocum et al. 1981). Approximately two-thirds of the remaining strongly bound Mn can be removed with heat, hydroxylamine or Tris-washing treatment (Amesz, 1983; Dismukes, 1986). If the remaining very strongly bound Mn is extracted from a PSII reaction centre, readdition of four Mn atoms per reaction centre gives the maximal reactivation of electron transport (Klimov et al. 1982). However, of these, only two Mn atoms per reaction centre are vital, as the other two can be replaced by other divalent cations without loss of activity. Chloride has also been shown to be a component of the oxygen-evolving complex. Its exact function is unknown but it may act as a bridging ligand between Mn atoms (Critchley, 1985).

Other components of PSII include a number of polypeptides. Three of these, which have molecular weights of 17, 23 and 33 kDa, respectively, are found in the oxygen-evolving complex (OEC) (Kuwabara and Murata, 1982, 1983; Yamamoto et al. 1981, 1983). These proteins have absorbance peaks at 275-276nm, but none in the visible region and are monomeric in solution. They

do not contain Mn, other metals, or chlorophyll (Jansson *et al.* 1983; Kuwabara and Murata, 1982, 1983; Yamamoto *et al.* 1983). Their function is unknown but may be catalytic, regulatory or structural. Recently, Hunziker *et al.* (1987) presented evidence for an association between the 33kDa protein and oxygen evolution, but Styring *et al.* (1987) found no requirement for this protein if sufficient Cl^- was present. Other polypeptides include two chlorophyll *a*-protein complexes with apoproteins of 47 and 50 kDa, respectively (Delepelaire and Chua, 1979). The first of these is associated with the secondary electron acceptor QB while the latter may be associated with the reaction centre of PSII. Also present are the 32 kDa polypeptide involved in the binding of QB, and cytochrome b_{559}, which has a molecular weight of 10 kDa.

2.3.2 Cytochrome b_6-*f* Complex

This section of the electron transport chain is an integral protein complex which includes two cytochrome polypeptides. These are the polypeptide of cytochrome *f* of 34 kDa, and a polypeptide with two cytochrome b_6 hemes of 23 kDa. Other components are the high potential Fe_2S_2 "Rieske" protein of 20 kDa and a bound plastoquinol. The complex structure, as known today, is completed with a structural polypeptide of 17 kDa and a small peptide of 5 kDa (Bendall, 1982; Cramer and Whitmarsh, 1977; Hauska *et al.* 1983). The precise mechanism of

electron transfer within this complex has yet to be elucidated.

2.3.3 Photosystem I

The PSI complex consists of the reaction centre chlorophyll P700, which functions as the primary electron donor of PSI, and five electron acceptors, as shown below:

$$P700 \longrightarrow a_0 \longrightarrow a_1 \longrightarrow X \longrightarrow (\text{centre B - centre A}),$$

where P700 is recognized as a form of chlorophyll *a*, but the precise structure is unknown; different investigators have provided evidence supporting a dimer (Norris *et al*. 1971), a monomer (O'Malley and Babcock, 1984b), and an enolized monomer (Wasielewski *et al*. 1981).

The charges separated in the reaction centre are stabilized by fast consecutive electron transfer through the chain of electron acceptors shown above. The recently detected initial acceptors a_0 and a_1 may be monomeric chlorophyll *a* anions (Gast *et al*. 1983; Malkin, 1982). Acceptor a_1 is closely associated with X, and if X is destroyed, does not participate in PSI electron transfer (Warden and Golbeck, 1987). The third electron acceptor, X, has properties similar to an iron-sulphur centre (Koike and Katoh, 1982; McIntosh and Bolton, 1976) but the exact structure is unknown. The final electron acceptors are the iron-sulphur centres A and B, which interact closely with each other (Malkin, 1982). It has been shown that these

are bound ferredoxins having Fe_4S_4 centres (Cammack and Evans, 1975). Their reduction can be observed as absorbance changes at 430nm (Ke, 1972). Electron transfer between X, and centres A and B has yet to be definitively elucidated. Initial reports of the redox potentials of these acceptors in spinach chloroplasts suggest linear transfer from X to B to A (Ke et al. 1973; Evans et al. 1974). However, redox potentials are different in some systems (Malkin, 1982). The successful reduction of A after inactivation of B (Golbeck and Warden, 1982) and the chemical reduction of B prior to A (Nugent et al. 1981b) has led to a hypothesis that X is the branch point leading to parallel function of centres A and B (Nugent et al. 1981b).

The primary electron donor, P700, and acceptors a_0 and a_1, are contained in the largest subunit of the PSI reaction centre complex which has a molecular weight of 70 kDa (Bengis and Nelson, 1977). The three later acceptors, X, A and B, are apparently located in two smaller subunits having molecular weights of approximately 15-18 kDa (Moller et al. 1981).

2.4 EPR Studies

EPR spectroscopy has been used extensively to study the components of the photosynthetic electron transport chain. In fact, many of the components were discovered through the use of EPR. With the exception of initial observations made regarding Signals I and II, the majority of the work has been done at liquid helium or liquid nitrogen temperatures using chloroplast and reaction centre preparations.

Initially, Commoner et al. (1956, 1957), working at 35C, discovered the presence of EPR signals in tobacco chloroplasts illuminated with light. One signal, now known as Signal I (Figure 2c), is associated with PSI. It consists of a single peak, has a g-value of 2.0024-2.0025, and a peak-to-peak line width of 7.5-9 gauss. In chloroplast preparations from healthy plants this signal is only induced by illumination with far-red (700-730nm) light. It is transient and disappears within milliseconds after termination of illumination (Warden and Bolton, 1974a). This signal is ascribed to the oxidized form of the chlorophyll a of the reaction centre of PSI (Beinert et al. 1962). Signal I is also formed upon irradiation of chloroplast suspensions with red (Blumenfeld et al. 1974; Babcock and Sauer, 1975a) or broad-band white light (Babcock and Sauer, 1975b) when electron transport from PSII to PSI is blocked by an inhibitor such as DCMU (Velthuys and Amesz, 1974).

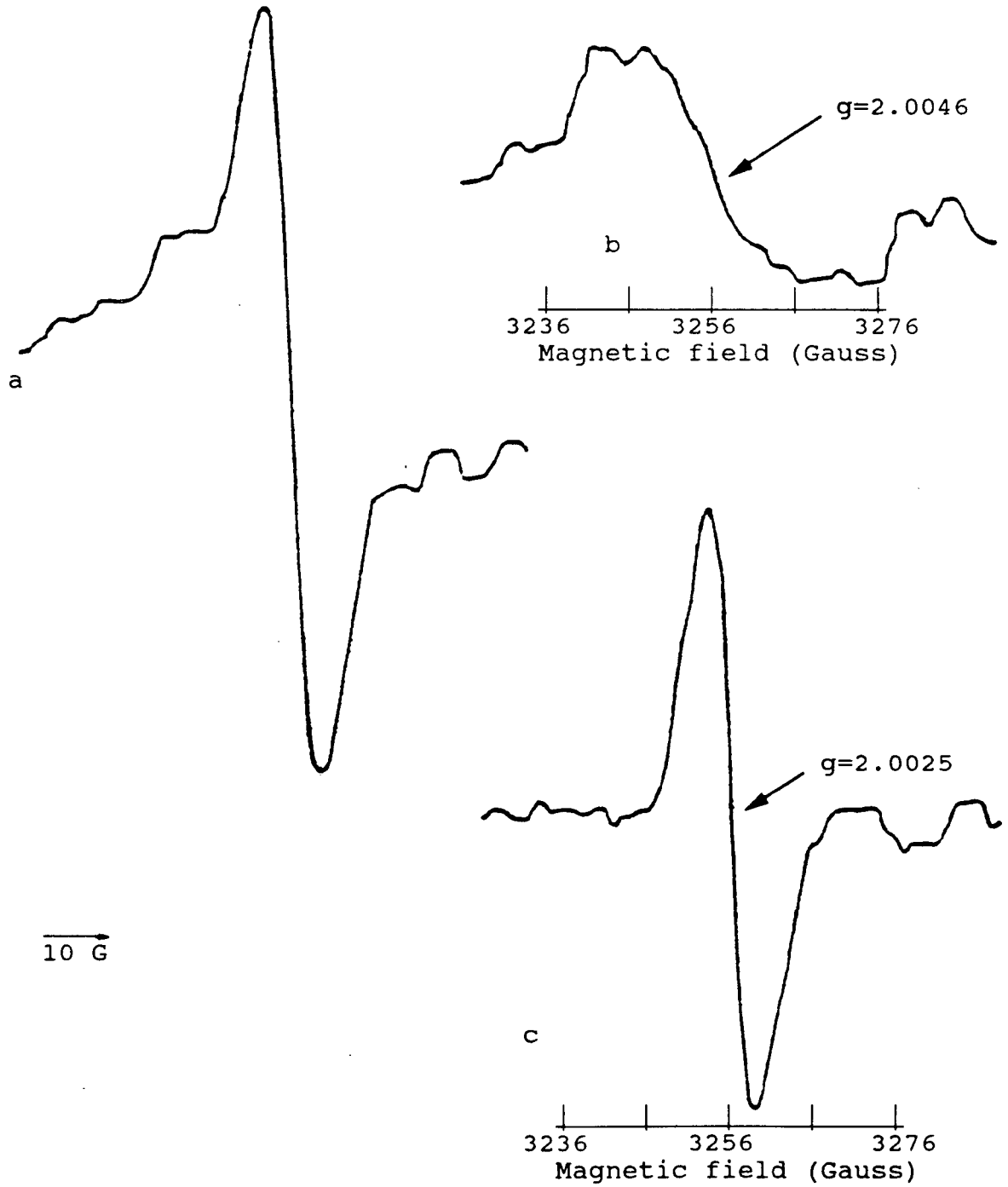

Figure 2. Primary photosynthetic signals found in reaction centre and chloroplast preparations and in intact leaf tissue. These signals were obtained in the present study from Kentucky bluegrass leaves. a. Combined Signal I and II_{u+s}; b. Signal II_{u+s}; c. Signal I (obtained by subtraction of b from a).

The second major signal discovered by Commoner et al. (1956,57), now known as Signal II (Figure 2b), is associated with Photosystem II, is asymmetrical, has five lines of unequal intensity and splitting, a g-value around 2.0046 and a peak-to-peak line width of 18-20 gauss (Esser, 1974a). This signal was first known as a dark signal, but subsequent investigations have shown that it, too, has components which are dependent upon light, as oxidation in darkness results in elimination of 50% of the signal (Weaver, 1968; Babcock and Sauer, 1975a). The two components of this signal are now known as Signal II_u and Signal II_s, with the subscripts, u and s, standing for unchanging and slow, respectively. The composite signal is known as Signal II_{u+s}. This signal is induced by broad-band white light and has several decay phases (Warden and Bolton, 1974b). The slowest of these phases has a half-life exceeding 2 hours (Weaver, 1968). Recent studies by Rutherford (1985) have shown that Signal II_{u+s} is composed of an overlap of two distinct four line signals. Which of these emanates from any given membrane is dependent upon the orientation of the membrane to the magnetic field (parallel or perpendicular). In whole plant tissues the signals overlap to form Signal II_{u+s}. DCMU and atrazine-type herbicides which inhibit PSII at QB (Velthuys and Amesz, 1974), do not prevent the formation of Signal II_{u+s} (Lozier and Butler, 1973; Esser, 1974b).

The exact structure of the species giving rise to Signal

II_{u+s} is not known but it was first attributed to a plastosemiquinone (Weaver, 1962; Kohl and Wood, 1969) or plastochromanoxyl radical (Kohl et al. 1969). Subsequently, it was proposed that Signal II_{u+s} originates from a plastosemiquinone anion radical perturbed by a metal cation (Hales and Case, 1981; Hales and Das Gupta, 1981). More recently, it was suggested that Signal II_{u+s} represents a plastoquinone cation radical in which the electron-donating ability of the quinol-OH groups has been decreased (O'Malley and Babcock, 1984a). The functional role of the species giving rise to Signal II_{u+s} has not been ascertained but early hypotheses suggested that Signal II_{u+s} reflected the behaviour of some quinoidal compound on the reducing side of PSII which was located near the electron transport chain (Weaver 1962; Warden and Bolton, 1974b). More recently, Signal II_{u+s} has been assigned to D, a donor on an auxiliary path to P680 (Boussac and Etienne, 1982a, 1982b) (see Figure 1).

Signal II_{u+s} is distinguished from two other signals, Signal II_f (Babcock and Sauer, 1975a, 1975b) and Signal II_{vf} (Blankenship et al. 1975a; Warden et al. 1976). The f and vf stand for fast and very fast, respectively. The latter signals, which represent light-generated free radicals detected in chloroplast suspensions by EPR, are the EPR manifestations of Z^+, the primary donor to P680 (Yocum and Babcock, 1981). The difference in nomenclature represents the fact that the

light-generated reduction of Z can be fast or very fast, depending upon the stage of the oxygen-evolving complex. In oxygen-evolving chloroplasts, Z^+ reduction occurs in the sub-millisecond time range; thus its EPR signal is designated Signal II_{vf}. When oxygen-evolving ability has been inhibited, Z^+ is stable well into the millisecond-range; thus its signal is designated Signal II_f (Babcock and Sauer, 1975b; Babcock et al. 1976). The various components of Signal II all have the same shape, g-value and line width (see Figure 2b).

Malkin and Bearden (1971) used EPR spectroscopy to demonstrate the presence of an iron-sulphur protein in chloroplast membranes maintained at liquid helium temperatures. Illumination of chloroplasts maintained at 10K produced a paramagnetic species with a spectrum having g-values of g_x=1.86, g_y=1.94 and g_z=2.05. This is now known as iron-sulphur centre A. The association of this centre with PSI was shown by Bearden and Malkin (1972a), since far-red light, which activates PSI, also reduces the iron-sulphur centre. Further association with P700 was indicated through the observed 1:1 stoichiometry between photo-oxidized P700 and the photo-reduced iron-sulphur centre A (Bearden and Malkin, 1972b). At cryogenic temperatures the oxidized P700 and reduced iron-sulphur centre A are stable in the dark after cessation of illumination. However, when the temperature is raised from 77K to 150K there is a back reaction arising from a charge

recombination between these species (Bearden and Malkin, 1972b; Malkin and Bearden, 1974; Visser et al. 1974). At 150K there is an approximate 40% decay in both the P700 and iron-sulphur centre A (Bearden and Malkin, 1972b). This decay is biphasic (Bearden and Malkin, 1972b), but the reason for the biphasic decay has yet to be explained except for the trivial analysis that there is heterogeneity in the PSI complex. This was attributed to consequences arising from freezing of the samples (Lozier and Butler, 1974).

A second iron-sulphur centre, B, was discovered concomitantly (Malkin and Bearden, 1971; Evans et al. 1972). The spectrum of this centre, which has g-values of g_x=1.89, g_y=1.94, g_z=2.05, overlaps that of Centre A, except when Centre A has been previously reduced chemically. A 1:1 stoichiometric relationship has been shown between centres A and B (Malkin and Bearden, 1978) and the disappearance of the 1.86 component of the EPR spectrum of Centre A correlates well with the appearance of the 1.89 component of Centre B (Ke et al. 1973; Evans et al. 1974). These centres appear to be bound ferredoxins having Fe_4S_4 centres (Evans et al. 1975). EPR signals from these centres have yet to be found at ambient temperatures.

The presence of the electron acceptor X was first shown by McIntosh and Bolton (1976) in studies using purified spinach

Photosystem I particles maintained at 10K. This acceptor, which has an EPR signal having g-values of g_x=1.75, g_y=1.86, g_z=2.07, is discernible if both Centres A and B are previously reduced. This centre may be another iron-sulphur protein (McIntosh and Bolton, 1976) or it may be a chlorophyll anion radical interacting with another paramagentic centre such as an iron atom (Rupp *et al*. 1979).

Shuvalov *et al*. (1979) used Photosystem I particles maintained at 5K to show the presence of an electron acceptor prior to X. This early acceptor was shown to have a free-radical signal at a g-value of 2.004, with a line width of approximately 10 gauss. Heathcote and Evans (1980), and Baltimore and Malkin (1980) attributed a free-radical signal which had a g-value of 2.003 and a line width of 12-14 gauss to a_1. This was assigned to a chlorophyll *a* monomer. Subsequently, Bonnerjea and Evans (1982) showed that the 12-14 gauss signal originated from the overlap of two free radicals; one having a g-value of 2.0051, and the second a g-value of 2.0024. When both signals were formed at cryogenic temperatures after 50min illumination, the composite EPR signal had a g-value of 2.0033 and a line width of 13 gauss. Concurrently, (Gast *et al*. 1983) working under strongly reducing conditions, found two free radicals, having g-values of 2.0017 and 2.0054, and respective line widths of approximately 11.5 and 10.8 gauss. The individual signals are now ascribed to the electron

acceptors a_0 and a_1, respectively. The identity of the species giving rise to these signals is not yet clear, but the a_0 signal value is compatible with that of a chlorophyll anion monomer (Bonnerjea and Evans, 1982).

Blankenship et al. (1975b) observed the first polarized EPR signal in photosynthesis. This signal resembled an inverted steady-state $P700^+$ spectrum and was first attributed to a triplet mechanism (MacIntosh and Bolton, 1979). Subsequently, upon the discovery of a_0 and a_1, it was shown that the radical pair mechanism was responsible. The signal, which has definite orientation effects (Dismukes et al. 1978), is now attributed to a radical pair interaction between $P700^+$ and a_0 (Gast and Hoff, 1979), or between $P700^+$ and a_1 polarized through exchange interaction with a_0 (Broadhurst et al. 1986; Hoff, 1984). This was confirmed when signals attributable to the polarized triplet state (P^T) were discovered (Frank et al. 1979a, 1979b; Rutherford and Mullet, 1981; Rutherford et al. 1981).

Other components of the photosynthetic electron transport chain have been minimally studied but Nugent et al. (1981c) showed that the primary acceptor of PSII, QA, was a quinone-iron complex giving rise to an EPR signal having a g-value of 1.82. This signal can be induced by illumination of reaction centre particles at low temperatures or by chemical reduction. A

recent study indicates that QB is also an iron-quinone complex which can be followed through the appearance of an Fe^{+3} signal at a g-value of 7.9 (Zimmermann and Rutherford, 1986). Other signals connected to the electron transport chain include a multiline Mn signal associated with the S_2 state of Mn in the oxygen-evolving complex (Dismukes and Siderer, 1981; Zimmermann and Rutherford, 1984), a newly discovered signal with a g-value of 4.1, also seemingly associated with the S_2 state (Casey and Sauer, 1984a, 1984b; De Paula and Brudwig, 1985) and various signals associated with cytochrome $\underline{b}_{559}$ (Rutherford *et al.* 1984a), cytochrome $\underline{b}_{563}$ (Bergstrom, 1985) and the cytochrome $\underline{b}_6$-$\underline{f}$ complex (Malkin and Vanngard, 1980; Nugent and Evans, 1980).

Plant leaves also show a manganous ion (Mn^{++}) EPR spectrum (Theg and Sayre, 1979; McCain *et al.* 1984). The exact role of this EPR-detectable Mn^{++} has yet to be elucidated, a situation which is complicated by the occurrence of several pools of bound Mn^{++} in chloroplasts (Amesz, 1983). The Mn^{++} detectable by EPR spectrometry without prior treatment is neither the Mn^{++} involved in water oxidation nor the hexaaquomanganese (II) ion (McCain *et al.* 1984). It appears to be the weakly bound or storage pool Mn^{++} (Goldfeld and Blumenfeld, 1979: Amesz, 1983) but its function is not known to date.

Most plant leaves also reveal a broad Fe^{++} signal which

slopes down from low to high field, and underlies the six-peak Mn^{++} signal (Treharne and Eyster, 1962). The function of the iron responsible for this signal is not known at present.

The effect of SO_2 upon free-radical Signals I and II_{u+s}, and the Mn^{++} signal, has not been extensively investigated to date. Rowlands et al. (1970) fumigated radish, pinto bean and soybean plants with SO_2 concentrations ranging from 0.05 to 300ppm. Daily exposure periods varied from 1 to 20 hours for spans of 18 to 27 days, depending upon the experiment. Subsequently, leaves were excised and spectra obtained were compared to spectra from control leaves at ambient (300 K) and liquid nitrogen (77 K) temperatures. After fumigation with low levels of SO_2 (0.05 and 0.5ppm) they found no differences in the spectra except for a change in the hyperfine splitting of the second and third lines of the Mn^{++} spectrum when the spectra were recorded at 77 K. However, when pinto bean leaves were fumigated with high concentrations (100-300ppm) of SO_2 for 1 hour for 18 days, spectra recorded at 300 K showed a large increase in the Mn^{++} signal and a decrease in a 'free-radical' signal having a g-value around 2.0023. They also state, (without providing data), that a similar effect occurred when a chloroplast suspension was exposed to a high but unspecified level of SO_2. The investigators offer only very tentative conclusions but suggest that the increase in the Mn^{++} spectrum may be associated with SO_2-caused changes in Photosystem II.

In a related experiment they compared the forms of signals, described as Signal I and Signal II_{u+s}, obtained with chloroplast suspensions prepared from spinach leaves, which were illuminated with white light, before and after exposure to 0.5ppm SO_2 for 4 hours and suggested that SO_2 had caused a change in the relationship of PSI to PSII to account for the differences.

Shimazaki et al. (1984b) fumigated spinach leaves with 2ppm SO_2 for 45 minutes and then traced the kinetics of Signal I in excised sections of these leaves. After the plants were removed from the fumigation chamber the leaf segments were illuminated with far-red light (>700nm). This irradiation, which induced the formation of Signal I, was then followed by either illumination with broad-band white light or by elimination of all light focused upon the spectrometer cavity window. They found that neither the formation of Signal I in far-red light nor its decay in darkness was affected by the SO_2 fumigation. However, the rate of decay of Signal I in white light was reduced by the fumigation. They concluded, from these data and others (Shimazaki and Sugahara, 1979, 1980; Shimazaki et al. 1984a), that the SO_2 fumigation reversibly inhibits the photosynthetic water-splitting enzyme system and injures the reaction centre of PSII when fumigation is prolonged.

EPR investigation of the effects of exposure to O_3 on the

formation of free radicals in plant leaves, chloroplast or subchloroplst preparations, is even more limited. Rowlands et al. (1970) fumigated soybean and pinto bean plants with 0.5ppm O_3 for 1 hour or with 0.05ppm O_3 for 4 hours, and compared the spectra obtained from fumigated sections of leaves with those of spectra previously obtained from unfumigated sections of the same leaf. At the lower concentration of ozone, no differences in the photosynthetic signals were found, nor was there evidence for the formation of new free radicals. At the higher concentration, there was a large increase in free radical formation around the g-value of "2.000". Unfortunately, their spectra were recorded, and are presented, over a scan range of 1000 gauss, thus prohibiting precise characterization of this signal. The increase appears to be independent of light as they do not mention irradiation of the spectrometer cavity. However, the imprecise g-value leads only to speculation regarding whether this increased signal is an increased Signal I, an increased Signal II_{u+s}, or is representative of a new free radical. The authors do not attempt to explain further the signal increase (Rowlands et al. 1970).

As yet, no EPR studies have been reported in which the in vivo EPR-detectable changes in Signal I and II_{u+s} which occur during fumigation with a gaseous pollutant were investigated.

3.0 DEVELOPMENT OF METHODOLOGY

3.1 Objectives

The objectives of this study were:

1) to develop a system capable of detecting free radicals in intact plant leaves, rather than cellular or subcellular preparations or excised leaf tissue, in order to detect signal formation or decay occurring *in situ*;

2) to make the system capable of detecting changes in free-radical signals resulting from exposure of the leaf to changes in atmospheric composition;

3) through identification, if possible, of any new free radicals and, through analysis of the changes which occur in the photosynthetic free-radical signals, to increase our understanding of the mechanisms by which gaseous air pollutants injure plant cells and disrupt the photosynthetic process.

3.2 Methods

3.2.1 Spectrometer Operation

Spectrometry was carried out at room temperature in an

X-band (9GHz) spectrometer (Century Series, Model E-109 Varian Instrument Division) with an attached computer (Model 9835B, Hewlett-Packard Co.). The TM_{110} cavity was used in the studies with excised leaf pieces placed in the standard biological tissue holder (Wang Laboratories Inc.). In subsequent studies using the cellulose acetate leaf holder (described below in Section 3.2.2), the E_{231} cavity and variable temperature accessory equipment were used. Both cavities have an access port for illumination, which was provided by a collimated beam from a 400W tungsten lamp (slide projector), directed towards the cavity port (Figure 3). Optical bandpass filters (PTR Optics Ltd.) inserted in the light path were used to obtain 650 and 710nm spectral bands. Broad-band white light was obtained by omitting filters from the path of the light beam. The relevant irradiation intensities achieved are presented in Table 1.

Instrument settings were varied to obtain maximum clarity of signals. In most cases, optimum photosynthetic signals were achieved with the following settings: time constant 0.5sec; scan rate 100G/min; modulation 1.0x10 G; receiver gain $5.0x10^4$; power 10mW. For better resolution, in some cases the ordinate was subsequently increased through use of the Varian factory software package and attached computer. Where the instrument settings varied from the above they are presented with the spectra in the appropriate figures.

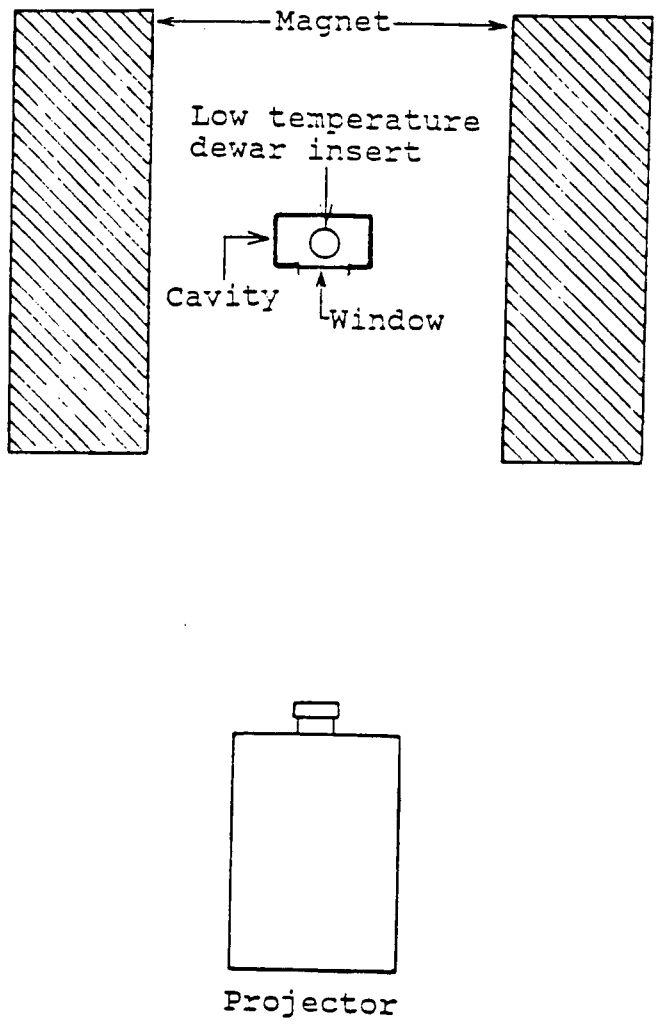

Figure 3. Cross sectional view of the equipment arrangement.

Table 1. Irradiation intensities relevant to the studies of this investigation.

Exposure condition	$\mu Em^{-2}s^{-1}$	Wm^{-2}
Within* spectrometer cavity		
650nm light	1.50	.68
710nm light	.75	.42
broad-band white light	72.00	46.00
Room light**		
within spectrometer cavity	3.60	.90
Full sunlight	$1.50x10^3$	$8.20x10^2$
In greenhouse (top of benches)	$4.65x10^2$	$2.35x10^2$
In greenhouse (below benches)	40.00	24.00

* Radiation intensities within the spectrometer cavity were based upon halving the intensities at the surface of the cavity, by the radiation port, as per manufacturer's specifications.

** These figures are only included for purposes of comparison as all spectrometry was done with the room light off, thus the only illumination was provided by the projector beam.

Kinetic traces were recorded directly onto EPR data paper. Free radical signals were recorded, using the Varian software package, onto the computer screen and then stored on tapes to provide the capability of subtracting signals recorded under different light or fumigation regimes from each other. The time required to record a signal, store it onto a tape and return to the scan module for a new scan was approximately 6 minutes. Signals which were found to decay rapidly, such as those subsequently described in Section 3.3.5, Effects of Photo-inhibition, were recorded directly onto paper, so that several signals could be recorded within a 6 minute span, thus allowing for comparison of signal size at various points in time.

Free radical g-values (see Appendix A) were determined by comparison with the known standard DPPH (1,1 diphenyl-2-picryl-hydrazyl), which has a g-value of 2.0037 (Appendix B).

3.2.2 Leaf Holder

The requirement for changing the composition of the surrounding air while the leaf was in the spectrometer cavity necessitated the development of a technique for keeping the leaf immobile in a flowing gas stream. Conventional use of the standard factory biological tissue holder is not suitable because the cover of this holder prevents gas exchange from occurring. Thus, for gaseous air pollutant studies, flux to the

leaf would be prevented. The use of leaves or leaf pieces without any supporting material is not possible because the gas flow required for in situ studies causes movement of the leaf in the cavity, which in turn prevents the establishment of resonance.

Initially, the following technique was used. The cover plate of the holder was removed and the leaf tissue was held in place with adhesive tape. This allowed ready access of the components of the gas system to one leaf surface. Since the factory quartz tissue holder (Figure 4) can be supported from the top of the cavity, this allowed atmosphere modification by passage of air through the bottom opening of the cavity via the teflon tubing used to transport nitrogen in controlled or low temperature studies. Consequently, the leaf tissue could be fumigated while it was in the cavity with the spectrometer functioning.

This initial procedure allowed in situ fumigation of excised pieces of leaves with some degree of success, but absolute holder stability was not always achieved. However, a major drawback was that the factory holder gave rise to a broad EPR signal which, while it did not interfere with detection of the relevant signals at receiver gain levels of up to 5.0×10^4, began to interfere at the higher gain settings needed for some leaf samples. While this extraneous signal could be corrected

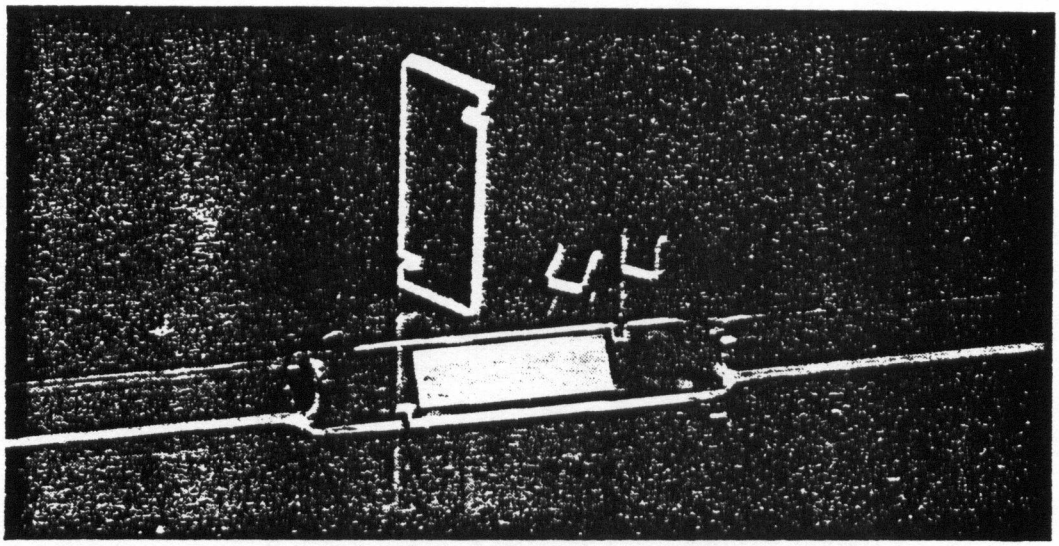

Figure 4. Conventional factory (Wang Laboratories Inc.) biological tissue holder.

for by spectral subtraction, a more suitable holder was sought. In order to maintain the leaf sample motionless in the cavity, it was decided to use the cavity dewar insert of the Varian variable temperature accessory as a guide. This insert has an internal diameter of 5mm. Its use necessitated changing to the E_{231} cavity, which is adapted for variable temperature studies (Figure 5).

Trials were conducted with holders made of several different materials, of various dimensions, as follows.

1) a glass microscope slide holder

Holders made from glass microscope slides were found to generate strong EPR signals including those attributable to Fe, Mn and Cu, and an unidentified free radical. Although these signals could be corrected by subtraction, this was an undesirable feature.

2) a microscope cover slip section

The use of this material caused much less noise than the conventional factory holder when the spectrometer was set at a high receiver gain. However, the material was very difficult to work with because of the fragility of the narrow pieces which were required to fit into the dewar insert.

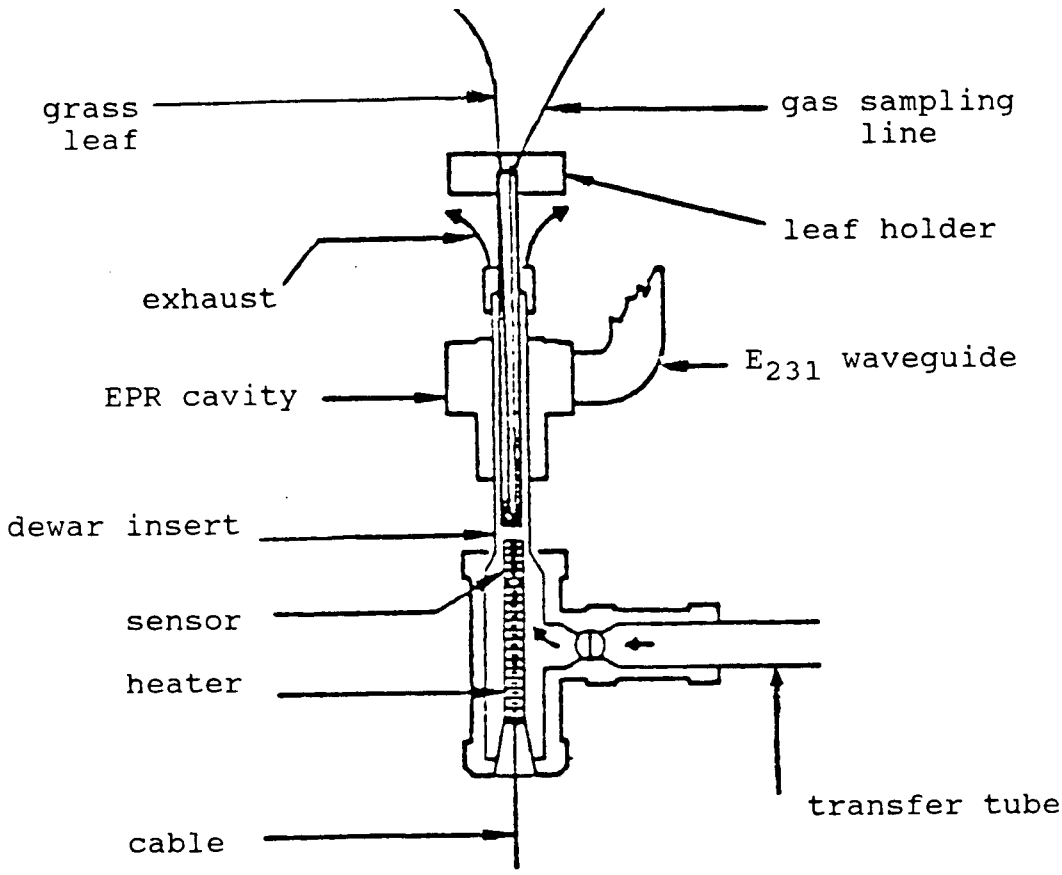

Figure 5. E_{231} cavity and dewar insert.

3) Teflon and film holders.

Various films of Teflon and other polymers were found to have stronger background signals than the microscope cover slip, but less than the microscope slide. They were usable but not optimal.

d) Cellulose acetate

Cellulose acetate film, 0.1mm thick, the material commonly used for overhead projection, was found to be ideal. This material was chosen because of its desired physical strength and robustness, and the fact that it did not reveal any EPR signals in the regions of interest. The dimensions of the 'T' shaped cellulose acetate holder finally adopted for use (Figure 6) were chosen so that the tail fitted snugly lengthwise into the cavity dewar, leaving ample room for unimpeded gas flow and for the insertion of a sample line through which gas samples could be withdrawn for analysis.

Intact leaves or excised leaf pieces (3x15mm) were attached to the tail of the holder with adhesive tape. The locations of the holder and the tape attachments are also shown in Figure 6. In all cases the abaxial surface of the leaf was placed against the holder.

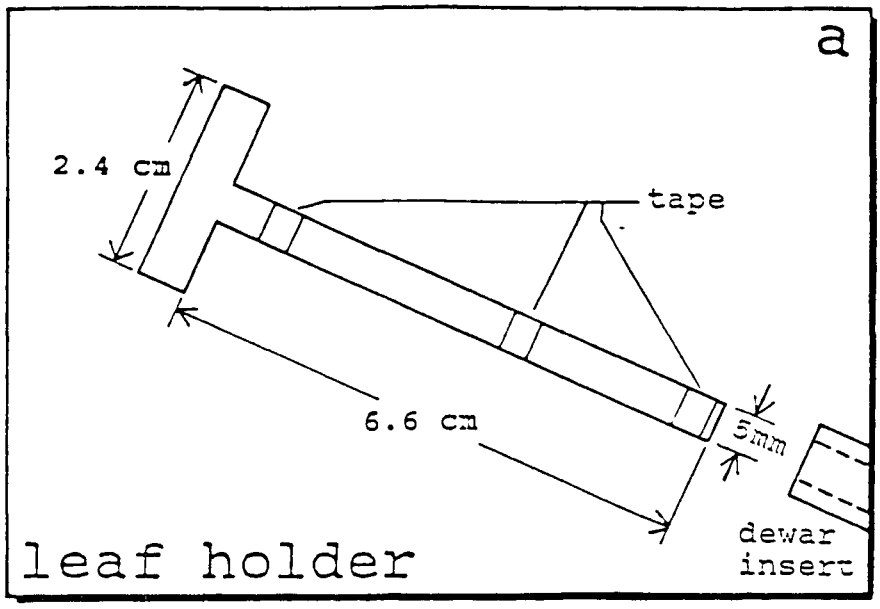

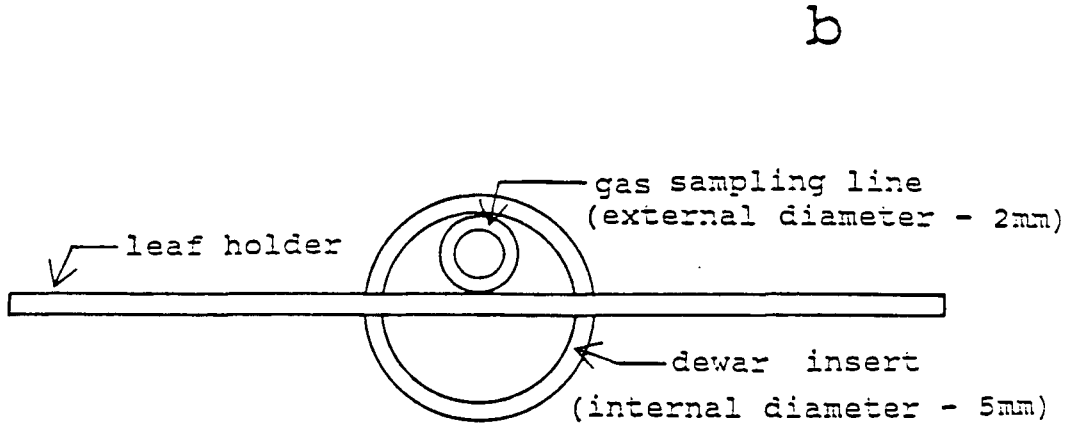

Figure 6. 'T'-shaped cellulose acetate leaf holder used in the EPR studies. a. Leaf holder; b. Cross section of holder in the variable temperature accessory dewar insert.

3.2.3 Atmosphere Modification

Since the cross-sectional area of the cavity dewar insert was 16.5mm^2, a velocity of 2 m/s was achieved with a flow rate of approximately 2 l/min, the conditions used in subsequent studies with ozone and sulphur dioxide. Preliminary results, obtained by illuminating radish leaf pieces with 710nm or 650nm light, had indicated that the magnitude of EPR Signals I and II_{u+s} obtained was unaffected by air flow rate.

Enriched levels of different gases were achieved by injecting a gas-in-air mixture into the air stream, flowing first through a mixing chamber, and then into the variable temperature accessory system via the tubing normally used to supply gases in controlled temperature studies. Ozone was generated by passing medical grade air through a charcoal filter and then through an ozone generator (Dasibi Instrument Co.). For the sulphur dioxide studies, a supply of standard 1 per cent sulphur dioxide in air was injected through a flowmeter/needle valve into the mixing chamber.

Pollutant concentrations within the dewar insert were monitored through a 2mm external diameter teflon sampling line inserted into the top of the dewar insert as shown in Figure 6. The sampling line was connected to either an ozone monitor (Model 1003AX, Dasibi Instrument Co.) or a sulphur dioxide

monitor (Model 43, Thermoelectron Corp.), depending upon the pollutant under investigation.

3.2.4 Spin Trapping

Numerous attempts were made to incorporate the free radical-specific spin traps DMPO (5,5-dimethyl-pyrroline-N-oxide) and Tiron (1,2-dihydroxybenzene-3,5-disulphonate), and the non-specific spin traps PBN (4-pyridyl-1-oxide-N-tert-butyl-nitrone), TEMPO (2,2,6,6-tetramethyl-1-piperidine-N-oxyl) and BPN (N-t-butyl-α-phenylnitrone), into plant leaves. Various approaches were tried. First, 20mM solutions of the spin traps were separately painted onto the exterior of the tissue holder. The appropriate pollutant was then released and a scan was recorded to act as a control. Subsequently the spin traps were painted onto the exterior of the leaf tissue, incorporation was attempted by uptake through the petiole for periods of 2, 24 and 48 hours and incorporation was attempted by vacuum infiltration. Spin trap concentrations were also decreased to 10mM and increased to 100mM. No spin adducts were formed, regardless of pollutant or method of attempted incorporation.

3.2.5 Plant Materials

Plants of radish (Raphanus sativus L. cv Cherry Belle), perennial ryegrass (Lolium perenne L.) and Kentucky bluegrass

(Poa pratensis L.) were grown from seed in pots containing standard greenhouse potting soil mix (85% loam; 15% peat) fertilized with 14-14-14 (Osmocote) fertilizer (Sierra Chemical Company; Milpitas, California, USA). For studies involving attached, intact leaves, the grass plants were grown in 5cm pots, which could be placed on a platform in front of the spectrometer magnet, to one side of the light beam directed at the cavity window (Figure 7).

3.3 Phenomena Associated with EPR Spectrometry of Leaf Tissue

3.3.1 Natural Variation in Photosynthetic EPR Signals in Excised Pieces of Leaves

The temporal variation in EPR signals from excised pieces of radish leaves is shown in Figures 8 and 9. Figure 8 shows the signals obtained immediately following excision and mounting in the cavity. Residual Signal II_{u+s}, attributable to a component of Photosystem II, is observed in darkness and is enhanced in 650nm light; Signal I, associated with Photosystem I, is superimposed when the signals are recorded in 710nm light. In healthy leaves, under broad-band white light of much higher intensity (Table 1), only a small Signal I is superimposed upon Signal II_{u+s} when signals are recorded immediately after excision (Figures 8a,8b). After subtraction (see Figure 2) of Signal II_{u+s} from the combined signal

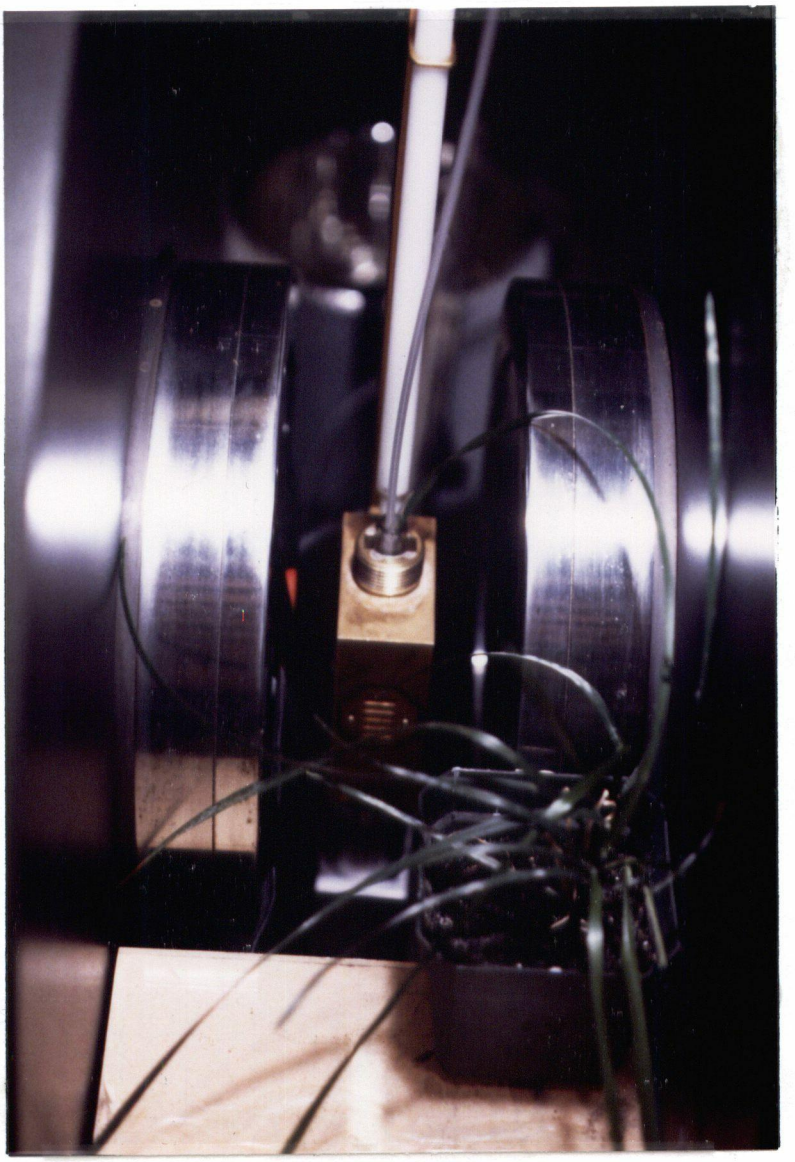

Figure 7. Equipment setup for studies with attached, intact grass leaves.

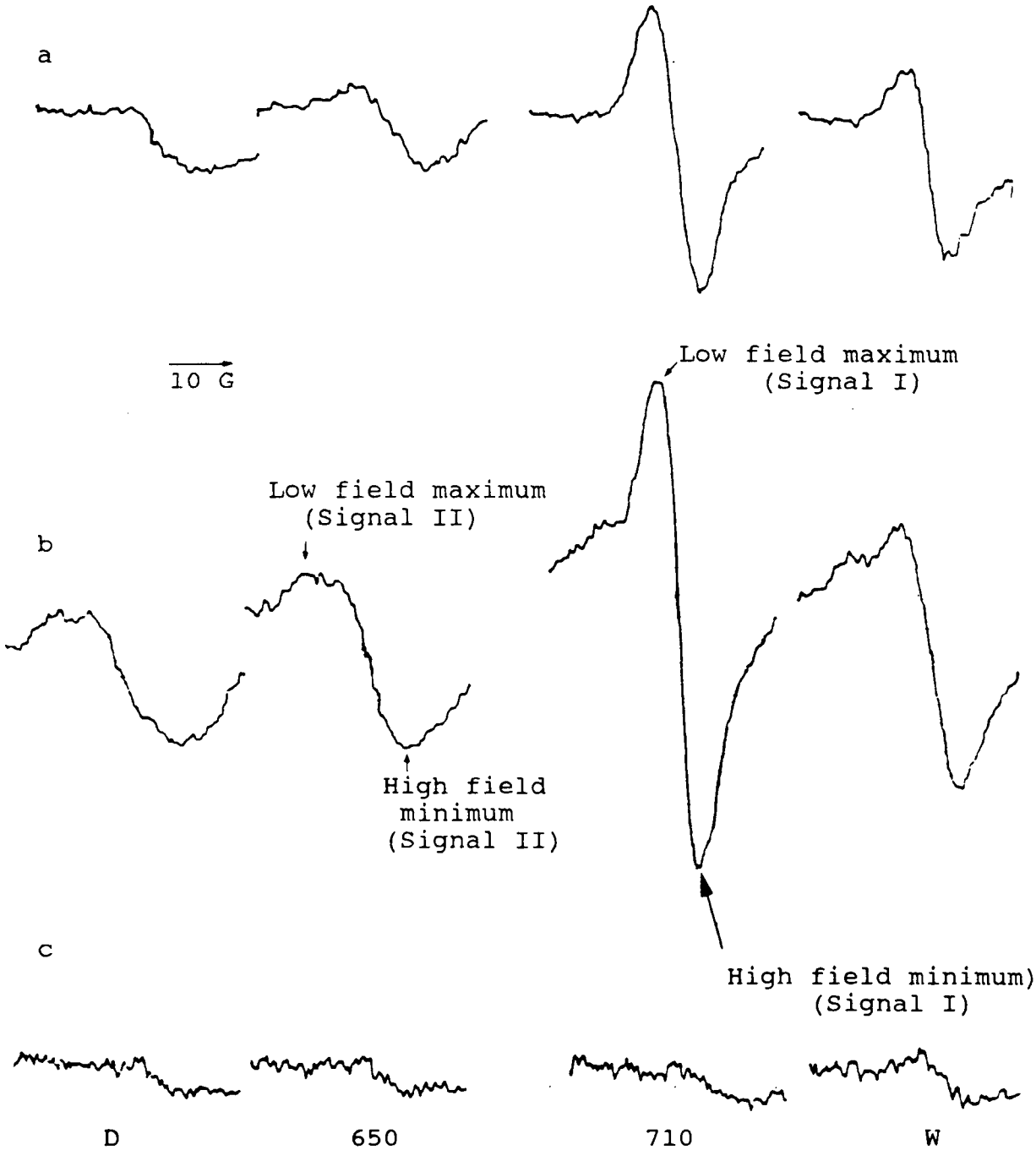

Figure 8. EPR signals obtained from healthy radish leaf pieces in different light regimes, recorded immediately after excision of the pieces. a. 4-week old pale green leaf; b. 6-week old dark green leaf; c. chlorotic, turgid leaf. Recorded in: D = dark; 650 = 650nm light; 710 = 710nnm light; W = broad-band white light.

obtained in 710nm light, Signal I was found to have a peak-to-peak width of 8-9 gauss and a g-value of 2.0025. Signal II_{u+s} was found to have a peak-to-peak width of approximately 19 gauss and a g-value of 2.0046. These characteristics are similar to those reported in the relevant literature (Appendix B).

Pieces of 6-week old radish leaves which were dark green typically yielded larger signals in semi-darkness, under 650nm light, under 710nm light and under broad-band white light (Figure 8a) than younger, pale green leaves (4 weeks old) (Figure 8b). For each type of leaf, the spectra were recorded in the sequence indicated, on the same piece of leaf, after exposure to 3 minutes of the appropriate light regime. The shade of greenness of the leaf was found to be a more important determinant of signal intensity than leaf age. The dependence of the signals upon the presence of chlorophyll was indicated by the lack of signals from completely chlorotic, but still fully turgid older leaves, such as those shown in Figure 8c. The dependence of the signals on functioning chloroplasts was verified using variegated Coleus sp. leaves. Irradiation of pieces taken from the green parts of such leaves revealed similar signals to those obtained from green radish leaves, while illumination of pieces taken from chlorophyll-free pink or white areas resulted in traces comparable to those obtained from the chlorotic radish leaves (Coleus sp. spectra not shown).

After two hours within the cavity, without illumination from the projector beam, the signals in Figure 9 were recorded for the same leaf pieces as those used for Figure 8. All signals can be seen to have changed, with the largest change occurring in the dark green, 6-week old leaves illuminated with 650nm or broad-band white light (Figure 9b). These changes in the signals were not directly attributable to desiccation, as trials with detached leaf pieces maintained in close to 100 per cent relative humidity showed comparable changes in the signals with time (spectra not shown).

The major part of the changes in the signals observed under any light treatment occurred in the second hour after detachment from the plant. Similar changes in signals were also observed in detached leaf pieces of perennial ryegrass and Kentucky bluegrass (spectra not shown).

3.3.2 Variability in Photosynthetic EPR Signals in Whole, Attached Grass Leaves

In contrast to the situation described for excised leaf pieces, when healthy, intact, attached grass leaves were maintained in the spectrometer cavity, no changes in the signals occurred for at least 72 hours. In these trials, using both perennial ryegrass and Kentucky bluegrass leaves, the test leaf remained mounted in the cavity for 5 days. The plants were

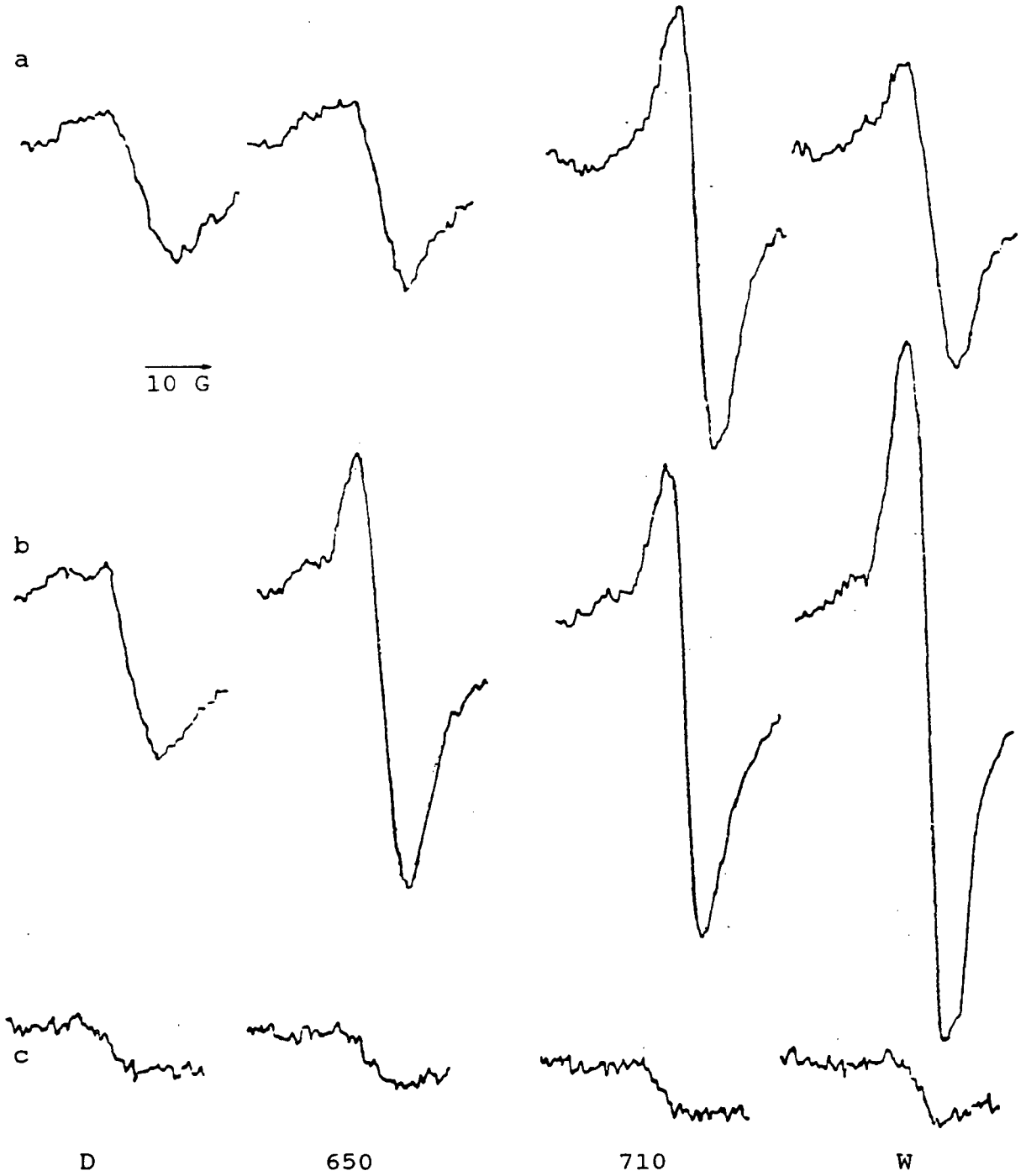

Figure 9. EPR signals obtained from the previously healthy radish leaf pieces depicted in Figure 8, in different light regimes, recorded 2 hours after excision, with the pieces held in darkness in the cavity during the interval. a. 4-week old pale green leaf; b. 6-week old dark green leaf; c. chlorotic, turgid leaf. Recorded in: D = dark; 650 = 650nm light; c = 710nm light; W = broad-band white light.

watered daily and were exposed to 14hr room light and 10hr darkness. During the intervals between the recording of the signals only indirect room light entered the cavity during the photoperiod and the leaf was illuminated by the projector beam only during signal measurement. EPR signals were recorded after the plants had been held in room light for 2 hours each day. The spectrometer was turned off after each day's measurements.

After five days in the spectrometer cavity, with the magnetic field off, several changes were observed to have occurred in the EPR signals. A representative series of spectra obtained with Kentucky bluegrass leaves is shown in Figure 10. The changes were: 1) the near elimination of the multiple band Mn^{++} signal typically associated with healthy bluegrass leaves (Figure 10a,b); 2) the concomitant elimination of typical Signal II_{u+s} (Figure 10a); and 3) the appearance of a new signal under broad-band white light (Figure 10b,d). These changes only occurred in the part of the specific leaf maintained in the cavity; signals from other parts of that leaf or from other leaves of the same plant, which were not in the cavity for the five day period, were not affected in this interval as shown in Figure 10c. The white light-induced signal observed after 5 days is shown more clearly in Figure 10d, following subtraction of the original signals. This signal, which has a g-value of 2.0046 and a peak-to-peak width of approximately 10 gauss, is clearly different from Signal I, which has a g-value of 2.0025

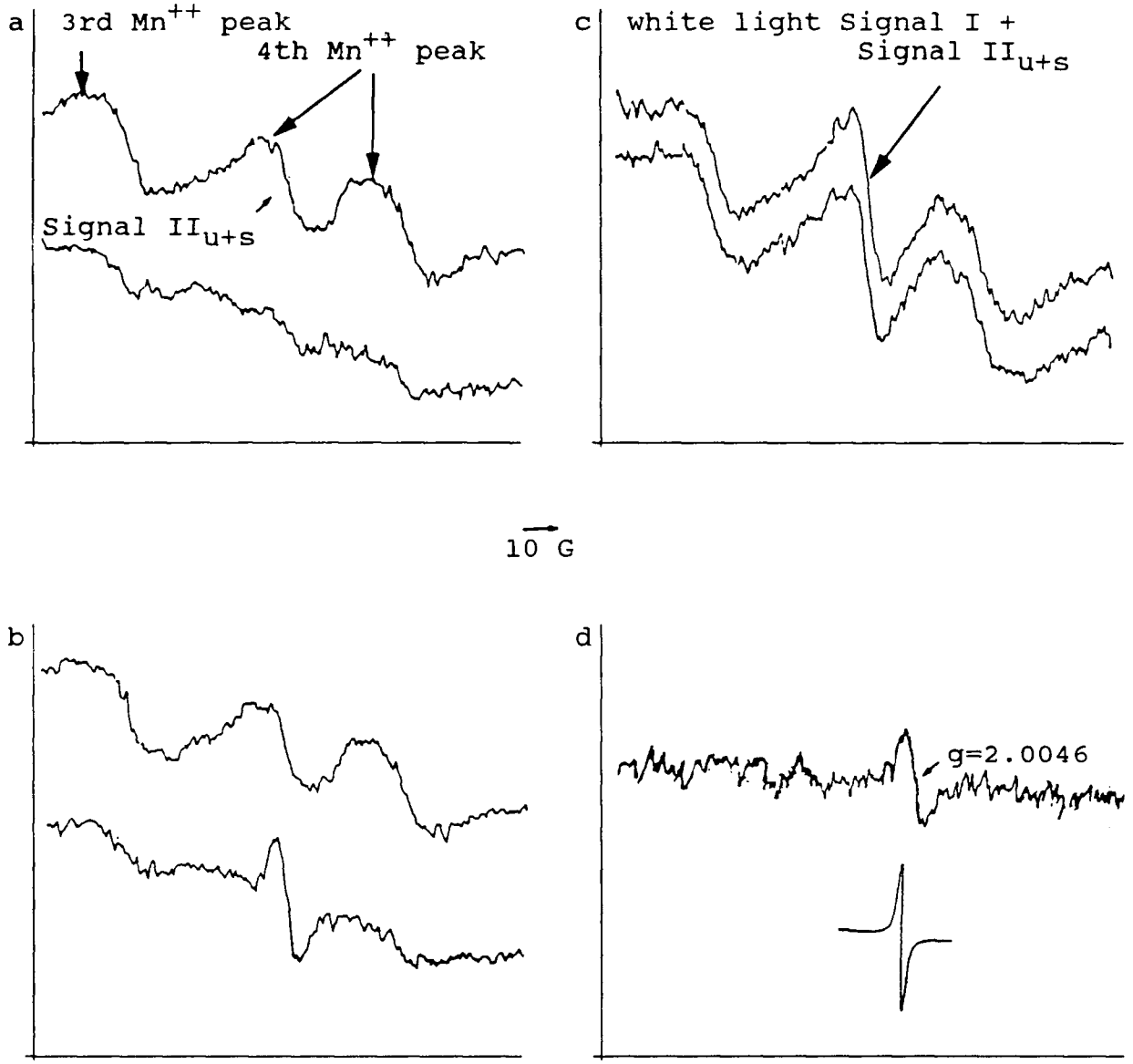

Figure 10. Changes in the Mn, dark, and white-light induced signals in intact, attached Kentucky bluegrass leaves after 5 days in the spectrometer. a. Top - dark signal at start; Bottom - dark signal after leaf taped to holder within cavity for 5 days; b. Top - white light signal at start; Bottom - white light signal after leaf taped to holder within cavity for 5 days; c. Top - white light signal at start from a different leaf on same plant as leaf used for Figures 10a and 10b; Bottom - white light signal from leaf used for 10c-Top after 5 days with the plant on the spectrometer platform but the leaf not taped to the holder; d. Top - (10b Bottom - 10b Top) - (10a Bottom - 10a Top); Bottom - DPPH (g=2.0037).

and a width of 7.5-9 gauss. The leaf-to-leaf differences which occur on the same plant are shown by the comparison of the upper spectra in Figures 10b and 10c, which were obtained in white light from different leaves of the same plant.

3.3.3 Possibilities and Limitations of Kinetic Studies

It is possible to follow the rise and decay of free-radical signals over time, by locking the spectrometer onto the low or high field peak of the appropriate signal. Prior to kinetic tracking it is necessary to first record the signal in order to ascertain its precise location in the magnetic field. Once its location in the magnetic field has been established, subsequent trials with different leaf pieces can be done to follow the kinetics of signal formation and decay. For example, the trace depicted in Figure 11 shows the typical changes which occur in Signal I in healthy radish leaf pieces exposed in sequence to the different light regimes. To obtain the data the spectrometer was locked onto the low field maximum (see Figure 8). The trace shows the appearance of a large Signal I upon irradiation with 710nm light, minimal occurrence of this signal on exposure to 650nm or broad-band white light, and the rapid decay of the signal when the quality of light is changed or illumination ceases. These observations are similar to those of Blumenfeld et al. (1974), who worked with pieces of leaves from several perennial species.

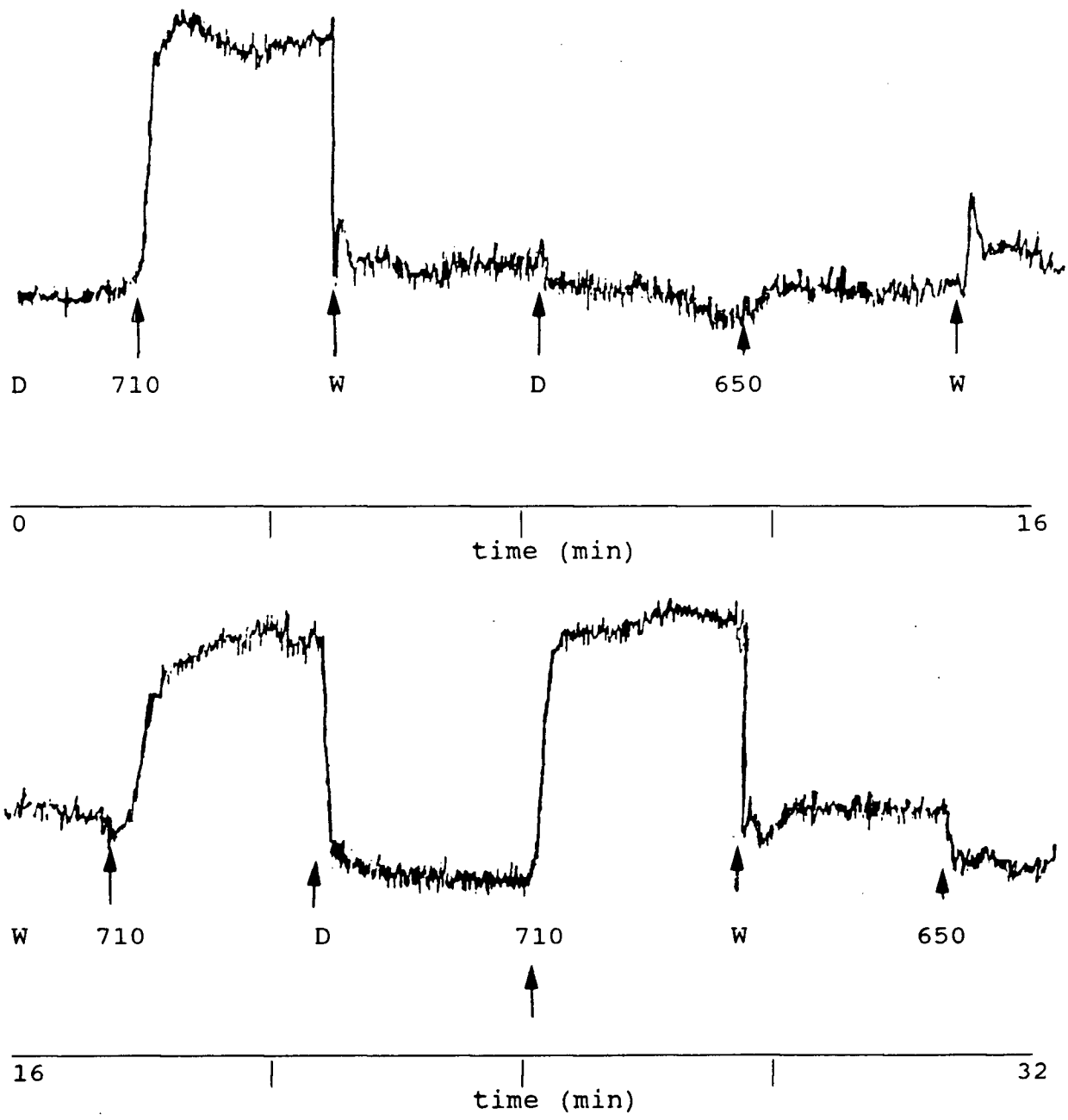

Figure 11. Kinetics of Signal I formation and decay in unfumigated radish leaf pieces with different light treatments. Arrows (⬆) indicate times at which light was changed. D = dark, 650 = 650nm light; 710 = 710nm light; W = broad-band white light.

In contrast, Figure 12 shows the changes in the low field maximum of Signal I during the same sequence of light regimes, which occur in pieces of radish leaves previously fumigated for 10 minutes with approximately 400ppm SO_2, a massive dose of this gaseous air pollutant. Again, in darkness, Signal I is barely detectable, and is markedly increased upon irradiation with 710nm light, although the rate of increase is less than in untreated tissue (Figure 11). However, following SO_2 treatment, signals of approximately comparable size result from irradiation with either 650nm or 710nm light and a still larger Signal I results from irradiation with the broad-band white light. These data, and other changes caused by exposure to SO_2 are discussed in detail in Section 5.0, but it is apparent that the massive influx of SO_2 into the leaf has affected the normal photosynthetic electron transfer process found in healthy leaves.

In radish leaves, using excised leaf tissue, it is thus possible to follow the EPR signals induced by treatment with different light qualities, and to determine how these signals may be influenced by gas treatment, within the limited 60 minute period following excision, before the changes induced by excision begin to be appreciable.

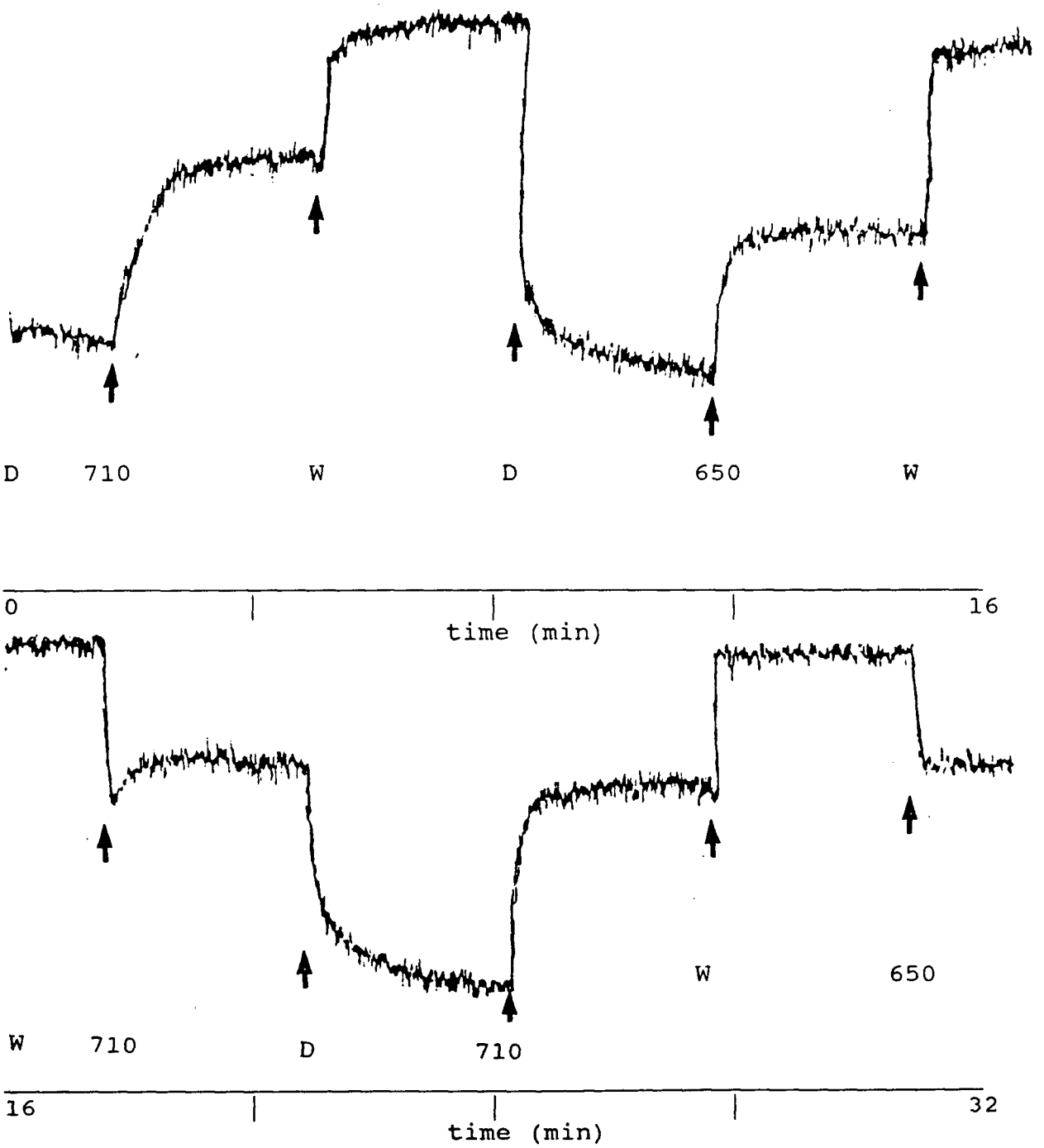

Figure 12. Kinetics of Signal I formation and decay in different light treatments in radish leaf pieces previously fumigated with approximately 400ppm SO_2 for 10 minutes. Arrows (▲) indicate times at which light was changed. D = dark, 650 = 650nm light; 710 = 710nm light; W = broad-band white light.

However, plant leaves are capable of adaptation (Blumenfeld et al. 1974; Ruuge and Tihkonov, 1972; Tihkonov and Ruuge 1975a, 1975b; Andreyeva et al. 1979). Prolonged exposure to either darkness or intense broad-band white light causes a delay in the formation of Signal I when the leaf is subsequently exposed to 710nm light. Several hours of darkness are required to delay its appearance, but as little as 3 minutes exposure to intense white light is sufficient to retard its formation upon exposure to 710nm light, as shown in the lower part of the trace in Figure 11. Thus, if one wishes to record the signals after a lengthy kinetic trace in either darkness or broad-band white light, the 710nm light-induced Signal I will not be formed immediately upon illumination with 710nm light. This can be of importance when the technique of signal subtraction is used to clarify the changes in spectra resulting from different treatments of the leaf as discussed below in Section 3.3.4. The period of time required to counter the effects of darkness or broad-band white light increases with increasing time of exposure to these light regimes (data not presented) and varies somewhat from leaf to leaf. In order to minimize this problem in long-term studies it is therefore necessary to illuminate the leaf with light of the appropriate wavelength (710nm or 650nm) for several minutes prior to recording the EPR spectra.

A more severe problem in attempting to track the photosynthetic Signals I and II_{u+s} occurs when the signals of

interest are superimposed upon other signals of comparable or larger magnitude, if these, too, change with experimental treatment. In leaves of many species, EPR spectrometry reveals the broad Fe^{++} and six-peak Mn^{++} signals discussed earlier in Section 2.4. Signals I and II_{u+s}, and all free-radical signals, are underlain first by the Fe^{++} signal and also by the fourth peak from the low field end of the Mn^{++} signal. Thus, if these signals change as a result of any treatment, the apparent rise or decay of the photosynthetic or other free-radical signals monitored by the kinetic scan may be completely inaccurate, especially in tissues in which the iron and manganese signals are much larger than the free-radical signals of interest.

Unfortunately, this appears to be the case for many, if not most, plant species. Figures 13-17 indicate the EPR spectra obtained from pieces of the leaves of five species selected arbitrarily. These spectra were recorded over 5000 gauss with the leaf pieces held in darkness in the cavity. In order to avoid truncating the spectra, the spectrometer receiver gain was halved to 2.5x10000. The six-peak Mn^{++} signal and the sloping Fe^{++} signal which underlies it are present in each spectrum and their intensities vary from species to species. At this lowered receiver gain, Signal II_{u+s} is not apparent in the spectra from the pine needle (Figure 13) and maple leaf (Figure 14), and is only present as a very small perturbation in the

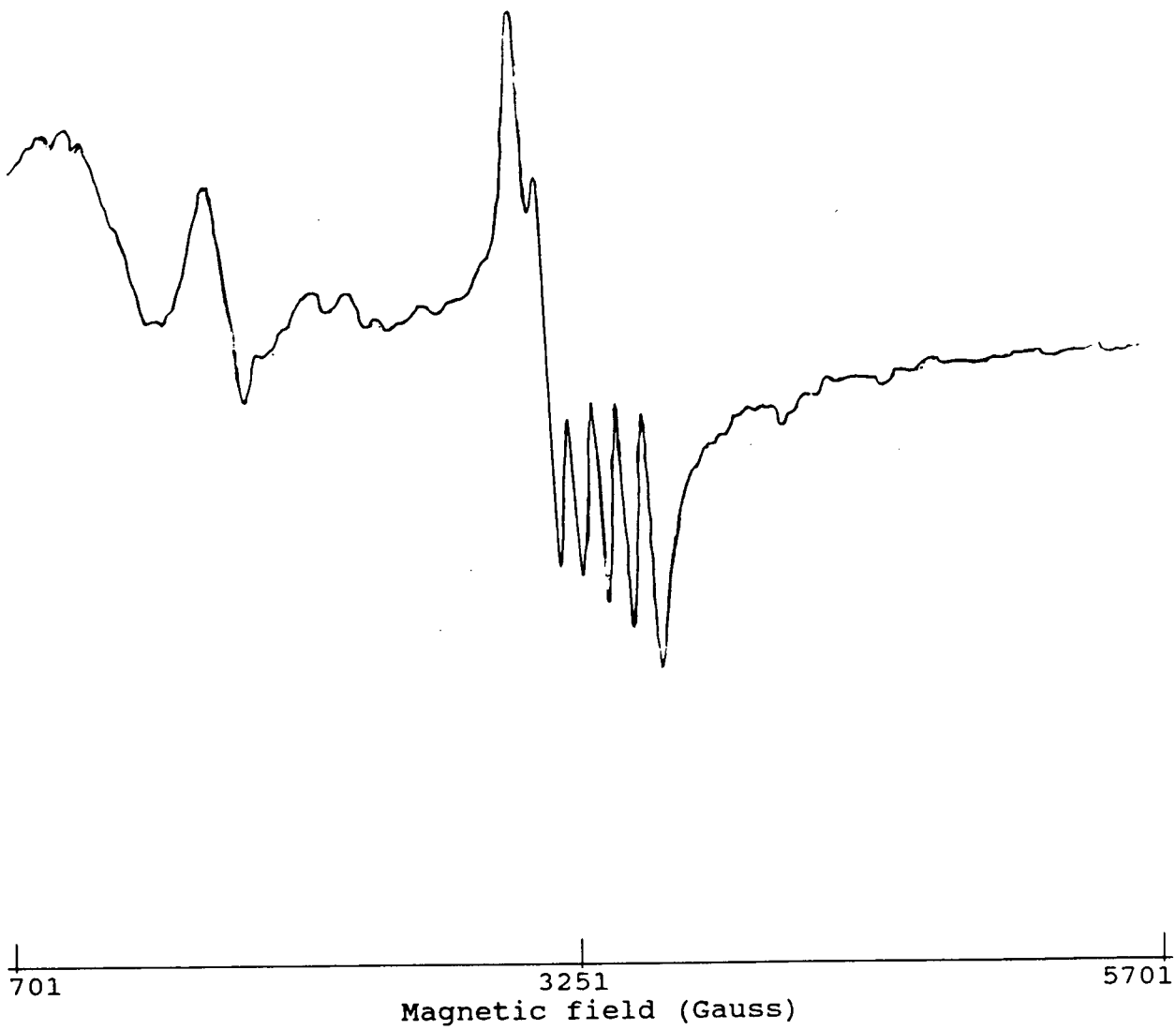

Figure 13. EPR spectrum from a detached pine needle. Recorded in darkness. Receiver gain - 2.5 x 10000; Microwave frequency - 9.188

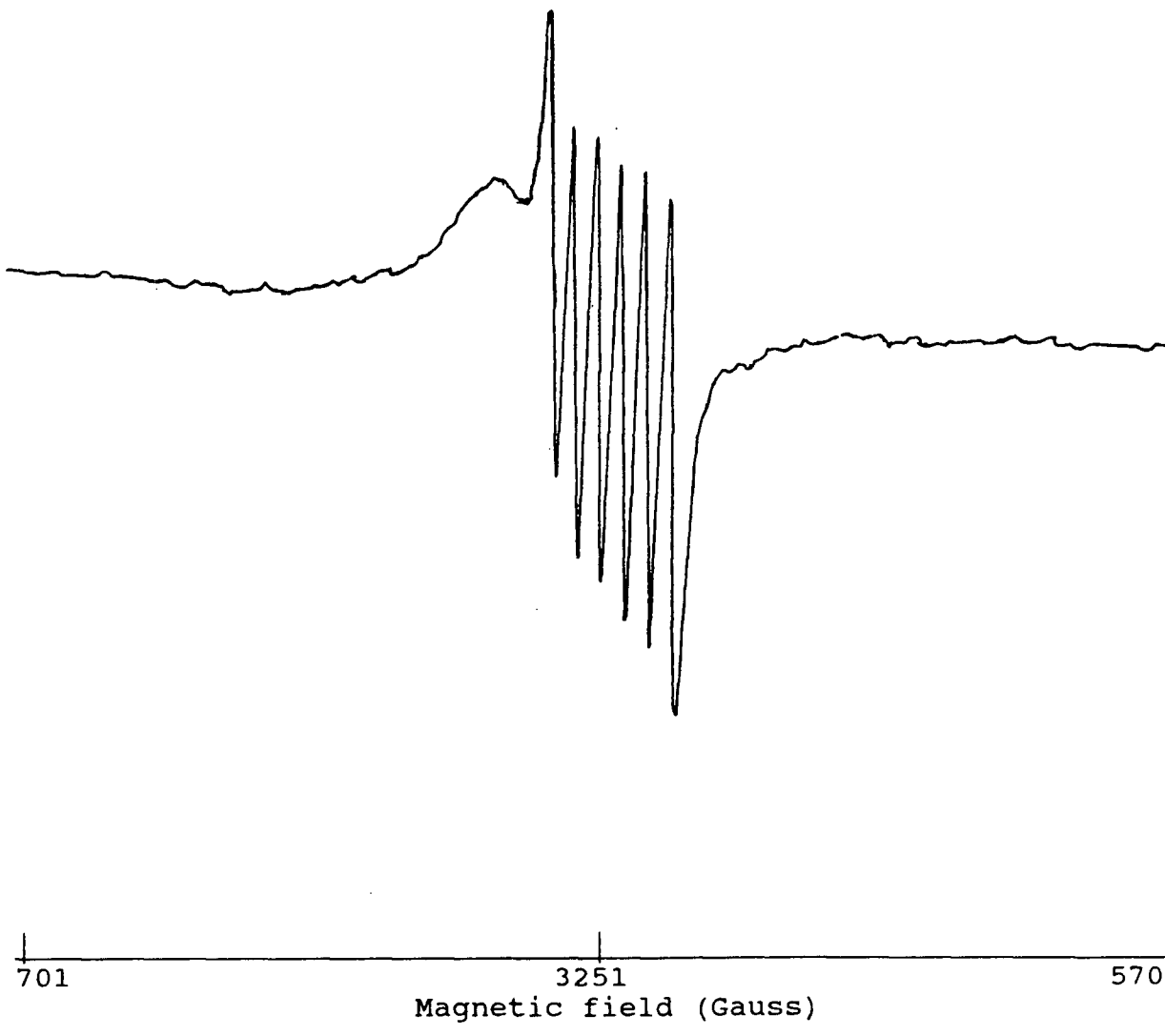

Figure 14. EPR spectrum from an excised maple leaf piece. Recorded in darkness. Receiver gain - 2.5 x 10000; Microwave frequency - 9.188

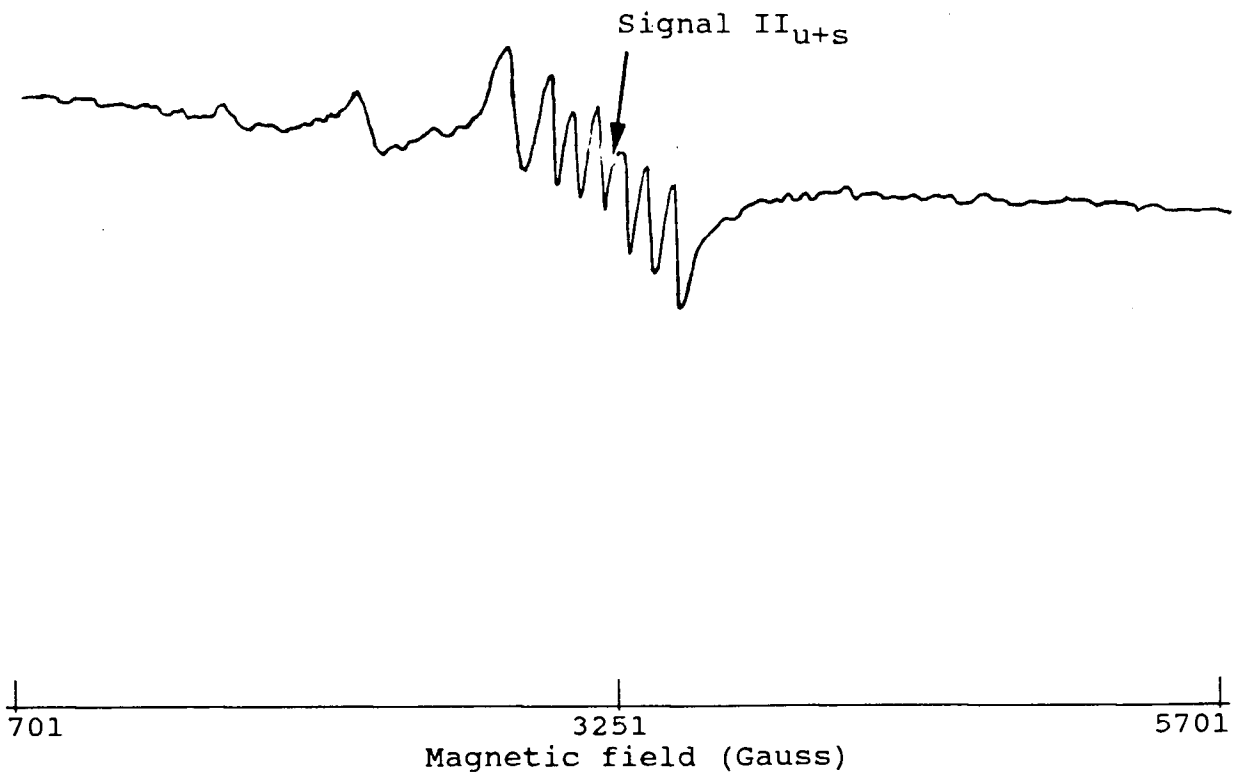

Figure 15. EPR spectrum from an excised oak leaf piece. Recorded in darkness. Receiver gain - 2.5 x 10000; Microwave frequency - 9.188.

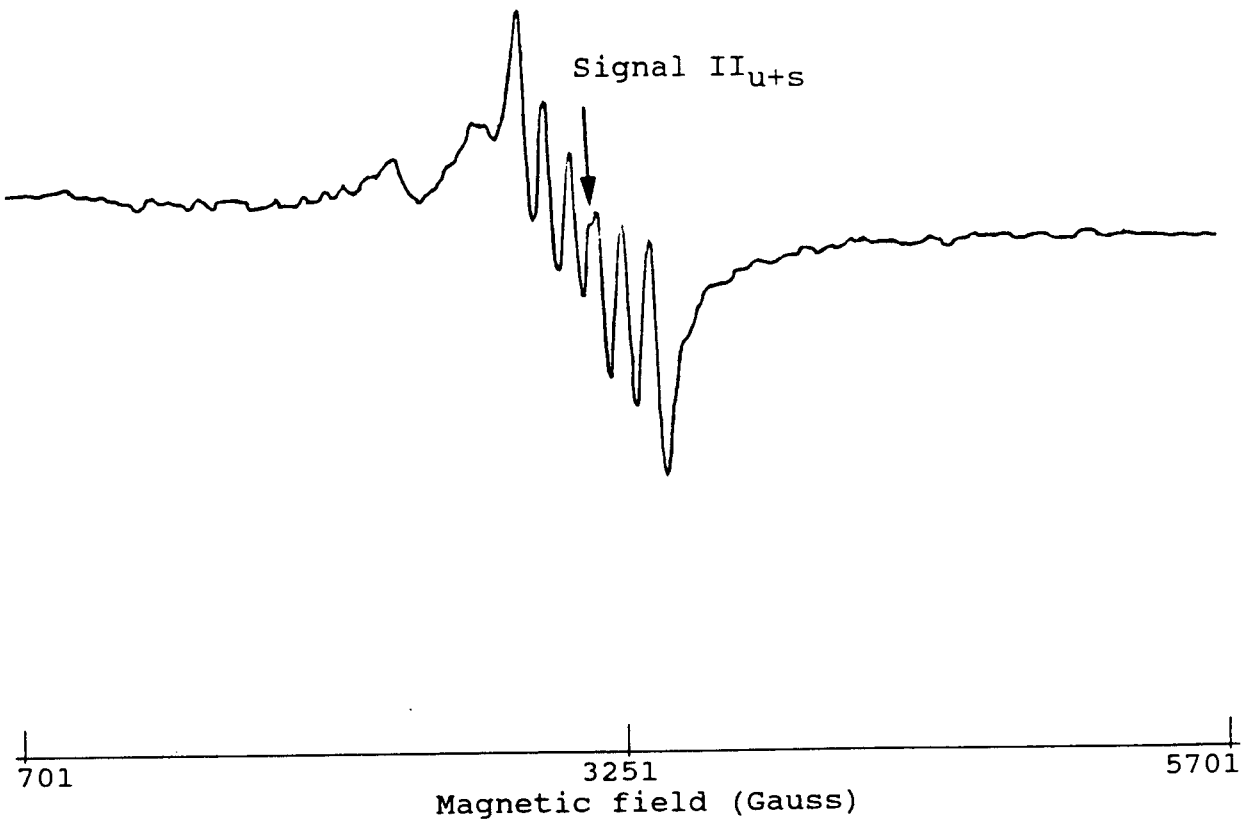

Figure 16. EPR spectrum from an excised ivy leaf piece. Recorded in darkness. Receiver gain - 2.5 x 10000; Microwave frequency - 9.188

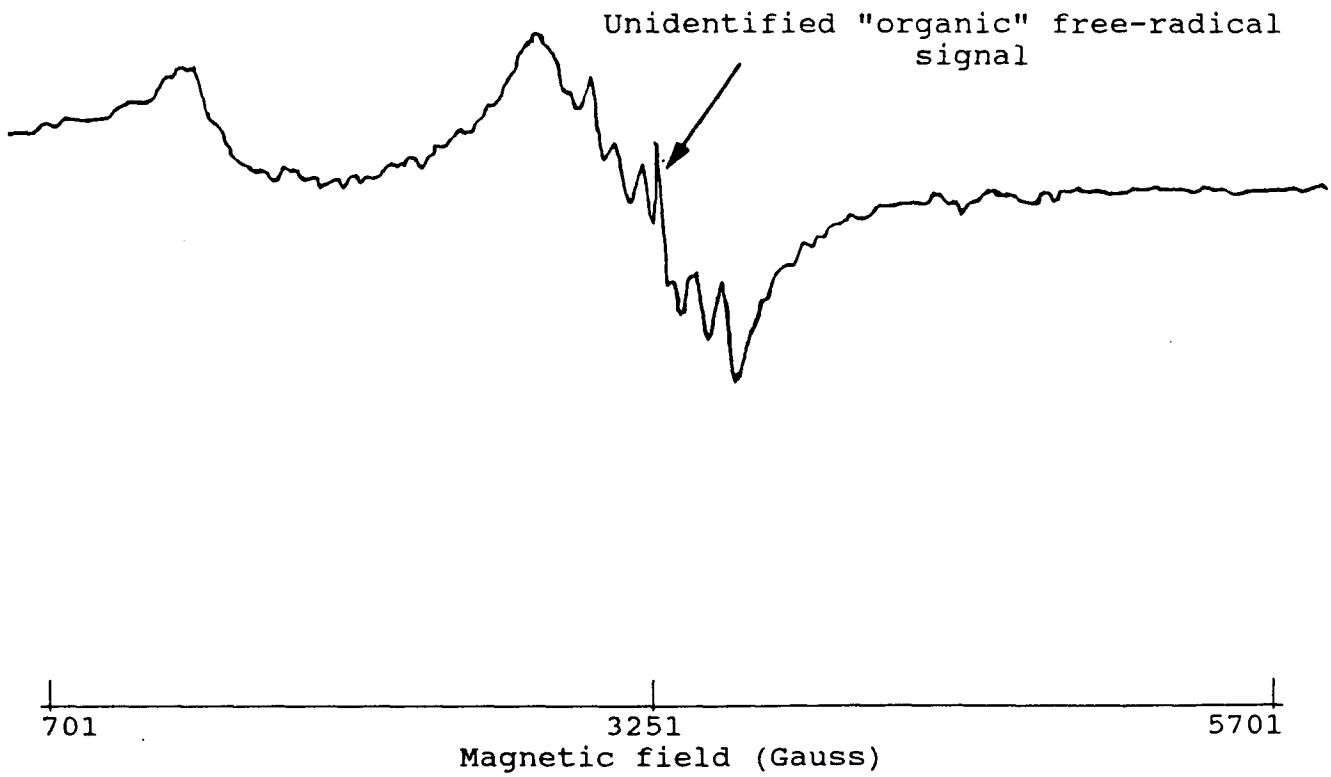

Figure 17. EPR spectrum from an excised cherry leaf piece. Recorded in darkness. Receiver gain - 2.5 x 10000; Microwave frequency - 9.188

fourth Mn^{++} peak in the spectra from the oak (Figure 15) and ivy (Figure 16) leaves. The spectra from the pine needle (Figure 13) and cherry leaf (Figure 17) show additional signals riding on the second and fourth Mn^{++} peak, respectively. At this scale it is impossible to discern the exact g-values of these signals. However, the cherry leaf signal with a g-value close to 2.000 cannot be Signal I, which requires light for induction, and is possibly the unidentified organic free radical signal (Mishra et al. 1971; Priestley et al. 1980) generally associated with aged plant material.

As is readily apparent, the manganese signals and the broad sloping iron signal upon which the manganese signals themselves ride are much larger than Signal II_{u+s}. Thus, any changes in these signals will distort the kinetic tracking of Signal II_{u+s}.

Although the use of grass leaves attached to the plant offers the advantage of providing stable photosynthetic EPR spectra over a much longer time period than excised leaf pieces, all of the grasses surveyed revealed distinct Fe^{++} and Mn^{++} spectra, as shown typically by the Kentucky bluegrass spectra in Figure 10. Just as these signals can change over time with prolonged residence in the chamber, so too can they be modified as a result of pollutant gas treatment. Such changes in an attached perennial ryegrass leaf treated with ozone are shown in

Figure 18. The spectrum in Figure 18a, recorded over 1600 gauss, under broad-band white light, shows typical composite Fe^{++}/Mn^{++} signals prior to fumigation with ozone. After 1 hour of fumigation with 1ppm ozone in the cavity, both the Mn^{++} and Fe^{++} signals have increased slightly (Figure 18b) but after 14 hours of exposure to the ozone and white light, the Mn^{++} signal has greatly diminished while the Fe^{++} signal has greatly increased (Figure 18c), as evidenced by the increase in overall slope in the centre of the spectrum. The imminent demise of the fumigated part of the leaf is indicated by the large free-radical signal found near the 2.000 g-value. However, even the tracking of this large free-radical signal would be confounded by the shifts in the underlying Mn^{++} and Fe^{++} signals.

These complications therefore limit the tracking of the changes in the photosynthetic free-radical signals induced by gaseous air pollutants to species such as radish, which have very minimal Mn^{++} and Fe^{++} EPR signals in relation to the size of their photosynthetic free-radical signals. In particular, it is unfortunate that such tracking does not appear to be usable with any of the grass species investigated, in spite of the attractiveness that they can be studied intact without the appearance of the artificial aging effects discussed earlier, and are thus potentially more useful for assessing the longer-term effects of low concentrations of gaseous pollutants.

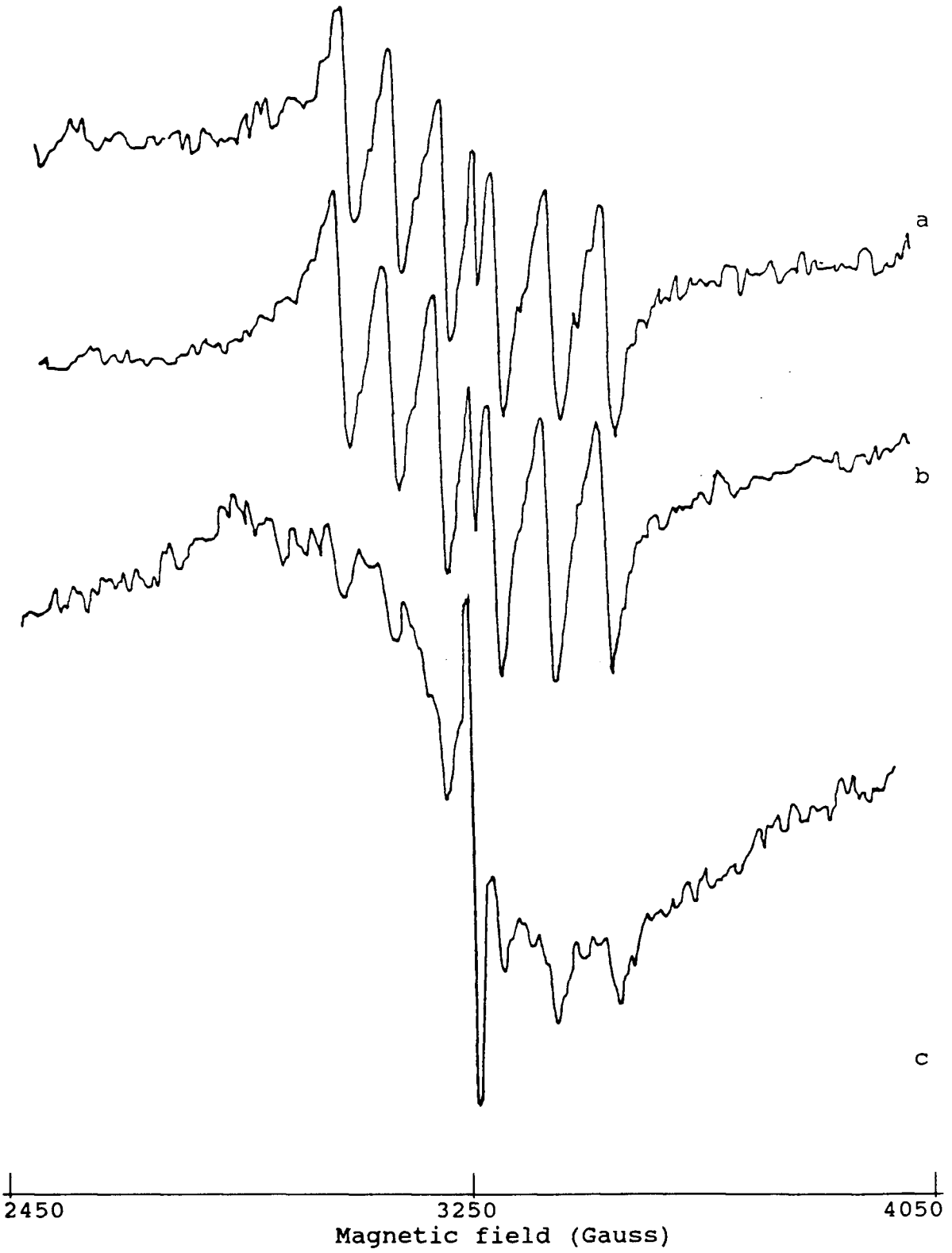

Figure 18. White light-induced spectra from an intact, attached perennial ryegrass leaf. Receiver gain - 10.0x10000; Microwave frequency - 9.184. a. prior to fumigation; b. after 30 minutes of 1ppm ozone; c. after 14 hours of 1ppm ozone. The leaf was maintained in white light continuously.

The only alternative appears to be to record the absolute signals with treated and control leaves under different light regimes at appropriate times, and then compare the specific spectra, for example by measuring peak-to-peak heights, or by signal subtractions conducted to adjust for these other signal changes, as described below.

3.3.4 Signal Subtraction

The Hewlett-Packard computer attached to the spectrometer permits the subtraction of spectra from each other. Control spectra can be stored on tape and subsequently subtracted from spectra obtained after treatment. This allows for the characterization of small, new free radicals which overlap established free radicals. A simple example of results attainable with this technique has been presented in Figure 2. The time required to record the signal, store it on tape and return to the scan module to record the next signal is 6 minutes.

3.3.4.1. A New Light-induced Free Radical Signal

When attached perennial ryegrass leaves were maintained in charcoal-filtered air in 710nm light in the spectrometer cavity for 7 hours, a downfield shift in the peak of the signal induced by 710nm light became apparent, with a concomitant shift in

g-value. This suggested the formation of a new signal with a higher g-value than Signal I. To clarify this new signal, the spectrum obtained in 710nm light at the start of the experiment was subtracted from the 710nm light-induced spectrum after 7 hours.

This subtraction revealed the small free-radical signal (Signal N_{710}) shown in Figure 19b. Subsequent trials with both attached Kentucky bluegrass and attached perennial ryegrass leaves disclosed that Signal N_{710} was formed after prolonged exposure to 710nm light. Depending upon the leaf, the signal appeared anywhere from 30 to 60 minutes after the onset of illumination, regardless of whether or not air was passing through the cavity. Signal N_{710}, which is revealed by subtraction of the light-induced signal at the onset of illumination, from the light-induced signal after 30 to 60 minutes of illumination, has a peak-to-peak width of 8.5 gauss, a g-value of approximately 2.0054 and is induced by 710nm light (Table 2). It reaches a maximum within 120 minutes of illumination. The maximum height of Signal N_{710} is approximately 45 per cent of the 710nm light-induced Signal I. It is clearly not an increase in Signal I as it differs in g-value (Signal I = 2.0025). The identity of Signal N_{710} is unknown; the g-value is identical to that of the early electron acceptor, a_1, described by Gast et al. (1983), but the line width is less (Appendix B).

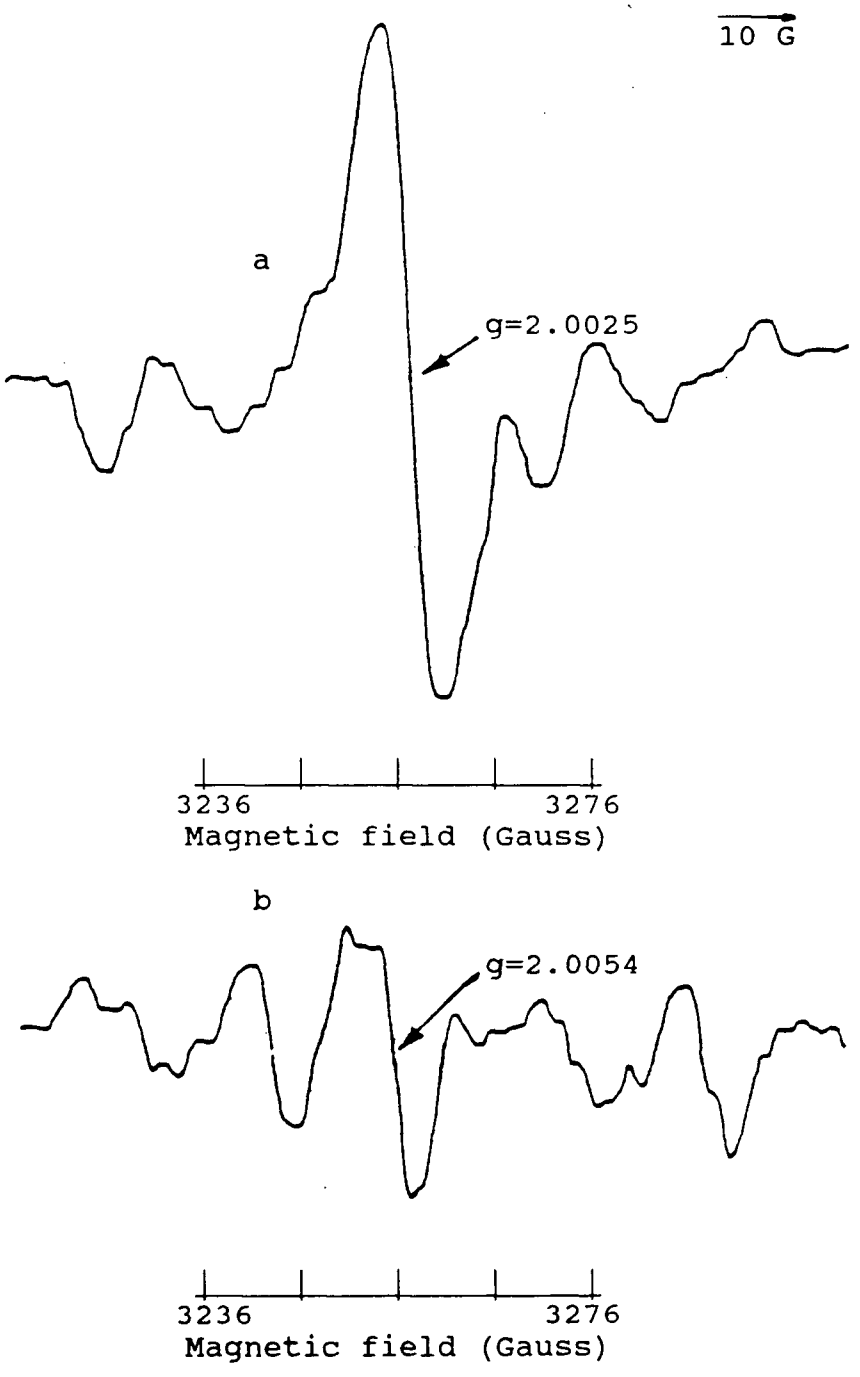

Figure 19. Comparison of original Signal I and Signal N_{710} in attached, intact Kentucky bluegrass leaves. a. Original Signal I (710nm light-induced signal - dark signal); b. Signal N_{710} after leaf held in 710nm light for 1 hour ((710nm light signal after 1 hour - dark signal after 1 hour) - original Signal I). Microwave frequency - 9.190.

Table 2. Relationship of appearance of the uncharacterized EPR free-radical signal (Signal N_{710}) in intact ryegrass leaves with time of exposure to 710nm light.

	Time of exposure (min)				
	30	120	240	320	420
New 710nm light-induced signal (Signal N_{710})**					
Peak-to-peak width	8	8.5	8.5	8.5	8.5
Height*	29	42	37	39	43
g-value	2.0055	2.0055	2.0054	2.0054	2.0054

*Relative units

**Obtained by subtraction of the original 710nm light-induced signal from the 710nm light-induced signal at the indicated times. In each case, the true light-induced signals were obtained by prior subtraction of the appropriate dark signals.

3.3.4.2 Oxygen Effects on Signals I and II_{u+s}

Changes in the oxygen content of the air passing over the leaf tissue supported in the cavity have a profound influence on the photosynthetic Signals I and II_{u+s}. Figure 20 depicts the combined signal (Signal II_{u+s} + Signal I) when Kentucky

bluegrass leaves are illuminated with 710nm light. Figure 20a shows the typical signal when air is passed through the cavity at the standard rate of 2 l/min. Figure 20b shows the decreased signal recorded after the leaf was held in 710nm light for 30 minutes during which O_2 was removed by flushing the system with N_2. Figure 20c shows the absence of Signal I induction by 710nm light following leaf exposure to 4 minutes each of darkness and white light. This signal was recorded after the leaf had been reexposed to 4 minutes of 710nm light in order to eliminate any possible light adaptation effects caused by the exposure to white light (see Section 3.3.3). Figure 20d shows the signal obtained after an additional hour in N_2 with the leaf held in 710nm light for that time, and suggests a composite reduced Signal II_{u+s} and reduced Signal I.

Figure 21 shows the signals obtained with no direct cavity illumination when the leaf was exposed to air (Figure 21a), and after 36 and 96 minutes exposure to N_2 (Figures 21b and 21c), and suggests a progressive decrease in Signal II_{u+s}. Figure 22 shows the signals obtained when the leaf was illuminated with broad-band white light during the same sequence of atmospheric conditions and suggests a decrease in both Signal II_{u+s} and the minimal white light-induced Signal I.

In order to reveal the changes in Signal I more clearly, the dark signals recorded at the appropriate times were subtracted

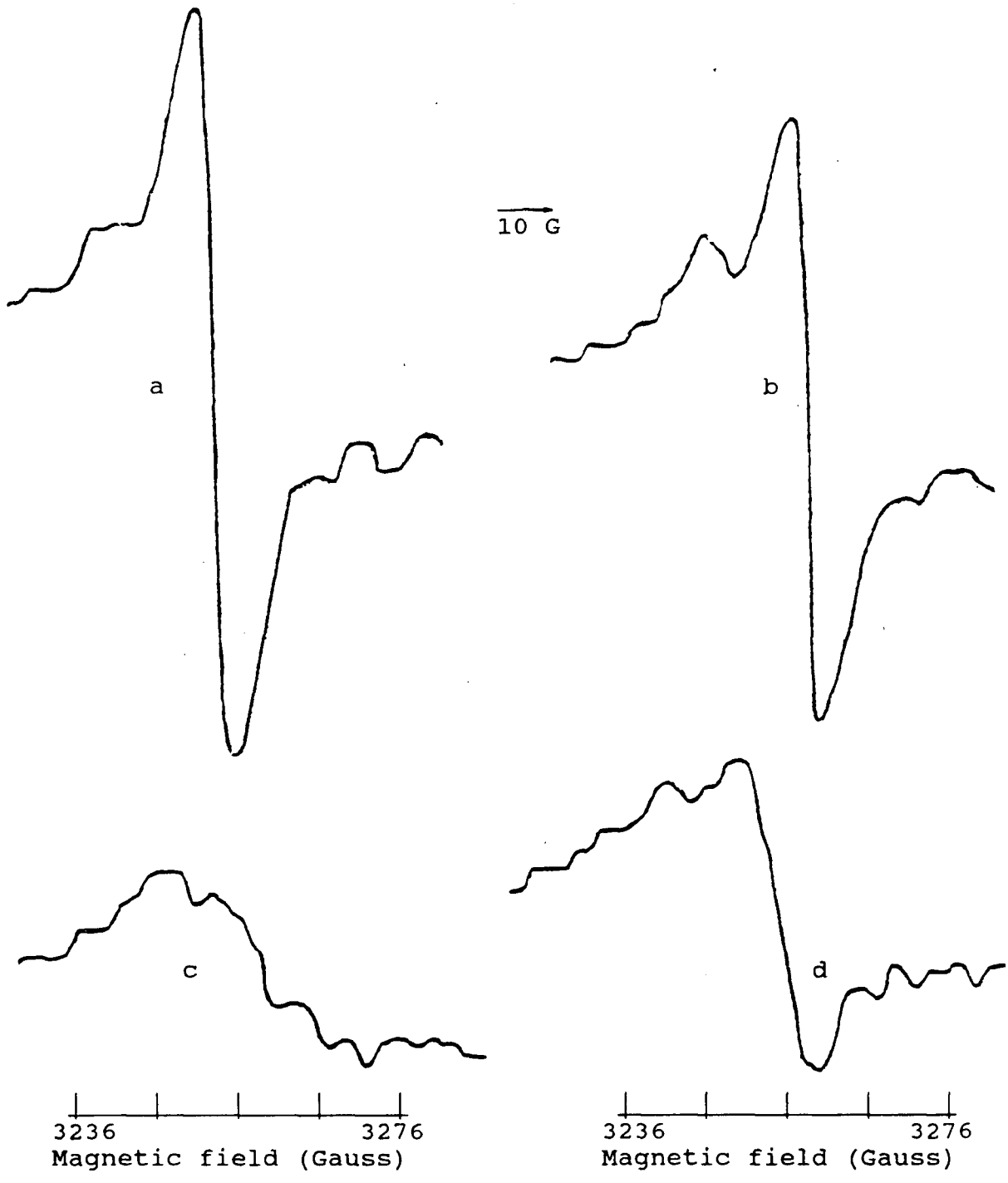

Figure 20. Combined Signals I and II_{u+s} from an attached, intact Kentucky bluegrass leaf. a. in air; b. in N_2 for 30 minutes; c. in N_2, 12 minutes after 20b; the leaf was in darkness for 4 minutes and white light for 4 minutes in the 12 minute interval; d. in N_2, 60 minutes after 20c. The leaf was held in 710nm light throughout except for the recording of the dark and white light-induced signals shown in Figures 21b and 22b, respectively. These were recorded in the interval between b and c of this figure. Microwave frequency - 9.190.

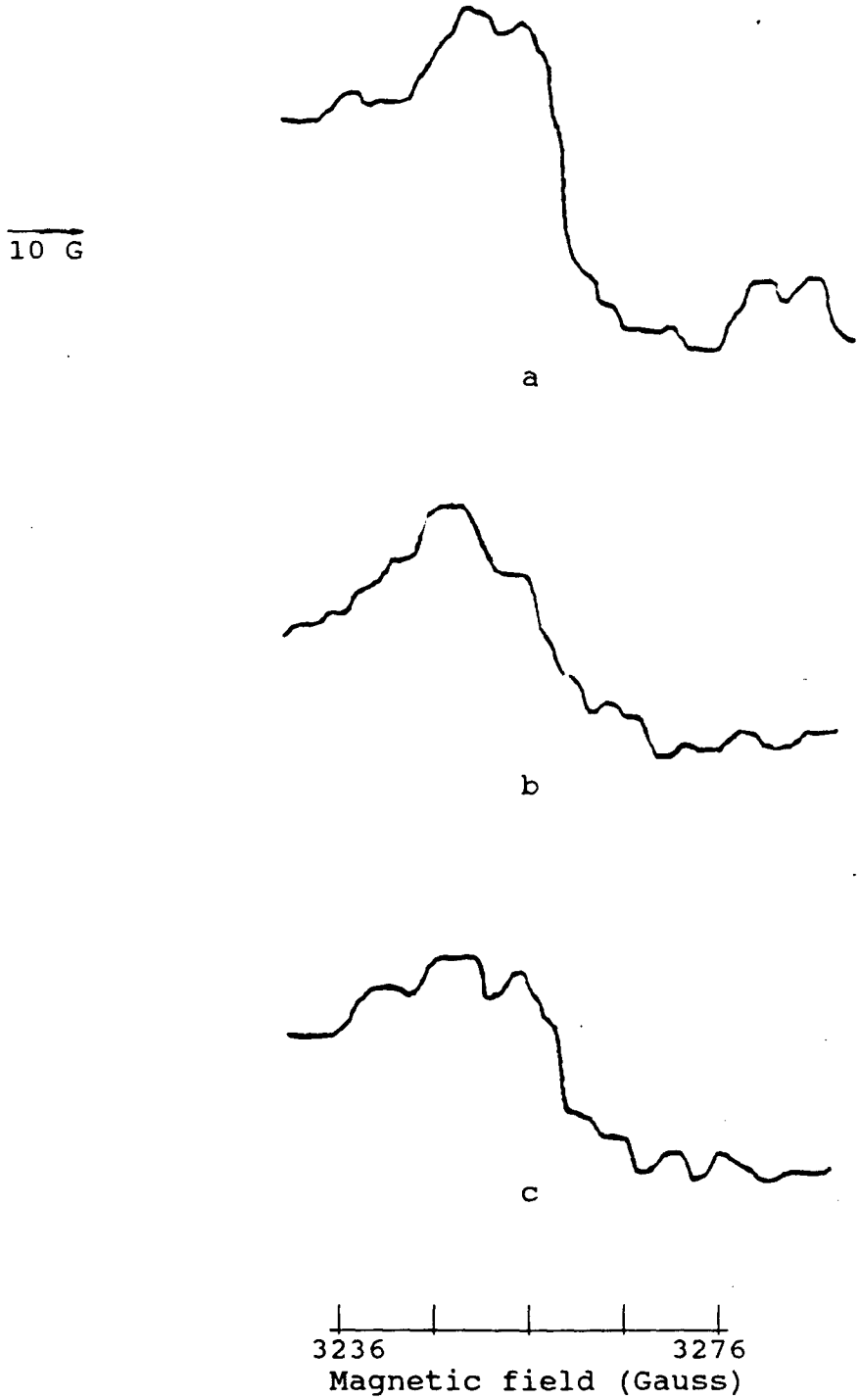

Figure 21. Signal II_{u+s} from an intact, attached Kentucky bluegrass leaf. a. in air; b. in N_2 for 36 minutes; c. in N_2 for 96 minutes. The leaf was held in 710nm light during the experiment except for the times when the traces shown in b (above) and Figure 22b were recorded. In this figure, a and c were recorded prior to, and after, exposure to the 710nm light, respectively. Microwave frequency - 9.190.

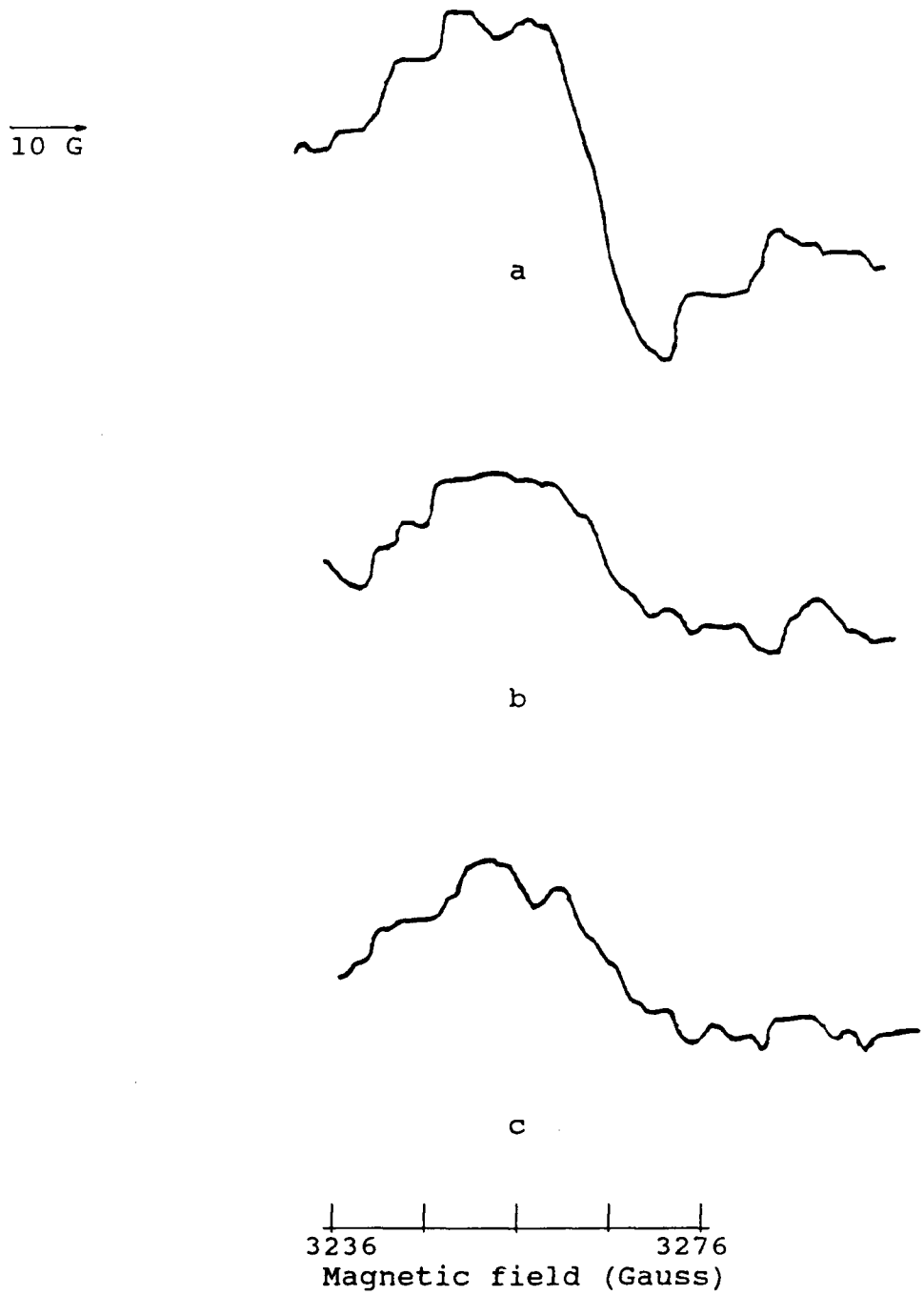

Figure 22. White light-induced signal from an attached, intact Kentucky bluegrass leaf. a. in air; b. in N_2 for 42 minutes; c. in N_2 for 102 minutes. The leaf was held in 710 light throughout, except for the times when the traces shown in b (above) and Figure 21b were recorded. In this figure, a and c were recorded prior to, and after, exposure to 90 minutes of 710nm light. Microwave frequency - 9.190.

from the composite signal as shown in Figure 23. Specifically, Figure 23a was obtained by subtracting 21a from 20a, Figure 23b by the subtraction of 21b from 20b and Figure 23c by the subtraction of 21c from 20d. The signals shown in Figures 23a-23c all have the peak-to-peak line width of 7.5 gauss and g-value of 2.0025 which is associated with Signal I (see Appendix B). Thus, it is apparent that once Signal I has been formed under conditions of clean air and 710nm light, minimal decay occurs when the oxygen is replaced by nitrogen (Figure 23b) for 30 minutes. However, if the light is then briefly turned off, then the signal is not restored within 4 minutes of exposure to 710nm light as previously shown. Hence there is evidence for some oxygen-dependence of the formation of the species represented by the signal since after 1 additional hour of exposure to 710nm light under nitrogen only approximately 40 per cent of Signal I is restored (Figure 23c).

Figure 24a shows the portion of Signal II_{u+s} which is lost as a result of the substitution of the N_2 for air. This was obtained by subtracting Figure 21c from Figure 21a. Figure 24b shows the difference signal obtained under broad-band white light. This was obtained by subtracting Figure 22c from Figure 22a. However, this change is a composite of the difference which occurs in darkness and the difference in the white light-induced component. Therefore, to obtain the real difference in the white light component it is necessary to

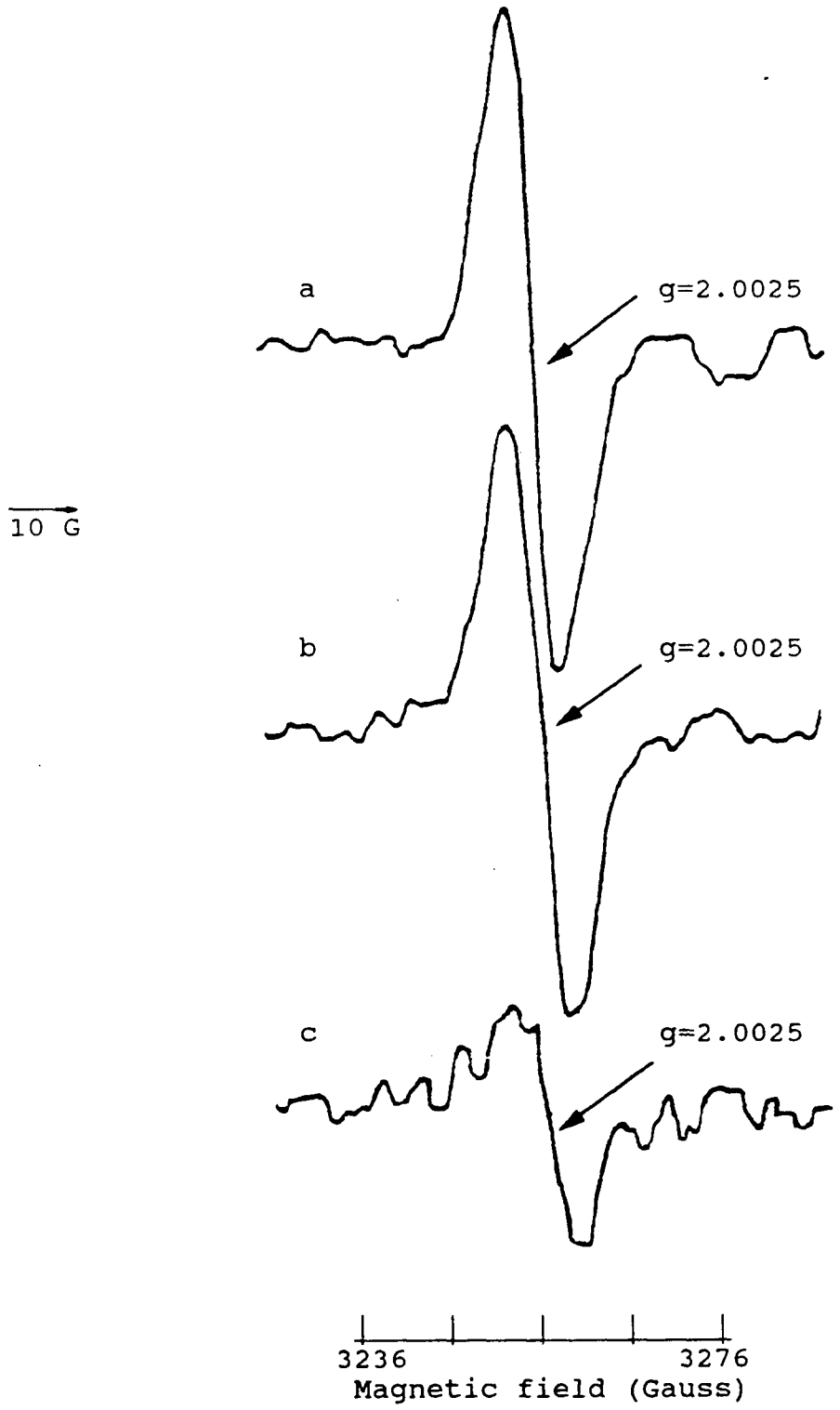

Figure 23. True 710nm light-induced signal (Signal I) from an intact, attached Kentucky bluegrass leaf. a. in air; b. in N_2 for 30 minutes; c. in N_2 for 90 minutes. All figures were obtained by subtracting the dark signal from the combined signal obtained in 710nm light. Microwave frequency - 9.190.

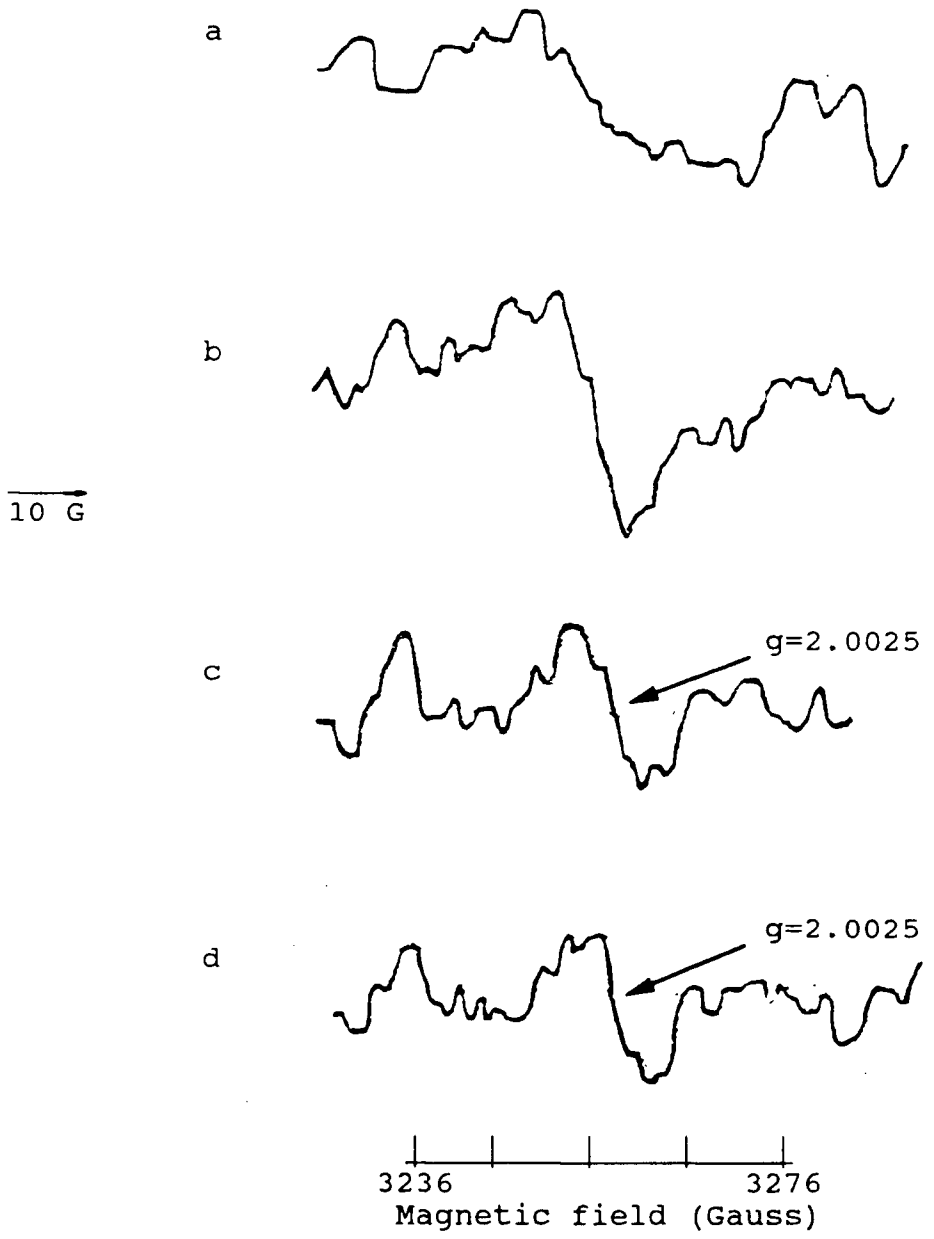

Figure 24. Changes in the dark and white light-induced signals in an intact, attached Kentucky bluegrass leaf caused by removal of O_2. a. Loss of Signal II_{u+s} caused by O_2 removal (Original dark signal - dark signal after 90 minutes N_2); b. difference in the white light-induced signal after removal of O_2 (Original white light induced signal after 90 minutes N_2; c. True difference in white light-induced signal caused by removal of O_2 (Figure 24b-24a); d. True white light-induced signal prior to removal of O_2 (Original white light-induced signal - original dark signal). Microwave frequency - 9.190.

subtract Figure 24a from Figure 24b. The result of this subtraction is shown in Figure 24c. This difference signal is nearly identical to the difference signal obtained when the original dark signal (Figure 21a) is subtracted from the original white light-induced signal (Figure 22a) as shown in Figure 24d. The small signals shown in Figures 24c and 24d have g-values of 2.0025 and peak-to-peak line widths of 7.5 gauss, identical to Signal I obtained upon irradiation with 710nm light.

Thus, the use of this subtraction technique indicates that the substitution of N_2 for O_2 causes a 60 per cent reduction in Signal I induced by 710nm light, eliminates all of the minimal Signal I induced by broad-band white light and causes a decay of approximately 30 per cent of Signal II_{u+s}. Signal II_{u+s} decays while the leaf is held under 710nm light but Signal I is only minimally affected during this period. The initial loss of Signal I under 710nm light is comparable in size to the loss of the Signal I lost under broad-band white light. However, once the 710nm light-induced Signal I formed under air decays in darkness, only 40 per cent of it can be restored in 710nm light under N_2 in the next hour.

These data support the earlier observations that Signal I is heterogeneous (Bearden and Malkin, 1972b) but also suggest that Signal II_{u+s} is heterogeneous and has some oxygen dependence.

3.3.5 Effects of Photoinhibition

In the present study, preliminary investigations showed that leaves of plants grown under conditions of high photon flux density (PFD) during the summers of 1986 and 1987 did not display the typical photosynthetic signals found in chloroplast suspensions and leaves grown under less intense light. Light intensity during this period was close to 1500μE $m^{-2}s^{-1}$ in full sunlight and just under 465μE $m^{-2}s^{-1}$ in the greenhouse. This confounding factor was eliminated by subsequently growing new experimental plants during the summer under the greenhouse benches at a reduced light intensity of approximately 40μE $m^{-2}s^{-1}$. However, leaves of plants grown in high PFD were studied in order to increase the current body of information pertaining to photoinhibitory effects of intense sunlight.

When C-3 plants grown in full summer sunlight or in the greenhouse at a light intensity reaching 465μE m^{-2} s^{-1} were used, excised pieces of radish, perennial ryegrass or Kentucky bluegrass leaves and intact, attached leaves of the grasses were found to yield a large EPR signal in darkness and when irradiated with 710nm or white light. Examples of this signal are presented in Figures 25 and 26, for Kentucky bluegrass and perennial ryegrass, respectively. These figures indicate two types of response, depending upon the leaf, regardless of species. The top spectra in each figure indicate the presence

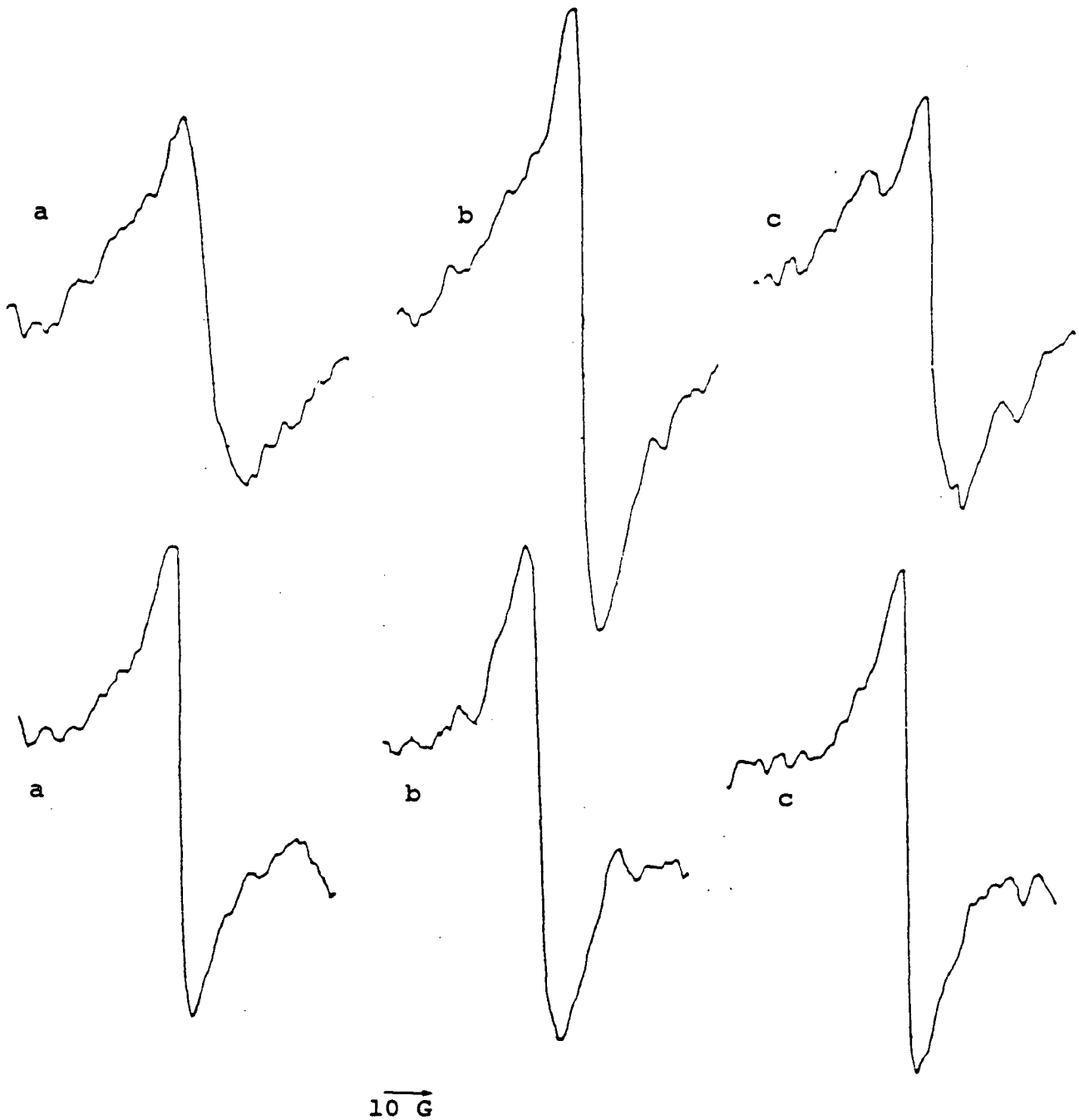

Figure 25. Examples of the free-radical signal found in Kentucky bluegrass leaves of plants grown under high photon flux density. a. darkness; b. in 710nm light; c. in white light. Top=typical response of leaves from plants grown in greenhouse; Bottom=typical response of leaves from plants grown in full sunlight.

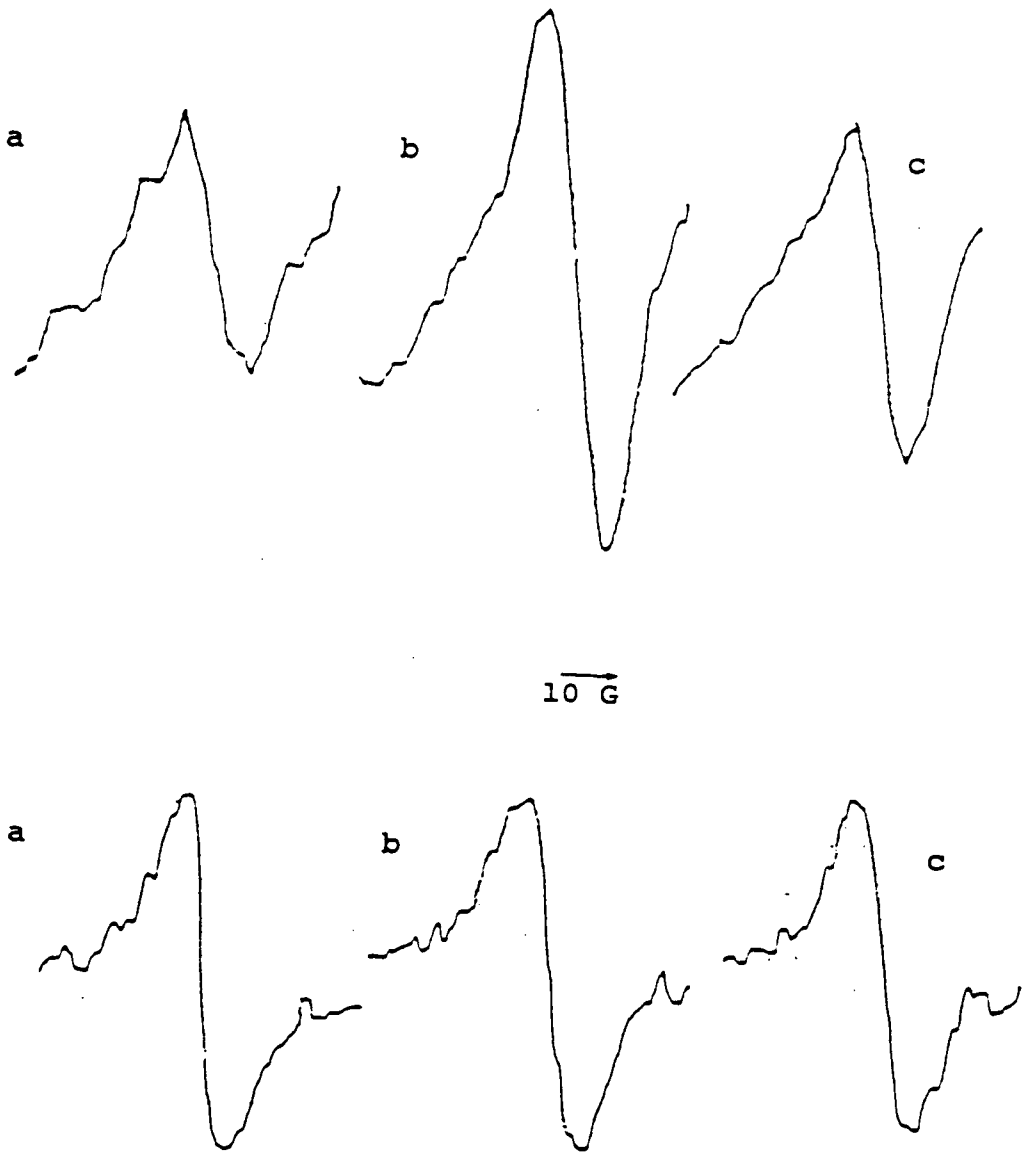

Figure 26. Examples of the free-radical signal found in leaves of perennial ryegrass plants grown under high photon flux density. a. darkness; b. in 710nm light; c. in white light. Top=typical response of leaves from plants grown in greenhouse; Bottom=typical response of leaves from plants grown in full sunlight.

of a new signal (Signal N_{PI}) in addition to the presence of the established Signal I and Signal II_{u+s}. This was the typical response in leaves grown on the greenhouse benches. The bottom spectra of each figure indicate the presence of Signal II_{u+s} and the new Signal N_{PI} but also indicate that Signal I, formed in 710nm light, has not been formed, since signals in all light regimes are identical. This was the typical response in leaves grown outside in full sunlight. While these were the most frequent responses of plants grown in the greenhouse and outside in full sunlight, respectively, some leaves of both species showed the opposite response. Approximately 5% of leaves grown outside still revealed the presence of Signal I and a similar percentage of leaves grown in the greenhouse did not reveal the formation of Signal I in 710nm light. The g-values of these combined signals are 2.0049 for Figures 25b and 26b (Top spectra) and 2.0051 for all other spectra in these figures. In all leaves of a C-4 plant, barnyard grass (Echinochloa crusgalli (L.) Beauv.), which was grown in full sunlight, Signal N_{PI} was revealed and Signal I was not formed in 710nm light (Figure 27). The g-value of the combined signal in barnyard grass leaves was found to be 2.0051.

Furthermore, once induced, this new signal is long-lived, as leaves of plants originally grown under high PFD, which were moved under greenhouse benches or to the spectrometry laboratory for periods of up to eight days, still revealed this signal, as

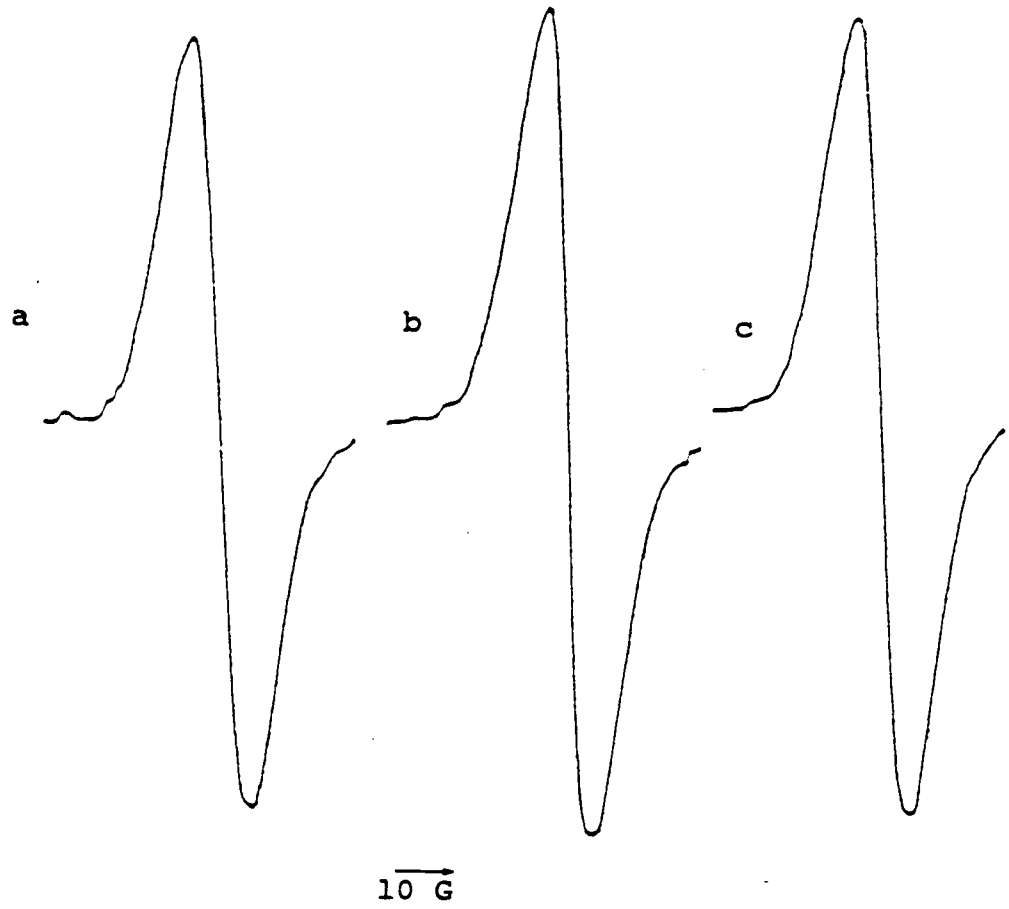

Figure 27. Examples of the free-radical signal found in leaves of barnyardgrass grown in full summer sunlight. a. darkness; b. in 710nm light; c. in white light.

shown in Figure 28. Similarly, if leaf pieces from plants grown under high PFD were excised and stored in water for eight days, Signal N_{PI} was still present (data not presented).

In most leaves, the signal was rapidly eliminated upon exposure of the leaf to microwave radiation in the spectrometer cavity. The kinetics of the signal decay were found to vary somewhat, from leaf to leaf, but a typical example is shown in Figure 29. These kinetics, which are independent of cavity light, were obtained by locking the spectrometer onto the low field maximum of the signal shown in Figures 25-28. Initially, there is a small increase in Signal N_{PI}, but within two minutes a maximum height is achieved and decay sets in. In nearly all leaves grown in the greenhouse (see below) the signal was found to disappear within 15 minutes of exposure to microwave radiation. The kinetic trace shown in Figure 29 was obtained with a Kentucky bluegrass leaf irradiated with 710nm light but the kinetics of the rise and decay of Signal N_{PI} were not affected by the irradiation of the leaf through the cavity port as similar results were obtained in 710nm light, in 650nm light, in broad-band white light and in darkness. A representative example of the absolute size of the signal in Kentucky bluegrass leaves held in darkness during exposure to microwave radiation in the cavity for various time periods is shown in Figure 30.

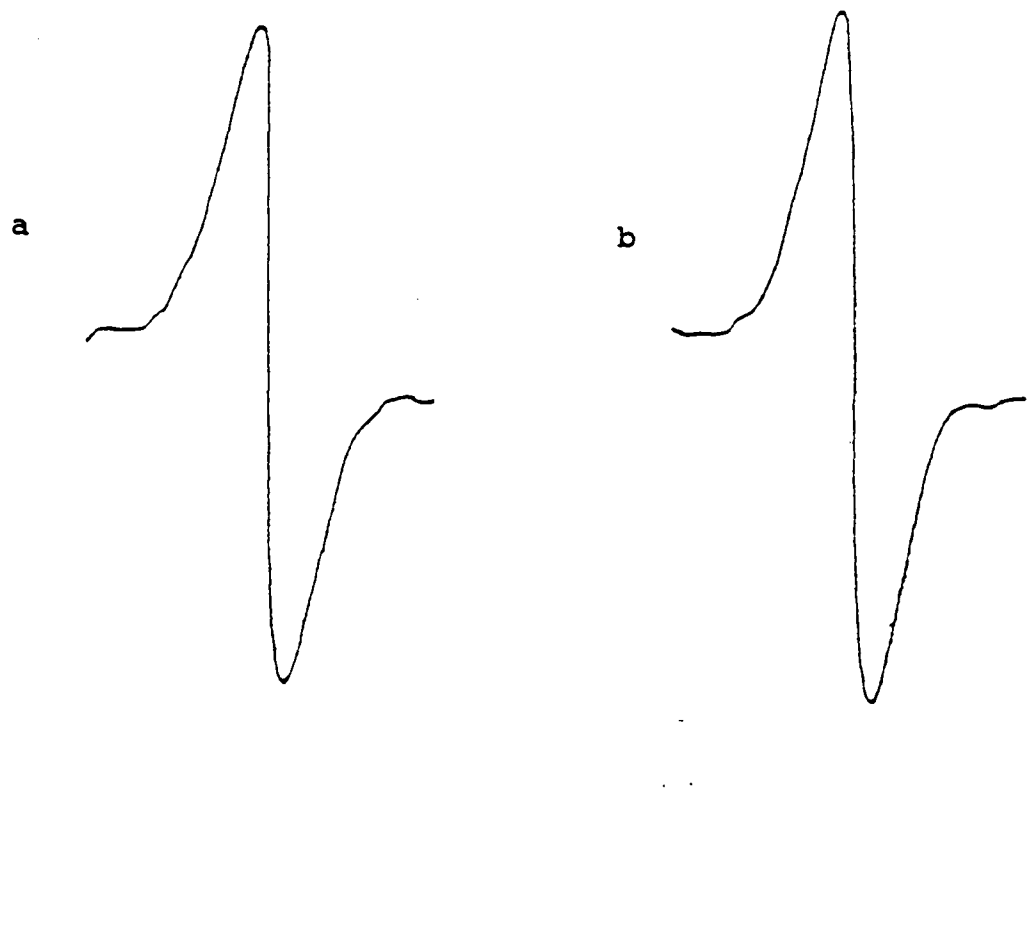

Figure 28. Examples of the free-radical signal found in leaves of Kentucky bluegrass plants grown under high photon flux density 8 days after the plants were moved to the spectrometry laboratory. a. in darkness; b. in 710nm light.

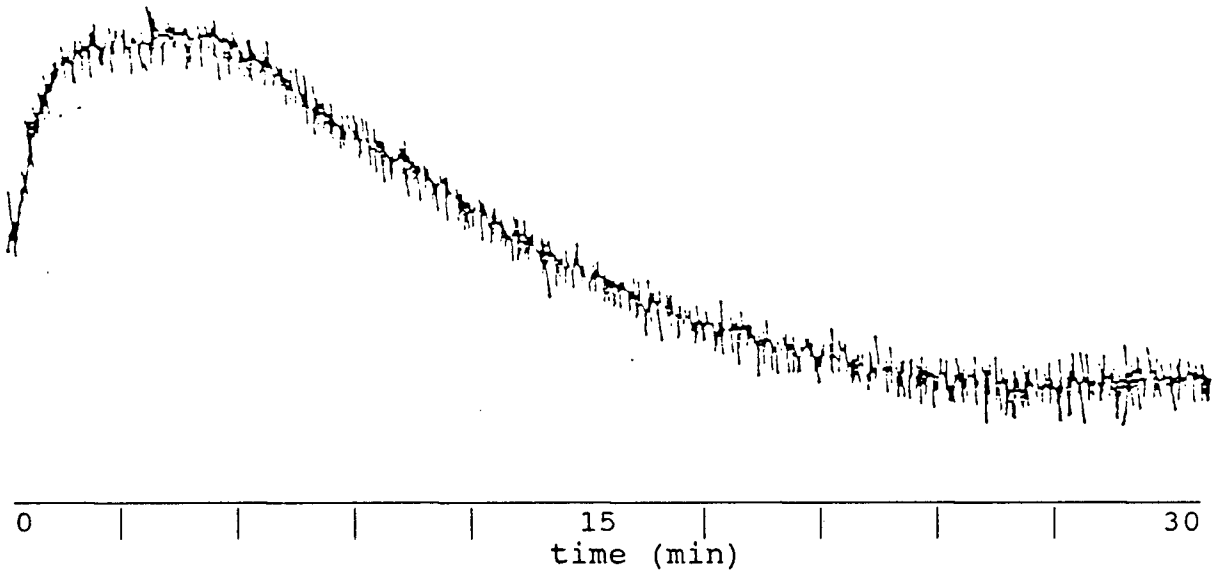

Figure 29. Decay of the free-radical signal found in Kentucky bluegrass leaves grown in conditions of high photon flux density, upon exposure to microwave radiation in the spectrometer cavity.

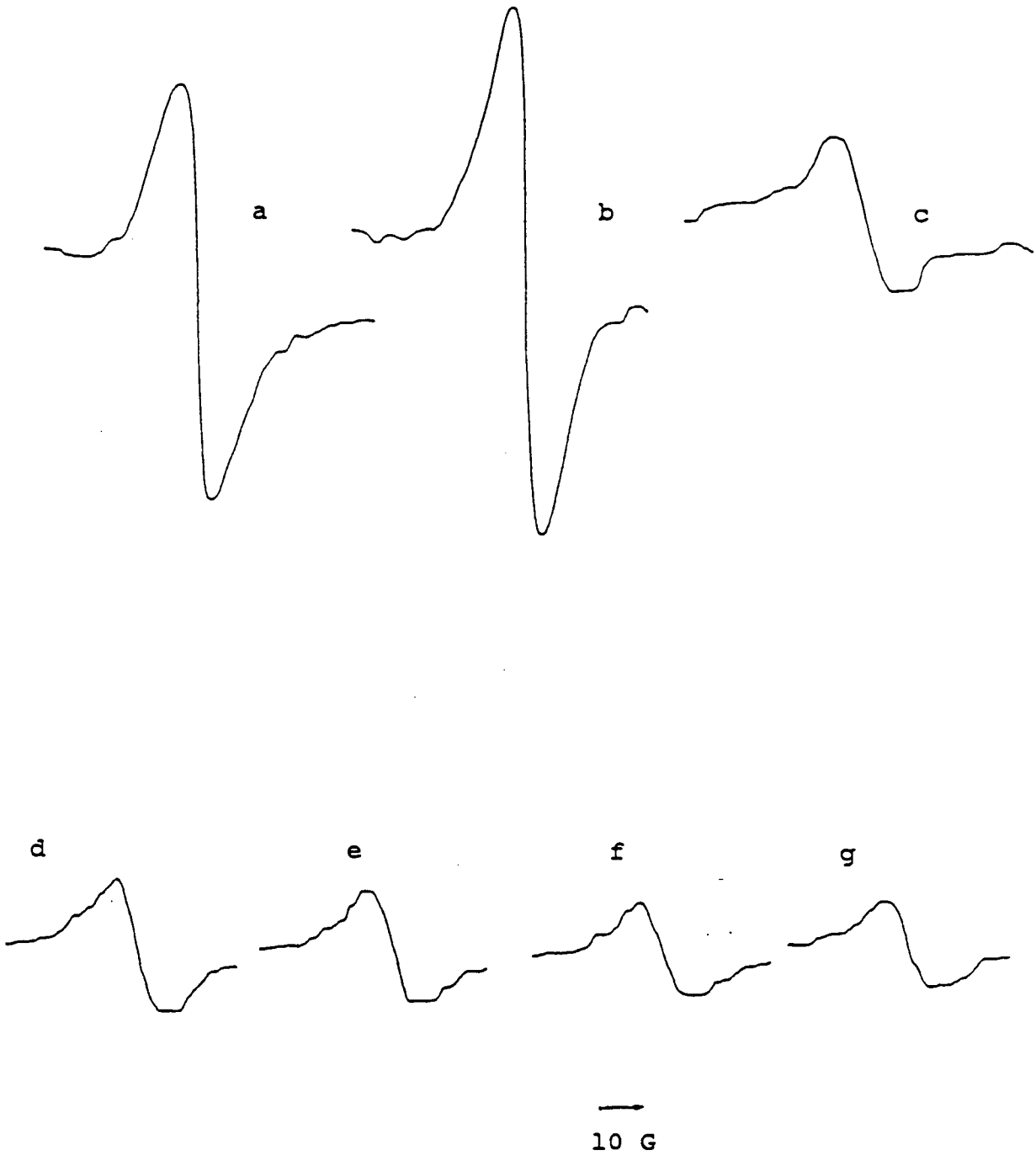

Figure 30. Spectra of the free-radical signal found in Kentucky bluegrass leaves grown under high photon flux density after exposure to microwave radiation in the spectrometer cavity for different time periods in darkness. a. 15 sec; b. 2 min; c. 6 min; d. 10 min; e. 15 min; f. 20 min; g. 30 min.

However, if the signal is recorded and the microwave radiation is immediately turned off, the identical decay occurs and no signal is found when the klystron is turned on again 15 minutes later, as shown in the spectra in Figure 31. On the other hand, if the leaf is maintained in the spectrometer cavity for periods up to 2 hours, without turning on the microwave radiation to record a signal, the signal shown in Figures 25-29 is still present. This is the case with or without the magnetic field turned on, indicating that the signal is not affected by the presence of the magnetic field (data not shown).

Photosynthetic Signal II_{u+s}, as shown in Figures 30f and 30g, appears to be unaffected, but Signal I may, or may not, be present in leaves which exhibit the new EPR signal, depending upon the leaf (Figures 25,26). The new signal (Signal N_{PI}) can be characterized as being symmetrical, with an approximate peak-to-peak width of 9 gauss and a g-value of 2.0056 (Figure 32c). This figure was obtained after reduction of Signal N_{PI} by exposure to microwave radiation in the spectrometer cavity and subtraction of Signal I and Signal II_{u+s} (Figure 32b) from the original composite signal shown in Figure 32a, which was recorded in 710nm light. These parameters do not match those of any signal in the relevant literature. An identical signal is revealed if Signal II_{u+s} is subtracted from the original composite signal recorded in darkness or broad-band white light, or if Signal II_{u+s} is subtracted from spectra recorded in

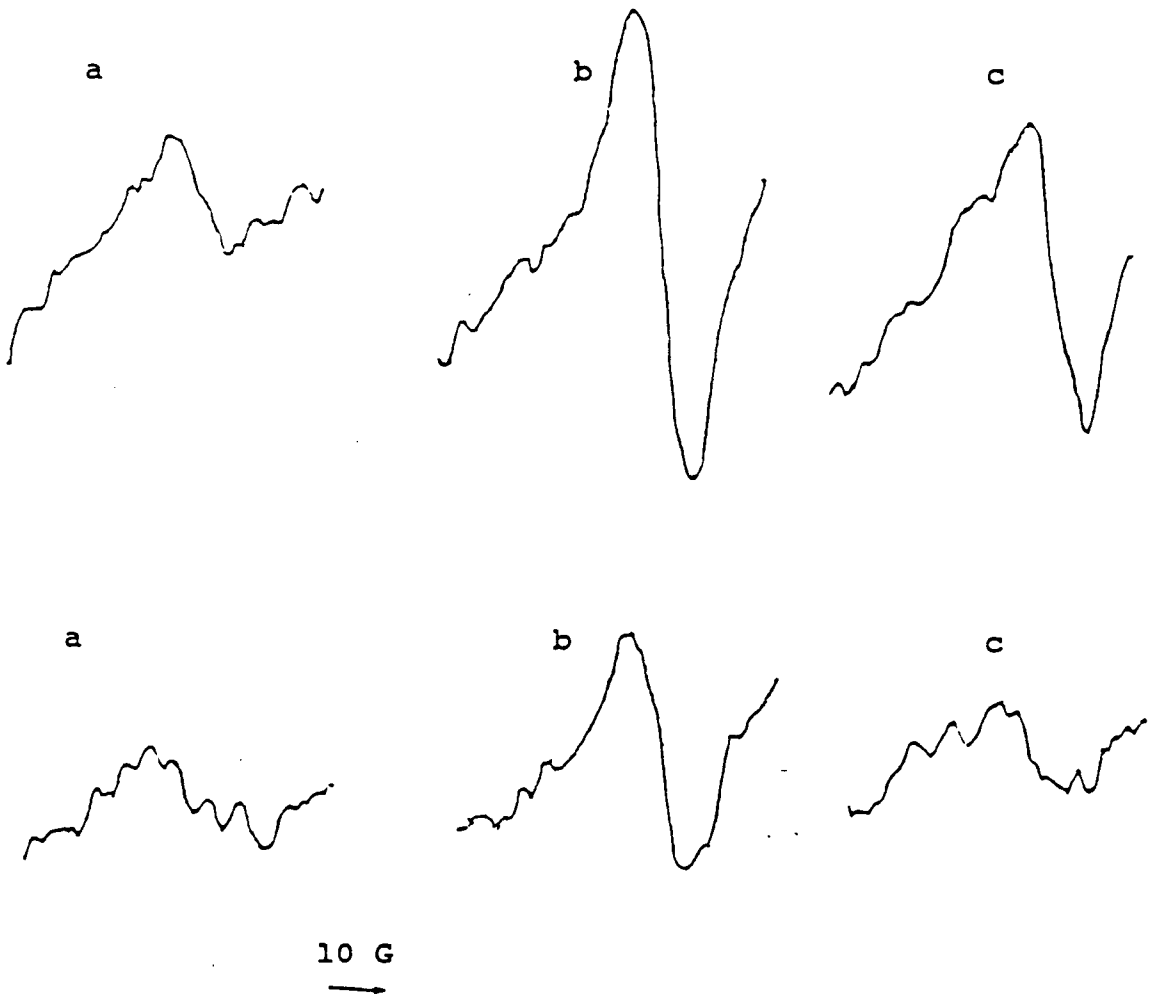

Figure 31. Spectra of perennial ryegrass leaves grown under high photon flux density. Top - at start of experiment; Bottom - 15 minutes after the top signals were recorded, with the klystron off in the interval. a. in darkness; b. in 710nm light; c. in white light.

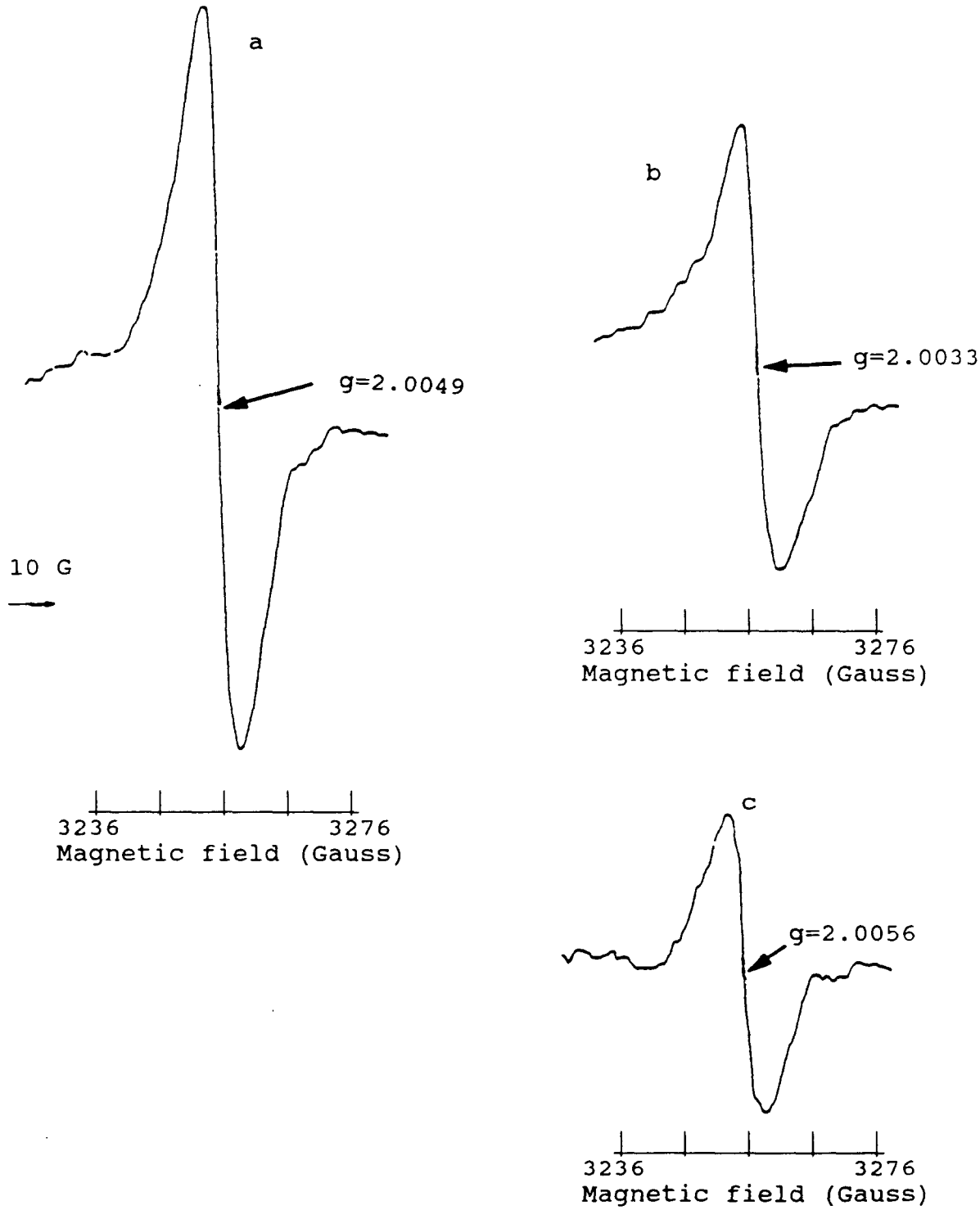

Figure 32. Signal N_{PI} of Kentucky bluegrass leaves exposed to high photon flux density. a. Composite signal recorded in 710nm light at start of experiment (Signal N_{PI}, Signal I and Signal II_{u+s}); b. Signal I + Signal II_{u+s} after elimination of Signal N_{PI} by exposure to 15 minutes microwave radiation; c. Signal N_{PI}, obtained by subtracting b from a. Microwave frequency - 9.190.

710nm light which do not reveal Signal I (data not shown).

After exposure to microwave radiation, leaves which are affected by exposure to high PFD differ in their capacity to revert to the established responses associated with the revelation of photosynthetic Signals I and II_{u+s} under various light regimes. The response of each species varies, depending upon the degree of damage and is illustrated in Figures 33 and 34 for Kentucky bluegrass. In extreme cases, Signal N_{PI} cannot be removed, even after 1 hour of exposure to microwave radiation in the spectrometer cavity, regardless of light regime (Figure 33a). This only occurred with a few leaves of plants grown in full sunlight outside the greenhouse, never with leaves of plants grown in the greenhouse. An alternative response from leaves grown in full sunlight is the elimination of Signal N_{PI}, but no appearance of Signal I, either under irradiation with 710nm or broad-band white light (Figure 33b). In such leaves, Signal I cannot be induced even by continuous irradiation with 710nm light for periods of up to 2 hours. This was the most prevalent response of leaves of barnyardgrass.

A third alternative is shown in Figure 34a. In this instance Signal N_{PI} has been eliminated and Signal I is formed upon irradiation with 710nm light. However, Signal I, as indicated by its g-value and peak-to-peak line width, is also formed upon irradiation with broad-band white light. The fourth

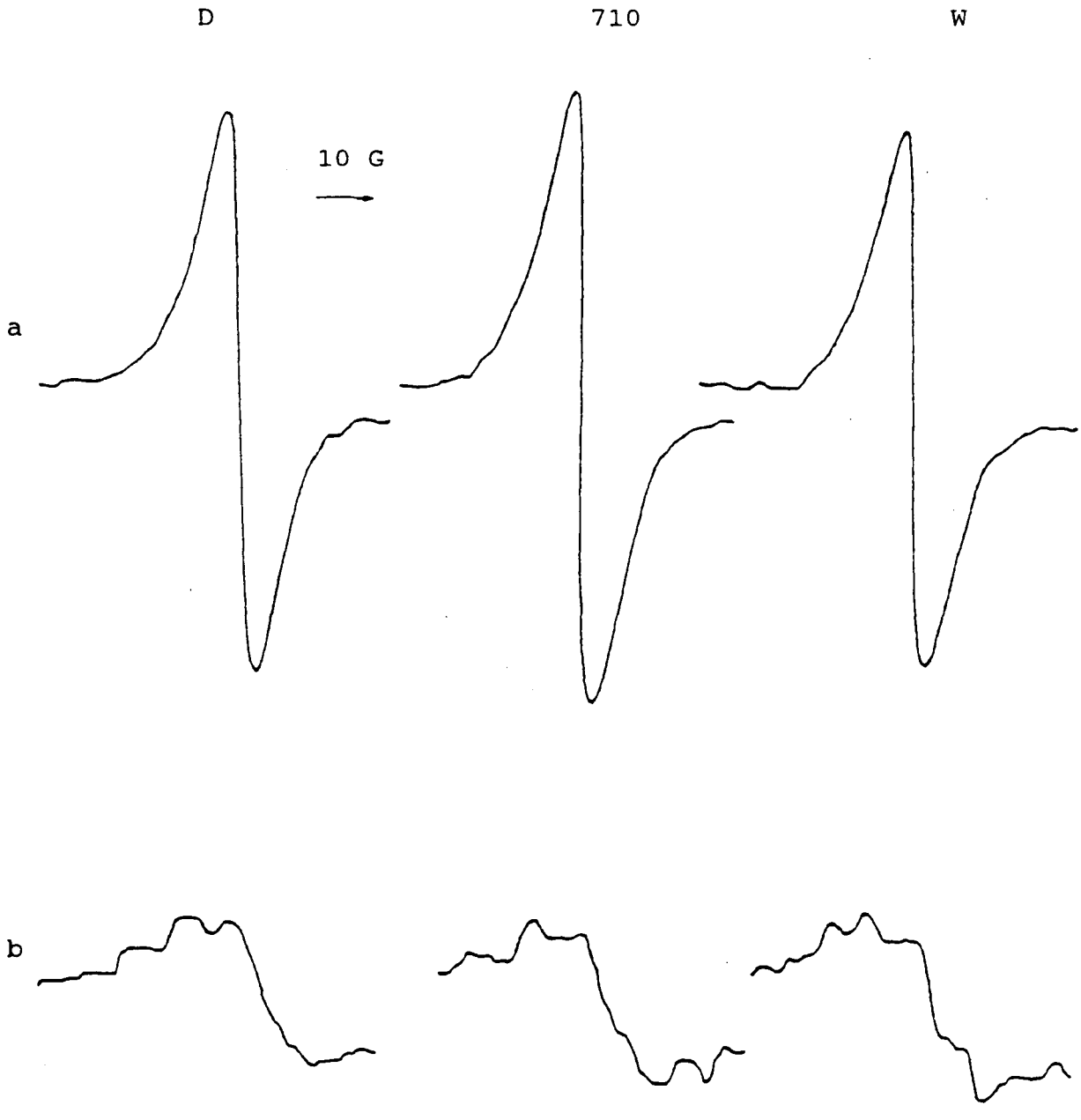

Figure 33. Alternative responses of Kentucky bluegrass leaves containing Signal N_{PI} after exposure to microwave radiation in the spectrometer cavity. a. retention of Signal N_{PI}; b. elimination of Signal N_{PI}, and a lack of generation of Signal I in 710nm light. D=darkness; 710=in 710nm light; W=in broad-band white light.

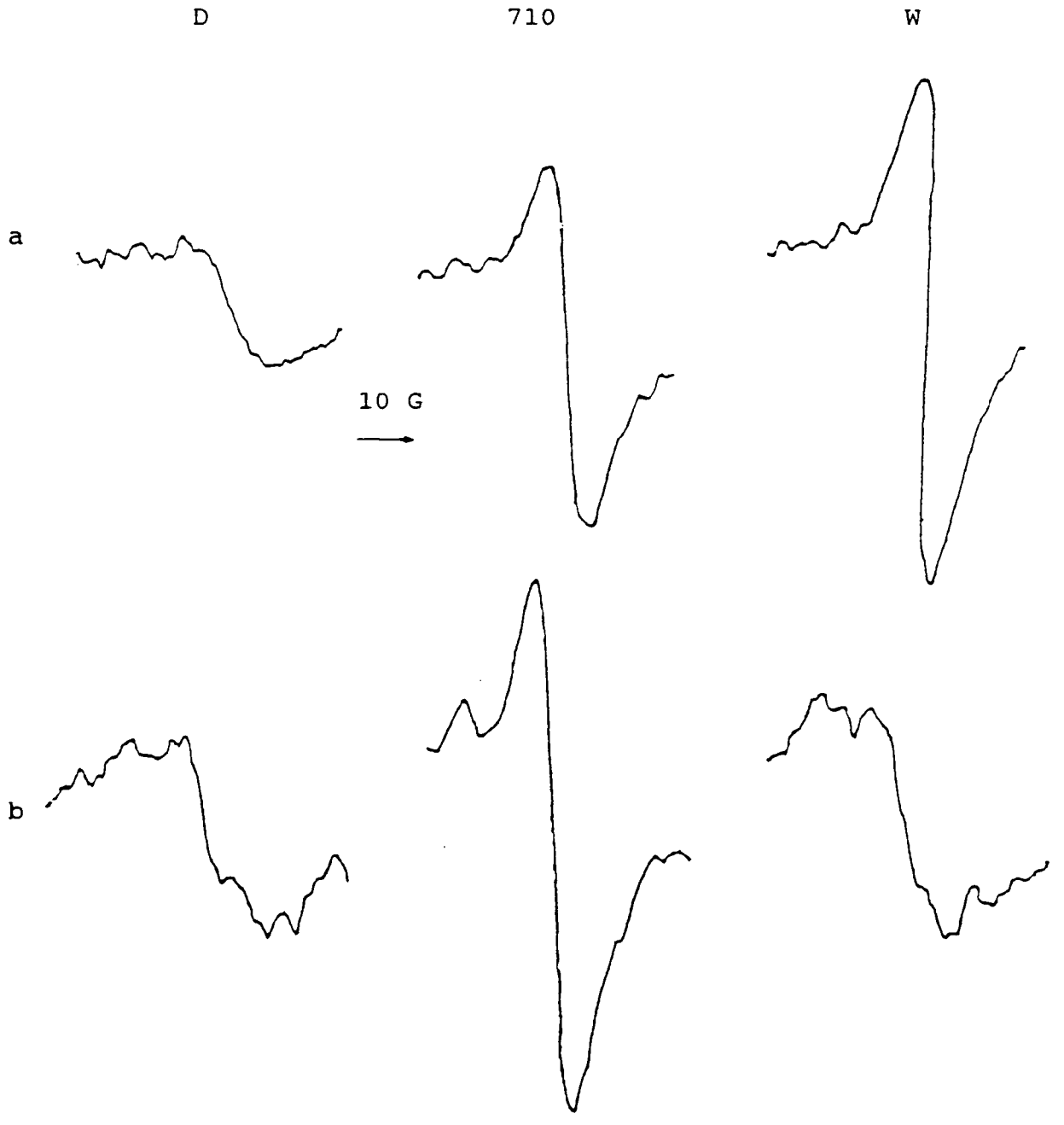

Figure 34. Alternative responses of Kentucky bluegrass leaves containing Signal N_{PI} after exposure to microwave radiation in the spectrometer cavity. a. elimination of Signal N_{PI} and formation of Signal I in white light; b. typical Signal I and II_{u+s} associated with leaves, chloroplast preparations and reaction centre preparations not exposed to high photon flux density. D=darkness; 710=in 710nm light; W=in broad-band white light.

possible response is shown in Figure 34b as a return to the signals found in healthy leaves with the formation of Signal I upon irradiation with 710nm light, but not upon irradiation with broad-band white light. This latter response was the most prevalent in Kentucky bluegrass leaves of plants grown in the greenhouse, while the additional formation of Signal I under broad-band white light was the most common response of perennial ryegrass plants grown in the greenhouse.

3.4 Discussion

The results presented illustrate the capability of the technique developed to determine free radicals in situ in leaf tissues. The methodology enables the investigator to follow changes in EPR signals resulting from exposure to pollutant gases, from other changes in gas composition or from other treatments. The technique illustrated in tracking changes in Signal I, associated with Photosystem I, can also be used to follow changes in Signal II_{u+s}, associated with Photosystem II, and the ubiquitous Mn^{++} signal if the underlying Fe^{++} signal is unaffected by the treatment. The appearance of new free-radical signals can be monitored by following the kinetics of signal appearance directly, if preliminary studies have shown that only one signal is affected. If two signals, which respond to different light regimes, are found to overlap, then both signals can be recorded sequentially under their respective

light regimes after various fumigation periods. Subsequent subtraction of the signals obtained at different times will reveal new EPR signals attributable to the effects of treatment.

The problems associated with the differences in inherent signal intensity from leaf to leaf are minimized by subtracting original signals found in leaves prior to fumigation from those found in the same leaves after fumigation, in order to observe the relative changes in the signals. Furthermore, if different changes in free-radical signal appearance occur in darkness than in light, the true light-induced free-radical signal can be determined by multiple subtractions.

The small differences in g-values and peak-to-peak widths of the various signals require instrument precision and accurate recording because the differences in these parameters are the basis upon which signals are differentiated. The spectrometer precision is attested to by the fact that that several hundred 710nm light-induced signals (Signal I) were all found to have a g-value of 2.0025, with an error range of 0.0002. This error is identical to the measurement error associated with the standard used for comparison, DPPH. Operator error is limited to faulty placement of the recording paper on the recorder. All signals discussed in this thesis were recorded at least 8 times, and yielded virtually identical g-values and line widths.

Studies involving fumigation of excised leaves have to be limited to periods of between 1 and 1.5 hours because of the effects of excision (wounding), which result in changes in free-radical signals in the vicinity of the 2.000 g-value associated with photosynthetic signals. However, this problem is largely overcome through the use of intact, attached grass leaves which can be placed in the cavity without wounding. The grass leaves can be held in air in the spectrometer cavity for 72 hours without the formation of new free-radical signals. This allows the use of realistic concentrations of pollutants while monitoring free radical changes over longer periods of time.

Although developed specifically to permit investigation of the effect of gaseous air pollutants on free radical formation in intact leaves, the method could be used to investigate changes resulting from other physical or chemical treatments. The permanence of any changes induced by treatments can also be investigated because the signals can be observed at various time periods after cessation of treatment. The method could also permit the detection of transient free radicals, such the superoxide and hydroxyl free radicals, if appropriate spin traps could be incorporated into excised plant leaf tissue.

The data presented also support the contention that free radical formation is a contributory factor in photoinhibition.

Unfortunately, the free radical (Signal N_{PI}) formed by the exposure to intensive light cannot be identified by EPR characteristics alone.

The differential response after leaves have been exposed to microwave radiation in the cavity is indicative of the degree of damage suffered by the plant. Plant leaves which either retain Signal N_{PI}, or show no Signal I after elimination of Signal N_{PI}, have been severely damaged and are not functional in the photosynthetic process at that time. Definite damage to Photosystem I is indicated by the lack of Signal I formation upon exposure to 710nm light. Photosystem II may, or may not be, damaged also, but this can not be ascertained in the absence of Signal I formation. Signal II_{u+s} is unaffected by the formation of Signal N_{PI}, but other components of Photosystem II may be damaged by the presence of the free radical revealed by the presence of Signal N_{PI}. However, it is necessary to ascertain the response of Signal I to different irradiation regimes before damage to Photosystem II can be postulated. As there is no formation of Signal I, even in 710nm light, in the above cases, consideration of interruption of electron transfer from PSII to PSI would only be speculation. Damage to these leaves has apparently passed the reversible photoinhibitory stage and may have reached the photooxidative stage leading to death.

Damage to Photosystem II, or the electron transport chain, is indicated in leaves in which Signal N_{PI} decays upon exposure to microwave radiation, but which also reveal the formation of Signal I upon irradiation with broad-band white light. The formation of the white light-induced Signal I indicates that the electron transfer from PSII to PSI normally associated with exposure to white light has been interrupted and the reduction of the light-oxidized chloropyll a free radical giving rise to Signal I is no longer occurring. Therefore, either PSII has been damaged or the electron transport chain is blocked.

The findings from these studies are consistent with the suggestions that photoinhibition precedes photooxidation, with the latter process resulting in death of the leaf (Kok et al. 1965). The fluorescence studies which indicated that PSII is consistently damaged by photoinhibition (Bjorkman, 1968; Powles and Bjorkman, 1983) cannot be confirmed by EPR spectrometry alone, but the studies which indicated that PSI may also be damaged (Bjorkman, 1968; Critchley, 1981) have been confirmed. The site of PSII damage can not be ascertained from EPR data but data showing elimination of Signal I are highly supportive of earlier data which indicated that the site of PSI inhibition is very close to the reaction centre of PSI (Satoh, 1970b).

The new unidentified free radical, depicted as Signal N_{PI},

may be the 'fluorescence quencher' discovered by Den Haan et al. (1973) and subsequently postulated to be the major cause of photoinhibition (Cleland and Critchley, 1985). However, the role of the free radical giving rise to Signal N_{PI} is currently unknown and before this can be clarified it is first necessary to identify the free radical shown in Figure 32c as Signal N_{PI}.

The greater and sometimes permanent damage suffered by leaves on plants grown in full sunlight confirms that photoinhibitory damage is dependent upon exposure (Critchley, 1981). The differing responses in free radical formation in Kentucky bluegrass and perennial ryegrass leaves upon exposure to microwave radiation suggest that Kentucky bluegrass is more tolerant to intense light than perennial ryegrass.

4.0 OZONE STUDIES

4.1 Introduction

The effect of ozone on vegetation ranges from visible injury which can lead to necrosis (Costonis, 1970), to less obvious changes in the metabolic processes of plants (Mudd et al. 1969,1971; Frederick and Heath, 1974; Tingey, 1974). Plant physiology and biochemistry can be affected with concomitant reductions in plant growth (Flagler and Youngner, 1982a, 1982b). Exposure to ozone causes reductions in photosynthesis (Coulson and Heath, 1974) and alters photosynthate pools (McLaughlin and McConathy, 1983) and partitioning among plant organs (Oshima et al. 1978). The degree of damage is a function of genetic (Wilton et al. 1972) and environmental factors (Heck and Dunning, 1967).

Free radicals have been implicated in ozone toxicity in plant systems (Rowlands et al. 1970; Asada et al. 1977). These may be formed by ozone decomposition in aqueous systems or by oxygen reduction in the chloroplasts (Weiss, 1935; Mehler, 1951). The present study was undertaken to investigate the in situ changes in free radical appearance and decay which occur when plant leaves are fumigated with different levels of ozone.

4.2 Methods

Plant materials, EPR spectrometry and the leaf holder were as described earlier (Section 3.2). Preliminary investigations with excised pieces of leaves indicated that no changes in free radical formation occurred upon exposure to low and intermediate levels of ozone (up to 250ppb) during time periods of up to one hour. Therefore, all further studies involved the use of 10-12 week old intact, attached Kentucky bluegrass and perennial ryegrass leaves.

Ozone was generated by passing medical grade air at a rate of 2 l/min through a charcoal filter, and then through a Dasibi ozone generator. Ozone levels were monitored with a Dasibi Model 1003AX monitor. Plants were moved into the spectrometry laboratory 2 hours prior to the start of any treatment. The room light was on during this period. Previous light adaptation effects (Tikhonov and Ruuge, 1975a) were then standardized by exposing the leaves to 30 seconds of 710nm light followed by 3 minutes of darkness in the cavity.

4.3 Results

Results were similar with both grasses. Hence, the majority of data presented here are from experiments with Kentucky bluegrass leaves, since they exhibit less interference from the

Mn^{++} and Fe^{++} signals discussed earlier (Section 2.4).

4.3.1 Effects of Low Levels of O_3

When leaves were fumigated at low levels of O_3, (up to 80ppb) for periods of time up to 8 hours, no changes occurred in the photosynthetic EPR signals, and no new EPR free-radical signals were evident. The small free radical (Signal N_{710}) which is formed under 710nm light is induced by the continual exposure to 710nm light, and is independent of ozone treatment. Details of this free radical are presented in Section 3.3.4.1. Knowledge of Signal N_{710} is critical for correct interpretation of results which occur when leaves are fumigated with higher levels of ozone.

4.3.2 Effects of Intermediate Levels of O_3

Fumigation of leaves exposed to 710nm or broad-band white light with ozone levels ranging from 80 to 250ppb causes changes in the photosynthetic free radicals if the fumigation is extended beyond 2 hours. Figures 35-39 present EPR signals from Kentucky bluegrass leaves fumigated with 100ppb O_3. Figure 35 shows the signals prior to fumigation, when the leaf was held in the dark, under 710nm light and under broad-band white light, respectively, after the initial standardization period. These spectra show a definite Signal II_{u+s} in darkness (Figure 35a),

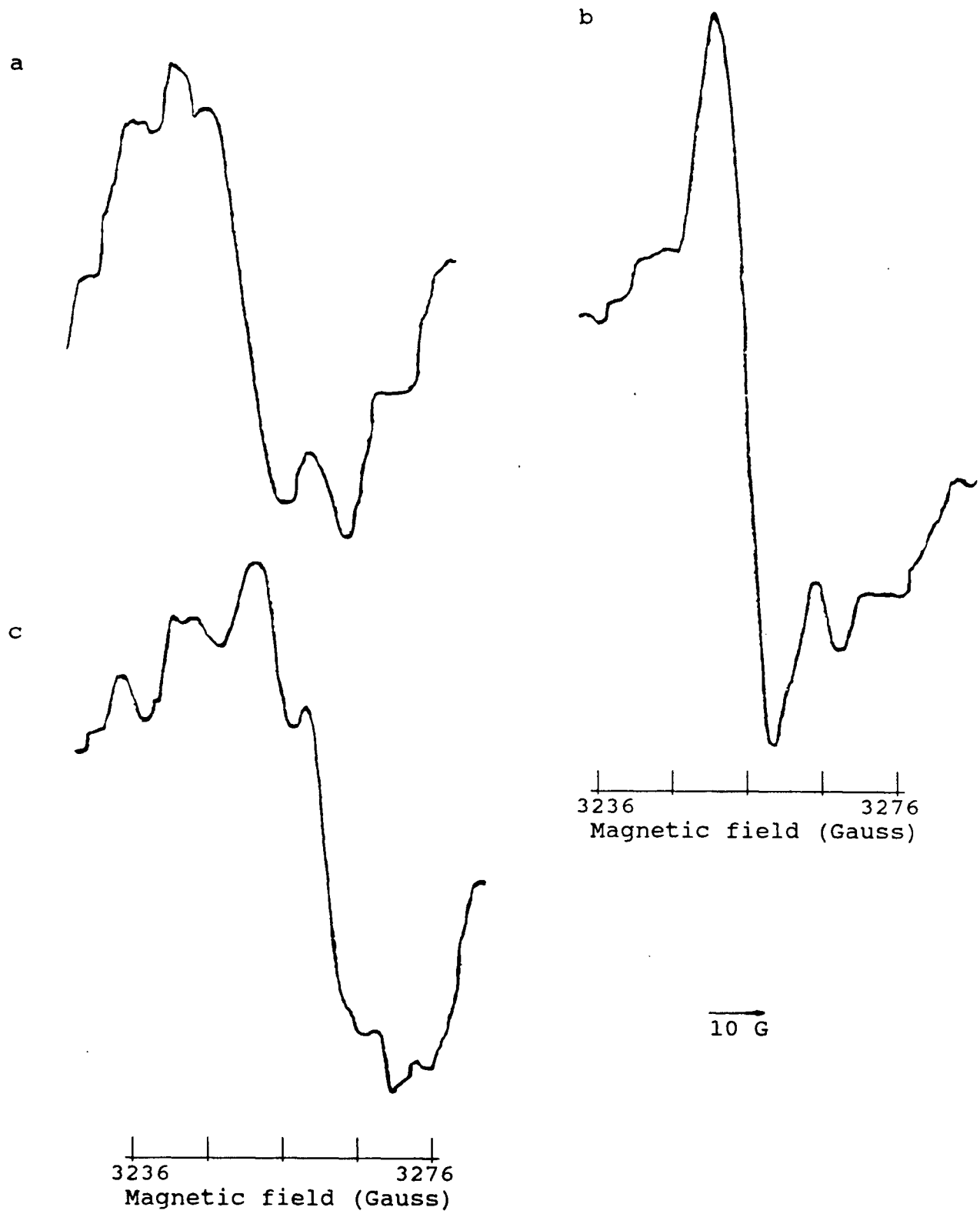

Figure 35. EPR signals from an intact, attached Kentucky bluegrass leaf prior to fumigation. a. in dark; b. in 710nm light; c. in white light. Microwave frequency - 9.190.

a strong Signal I superimposed upon Signal II_{u+s} under 710nm light (Figure 35b) and a very small Signal I imposed upon Signal II_{u+s} under broad-band white light (Figure 35c). Figures 36a and 36c, recorded after 2 hours of fumigation with 100ppb O_3, with the leaf held in 710nm light during this period, show the appearance of a new signal superimposed upon Signal II_{u+s}, when the spectra were recorded in darkness or under broad-band white light, respectively. Figure 36b indicates little change in the height of the signal recorded with the leaf held under 710nm light at this time. However, the peak-to-peak width of this latter signal has increased from 8 gauss to approximately 10.5 gauss and the g-value has shifted to approximately 2.0035, suggesting that this, too, is now a composite signal which includes Signal II_{u+s}, Signal I and a new free-radical signal. Subtraction of the spectra in Figure 35 from the appropriate spectra in Figure 36 revealed the formation of a very small new free-radical signal (Signal N_{O1}) having a g-value of approximately 2.004 and a peak-to-peak line width of approximately 10 gauss (data not shown).

Figure 37 shows the signals obtained when fumigation was continued for one more hour with the bluegrass leaf still maintained under 710nm light. By this time the free-radical signals obtained from the leaf under each light regime are identical. The 710nm light-induced Signal I has disappeared and the new free-radical signal (Signal N_{O1}) with a g-value of

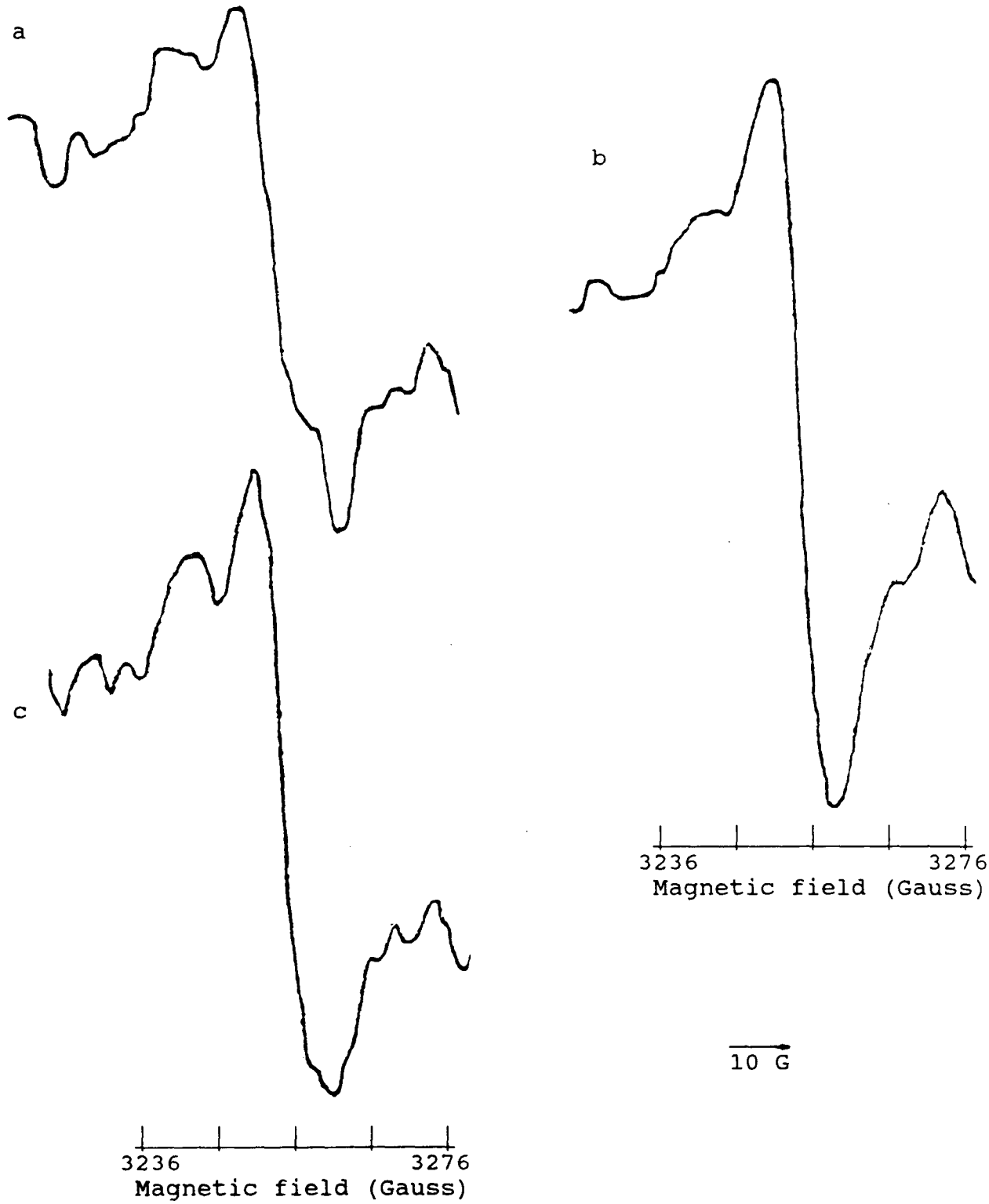

Figure 36. EPR signals from an intact, attached Kentucky bluegrass leaf after exposure to 100ppb ozone for 2 hours. The leaf was maintained in 710nm light during the 2 hours of fumigation. a. in dark; b. in 710nm light; c. in white light. Microwave frequency - 9.190.

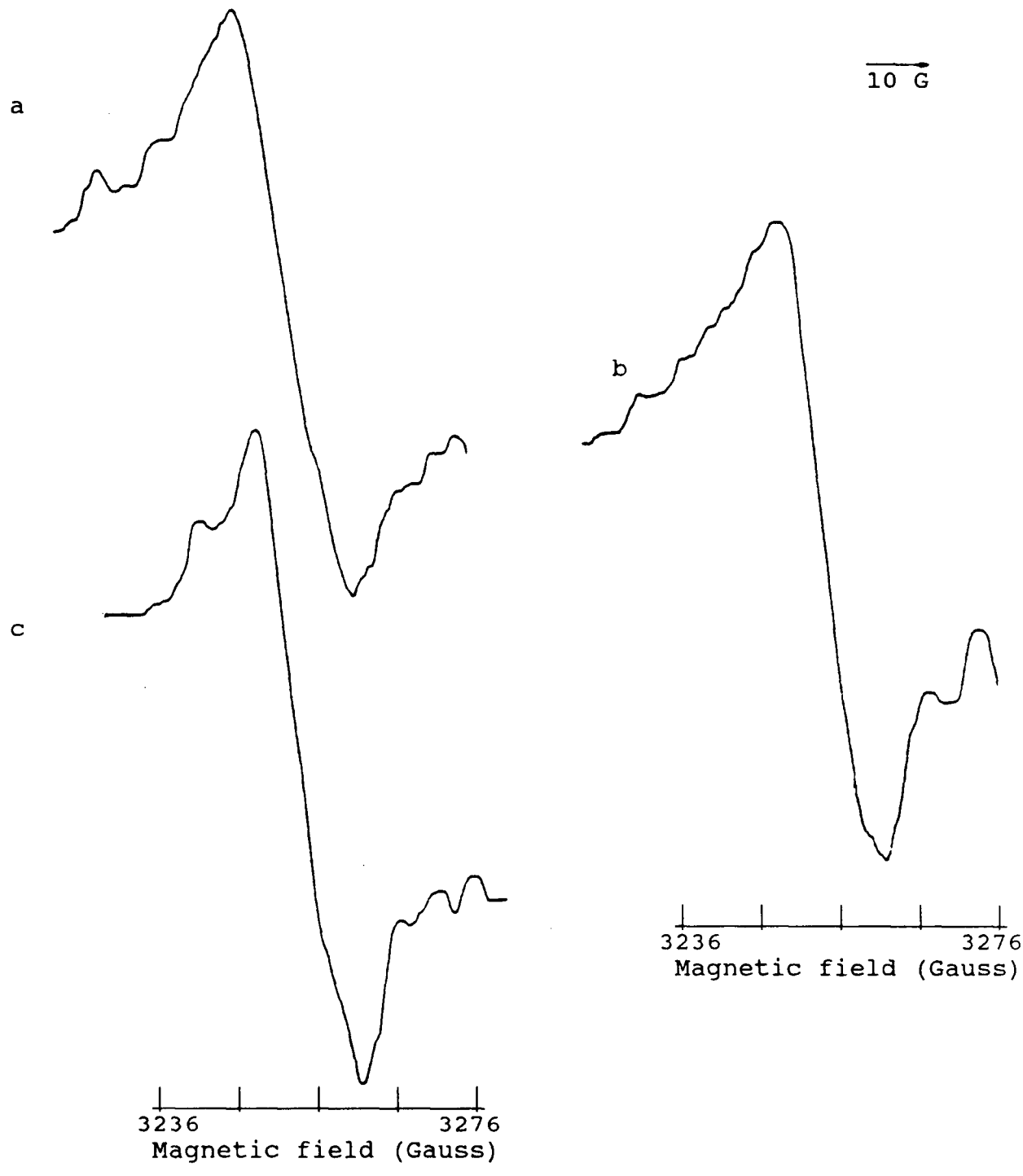

Figure 37. EPR signals from an intact, attached Kentucky bluegrass leaf after exposure to 100ppb ozone for 3 hours. The leaf was maintained in 710nm light during the 3 hours of fumigation except for the 8 minutes when the signals shown in Figures 36a and 36c were recorded. a. in dark; b. in 710nm light; c. in white light. Microwave frequency - 9.190.

2.0041 and a peak-to-peak line width of 10 gauss is observed under all light regimes.

The exact concentration level and time period needed to induce these changes varied from leaf to leaf, and even between parts of any given leaf. Ryegrass leaves were generally more sensitive and usually showed the change to Signal N_{O1} shortly after 2 hours of fumigation at concentrations as low as 80ppb O_3. Kentucky bluegrass leaves, on the other hand, generally required O_3 levels of at least 100ppb and a fumigation time period often approaching 3 hours.

These signal changes were reversible once fumigation was terminated. Figure 38 indicates the signals obtained 20 minutes after the end of fumigation of a bluegrass leaf. During this 20 minute period filtered air was passed through the cavity and the leaf was maintained in 710nm light. The signal obtained with 710nm light has reverted back to 8 gauss in width and a g-value of 2.0025 (Figure 38b). The signals obtained in darkness and under broad-band white light (Figures 38a and 38c) show no sign of the O_3-induced free-radical signal (Signal N_{O1}), but also show a somewhat distorted Signal II_{u+s} when compared to the comparable signals (Figures 35a and 35c) at the start of the experiment.

After the signals shown in Figure 38 were recorded, the leaf

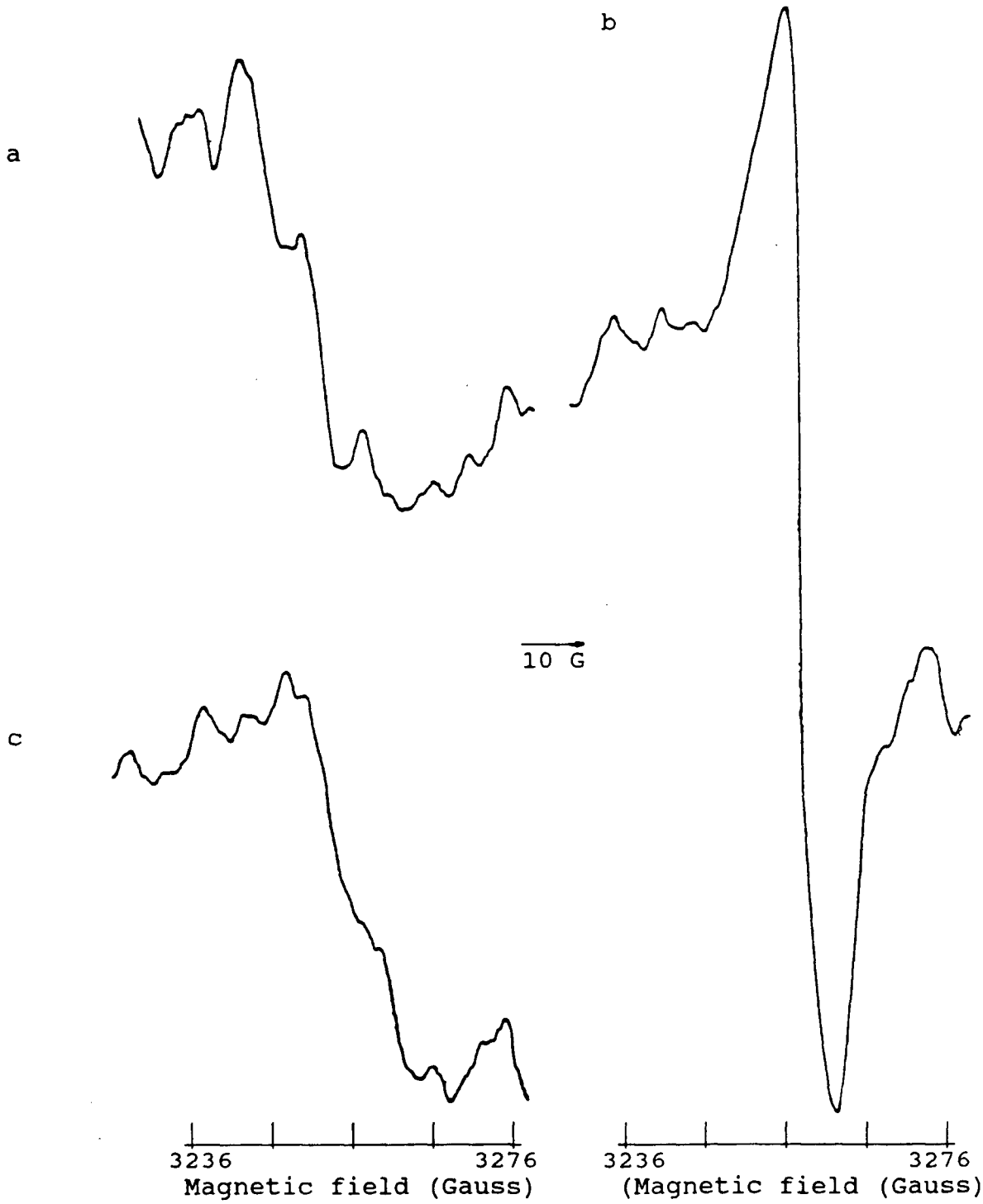

Figure 38. EPR signals from an intact, attached Kentucky bluegrass leaf 20 minutes after termination of a 3 hour exposure to 100ppb ozone. The leaf was maintained in 710nm light throughout, except for the 8 minute periods during which the signals shown in Figures 37a, 37c and 38a, 38c were recorded. a. in dark; b. in 710nm light; c. in white light. Microwave frequency - 9.190.

was removed from the cavity but remained attached to the holder to permit precise relocation in the cavity. The plant was held in darkness for 8 hours followed by room light for 8 hours. Following replacement of the leaf in the cavity, the signals were again recorded. Figure 39b indicates no further change in the 710nm light-induced signal while Figures 39a and 39c indicate a near complete return to the original Signal II_{u+s}, (cf. Figures 35a,35c,) by this time.

The amount of time necessary for complete recovery of the leaf varied greatly among different leaves but was generally correlated to the length of time the leaf was exposed to the pollutant. If the time of fumigation was extended to periods exceeding 3 hours (e.g. 5 hours), the time required to reverse the signals increased, in some cases, requiring 48 hours exposure to clean air. Accurate dose-response and recovery curves could not be constructed because of this extreme variability in sensitivity among leaves.

At no time during these experiments were visible signs of ozone injury apparent.

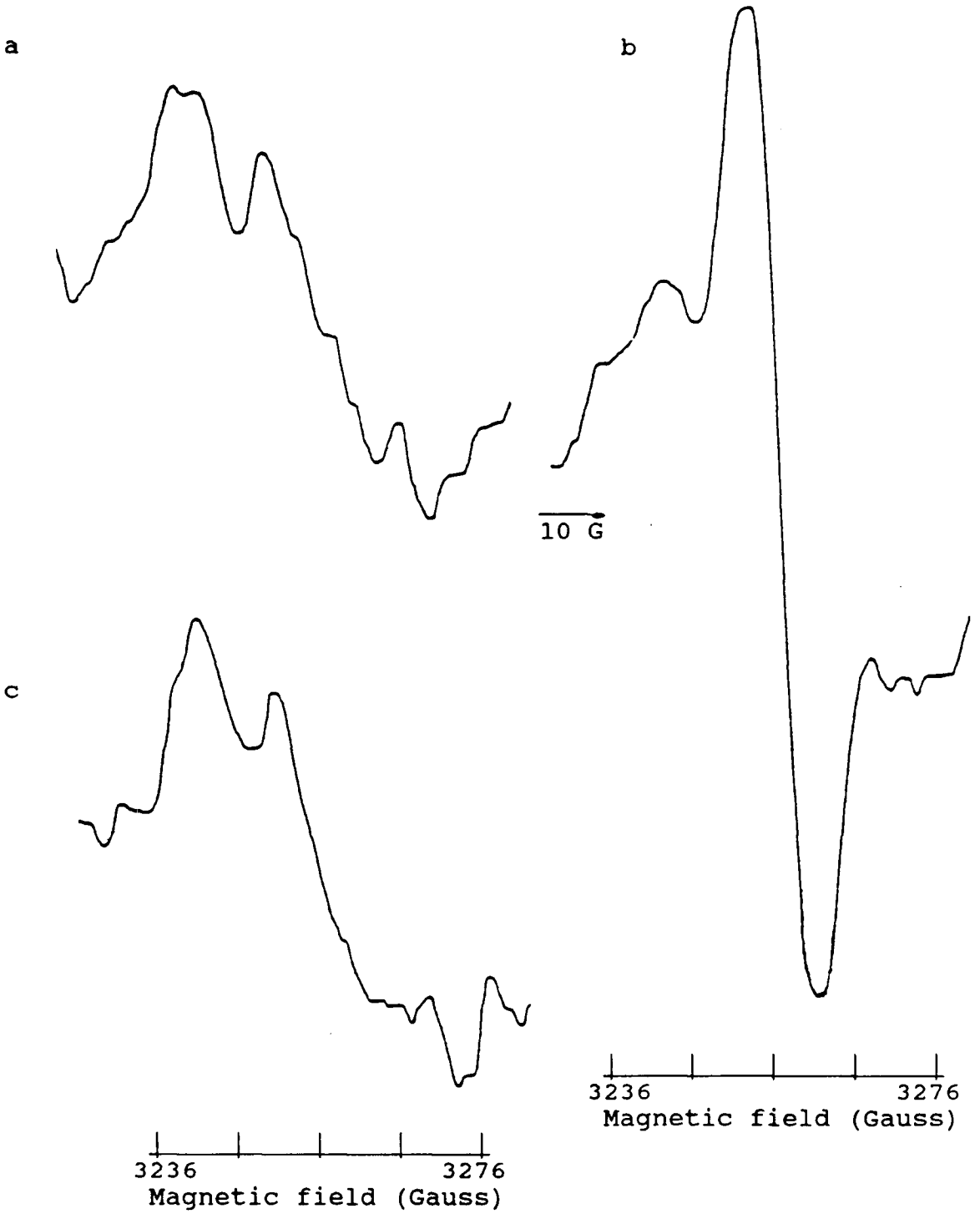

Figure 39. EPR signals from an intact, attached Kentucky bluegrass leaf 16 hours and 20 minutes after a 3 hour exposure to 100ppb ozone. After fumigation ended, the leaf was maintained in 710nm light for 20 minutes, darkness for 8 hours and room light for 8 hours. a. in dark; b. in 710nm light; c. in white light. Microwave frequency - 9.190.

4.3.3 Effects of High Levels of O_3

There was a marked contrast in free-radical signal responses when leaves were exposed to high levels of O_3 (250ppb to 1ppm) for periods exceeding 1 hour. Data presented here indicate changes which occurred when Kentucky bluegrass leaves were fumigated with 500ppb O_3 for 1.5 hours.

Figure 40a indicates the true Signal I at the start of the experiment. This signal, obtained by subtracting Signal II_{u+s} (recorded with the leaf in darkness) from the composite of Signal I and II_{u+s} (recorded with the leaf under 710nm light) has the typical g-value of 2.0025 and a line width of 7.5 gauss. Figure 40b indicates the new signal (Signal N_{710}), discussed earlier in Section 3.3.4.1, which is induced by constant exposure to 710 nm light. This signal, obtained by subtracting the original Signal I shown in Figure 40a, from the 710nm light-induced signal after 45 minutes exposure to 710nm light has a g-value of approximately 2.0054 and a line width of 8.5 gauss. Signal II_{u+s} was subtracted in each case. In leaves, the time of appearance of Signal N_{710} varies but it is always present within one hour of constant exposure to 710nm light.

Figure 41 indicates the changes in the true 710nm light-induced and dark signals which occur after 1.5 hours of

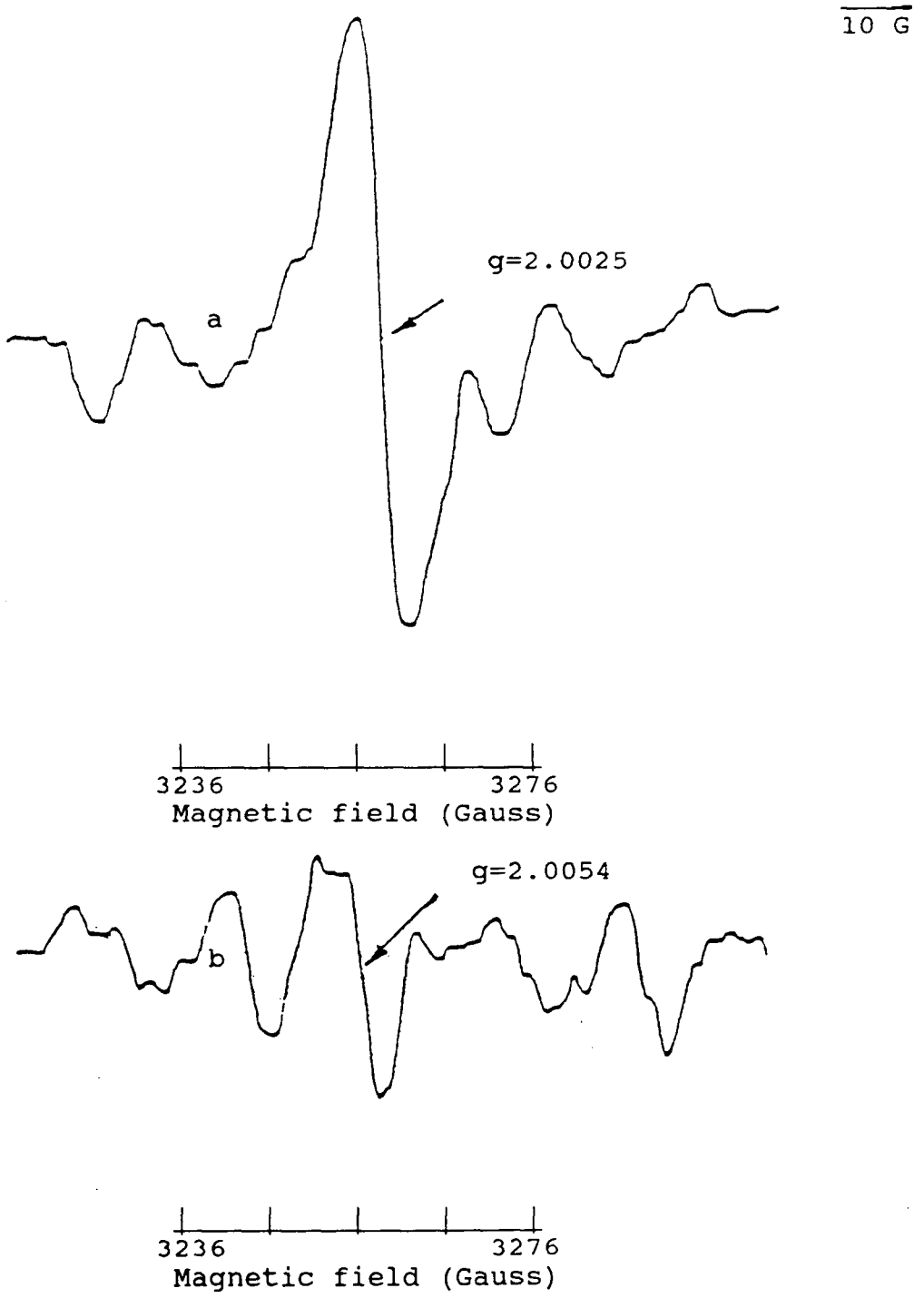

Figure 40. 710nm light-induced signals from an intact, attached Kentucky bluegrass leaf prior to fumigation. a. True Signal I; b. True Signal N_{710}, induced by exposure to 1 hour of 710nm light. Microwave frequency - 9.190.

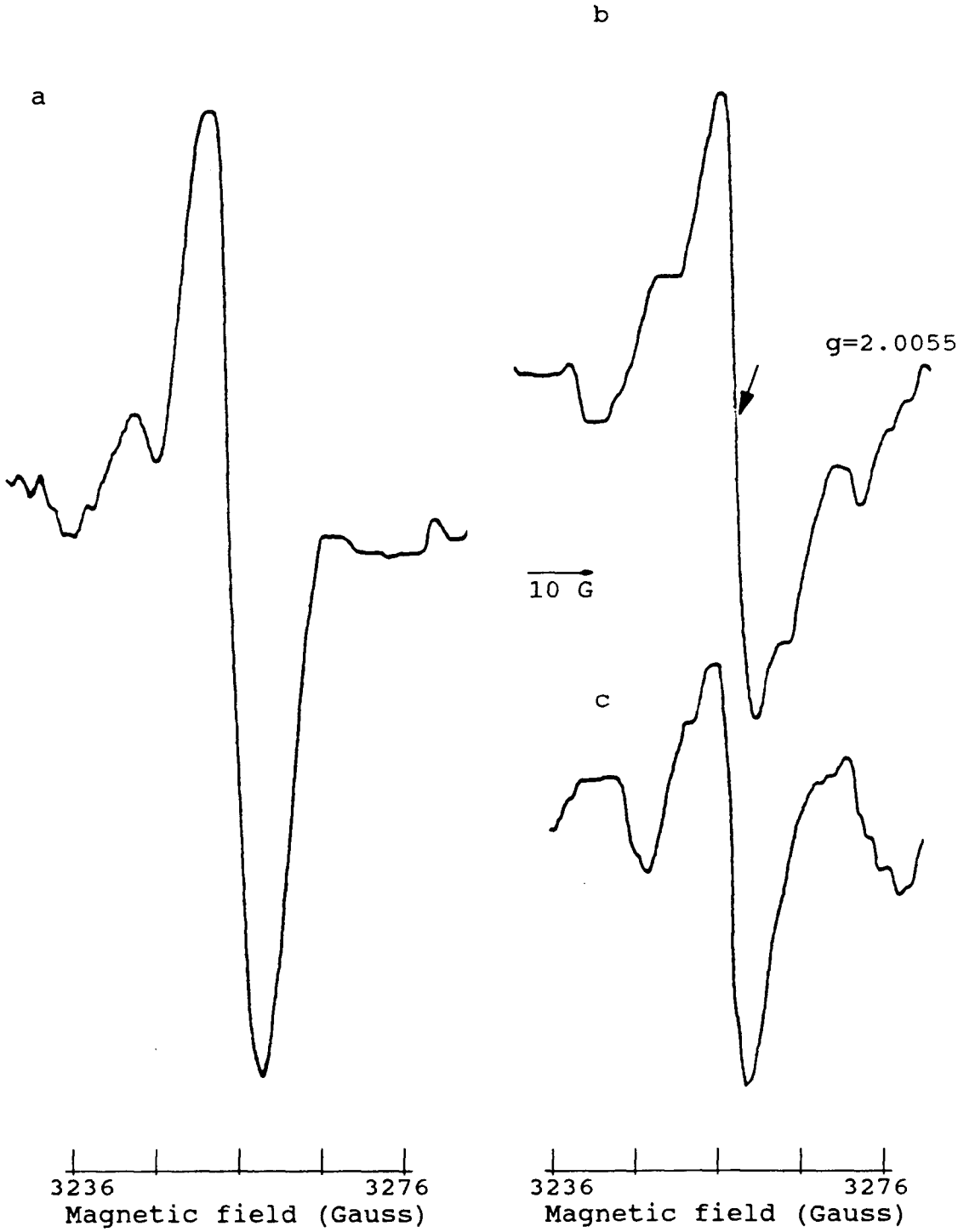

Figure 41. Differences in free-radical signals in intact, attached Kentucky bluegrass leaves after exposure to 0.5ppm ozone for 1.5 hours. a. Difference in signal obtained in 710nm light; b. Difference in signal in darkness; c. True change in 710nm light-induced signal (Figure 41a - 41b). Microwave frequency - 9.190.

fumigation with 500ppb O_3. Figure 41a was obtained by subtracting the 710nm light-induced signal obtained at the start of the experiment from the 710nm light-induced signal after 1.5 hours of fumigation. However, this difference in signal is composed of the change in free radical formation which occurs in darkness, and the change which occurs under 710nm light. This high ozone treatment was found to result in an appreciable change in the true dark signal as shown in Figure 41b. This figure was obtained by subtracting the signal obtained in darkness at the start of the experiment from the signal obtained in darkness after 1.5 hours of fumigation. This new symmetrical 'dark' free-radical signal (Signal N_{O2}) has a g-value of 2.0055 and a line width of 7-8 gauss. These parameters are similar to the those of Signal N_{710} discussed in Section 3.3.4.1, but the signals are clearly different as formation of Signal N_{710} is dependent upon irradiation of the leaf while in the spectrometer cavity, while this 'dark' signal (Signal N_{O2}) is present in the absence of leaf irradiation at the time of measurement. The real difference in the 710nm light-induced signal is shown in Figure 41c, obtained by subtracting Figure 41b from Figure 41a.

However, the signal shown in Figure 41c still includes the 710nm light-induced signal (Signal N_{710}) discussed in Section 3.3.4.1 (see Figure 40b), which is not dependent upon fumigation. When this signal, shown in Figure 40b, is also

subtracted from the signal in Figure 41c, the signal shown in Figure 42a is revealed. This latter signal (Signal N_{Sox}) is asymmetrical, has a g-value of 2.001, a line width of approximately 10 gauss and shows a small rise in the g=2.08 region. The latter feature (Figure 42a) alone, could be dismissed as 'noise', but combined together with the other identifying parameters, indicates that this signal has the attributes of the signal assigned to the superoxide anion radical (Knowles et al. 1969; Ballou et al. 1969; Bray et al. 1970). For purposes of comparison, an example of the superoxide signal from the relevant literature is shown in Figure 42b (Figure 8c from Ballou et al. 1969). Once it has been induced, Signal N_{Sox} can also be revealed by simply subtracting the signal obtained in darkness after fumigation from the signal obtained under broad-band white light after fumigation. This is shown in Figure 42c. There is no evidence for the detection of Signal N_{Sox} in darkness.

If fumigation is continued for another hour, with the leaf still maintained in 710nm light, Signal I is eliminated. Upon elimination of Signal I, the free radical changes are irreversible upon termination of fumigation, even though there are no visible signs of O_3 injury at this point in time.

Signal N_{Sox} is also revealed, using the same subtraction technique, when excised pieces of radish leaves are fumigated

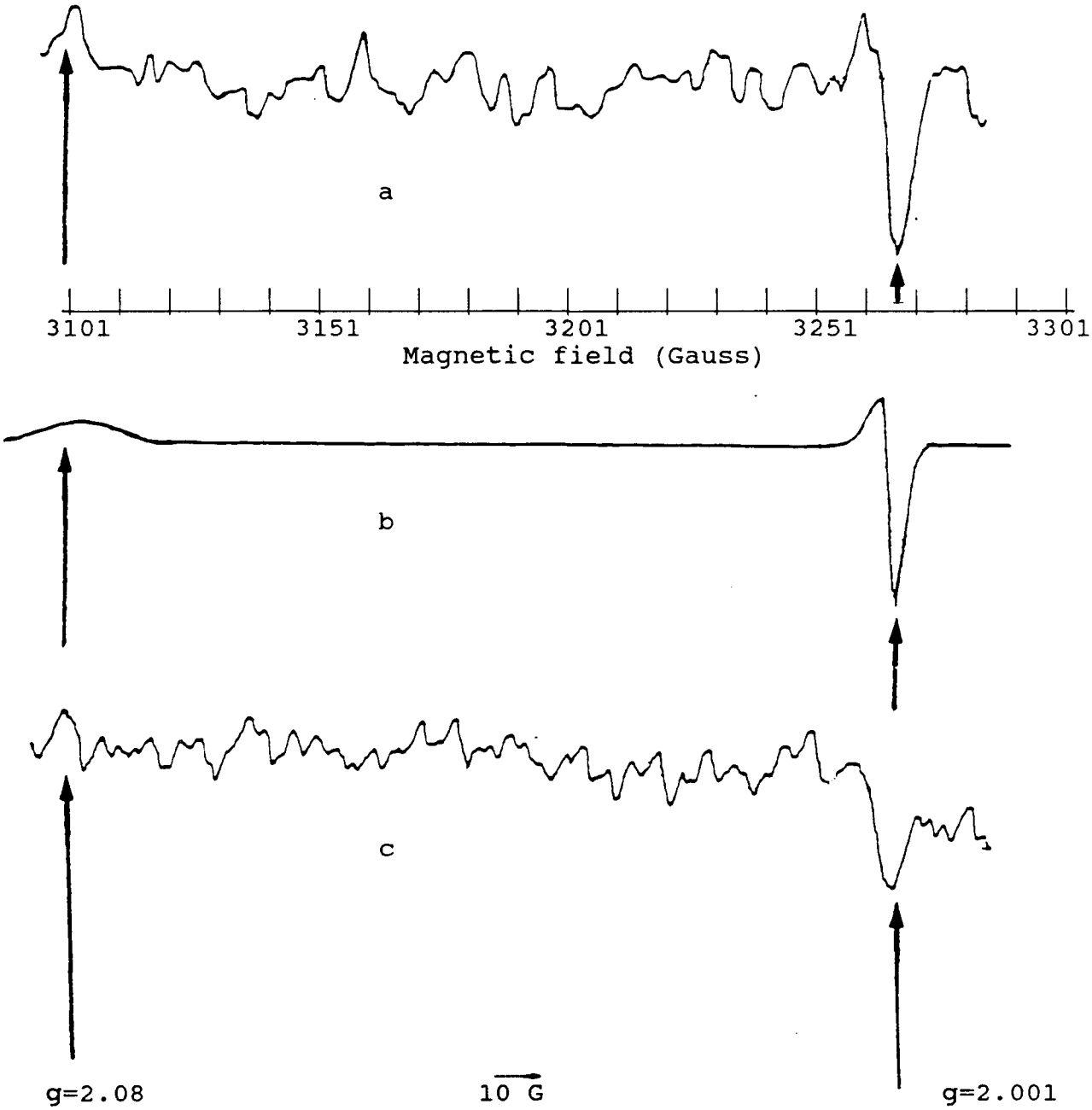

Figure 42. Light-dependent free-radical signals in intact, attached Kentucky bluegrass leaves after 1.5 hours of fumigation with 0.5ppm ozone. a. Signal N_{Sox} (Figure 41c - 40b) with ordinate doubled to facilitate comparison with Figure 42b. b. Free radical signal attributed to the superoxide anion free radical by Ballou et al. 1969; c. Difference of white light-induced signal minus dark signal after 1.5 hours of fumigation with 0.5ppm ozone. Microwave frequency - 9.190.

with 1ppm ozone for 30 minutes (data not presented). Similar changes also occur in perennial ryegrass leaves upon fumigation with high levels of O_3. However, the spectra are more difficult to interpret because of the larger Mn^{++} and Fe^{++} signals underlying the photosynthetic signals (see Section 2.4). In each spectrum shown in Figure 43, Signal II_{u+s} has been subtracted from the composite signal. These spectra show the original Signal I (Figure 43a), the increase in the combined dark and 710nm light-induced signal after fumigation of perennial ryegrass leaves with 1ppm O_3 for 30 minutes (Figure 43b), the dark signal increase after this fumigation (Figure 43c) and the small increase in the 710nm light-induced signal after subtraction of the dark signal increase (Figure 43d). The new dark signal (Figure 43c) is clearly the same as that found in Kentucky bluegrass leaves (Signal N_{O2}) (Figure 41b) but the shifts in the metal signals distort the light-induced signal (Figure 43d) to the extent that attribution to the superoxide anion radical, or any other specific free-radical signal, is not possible from these ryegrass leaf spectra.

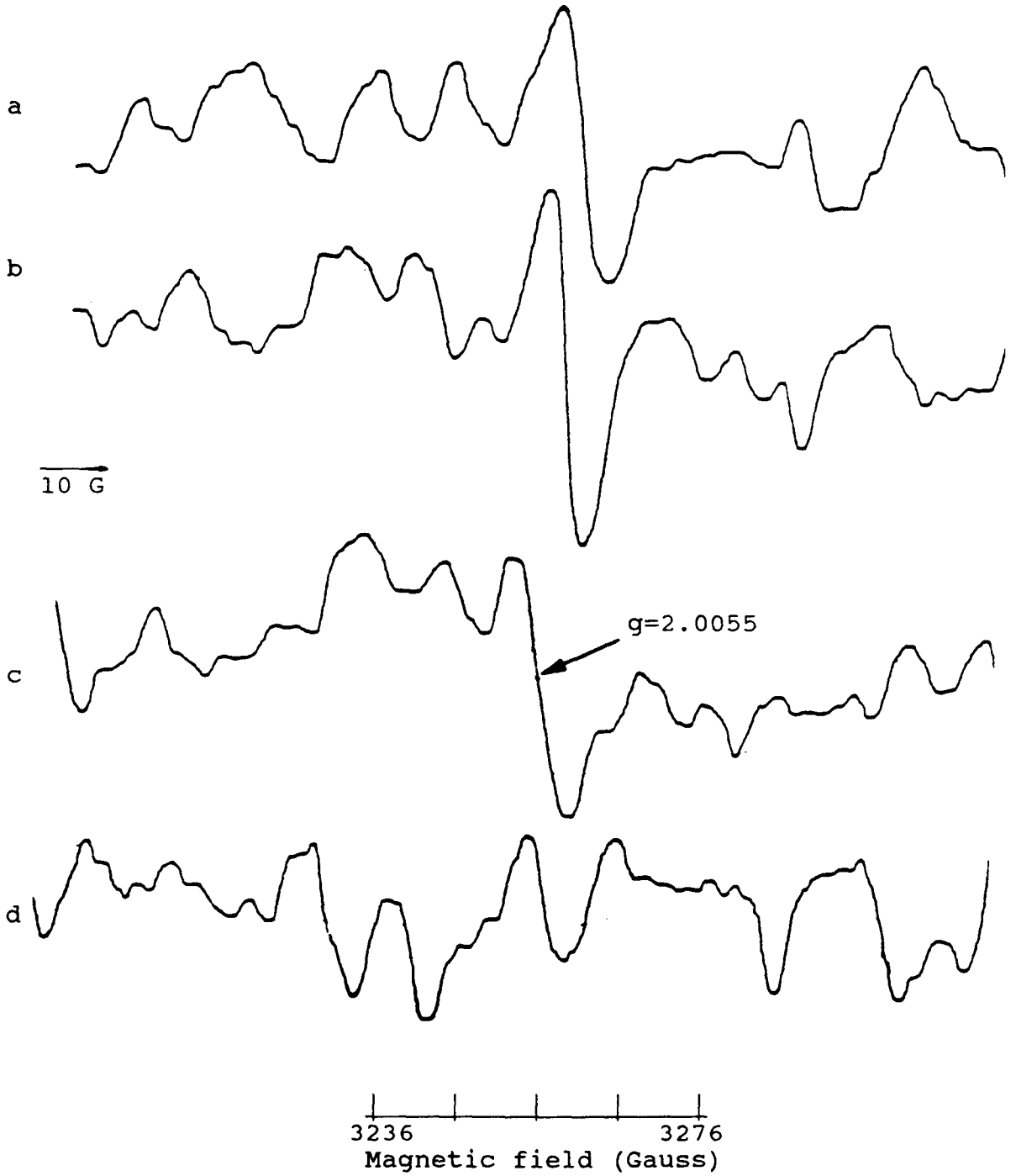

Figure 43. Free-radical signal differences in intact, attached perennial ryegrass leaves fumigated with 1ppm ozone for 30 minutes after subtraction of initial Signal II_{u+s}. a. Signal I prior to fumigation; b. Difference in 710nm light-induced signal after fumigation with 1ppm ozone for 30 minutes; c. Difference in dark signal after fumigation with 1ppm ozone for 30 minutes; d. Apparent new signal induced by ozone fumigation in 710nm light (Figure 43b -43c).

4.4 Discussion

The studies with different levels of O_3 indicate that total exposure to the pollutant substantially affects the response within the plant. Fumigation with low levels of ozone (up to 80ppb) for periods up to 8 hours failed to reveal any distinct or consistent changes in EPR spectra from those associated with unfumigated leaves.

Studies with intermediate levels of O_3 (80-250ppb) indicate that two independent events occur. First, there is the initiation of the formation of a new free radical depicted as Signal N_{O1}, with a g-value of 2.0041 and a peak-to-peak width of approximately 10 gauss. This radical is not dependent upon light as it is formed in darkness, under broad-band white light and in 710nm light. The initial appearance of this signal in darkness and white light is shown in Figures 36a and 36c, respectively. The presence of this signal is apparent in Figure 36b in the larger peak-to-peak line width and change in g-value of the 710nm light-induced signal. At this time, Signal I is still present in Figure 36b. After another hour of fumigation, Signal I has disappeared (Figure 37b) and Signal N_{O1} has reached a maximum (Figures 37a,37b and 37c), regardless of light regime. Apparently, the light-induced oxidation of the reaction centre chlorophyll a which results in the formation of Signal I has been interrupted as a result of fumigation. The loss of

Signal I is reversible but the length of time required to restore it after termination of fumigation is dependent upon total exposure. The identity of the species giving rise to Signal N_{O1}, having a g-value of 2.0041 and a peak-to-peak width of approximately 10 gauss, can not be ascertained from these data. However, it is possible that the free radical concerned is responsible for the elimination of Signal I.

At high concentrations of O_3 (500ppb) Signal I is also lost at approximately the same rate. However, prior to this loss there is the emergence of a different free-radical signal (Signal N_{O2}), which is also not light-dependent. This is not the same signal (Signal N_{O1}) which appears at lower concentrations, since Signal N_{O2} has a g-value of 2.0055 and a line width of 7-8 gauss. This signal may be due to the precursor of the 'organic' free-radical signal found in aged plant material (Mishra et al. 1971; Priestley et al. 1980).

The appearance of the small light-induced signal (Signal N_{Sox}) which has the characteristics of the signal ascribed to the superoxide anion radical is likely an effect of the damage caused by the other free radicals which have been created as a result of fumigation with O_3. This signal appears after the other free-radical signals have been formed and is probably the result of accelerated senescence, caused by the other free radicals. The sequence of events makes it unlikely that the

free radical depicted as Signal N_{Sox} is the precursor of damage. In young, healthy leaves, free-radical scavengers such as superoxide dismutase (SOD), α-tocopherol (Vitamin E), ascorbic acid (Vitamin C), catalase and β-carotene counter the effect of toxic species such as the superoxide and hydroxyl free radicals, and singlet oxygen. However, in aged tissue the capacity of plant tissue to scavenge these deleterious compounds decreases because activity of the scavengers declines with aging (Thompson et al. 1987). Hence, if the formation of free radicals depicted as Signals N_{O1} and N_{O2} accelerates tissue senescence, the scavenging capacity of the plant tissue will be reduced over time. Alternatively, the cumulative effect of continued fumigation with high levels of O_3 may overwhelm the capacity of the anti-oxidant scavengers even if their activity stays constant over the fumigation period. In either case, the lag time prior to the formation of Signal N_{Sox} seen in this study would be expected.

The discovery of the small 710nm light-induced signal (Signal N_{710}) which occurs in the first hour of exposure to far-red light was crucial to correct subtraction of signals in these ozone-fumigation studies. Prior to discovery of this signal, data from the start of exposure to 710nm light were used as the base which must be subtracted from data at any other time to establish the change in the 710nm light-induced signal caused by exposure to O_3. However, with the discovery of this signal

it became apparent that it was necessary to include this signal as a part of the base-line data, since otherwise its presence would confound results. The true effects of fumigation with O_3 can be obtained using the complex series of subtractions described in Section 4.3.3. Alternatively, they can be revealed by using the data obtained once the small signal has been induced, as the base which needs to be subtracted. This latter approach is only valid if no changes have occurred in the dark signal in the interval.

5.0 SULPHUR DIOXIDE STUDIES

5.1 Introduction

In an effort to increase knowledge of the mechanisms through which SO_2 affects vegetation, numerous investigators have studied the biochemical (Ewald and Schlee, 1983; Malhotra and Hocking, 1976; Malhotra and Sarkar, 1979; Robinson and Wellburn, 1983; Wellburn et al. 1981) and physiological changes (Le Sueur-Brymer and Ormrod, 1984; Majernik, 1971; Majernik and Mansfield, 1971, 1972; Taylor and Tingey, 1981) which occur in plants exposed to SO_2. One metabolic process affected by exposure to SO_2 is photosynthesis (Black et al. 1982; Carlson, 1979, 1983a, 1983b; Thomas and Hill, 1937). The vast majority of studies indicate that exposure to SO_2 causes reductions in the photosynthesis of plants (Lamoreaux and Chaney, 1978; Ormrod et al. 1981; Takemoto and Noble, 1982; Winner and Mooney, 1980), although little is known of the mechanisms of toxicity.

At the molecular level, the formation of toxic free radicals has been postulated as one of the primary events in the processes by which air pollutants such as SO_2 may adversely affect photosynthesis (Tanaka and Sugahara, 1980). A general pollutant-induced production of the superoxide and other radicals has been proposed as the primary cause of impairment of membrane function throughout the cell after pollutant uptake

(Mudd, 1973,1982).

These studies were carried out with leaves or chloroplast preparations from leaves after fumigation with SO_2. In order to determine the changes in free radicals which occur during fumigation, the present study investigated the <u>in vivo</u> EPR-detectable changes in Signals I and II_{u+s} during fumigation with SO_2.

5.2 Methods

Plant materials, and the experimental protocols used, were essentially the same as those described earlier (Sections 3.2 and 4.2). Preliminary investigations showed that, in radish, the magnitude of Signal I, Signal II_{u+s} and the Mn^{++} signal varied from leaf to leaf, even if the chronological ages of the leaves were identical. The least variation in signal intensity occurred with leaves of similar age which were also visually comparable in terms of greenness. Subsequent investigations showed that greater consistency could be obtained by sequentially using different segments of the same leaf. Thus, the experiments using radishes described below which included several treatments were done by using excised segments from the same leaf to obtain control and treatment data. Leaf segments were cut parallel to the midrib. In order to minimize aging effects and concomitant signal perturbation (Section 3.3.1), the

leaves from which the laminar segments were excised were not detached from the radish plants.

Instrument settings for all kinetic traces were as follows: time constant 0.250s; modulation 1.0 x 10 gauss; receiver gain $5.0x10^4$; power 10mW. For other traces the instrument settings were as described previously (Section 3.2).

SO_2 was controlled by injecting a SO_2 in air mixture into a medical grade air stream flowing at a rate of 2 l/min through a mixing chamber. SO_2 concentrations in the cavity were monitored with a Thermoelectron Model 43 SO_2 monitor.

5.3 Results

5.3.1 Detached Radish Leaf Segments

5.3.1.1 Signal I Studies

Numerous experiments were conducted using excised pieces of radish leaves. Because of the limited 60 minute period available (Section 3.3.1) for studying signal dynamics in detached leaf pieces, a wide range of concentrations (up to 400ppm) was used. Hence, the results presented in this section should be viewed with caution in relation to their relevance to changes induced by polluted atmospheres.

For Signal I (attributed to Photosystem I) kinetic studies, changes in the low field maximum were followed (see Figure 8). This peak was chosen to avoid possible confusion with changes which may occur in Signal II_{u+s} (attributed to D, a component of Photosystem II). Signal II_{u+s} is present in healthy leaves, regardless of the immediate light regime, unless the leaf has been held in absolute darkness for over 24 hours. However, it does not interfere with tracking the low field Signal I maximum at this point because this is the point at which the baseline crossover of Signal II_{u+s} occurs. Previous light adaptation effects (Tikhonov and Ruuge, 1975a) were standardized by exposing the leaf segment to 30 seconds of 710nm light followed by 3 minutes of darkness in the cavity. The leaves were then illuminated with the appropriate light.

Figure 44 shows kinetics of signals from unfumigated leaves. Signal I was not formed in darkness, a very small increase occurred under 650nm light, a large Signal I was induced by 710nm light and an intermediate size signal was formed under illumination with broad-band white light. The kinetics of the dark, 650nm and 710nm signals were consistent from leaf to leaf, differing only in signal magnitude. However, the multiphasic kinetics of the white light signal varied considerably. Similarly, the initial rise and increase in signal intensity in the second half hour after detachment of the leaf from the plant also varied from leaf to leaf. Major

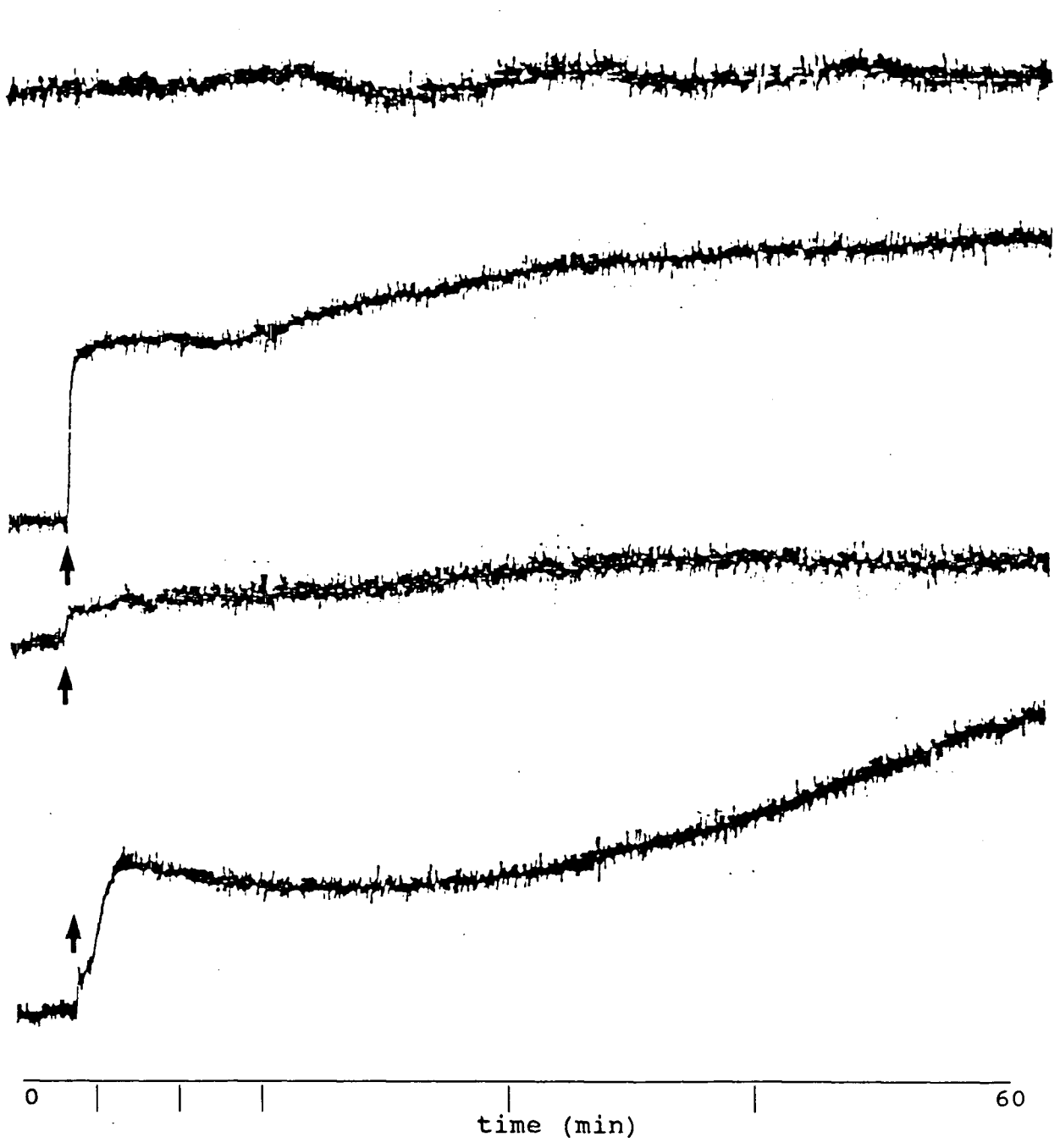

Figure 44. Kinetics of Signal I formation in excised unfumigated radish leaf pieces in different light regimes. a. dark; b. 710nm light; c. 650nm light; d. white light. All traces begin in darkness; arrows (↑) indicate time at which light was turned on.

differences occurred even in segments from the same leaf. Thus, the white-light induced traces shown in Figure 44d can only be regarded as a general outline of white light signal kinetics.

Figure 45 indicates changes in Signal I kinetics which occurred upon fumigation with a high concentration of SO_2, approximately 400ppm. Following the start of fumigation no changes occurred in the dark signal (Figure 45a), but under 710nm light, (Figure 45b), needed to invoke Signal I in healthy leaves, there was a small increase in signal magnitude that commenced after 30 to 45 seconds of fumigation. This was superimposed upon the Signal I normally induced by 710nm light. However, this difference in signal was so small that, even with signal subtraction, it could not be positively ascribed to either an increased Signal I or to a new free-radical signal which overlaps Signal I. Under 650nm light, which invokes virtually no Signal I response in healthy leaves (Figure 44c), an increase in signal intensity began after 30 to 45 seconds of fumigation, and the signal (Figure 45c), after 50 minutes, was comparable in magnitude to the 710nm light-induced signal. A similar increase, induced by SO_2, was observed in the signal induced by white light (Figure 45d).

On termination of fumigation (50min SO_2) the relative sizes of the three light signals had changed markedly. The absolute signals varied from leaf to leaf, but, in all cases,

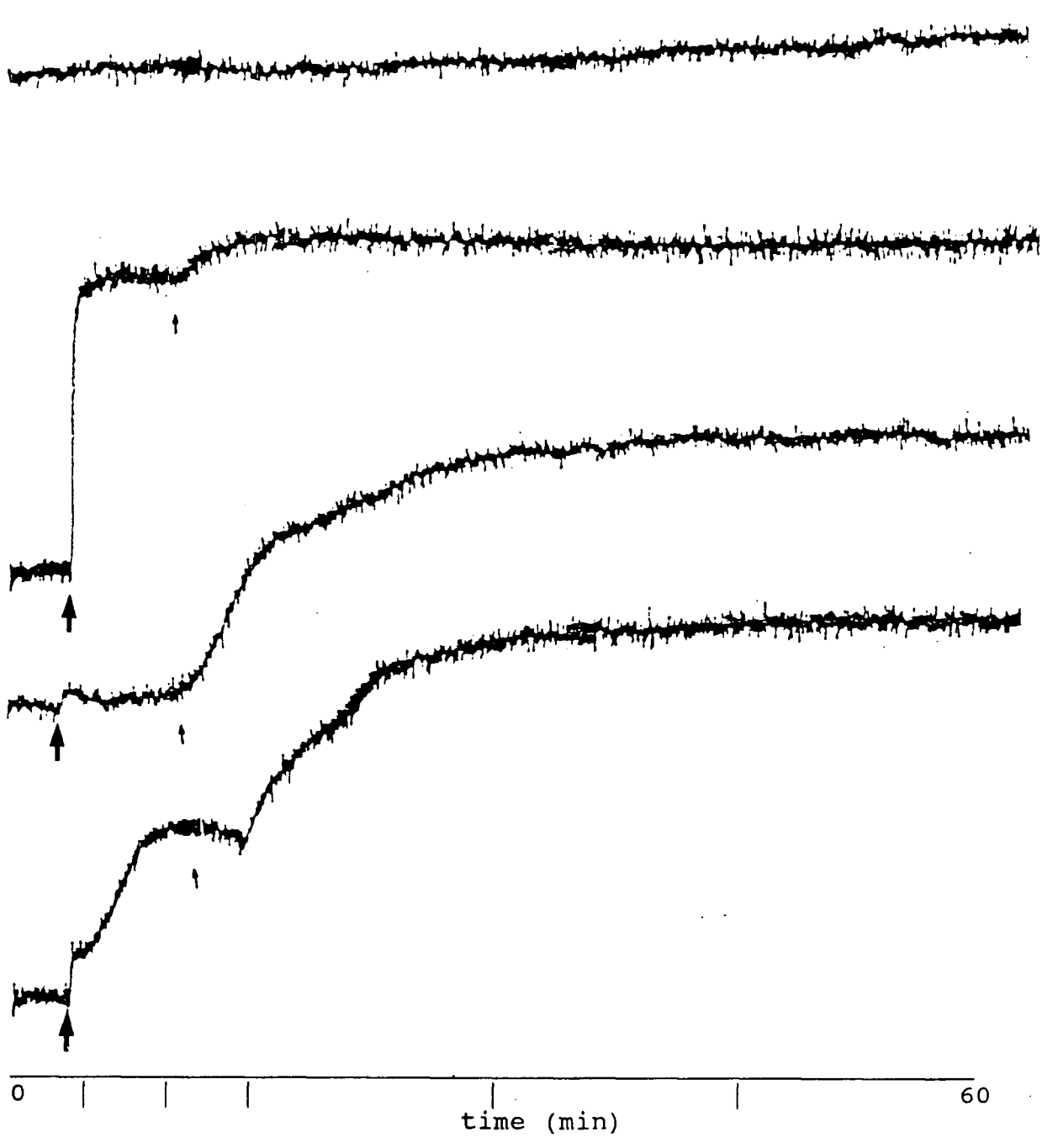

Figure 45. Kinetics of Signal I formation in SO_2-fumigated (400ppm) radish leaf pieces in different light regimes. a. dark; b. 710nm light; c. 650nm light; d. white light. All traces begin in darkness; large arrows (↑) indicate time at which light was turned on; small arrows (↑) indicate time at which SO_2 fumigation began.

were correlated with the size of the 710nm light-induced signal from each leaf prior to fumigation. After fumigation, the white light-induced signal exceeded the 710nm light-induced signal, while the signal induced by 650nm light (which normally only invokes Signal II_{u+s}, associated with Photosystem II) was now virtually identical to the 710nm light-induced signal. Figure 46 shows the signal spectra after 50 minutes of fumigation in 650nm light. In all cases the g-values and peak-to-peak line widths are identical to those associated with the 710nm light-induced Signal I, indicating that the increased 650nm and white light signals are indistinguishable from Signal I, and are not unknown free-radical signals with similar parameters.

These changes occurred regardless of whether the fumigation took place in darkness, in 650nm light, in 710nm light or in broad-band white light. The increases in the signals appeared to be irreversible; continuation of the kinetic trace showed no decrease in the signals during the following hour.

The increase in signal intensity was directly related to the uptake of SO_2, as shown by experiments in which the duration of the exposure to SO_2 was varied. At this high level of fumigation, steady-state levels of the increased signals were achieved after fumigation times ranging from 9 to about 15 minutes, depending upon the the leaf piece used. Figure 47 shows that 2 seconds of fumigation did not induce the rise in

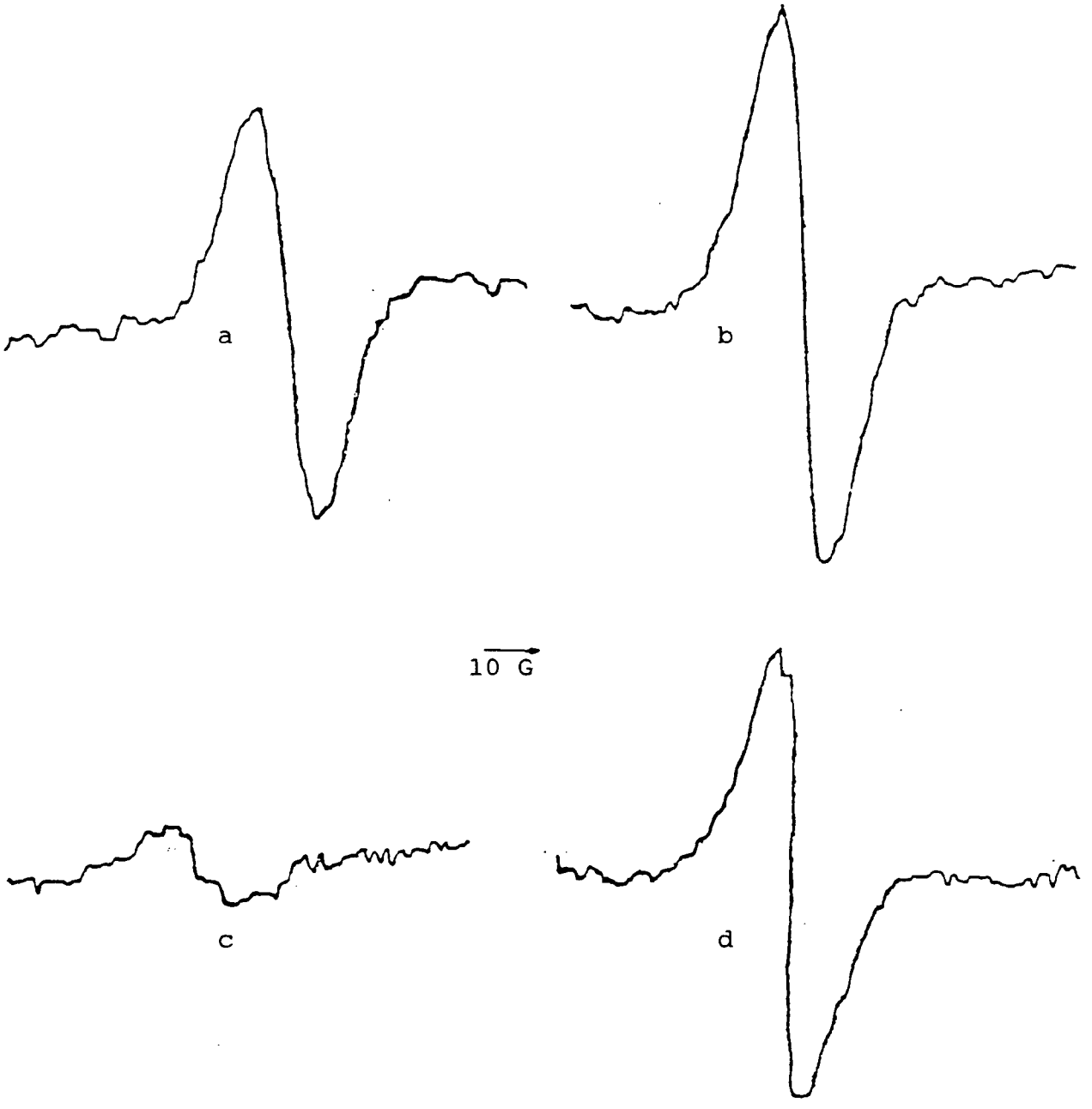

Figure 46. EPR signals in different light regimes from a radish leaf piece after 50 minutes of fumigation with 400ppm SO_2. The cavity was illuminated with 650nm light during fumigation. a. 710nm light; b. white light; c. dark; d. 650nm light.

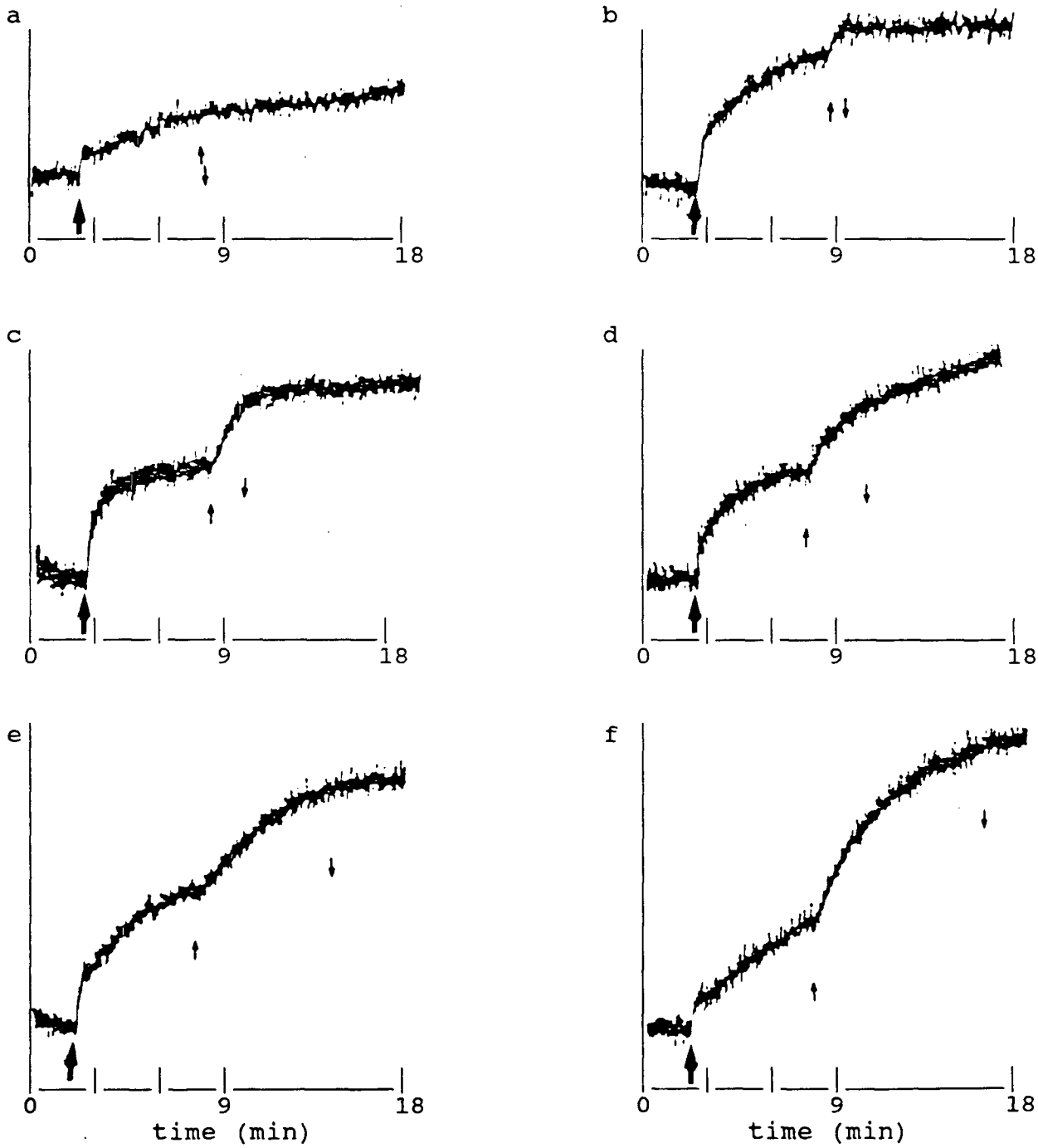

Figure 47. The effect of 400ppm SO_2 fumigation duration on the intensity of the white light-induced Signal I in excised radish leaf pieces. Traces begin in darkness; large arrows (↑) indicate time at which light was turned on; small arrows indicate time at which fumigation began (↑) and ended (↓). Fumigation duration; a. 2 sec; b. 36 sec; c. 1.5 min; d. 3 min; e. 6 min; f. 9 min.

the white light-induced signal, which became distinct within 36 seconds of fumigation. The increase in signal size became larger as fumigation time increased from 36 seconds to 9 minutes. Figure 47 also provides some indication of the variability among different leaf pieces in their response to white light, prior to fumigation, as revealed by the different magnitudes of the increases observed with the onset of illumination.

If fumigation was terminated after less than 9 minutes, the rise of Signal I under white (or 650nm light) was halted and a new steady state was attained. Subsequently, if, after achievement of this new steady-state in the signal, fumigation recommenced, then signal intensity increased to a new level, up to a maximum, for any given leaf (Figure 48).

Similar increases in the white and 650nm light-induced signals were found to occur at lower SO_2 concentrations, down to 10ppm. However, at the lower concentrations, there was a distinct lag period during which the signal remained unchanged. The data shown in Figure 49 are representative of trials with numerous leaf pieces. Exposure to 100ppm SO_2 resulted in a lag period of approximately 17.5 minutes before the increased signal could be detected, while at a fumigation level of 10ppm, the increase in signal did not occur until after 90 minutes of fumigation had taken place. For the latter observation the

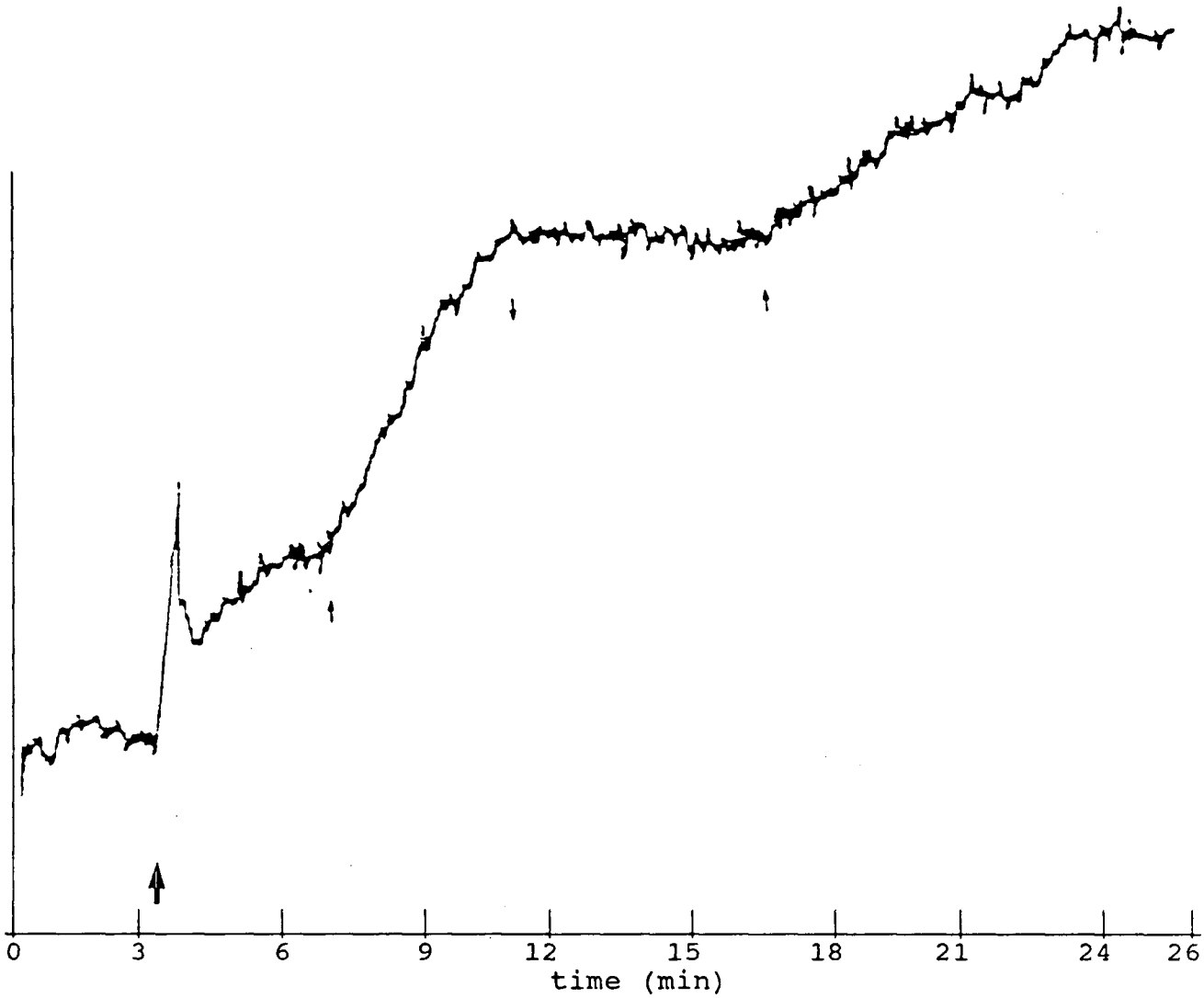

Figure 48. The effect of interruption of 400ppm SO_2 fumigation on the kinetics of the white light-induced formation of Signal I in excised radish leaf pieces. Trace begins in darkness; large arrow (↑) indicates time at which light was turned on; small arrows indicate times at which fumigation began (↑) and ended (↓).

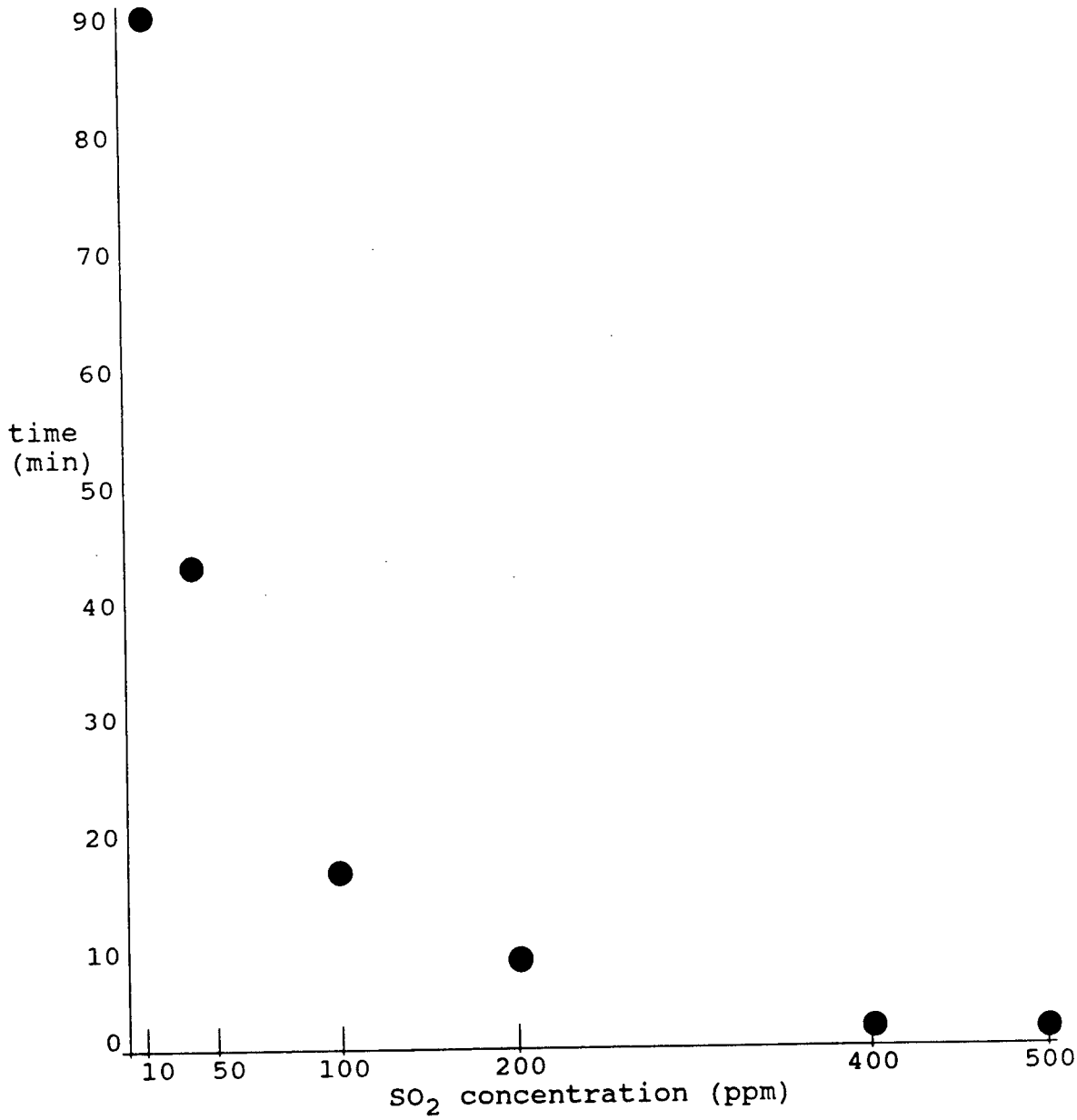

Figure 49. The lag time prior to the induction of the white light-induced Signal I in relation to SO_2 concentration.

kinetic scan was extended past 1 hour, but, despite the gradual increase in the white light signal which occurred because of aging (see Section 3.4.1), the effect of the SO_2 was discernible as a distinct jump in signal intensity at the 90 minute mark. Lowering the SO_2 concentration below 10ppm did not cause a detectable signal increase within 2 hours and the confounding aging effects discussed in Section 3.3.1 precluded the use of a longer scan period.

The effect of air flow on the kinetics of the rise in the white light-induced signal was also studied. The same increase occurred at identical SO_2 concentrations, regardless of air flow rate over the range of 1 l/min to 3 l/min (velocity 1m/s to 3m/s).

These changes in Signal I were confirmed by locking the spectrometer on the high field minimum (see Figure 8). Data from this peak are potentially confounded by the additional presence of Signal II_{u+s}, but kinetics from this peak were found to be nearly identical to those obtained from the low field peak (data not shown). The gradual decrease in Signal II_{u+s} discussed below (Section 5.3.1.3) was almost completely obscured by the much larger increase in Signal I.

5.3.1.2 Mn^{++} Signal

In healthy radish leaves the Mn^{++} signal is very small regardless of light regime. However, upon fumigation with 400ppm SO_2 the signal was found to increase gradually over 1 hour. The Mn^{++} signals from healthy and fumigated radish leaves are shown in Figure 50. The Mn^{++} signal kinetics were monitored by locking the spectrometer onto the far low field peak (see Figure 50) or onto the minimum associated with the second peak from the high field end of the spectrum. The kinetics of the increase of the overall Mn^{++} signal in the leaves fumigated with SO_2 are shown in Figure 51a, obtained by tracking the rise in the low field peak.

5.3.1.3 Signal II_{u+s}

For signal II_{u+s} studies the spectrometer was locked onto the high field minimum of Signal II_{u+s} (see Figure 8). In darkness, Signal II_{u+s} is not confounded with Signal I at this position because light is required to induce Signal I. Signal II_{u+s} was also followed at the low field maximum (see Figure 8) under all light regimes. Kinetics were identical, regardless of light; thus only the high field minimum kinetics recorded in darkness are shown in Figure 51b. Unfumigated leaves held in darkness showed a very small change in Signal II_{u+s} during one hour (Figure 44a). In contrast, leaves fumigated with 400ppm

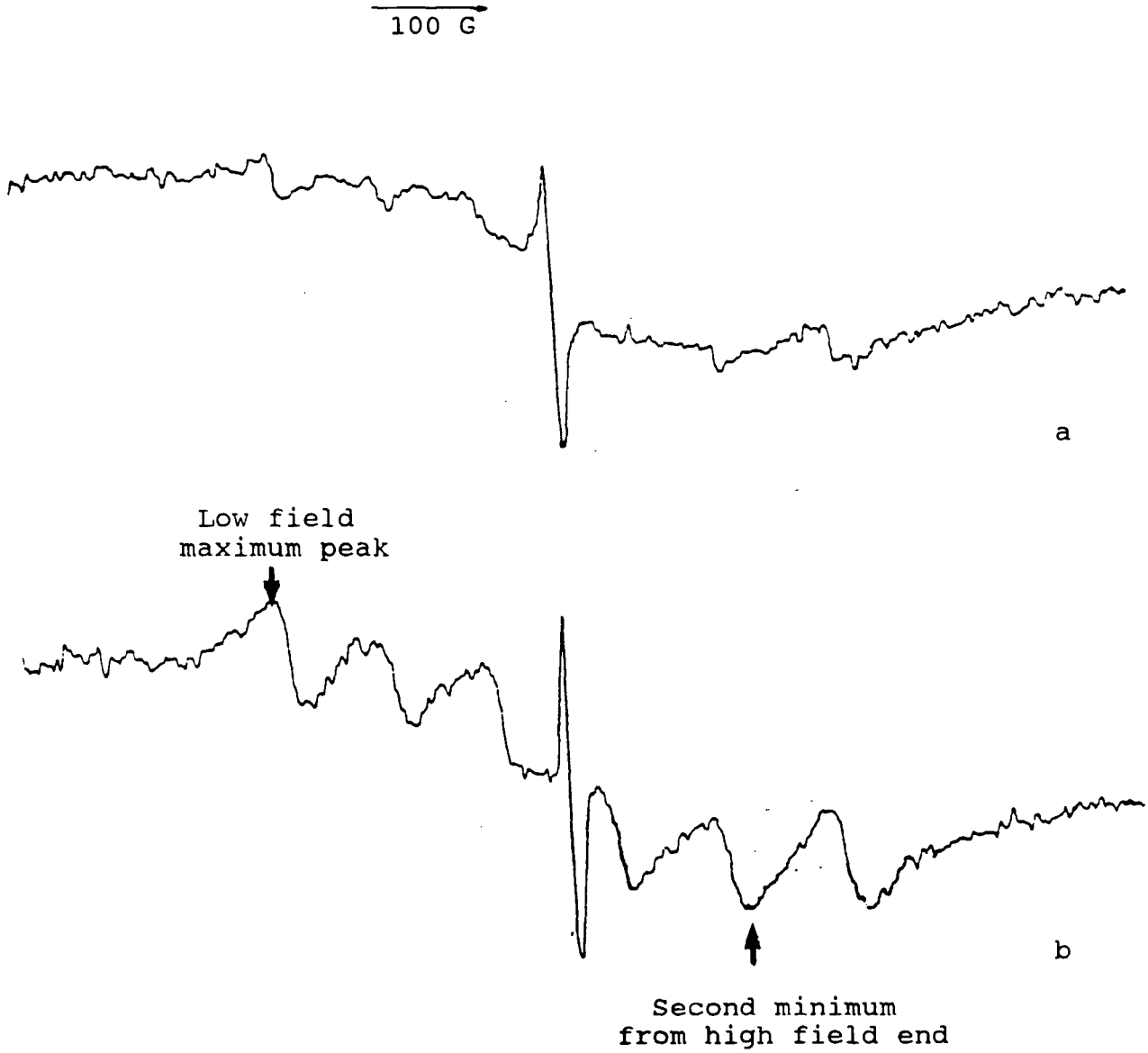

Figure 50. The Mn^{++} signal in healthy and fumigated radish leaf pieces. a. Healthy leaf; b. Same leaf after fumigation with 400ppm SO_2 for 50 minutes. The cavity was illuminated with 710nm light during fumigation and recording of the traces.

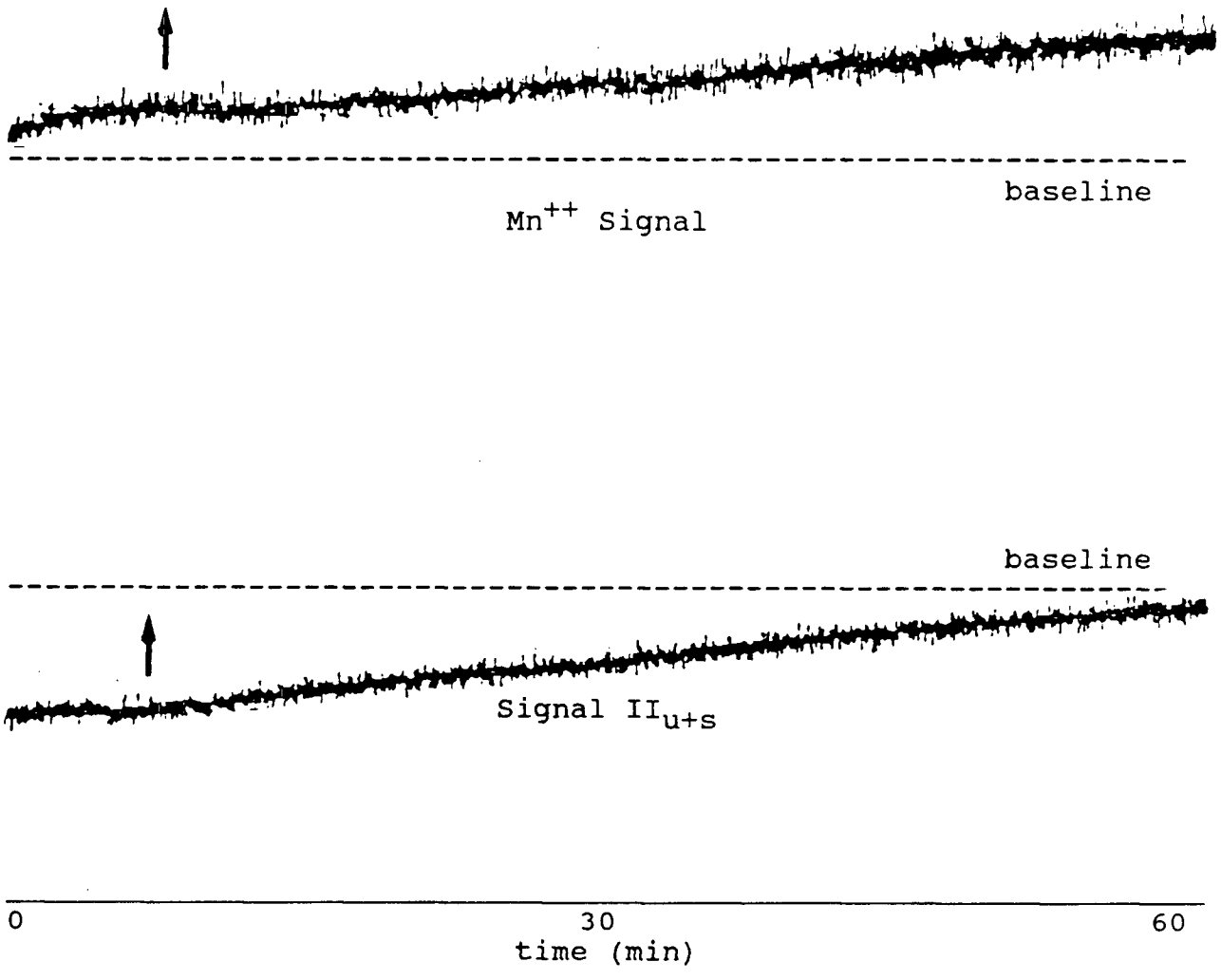

Figure 51. Comparative kinetics of the increase in the Mn^{++} signal and the decrease in Signal II_{u+s} in excised radish leaf pieces during fumigation with 400ppm SO_2. The cavity was not illuminated during fumigation and recording of traces. Arrows (↑) indicate time at which fumigation began.

SO_2, showed a gradual decrease in Signal II_{u+s} during the course of fumigation. After 1 hour of fumigation Signal II_{u+s} essentially disappeared, leaving only the small quinoidal signal shown in Figures 8c,9c.

A point of interest was the finding that curves of Signal II_{u+s} decrease and Mn^{++} signal increase had similar slopes (Figures 51a and b).

5.3.2 Attached, Intact Grass Leaves

5.3.2.1 High SO_2 Levels

At high (100-500ppm) SO_2 levels, changes identical to those which occured in Signal I under white and 650nm light in excised pieces of radish leaves, also occurred in intact, attached Kentucky bluegrass and perennial ryegrass leaves. The top traces in Figure 52 shows EPR signals from a healthy perennial ryegrass leaf held in the different light regimes prior to the start of fumigation. The bottom traces in Figure 52b show comparable signals from the same portion of the leaf after 40 minutes of fumigation with 100ppm SO_2. The leaf was illuminated with 710nm light during the fumigation period. The signal recorded in darkness (Signal II_{u+s}) has only changed marginally, while large differences have occurred in the signals recorded in 650nm, 710nm and broad-band white light. The

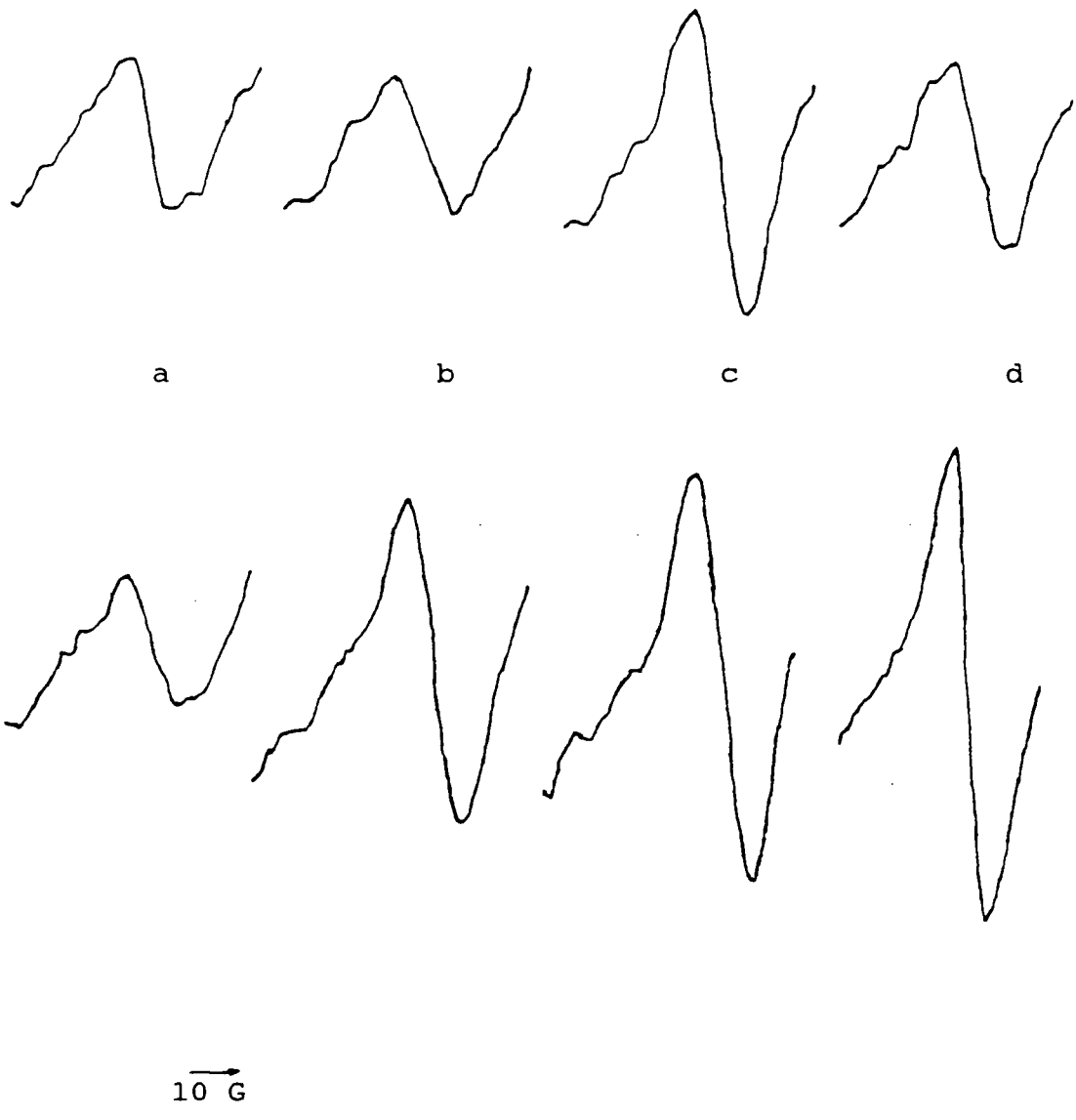

Figure 52. EPR signals from healthy and SO_2-fumigated attached, intact perennial ryegrass leaves. Top = healthy leaf; Bottom = same leaf after 40min fumigation with 100ppm SO_2. Spectra recorded in a. darkness; b. in 650nm light; c. in 710nm light; d. in white light. The cavity was illuminated with 710nm light during fumigation.

kinetics of the changes could not be accurately followed because of shifts in the Mn^{++} and Fe^{++} signals which underly the photosynthetic signals. However, it was apparent that very high concentrations of SO_2 caused a more rapid increase in the signals then comparatively low concentrations. As with radish, similar changes in the 650nm and broad-band white light-induced signals occurred with SO_2 concentrations of 100, 200, 300, 400 and 500ppm if the plants were fumigated in darkness, 650nm light, 710nm light or broad-band white light (data not shown).

5.3.2.2 Low SO_2 Levels

The use of intact leaves allows for longer time periods of fumigation at lower concentrations without the confounding of results caused by the artificial aging (see Section 3.3.1) which occurs with excised leaf pieces. Results with Kentucky bluegrass and perennial ryegrass were identical. The spectra presented here were obtained from Kentucky bluegrass leaves, which reveal the smaller Mn^{++} signals, thus allowing more reliable calculation of g-values and line widths.

Figure 53 shows the 710nm light-induced EPR signals of a Kentucky bluegrass leaf recorded prior to fumigation (Figure 53a) and after 120 minutes fumigation with 600ppb SO_2 (Figure 53b). It also shows the signal induced by white light after 120 minutes of fumigation with 600ppb SO_2 (Figure 53c). The

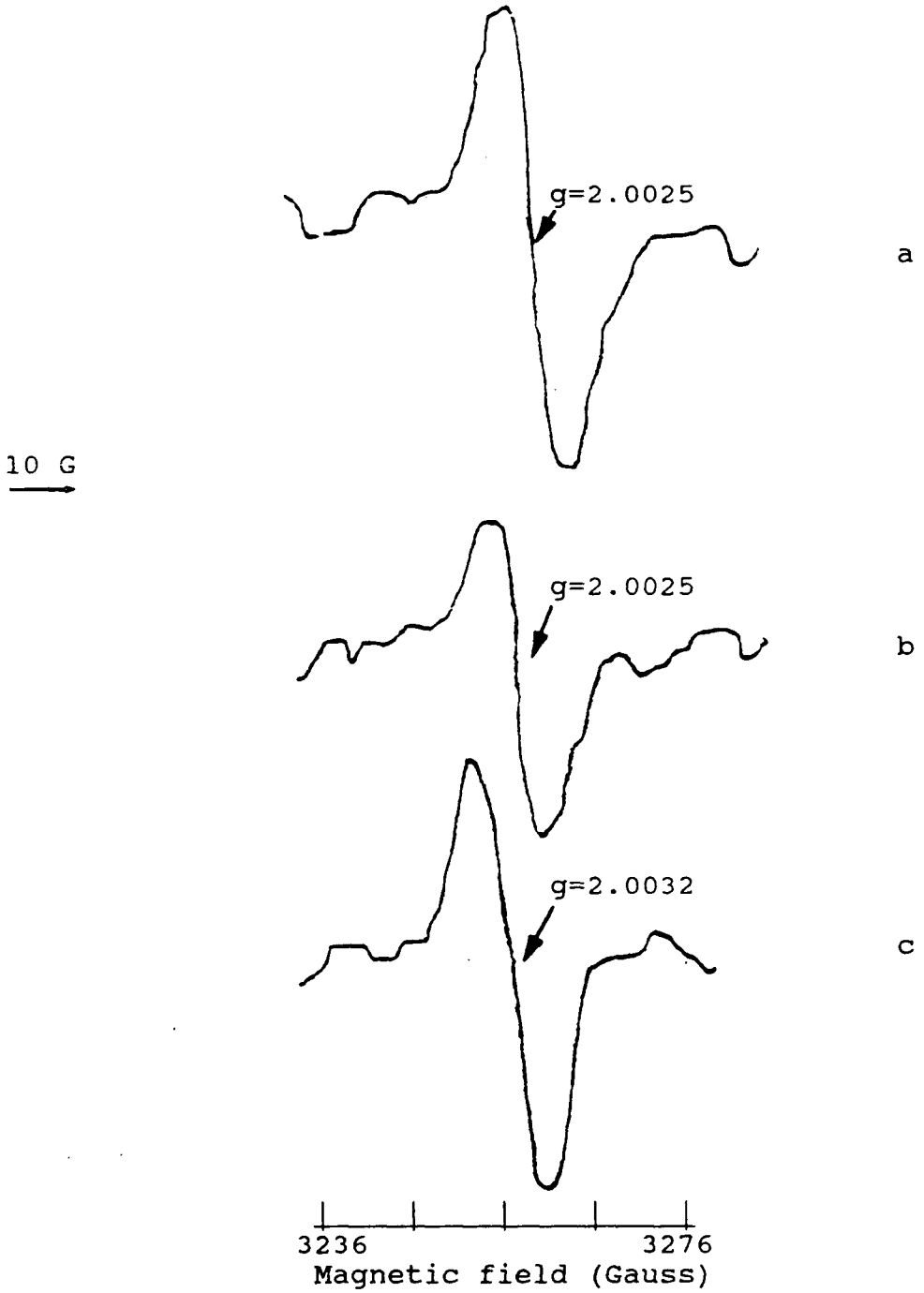

Figure 53. Light-induced EPR signal changes in attached, intact Kentucky bluegrass leaves fumigated with 600ppb SO_2. The cavity was illuminated with 710nm light during fumigation, except when traces were recorded in darkness and in white light. All traces indicate the signal obtained by subtracting Signal II_{u+s}, obtained in darkness, from the signal obtained in light. a. In 710nm light, prior to fumigation; b. In 710nm light, after 120min fumigation; c. In white light; after 120min fumigation. Microwave frequency - 9.190.

traces in these figures were obtained by subtracting Signal II_{u+s}, obtained in darkness, from the combined signals obtained in 710nm light and in white light. The leaf was maintained in 710nm light during the fumigation period except during the recording of the signals obtained in darkness and in white light. Figure 53b indicates a diminuation of Signal I after 120 minutes of fumigation as the g-value and peak-to-peak width of this signal are identical to those of Signal I shown in Figure 53a.

In contrast, Figure 53c indicates the formation of a new free radical when the fumigated leaf is exposed to broad-band white light. This new white light-induced signal (Signal N_{S1}) appears to be similar to Signal I but has a higher g-value and slightly larger line width. The peak-to-peak line widths of Signal I and Signal N_{S1} are 7.5 and 8.0 gauss, respectively. Such a small difference could be attributed to recorder error, especially as Signal I line widths ranging from 7.5 to 9.0 gauss are reported in the literature, but the g-values are clearly different: Signal I has a g-value of 2.0025 while Signal N_{S1} has a g-value of 2.0032. Thus, it is clear that this is a new signal, not a white light-induced Signal I.

If fumigation is continued beyond 120 minutes, further changes occur. Figure 54 shows the EPR difference signals when fumigation is continued for an additional 60 minutes. After 180

minutes of fumigation with 600ppb SO_2, Signal I is no longer present when the leaf is illuminated with 710nm light and a different free-radical signal (Signal N_{S2}) is revealed (Figure 54a). Figure 54b shows the white light-induced signal after 180 minutes of fumigation. Once again, to obtain the signals shown in Figures 54a and 54b, Signal II_{u+s}, recorded with the leaf in darkness, has been subtracted out from the combined spectra obtained with the leaf held in 710nm and broad-band white light. Figure 54c, obtained by subtracting the spectrum in Figure 53c from that in Figure 54b, shows the change in the white light-induced signal which occurs in the interval between 120 and 180 minutes of fumigation with 600ppb SO_2. This signal is indistinguishable from Signal N_{S2} shown in Figure 54a.

Signal N_{S2}, shown in Figures 54a and 54c, is nearly identical in line shape and peak-to-peak width to the radical pair signal first shown by McIntosh and Bolton (1979). The published g-values for this signal vary from 2.0026 to 2.0051, depending upon the orientation of the sample (Hoff, 1984). The g-value of Signal N_{S2} is 2.0042.

These changes in the 710nm and white light-induced signals are long-lived, but not permanent. If the leaf is exposed to clean air for 1 hour after the end of fumigation there is no change in the new signals (spectra not shown), but if the leaf

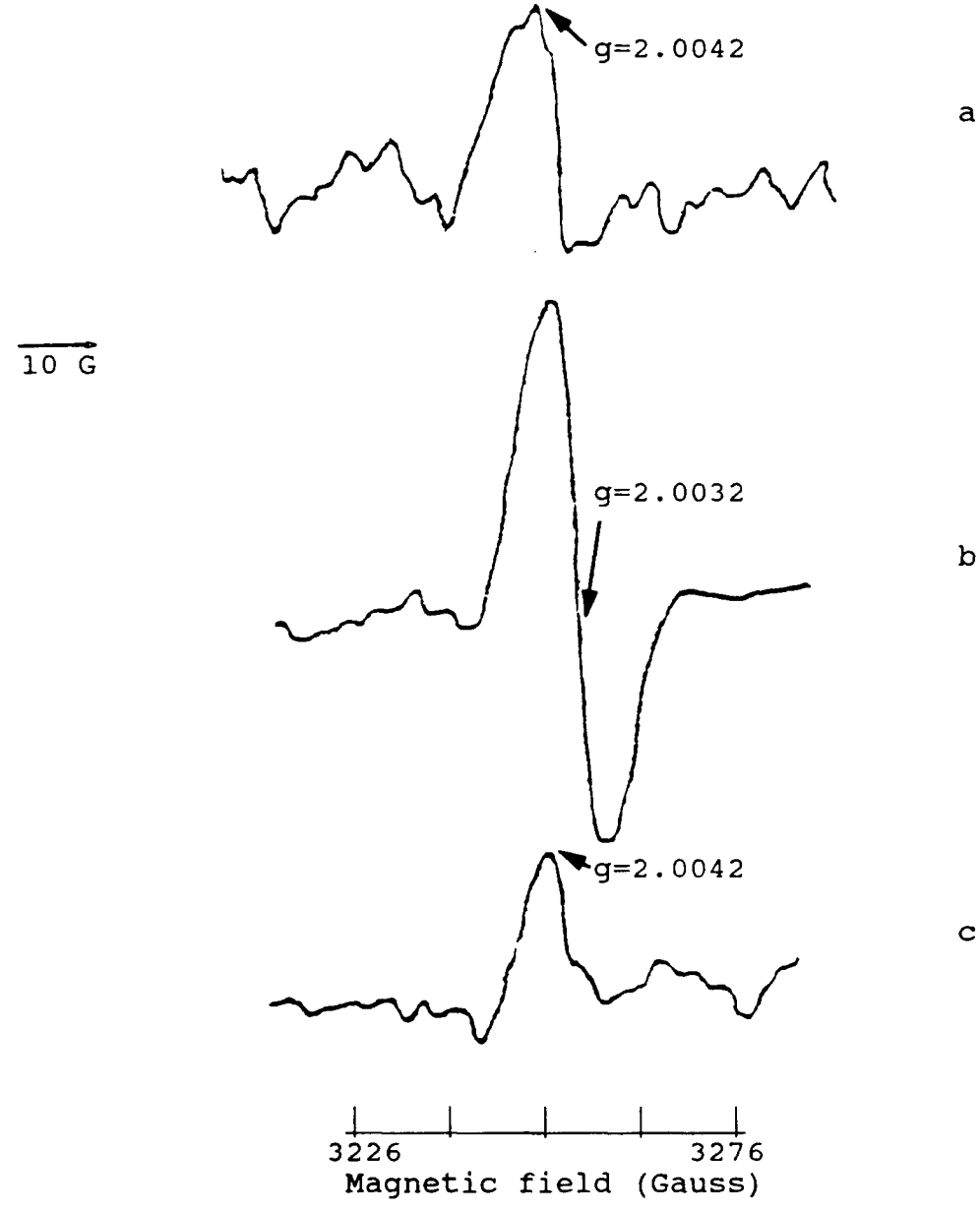

Figure 54. Light-induced EPR signal changes in attached, intact Kentucky bluegrass leaves fumigated with 600ppb SO_2. The cavity was illuminated with 710nm light during fumigation, except when traces were recorded in darkness and white light. All traces indicate the signal obtained by subtracting Signal II_{u+s}, obtained in darkness, from the signal obtained in light. a. In 710nm light, after 180min fumigation; b. In white light, after 180min fumigation; c. Change in white light signal between 120 and 180 min fumigation (Figure 54b - 53c). Microwave frequency - 9.190.

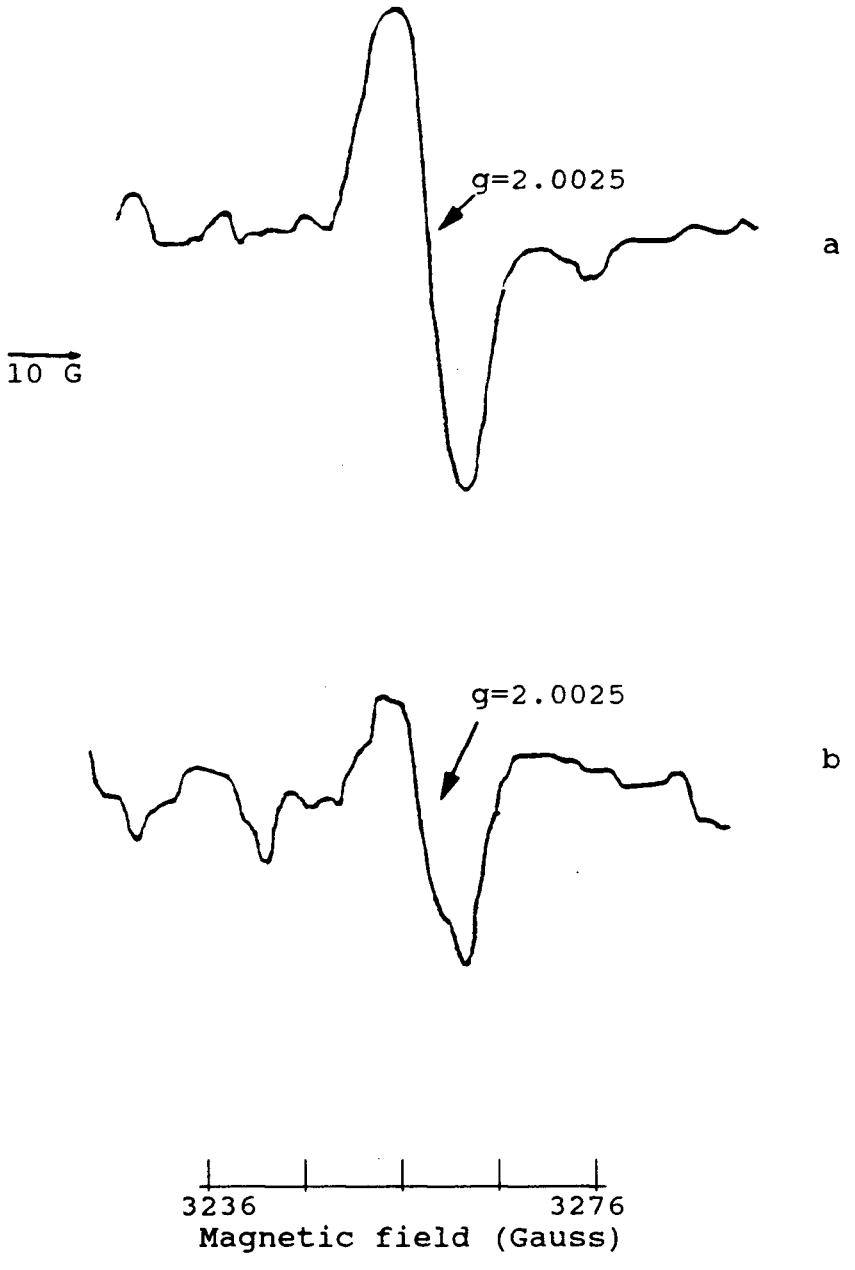

Figure 55. EPR 710nm light-induced and white light-induced signals in intact, attached Kentucky bluegrass leaves 16 hours after termination of fumigation with 600ppb SO_2. Traces indicate the differences after Signal II_{u+s}, obtained in darkness, was subtracted from the signals obtained in 710nm and broad-band white light. The cavity was illuminated with 710nm light during the 16 hour exposure to clean air. a. In 710nm light; b. In white light. Microwave frequency - 9.190.

is maintained in clean air for 16 hours, under 710nm light, most SO_2-caused changes have disappeared (Figure 55). Approximately 95 per cent of the 710nm light-induced Signal I has recovered (cf. Figures 55a and 53a) while all of the white light-induced signal caused by SO_2 (Signal N_{S1}) has disappeared, being replaced by a small white light-induced Signal I (cf. Figures 54b and 55b). Signal N_{S2} has also disappeared.

However, if fumigation is continued beyond 180 minutes, the signal which has parameters similar to the superoxide anion radical signal discussed in Section 4.3 is formed. Figure 56 shows this signal (Signal N_{Sox}) after 240 minutes of fumigation with SO_2. This signal was obtained through subtraction of the white light-induced signal after 180 minutes of fumigation from the white light-induced signal after 240 minutes of fumigation. Once this stage is reached Signals N_{S1} and N_{S2} appear to be irreversible as subsequent exposure to 24 hours of clean air does not result in their elimination. However, despite the apparent disruption of electron transport, visible signs of chlorosis and subsequent necrosis are not apparent at this time.

The results discussed above were obtained at fumigation levels ranging from 600 to 2000ppb SO_2. In all cases, the changes in these signals were first noticeable between 100 and 150 minutes of fumigation, depending upon the individual leaf.

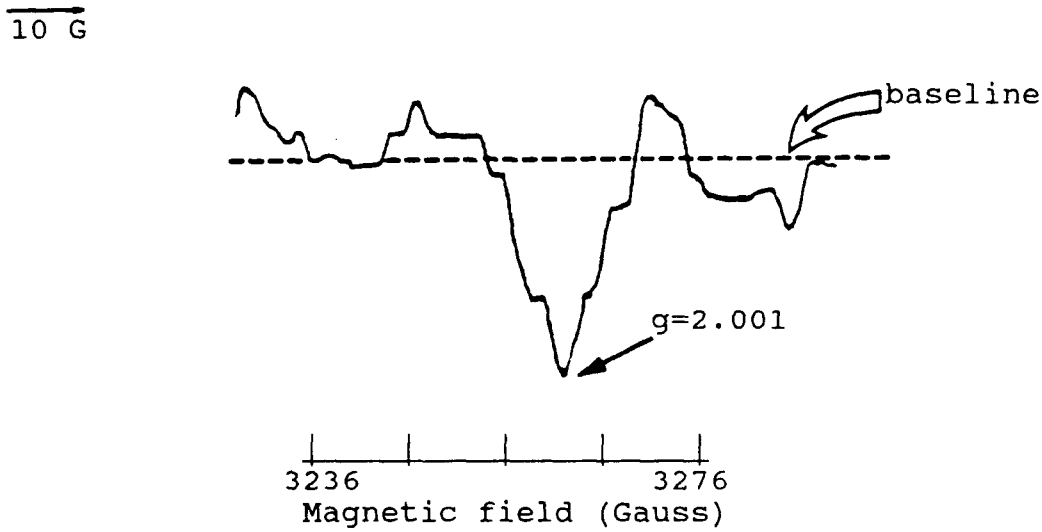

Figure 56. Signal N_{Sox}, found in attached, intact Kentucky bluegrass leaves after fumigation with 600ppb SO_2 for 4 hours. Obtained by subtraction of the light-induced signal after 180 minutes of fumigation from the light-induced signal after 240 minutes of fumigation. (Irrespective of light regime). Microwave frequency - 9.190.

5.4 Discussion

EPR Signal I, which is found in plant leaves illuminated with far-red (710nm) light, is induced with light of low irradiance and reaches saturation at an irradiance of approximately 1W m^{-2} (Blumenfeld et al. 1974). This signal can also be induced by broad-band white light of "sufficient" intensity (Tikhonov and Ruuge, 1975a). Upon leaf illumination with red light (634nm), Signal I is not induced at irradiation intensities which saturate the signal when 710nm light is used as the irradiation source. When higher intensities of 634nm light are used for irradiation, then Signal I is formed, but saturation is not achieved at intensities as high as 100W m^{-2} (Blumenfeld et al. 1974). The electron intersystem transport chain in chloroplast suspensions can be blocked by inhibitors such as DCMU, which block reoxidation of QA by QB (Velthuys and Amesz, 1974). Thus, when chloroplast suspensions are treated with DCMU, Signal I can be induced by red (Babcock and Sauer, 1975a) and white (Babcock and Sauer, 1975b) light. Similarly, when leaf pieces are infiltrated with DCMU, comparable intensities of Signal I are achieved at irradiation intensities of 1.2W m^{-2} with irradiation by either 710 or 634nm light (Blumenfeld et al. 1974).

Data presented here, based on fumigation of pieces of radish leaves, suggest that a similar blockage of the electron

transport chain is caused by fumigation of leaves with levels of SO_2 exceeding 10ppm. In the absence of fumigation, broad-band white and 650nm red light only induced a minimal Signal I formation in healthy leaves (Figure 44). After fumigation, the white-light induced signal exceeded that of the 710nm light-induced signal while the 650nm light-induced signal was comparable to the 710nm light-induced signal (Figure 44). This is readily explained by the fact that the white light used in this study was of considerably higher intensity than the 710nm light. In contrast, the 650 and 710nm light beams were of more comparable intensity (Table 1). Signal formation was light-dependent, but the blockage of the intersystem transport chain was not light dependent, as the relative post-fumigation signal intensities were similar upon irradiation with 710nm, 650nm and broad-band white light, regardless of whether the fumigation occurred in any light regime or in darkness.

Figures 47-49 indicate that the blockage is dependent upon total exposure to SO_2. After an initial lag period of just over 30 seconds, Signal I increased steadily as fumigation continued, until a maximum steady-state signal was attained after 9 to 15 minutes of fumigation, depending upon the leaf. If fumigation occurred for less than 9 minutes, a steady state signal of less than maximum intensity was attained. Maximum and less than maximum steady-state signals were irreversible. Once a specific level of blockage had occurred, the subsequent

termination of fumigation did not reverse the process. Signal I obtained with white or 650nm light remained at the height attained during fumigation. Similar effects of SO_2 on Signal I were observed at concentrations down to 10ppm. However, the lag period prior to induction of the white and 650nm light-induced Signal I progressively increased as SO_2 concentration was decreased. The total exposure required to initiate the increase in Signal I was similar, considering the variability within individual leaf segments, at concentrations of 50, 100 and 200ppm SO_2. However, when the concentration was reduced to 10ppm the exposure required to induce Signal I with white or 650nm light was reduced by approximately 50 per cent. This is attributable to the lowering of the relative humidity caused by the passage of the dry air stream through the cavity for the 90 minute period. Radish stomata have been shown to open as relative humidity decreases (Black and Unsworth, 1980) and thus the actual flux of the pollutant may well have increased over time. This is significant since it is the actual flux of the pollutant into the plant which determines the extent of damage, not the ambient air pollutant concentration (Runeckles, 1974).

Increased or decreased air flow, when the concentration of SO_2 was maintained at identical levels, caused no change in the lag period needed to induce the signal increase. Ashenden and Mansfield (1977) showed that plants were more susceptible to

air pollutants as the wind speed increased. This was attributed to a breakdown of the boundary layer component of plant resistance to pollutants. The changed air flow in this study did not have a similar effect, thus suggesting that even the lowest air flow of 1 l/min (velocity 1 m/s) was adequate to reduce boundary layer resistance and that the actual flux of the pollutant was comparable at all three air flow rates.

The precise mechanism through which SO_2 blocks electron transport from PSII to PSI cannot be elucidated from results of this study, but most of the data are consistent with the frequently stated hypothesis that air pollutants affect vegetation through the induction of various toxic active oxygen species such as the superoxide and hydroxyl free radicals, and singlet oxygen (Tanaka and Sugahara, 1980; Shimazaki et al. 1980; Sakaki et al. 1983). The hydroxyl free radical has been implicated in the destructive photooxidation of chlorophyll (Harbour and Bolton, 1978) while superoxide formation was shown in illuminated chloroplast suspensions under elevated levels of oxygen (Harbour and Bolton, 1975). McRae and Thompson (1983) found elevated levels of superoxide as plant leaves aged while Dupont and Siegenthaler (1986) suggested that the parallel breakdown of cytochromes and bleaching of pigments in aging thylakoid membranes may occur as the result of free radical activity.

The results presented in Figures 47-49 are consistent with the hypothesis that plant leaves are able to tolerate free radical production up to a threshold through the protective mechanisms of endogenous free radical scavengers such as superoxide dismutase, catalase, and -tocopherol. However, once this threshold is reached, the scavengers can no longer protect the leaves, and damage occurs. Support for this hypothesis is shown in Figure 49 as an increase in lag time with decreasing concentrations of SO_2. However, while active oxygen species, or other free radicals, may have some involvement in this blocking of electron transport, the studies with excised pieces of radish leaves subjected to high levels of sulphur dioxide do not provide any evidence for their presence. There is no spectrometric evidence in the studies using excised radish leaf pieces and high levels of SO_2 for the presence of the superoxide anion radical. The formation of Signal I under 650nm and broad-band white light occurs even if the fumigation took place in darkness. However, studies (Harbour and Bolton, 1975,1978; van Ginkel and Raison, 1980) indicate that light is necessary for the induction of the superoxide anion radical in chlorophyll-containing systems. Thus, it must be concluded that, if active oxygen species play a role in this impairment of electron transfer caused by high levels of SO_2, it is only a minor role, in relation to effects induced by SO_2 itself or the bisulphite ion. Sakaki and Kondo (1983) showed that intracellular sulphite accumulation in protoplasts in an

unmetabolized state was responsible for the inhibition of protoplast photosynthesis.

The blockage of electron transfer may occur as a result of perturbation of QB, resulting in a blockage of the plastoquinone binding site affected by DCMU and related herbicides. Daniell and Sarojini (1981) suggested that the mechanism of sulphite action in chloroplast suspensions is perturbation of the Q pool (QA+QB). Alternatively, the plastoquinone, cytochrome complex or plastocyanin components of the transfer chain may be affected or some component of Photosystem II, other than QB, may be altered. However, the similarity of response when leaves are treated with either DCMU (Blumenfeld et al. 1974) or SO_2 (this study) suggests that the site of perturbation is QB, but the evidence is not conclusive.

The longer-term low level SO_2 studies with attached, intact Kentucky bluegrass leaves discussed in Section 5.3.2.2 indicated that a free-radical signal with parameters similar to the superoxide anion radical is detectable if fumigation is extended. Thus, it must be concluded that if superoxide is formed during brief periods of fumigation with high levels of SO_2, then its signal is so transient that it is undetectable. The lack of detectable superoxide free-radical signal in the present studies provides support for the investigation by Covello and Thompson (1985). These investigators found neither

the spin-trapped signal from the superoxide free radical nor that from the hydroxyl free radical with the use of the spin traps, Tiron and DMPO, respectively, when chloroplast suspensions which contained bisulphite ions at concentrations ranging from 1 to 5mM were illuminated. However, the addition of SOD to these amended chloroplast suspensions eliminated the formation of the spin-trapped sulphur trioxide free-radical signal. These results suggest that the superoxide free radical is necessary for the initiation of sulphite oxidation but does not participate in the chain reaction of sulphite oxidation by chloroplasts (Covello and Thompson, 1985). Thus, it is more likely that the demonstrated effect on free radical formation in the high-level SO_2 experiments of the present study is the result of a gradual elimination of binding sites on QB, not an immediate increase in superoxide formation. The data in Figures 47-49 can be validly interpreted to support this hypothesis.

The results have confirmed the earlier investigations of Rowlands et al. (1970) with regard to the increase in the Mn^{++} signal and the decrease in Signal II_{u+s} after fumigation with high concentrations of SO_2 for 1 or more hours. Figure 51 shows the parallel increase in the Mn^{++} signal and decrease in Signal II_{u+s} which occur when leaves are fumigated with SO_2. The disappearance of Signal II_{u+s} indicates that the oxidation of the unknown species needed to produce this signal has been eliminated. Since Signal II_{u+s} is attributed to D

(Boussac and Etienne, 1982a, 1982b), a secondary donor to $P680^+$, which is located near the reaction centre of PSII (Govindjee et al. 1985), the disappearance of Signal II_{u+s} may be indicative of damage to the reaction centre of PSII as hypothesized by Shimazaki et al. (1984b).

The exact manganese component of the leaf which gives rise to the increased Mn^{++} signal can not be definitively identified from the data available. However, the parallel inverse kinetics of the Mn^{++} signal and Signal II_{u+s} shown in Figure 51 strongly suggest that the gradual decrease in Signal II_{u+s} is related to the change in state of the manganese pool represented by the Mn^{++} signal.

It has been shown that the environment of Mn^{++} proteins can greatly affect both the intensity and shape of the Mn^{++} EPR spectrum (Reed and Cohn, 1970,; Reed and Ray, 1971; Reed et al. 1971). Thus, it is possible that changes in the environment of either the weakly or very strongly bound pools of Mn^{++} are responsible for the Mn^{++} signal increase. Alternatively, the increase in the Mn^{++} signal may be attributed to a loosening of the strongly bound pool of Mn^{++} actively associated with oxygen evolution. SO_2 may thus act in a manner similar to Tris (Blankenship and Sauer, 1974) or heat treatment (Wydrzynski and Sauer, 1980), which release the strongly bound Mn^{++} to the interior of the thylakoid membrane and result in the concomitant

appearance of the Mn^{++} EPR signal. The Mn^{++} EPR signal may also result from a shift in manganese valence from the higher oxidation states, which are EPR silent, to Mn^{++}. This could occur from a SO_2-induced block in the S-state model of Kok et al. (1970). In either case, SO_2-caused perturbation of the oxygen-evolving complex is indicated. The parallel kinetics suggest that not only does the Mn^{++} donate an electron to Z^+, the primary donor to $P680^+$, but also to D, the auxiliary donor represented by Signal II_{u+s}.

Previously, Shimazaki and Sugahara (1980) presented evidence from fluorescence studies which indicated that SO_2 fumigation caused a decrease in the size of the Q pool. This was attributed to a SO_2-caused decrease in photoreduction of Q resulting from SO_2 inactivation of the primary electron donor or the reaction centre of PSII. Subsequently, Shimazaki et al. (1984b), again using fluorescence studies, showed reaction centre damage to the water-splitting enzyme system. The evidence presented here, showing the decrease in EPR Signal II_{u+s} and concomitant increase in the Mn^{++} signal is consistent with these conclusions of at least an indirect perturbation of the oxygen-evolving system and concomitant impairment of the reaction centre of PSII. However, since the EPR spectra do not indicate which Mn^{++} pool is represented by the enhanced signal, and, as the role of D, which is represented

by Signal II_{u+s}, is only marginally understood at present, the EPR data presented herein are not conclusive. Nonetheless, the data of Figure 51 suggest a definite interaction between the species responsible for Signal II_{u+s} and the Mn^{++} signal.

The Japanese investigators did not find any evidence for impairment of the intersystem transport chain (Shimazaki et al. 1984b). The reason for this discrepancy between their results and results of this study is related to the total exposure required to cause intersystem transport breakdown. They studied chloroplasts isolated from leaves fumigated with 2ppm SO_2 for 45 minutes. In contrast, the studies with leaf pieces reported in the present investigation indicated that 90 minutes of fumigation at 10ppm SO_2 was required to induce the blockage of electron transport from PSII to PSI.

The fact that similar results were obtained with excised radish leaf pieces and intact, attached Kentucky bluegrass and perennial ryegrass leaves indicates that the changes in signals are a function of the high concentrations of SO_2, not of the excision. It appears that the plants suffer a massive 'shock' when exposed to these high levels of SO_2. However, when the results from these high level SO_2 studies are contrasted with results obtained from studies using lower, more realistic concentrations of fumigant and intact leaves, it is readily apparent that the results with the high gas concentrations can

not be extrapolated to most real world situations because such high concentrations of SO_2 are likely to occur only in brief episodes caused by industrial accidents.

The data from the studies involving lower concentrations of SO_2 are much more relevant to realistic SO_2 pollution episodes. Here, the elimination of Signal I suggests that fumigation with SO_2 eliminates the light-catalyzed oxidation of the chlorophyll a of the reaction centre of PSI. This may occur because the SO_2 destroys the chlorophyll of either the reaction centre or the light-harvesting complex. The destruction of chlorophyll by bisulphite has been demonstrated in in vitro systems (Peiser and Yang, 1977).

The new white-light induced signal (Signal N_{S1}), while not conclusively identifiable, may well be the EPR manifestation of the appearance of the SO_3^- free radical. The g-value of Signal N_{S1} in this study is 2.0032 while reported g-values for the SO_3^- free-radical signal range from 2.0030 to 2.0033 (Behar and Fessenden, 1972: Flockhart et al. 1971; Mottley et al. 1982b). The DMPO-spin-trapped signal from the SO_3 free radical has been shown to occur in illuminated chloroplast suspensions amended with bisulphite (Covello and Thompson, 1985) and in the prostaglandin hydroperoxidase-catalyzed oxidation of bisulphite (Mottley et al. 1982a). Signal N_{S1} is not the EPR manifestation of either the SO_2^- or SO_4^- free radical as

these have g-values of 2.0058 (Norman and Storey, 1971) and 2.0125 (Ershov et al. 1971), respectively.

The appearance of the radical pair signal (Figures 54a, 54c) after extended fumigation is explainable if it assumed that SO_2, which is a reductant, is capable of reducing electron acceptors X, B and A. The presence of the initial acceptors, a_0 and a_1, has only been shown in strongly reducing conditions (Gast et al. 1983; Bonnarjea and Evans, 1982) or with the later acceptors previously inactivated (Baltimore and Malkin, 1980). Under these conditions a back reaction occurs between P700 and the early acceptors, and through the radical pair mechanism (Hoff, 1984) a signal similar in line-shape and g-value to that shown in Figures 54a and 54c appears.

The presence of detectable amounts of the superoxide anion free radical after 4 hours of fumigation is the start of the process of necrosis in plants discussed earlier in Section 4.0. This appears to be not uniquely attributable to SO_2 pollution but occurs whenever the defenses of plants are overcome through exposure to different stresses, including SO_2.

6.0 GENERAL DISCUSSION

The general purpose of these studies was the investigation, using X-band EPR spectroscopy at room temperature, of free radical changes in plant leaves, which are caused by exposure to the gaseous air pollutants, ozone and sulphur dioxide. This entailed investigation of changes in the established photosynthesis-associated free radicals represented by Signal I and Signal II_{u+s}, and investigation of the formation and decay of other free radicals which occur as a result of exposure of leaves to these air pollutants. Previous investigations of such changes were limited (Rowlands et al. 1970; Shimazaki et al. 1984b), and were confined to the description of changes in free-radical signals after completion of fumigation. However, these studies could not reveal the chronology of any changes in free radical formation which might occur during fumigation of plant leaves. To attempt to investigate such changes, it was necessary to develop a methodology whereby in situ free-radical signals could be detected and followed during the course of fumigation. Consequently, techniques were developed to permit the investigation of free-radical signal changes during fumigation of, firstly, small excised leaf segments and, subsequently, of intact, attached leaves of long, narrow-leaved plants such as grasses.

Prior to the investigation of free-radical signal changes

caused by fumigation with ozone and sulphur dioxide, several issues relating to the potential for free radical formation *in situ* in plant leaves needed investigation. These were: a) the elucidation of constraints imposed by different plant materials; b) the effect of leaf adaptation to light on free-radical signal formation; c) the effect of the composition of the air in the cavity on the formation of Signals I and II_{u+s}; d) the effect of spectrometer operation on free radicals in leaf tissue; and e) the potential for identifying individual free-radical signals in mixed spectra by the use of subtraction techniques.

Initial investigations revealed two problems related to the plant material available for use in EPR studies of free radical formation and decay in plant leaves. The first of these pertains to the use of excised leaf pieces. The present studies with excised leaf pieces provide confirmatory evidence that an unknown free radical(s) is formed upon aging of plant leaves. Previous studies had indicated that a free radical yielding a signal having a g-value of approximately 2.000 is formed in plant leaves subjected to salt or water stress (Kharitonenkov and Kalichava, 1966; Chetverikov *et al*. 1967) and upon natural aging (Mishra *et al*. 1971; Priestley *et al*. 1980). Rowlands *et al*. (1970) also showed the formation of a similar free-radical signal upon extended fumigation of soybean and pinto bean leaves with high levels of ozone. Unfortunately, in none of the above

studies was the free-radical signal characterized more precisely (g=approximately 2.000).

In the present study, the free-radical signal associated with senescence was shown, by subtraction of the spectrum obtained prior to aging from the spectrum obtained after aging, to have a g-value of 2.0046 and a line width of approximately 10 gauss (Figure 10d). This signal may also be present in the spectrum obtained from a cherry leaf (Figure 17). The signal from the cherry leaf was not investigated further, but younger cherry leaves did not show a similar signal.

Regardless of its identity, the appearance of this senescence-related free-radical signal negates the use of excised leaf pieces for fumigation studies which exceed one hour. After that time it becomes impossible to determine if changes in the vicinity of the 2.000 g-value are a result of treatment or arise from the formation of this free radical. Furthermore, it is not possible to correct for this signal by subtraction because the degree of free radical formation is unknown, and appears to vary from leaf to leaf. Once formed, the signal is permanent, and hence it is impossible to first record it and then return the leaf to a healthy state to ascertain the effects of treatment. Therefore, in order to undertake studies which involve realistic, low levels of air pollutants and thus require time periods exceeding 1 hour, it

became necessary to use intact leaves attached to plants.

The dimensions of the cavity dewar insert limit such studies to plants such as grasses which have long, narrow leaves. However, neither of the grasses investigated, Kentucky bluegrass (Poa pratensis L.), and perennial ryegrass (Lolium perenne L.), permitted investigation of the kinetics of the EPR signals related to photosynthesis as affected by the air pollutants. In each of these species, kinetic tracking of changes in the photosynthetic signals may be masked by changes in the strong underlying Mn^{++} and Fe^{++} signals, since these latter signals are also affected by treatment with light and fumigants (Figure 18). In addition to these species used extensively for the present studies of air pollutant effects, other grass species such as barnyardgrass (Echinochloa crusgalli (L.) Beauv.), red fescue (Festuca rubra L.), bentgrass (Agrostis tenuis Sibth.) and annual bluegrass (Poa annua L.) also revealed pronounced iron and manganese signals.

However, kinetic tracking is possible in leaves which reveal only minimal Mn^{++} and Fe^{++} underlying signals. Hence, in spite of the limitations imposed when using excised leaf pieces, the low levels of the Mn^{++} and Fe^{++} signals present in radish leaf tissue permitted the following of the changes in photosynthetic signals induced by sulphur dioxide, albeit at relatively high concentrations of the pollutant.

A second problem related to the selection of plant material concerns the light intensity of the ambient environment of the location where the plants were grown. Leaves from plants grown in the greenhouse from September to May were found to reveal the established photosynthesis-related Signals I and II_{u+s} (Figure 2), which are also found in chloroplast and subcellular preparations. However, leaves of plants grown on greenhouse benches or outside in full sunlight from June to August, revealed a new free-radical signal (Signal N_{PI}) superimposed upon Signal II_{u+s}. Depending upon the leaf, Signal I may, or may not, be revealed upon irradiation of such leaves with 710nm light. In most leaves (see section 3.3.5) Signal N_{PI} could be eliminated upon exposure to microwave radiation in the spectrometer cavity for 15 minutes, but, upon elimination of this signal, many leaves revealed different responses in free-radical formation to irradiation with the different light regimes than the responses associated with leaves from plants grown under lower light intensities. These changes were attributed to photoinhibition damage caused by leaf exposure to high photon flux density. Since leaves of plants grown in partial shade tended to respond more uniformly and predictably, subsequent studies in summertime were carried out with leaves of plants grown in partial shade under greenhouse benches. These did not reveal Signal N_{PI}, but did show the typical photosynthetic free-radical signals, and were thus presumed to be undamaged by the high light intensity of unsheltered areas.

However, the discovery of this previously unreported Signal N_{PI} raises an interesting point. Since the appearance of Signal N_{PI} in plants grown in full sunlight prevents the detection of Signals I and II_{u+s}, as discussed in Section 3.3.5, the question is raised as to whether the free radicals giving rise to these signals can still be induced in such tissues by different light treatments, or whether they only occur in tissues grown at reduced light intensities. The only possible evidence for their occurrence in tissue grown in high light intensities comes indirectly from the various studies on isolated chloroplasts and chloroplast fractions prepared from plants grown under a wide, but unspecified, range of light intensities (Commoner et al. 1956,1957). These studies consistently reveal Signals I and II_{u+s}, identical with those found in the present studies with intact tissues. If, as suggested by the studies discussed in Section 3.3.5, the accepted electron transport system of the photosynthetic process is changed under conditions of high light intensity, why do plants continue to grow during the summer? It appears that an unknown compensatory mechanism may occur in the summer.

Another factor relevant to the use of EPR spectroscopy for the study of free radical formation in leaf tissue concerns the effect of exposure to light of the different wavelengths needed to differentiate between Signals I and II_{u+s}, on the formation of the radicals responsible for these signals. For example,

prolonged exposure to darkness or broad-band white light influences the formation of Signal I when the leaf is subsequently exposed to far-red light. If leaves are kept in darkness prior to irradiation with far-red light there is a lag period prior to the formation of Signal I. The time period in darkness required for induction of this lag period varies greatly among species, but can be as short as 5 minutes for Chinese rose (Hibiscus sp.) leaves (Ruuge and Tikhonov, 1975). The lag period increases as the time the leaf is held in darkness is increased. The cause of this delay in Signal I formation has been attributed to a build-up of reductants in the darkness (Khangulov and Gol'dfel'd, 1977). However, a more reasonable explanation was proposed by Tikhonov and Ruuge (1975a). After infiltration of leaves with an artifical electron acceptor, methyl viologen, they found that the lag period did not occur in dark-adapted leaves. In contrast, when leaves were infiltrated with monuron, which blocks electron transport from PSII to PSI, the lag period still occurred in dark-adapted leaves. Consequently, they suggested that the lag period in dark-adapted leaves is associated with altered redox states of the electron acceptors of PSI.

A similar lag period also occurs when leaves are exposed to broad-band white light or red light (Tikhonov and Ruuge, 1975b). However, in this case the lag period occurs as a result of the action of the electron transport chain carriers which

were reduced during exposure to the white or red light, and thus provide electrons for immediate reduction of the species represented by Signal I.

Consequently, if one wishes to investigate the effect of extended fumigation on the formation of far-red light-induced Signal I for any given duration of fumigation, it is necessary to maintain the leaf in far-red light during the fumigation period. If this is not done, the formation of Signal I will be delayed, and if changes in Signal I which are induced by fumigation are reversible, the time required to restore Signal I after termination of fumigation may result in the reversal of these changes.

It is also necessary to be aware of the previously unreported signal (Signal N_{710}) formed in undamaged leaves upon prolonged exposure to 710nm light. The identity of the species represented by Signal N_{710} is uncertain but the signal has similarities in g-value to that of the early electron acceptor a_1 of PSI, but is narrower in peak-to-peak line width. However, the precise attributes of a_1 and a_0 have not been conclusively established; various investigators have reported slightly different g-values and peak-to-peak line widths (Shuvalov et al. 1979; Heathcote and Evans, 1980; Baltimore and Malkin 1980; Bonnerjea and Evans, 1982; Gast and Hoff, 1979; Gast et al. 1983). Nonetheless, regardless of the

identity of the species which gives rise to this signal, the formation of Signal N_{710} within 1 hour of exposure to 710nm light requires the inclusion of this signal in the baseline data which must be subtracted if new free-radical signals revealed during leaf exposure to gaseous pollutants are to be characterized accurately.

The transition from one light regime to another causes brief, but complex, shifts in the kinetic curve of Signal I induction. The exact shape of the kinetic curve is dependent upon the intensity and spectral composition of the light, the plant species and its physiological state (Tikhonov and Ruuge, 1975a). When a leaf already illuminated with far-red light is exposed to additional red (Tikhonov and Ruuge, 1975a) or broad-band white (Andreyeva et al. 1980) light, the intensity of Signal I rapidly drops, quickly rises to an overburst, and rapidly decreases again, before attaining an intermediate steady-state level. The entire sequence occurs in less than one minute. The present studies using the Varian E-109 spectrometer and attached Hewlett-Packard 9835B computer required approximately 4 minutes for the storage of the signal on tape for subsequent retrieval. Hence the steady-state white light signal could be obtained if the leaf was illuminated by white light during the 4 minute data transfer period and subsequently during the scan period.

The precise cause of these rapid shifts in Signal I intensity is unknown at present. Tikhonov and Ruuge (1975a) infiltrated leaves with NH_4Cl, an uncoupler of photophosphorylation, and found a monotonic decrease to the steady-state level of Signal I upon addition of red light illumination to a leaf already exposed to far-red light. They hypothesize that the rapid shifts in the kinetic curve occur as a result of redistribution of energy between the photosystems due to photo-induced rearrangement of the membranes of the chloroplasts, coupled with the process of photophosphorylation. The addition of uncouplers may prevent this rearrangement.

The present study shows that similar shifts in the kinetic trace of Signal I, obtained from unfumigated radish leaf pieces, occurred when the light regime was changed from 710 or 650nm light to broad-band white light (Figure 11). In contrast, when leaf pieces were exposed to 400ppm SO_2 for 10 minutes, these rapid kinetic shifts did not occur, and a steady-state signal was achieved without the appearance of a multi-phasic kinetic trace (Figure 12). Thus, high levels of SO_2 may act in a manner analogous to the uncouplers of phosphorylation discussed above.

The subtraction of signals obtained at different points in time was used to characterize new free-radical signals resulting from fumigation of leaves with ozone and sulphur dioxide, and

other new signals, such as Signal N_{710} and Signal N_{PI}, caused by extended exposure to 710nm light and exposure to high photon flux density, respectively.

The use of this technique is necessary because the signals discussed in the present study occur in a very narrow band and are superimposed upon each other. Specifically, it can be used to clarify the true changes in light-induced free-radical signals if underlying signals present in darkness are also changed by treatment. This entails firstly the subtraction of the signal obtained in the appropriate light regime prior to treatment, from the signal obtained during or after treatment in the identical light regime. Then the light is turned off, and the signal obtained in darkness prior to treatment is subtracted from the signal obtained in darkness during or after treatment. This is followed by the subtraction of the difference signal obtained in darkness from the difference signal obtained in light, to reveal the true change in the light-induced signal. Implicit in the use of this technique is the assumption that the signal obtained in light, prior to subtraction, is a composite signal which includes the signal obtained in darkness. This assumption has been shown to be valid for the photosynthetic-related signals (Signals I and II_{u+s}) shown in Figure 2. If PSI preparations are illuminated, only Signal I is revealed, (Malkin and Bearden, 1974; Warden and Bolton, 1974b) while PSII preparations reveal only Signal II_{u+s} (Warden and Bolton,

1974a; Boussac and Etiennne, 1982a). Identical signals are revealed when chloroplast suspensions containing both photosystems are examined, and the signal obtained in darkness (Signal II_{u+s}) is subtracted from the combined signal revealed upon irradiation of the suspension with far-red light (Weaver, 1968; Haehnel, 1984).

The lack of capability to accurately track the kinetics of formation and decay of free-radical signals which are superimposed upon the strong Mn^{++} and Fe^{++} signals of grass species, which also change upon treatment, can be minimized by the use of signal subtraction techniques. The rate of increase or decrease of the free-radical signal under study can not be continuously followed with confidence because the free-radical signals are minimal compared to the paramagnetic metal signals, and a small change in the latter signals would obscure major changes in the free-radical signals. However, by subtraction of the initial combined signal from the combined signal at various points in time, it is possible to measure the height (intensity) of the free-radical signal under study since changes in the metal signals which would affect the height of a kinetic trace of the free-radical signal are accounted for in the combined signal. Confusion between the metal signals and the free-radical signals is extremely unlikely as the metal signals exceed 400 gauss in width while free-radical signals in the present study are under 25 gauss in width. If composite signals

were recorded at short intervals, a reasonable kinetic record of the formation and decay of the free-radical signal in question could be obtained through measurement of the height of the signal after subtraction of the control spectra at each point in time.

A final point regarding methodology of EPR investigation of plant leaves pertains to the requirement for oxygen. The rates of formation of EPR Signals I and II_{u+s} have been shown to change as seedlings developed in different light regimes (Chetverikov et al. 1982, 1984) and two types of reduction processes have been demonstrated in the reaction centres of $P^{+}700$ in the leaves of Chinese rose plants (Khangulov and Gol'dfel'd, 1977). Also, the induction curve of far-red light-induced Signal I is biphasic (Tikhonov and Ruuge, 1975a, 1975b; Ruuge and Tikhonov, 1975) and there is a 40% biphasic decay in P700 and iron-sulphur centre A at 150K (Bearden and Malkin, 1972b). Consequently, it has been suggested that the species giving rise to Signal I is heterogeneous at cryogenic temperatures (Bearden and Malkin, 1972a, 1972b; Lozier and Butler, 1974).

The present studies which involved replacement of the air flowing through the dewar insert with nitrogen complement these earlier studies which suggested a lack of homogeneity in the species represented by Signal I. The data in Section 3.4.1.2

indicate that Signal I, once formed in 710nm light, is not affected by the removal of oxygen. However, to induce the formation of Signal I, oxygen is required as only 40% of Signal I can be formed if the leaf is briefly held in darkness under nitrogen and is then irradiated with 710nm light while still under nitrogen. These data support the view that the species giving rise to Signal I is heterogeneous and suggest that 60% of this signal is oxygen-dependent. The present data could also be interpreted as evidence for the requirement of CO_2 for Signal I formation since CO_2 is the terminal physiological acceptor of the photosynthetic electron transport chain.

The appearance of different new free-radical signals when different air pollutants are used as the fumigant suggests that SO_2 and O_3 cause damage to plant leaves via different mechanisms. This is not unexpected as SO_2 is a reductant while O_3 is an oxidant. The identity of the free radicals responsible for Signals N_{O1} and N_{O2}, which are revealed upon exposure to ozone, is not known since their g-values and peak-to-peak line widths do not appear to match those of any signals reported in the relevant literature. On the other hand, Signal N_{S1}, which is revealed upon prolonged exposure to sulphur dioxide, may be representative of the SO_3^- free radical since its g-value and line width are similar to those reported by Mottley et al. (1982b) for the SO_3^- free-radical signal (Appendix B).

The subsequent appearance of Signal N_{S2} after continued fumigation with sulphur dioxide suggests that the reduction of electron acceptors X, B and A occurs as a result of extended fumigation with SO_2. If these later electron acceptors are reduced (Gast et al. 1983) or otherwise inactivated (Baltimore and Malkin, 1980), the presence of the early electron acceptors a_0 and a_1 is revealed at room temperature (Bonnarjea and Evans, 1982). A signal similar in line-shape to Signal N_{S2} was detected by McIntosh and Bolton (1979) and was attributed to PSI radicals. Subsequent work (Gast et al. 1983; Hoff, 1984) indicated that this arises from the combined $P700^+$ and a_1^- radical. Definite identification of the radical responsible for Signal N_{S2} is not possible, but its 2.0042 g-value is within the range of g-values (2.0026-2.0051) reported, depending upon the orientation of the combined $P700^+a_1^-$ signal (Hoff, 1984).

The studies with high levels of SO_2 which revealed the formation of Signal I in broad-band white light (Figure 46) suggest that either the electron transport chain is blocked or PSII has been damaged by the fumigation with SO_2. A similar situation occurs as one of the alternative responses in leaves grown under high photon flux density after the leaves were exposed to microwave radiation in the spectrometer cavity (Figure 34a). In both cases it is clear that the electron transport from PSII to PSI needed to reduce Signal I in white

light in undamaged leaves is not occurring. However, it is by no means certain that the site of damage to the leaves is identical in these two cases. It is possible that SO_2 causes a blockage of the electron transport chain at QB similar to that caused by DCMU or Tris (Velthuys and Amesz, 1974) while exposure to high PFD impairs the reaction centre of PSII (Powles and Borkman, 1983). Kyle et al. (1983) suggested that the loss of the 32kDa herbicide-binding polypeptide of QB is the primary cause of interruption of electron transport and photoinhibition of PSII. However, Cleland and Critchley (1985) were unable to confirm this, and suggested that the loss of the 32kDa polypeptide is a consequence, not a cause, of photoinhibition of PSII. From the EPR standpoint the result would be identical, as Signal II_{u+s} would not be affected since it represents D, which precedes the reaction centre of PSII in the electron transport chain (Figure 1), and Signal I would be formed in white light if electron transfer from PSII is not occurring.

The hypothesis that the formation of oxy-free radicals is the initial step in air pollutant-caused damage to vegetation (Sakaki et al. 1983) is seductive, but can neither be verified nor refuted from the present studies. The present studies using ozone (Section 4.3.3) indicated that leaves fumigated with ozone show the presence of a new, small signal (Signal N_{Sox}) in intact plant leaves after several hours of fumigation. The signal, which is permanent once induced, but only resolvable

after a series of signal subtractions, appears to be identical to that attributed to the superoxide anion radical in xanthine-xanthine oxidase rapid flow systems (Palmer et al. 1964; Bray et al. 1964; Knowles et al. 1969; Ballou et al. 1969). Also, the longer-term studies with low levels of SO_2 (Section 5.3.2.2) disclosed the formation of the same signal after extended fumigation. Therefore, results from both the ozone and sulphur dioxide studies suggest that it is possible to detect the superoxide anion free radical in plant leaves.

However, the conditions under which this signal, attributed to the superoxide anion free radical, can be detected, suggest that its formation, in amounts detectable by EPR spectroscopy, occurs as a result of damage caused by the other free radicals which have been created as a result of fumigation with either O_3 or SO_2. Signal N_{Sox} appears after Signals N_{O1}, N_{O2}, N_{S1} and N_{S2} have been formed, and is probably the result of accelerated senescence, caused by the free radicals represented by these latter four signals. The sequence of events suggests that, if the formation of the superoxide anion free radical is the primary event in air pollutant damage to plant leaves, then the formation and decay of this free radical in the initial stages of air pollutant-induced damage to plant leaves is so rapid that its EPR-detectable free-radical signal can not be recorded at these initial stages, using the methodology of this study.

On the other hand, its accumulation to the level of detectability may reflect damage to the endogenous defense mechanisms found within plant leaves. The defense mechanisms against free radical damage can be grouped into two categories; prevention of free radical formation, and scavenging or quenching of present free radicals (Leshem, 1981). Within plant leaves the most prevalent antioxidants which prevent the formation of free radicals are α-tocopherol (Vitamin E), ascorbic acid (Vitamin C), β-carotene, catalase and glutathione peroxidase. The most prominent free radical scavenger is superoxide dismutase, which combines with superoxide to form molecular oxygen (see Section 2.1). In reality, SOD is a family of enzymes differentiated by their metal co-factor (Fridovich, 1976a, 1976b). Eukaryotes have enzymes which include both copper and zinc (CuZnSOD) while prokaryotes have enzymes which contain either iron (FeSOD) or manganese (MnSOD) (Baum and Scandalios, 1981; Bridges and Salin, 1981; Elstner, 1979; Giannopolitis and Ries, 1977; Puget and Michelson, 1974). Cytokinins, which are known to retard senescence (Runeckles and Resh, 1975), may also act as free radical scavengers (Leshem, 1981; Leshem et al. 1981), while chemicals such as propyl gallate, sodium benzoate (Leshem, 1981) and ethylene diurea (EDU) (Carnahan et al. 1978; Legassicke and Ormrod, 1981; Bisessar and Palmer, 1984)) can provide protection against free radical formation and ozone toxicity, respectively.

The exact role of any of these protective agents cannot be established from EPR studies alone. However, it is probable that they play a major role in plant defense mechanisms against air pollutants such as ozone and sulphur dioxide. The time lag in the formation of Signal N_{Sox} during fumigation with either pollutant suggests that endogenous defense mechanisms exist to counter the deleterious effects of the pollutants. Extended fumigation appears to overcome the protectants and various free radicals represented by Signals N_{O1}, N_{O2}, N_{S1}, N_{S2} and N_{Sox} are formed after different fumigation time periods.

The possible involvement of free-radical scavengers was also indicated in the high-level SO_2 studies which revealed the formation of Signal I in broad-band white light after a lag period which decreased as the SO_2 concentration was increased (Figure 49). The total external exposure (concentration x time), and probable uptake of the pollutant, necessary to induce the formation of the white light-dependent Signal I was similar at concentrations of 50, 100 and 200ppm SO_2. Thus, it appears that the endogenous scavengers can counter the effect of the SO_2 until a threshhold has been reached, but after this limit has been reached they are overcome, and metabolic pathways are affected by additional absorption of the pollutant.

The delayed appearance of Signal N_{Sox} is one possible explanation for the lack of success with the spin traps as

excised leaf pieces cannot be maintained in the spectrometer cavity for the time needed to generate the free radical represented by the Signal N_{Sox}. Free radical scavengers, such as SOD, which protect the leaves from toxic free radicals, may be successful in countering the effects of the free radicals during the time period (1 hour) that excised leaf pieces can be maintained in the spectrometer cavity without the appearance of confounding effects caused by artificial aging. Alternatively, the lack of spin adduct formation may be a function of inability to successfully incorporate the spin traps into the leaf cells.

Also, it is possible that free radicals such as the superoxide anion free radical are formed in the initial stages of exposure to gaseous air pollutants, but are so transient that they can not be detected using the methodology of this study. For instance, Covello and Thompson (1985) showed that the spin-trapped sulphur trioxide free-radical signal was formed when chloroplast suspensions amended with sulphite were illuminated. They found no evidence for the formation of the spin-trapped superoxide free-radical signal, but when SOD was added to the suspension, the sulphur trioxide free-radical signal was not formed. From these data they concluded that superoxide formation was necessary to initiate the oxidation of sulphite but superoxide was not involved in the propagation of the chain reaction of sulphite oxidation. It may be possible to detect this transient formation of the superoxide free-radical

signal through the use of rapid scan spectrometry which allows for the scanning of the magnetic field in milliseconds. However, this would require further modification of the present system as the E-271A rapid scan cavity is not compatible with the dewar insert used to aid in stabilization of the leaf and to guide the flow of treatment pollutant gases.

All of the present studies have confirmed that when plants are subjected to stress such as exposure to sulphur dioxide or ozone, free radicals, likely deleterious, are formed. The identification, through the use of EPR alone, of these stress-induced free radicals is tenuous at best. Changes also occur in Signals I and II_{u+s} when plants are subjected to stress associated with exposure to gaseous pollutants, thereby suggesting that both Photosystems I and II are impaired, and normal electron transport from H_2O to NADP is no longer possible. Consequently, the growth reductions reported in the literature (Bell and Clough, 1972; Roberts, 1976; Milchunas et al. 1981; Ayazloo et al. 1982;) are to be expected even if symptoms of stress are not apparent.

7.0 SUMMARY AND CONCLUSIONS

1. Methodology was developed which allows for the monitoring of EPR free-radical signal changes occurring *in vivo* in attached, intact leaves of narrow-leafed plants, such as grasses, which are subjected to gaseous air pollutants or other treatments.

2. The same technique permits the use of excised leaf pieces instead of intact, attached leaves if the experiment time length does not greatly exceed one hour. In the second hour after excision, excised leaf segments reveal a large free-radical signal with a g-value of 2.0046. The formation of this 'senescence' (Mishra *et al.* 1971) or 'organic' (Priestley *et al.* 1980) free-radical signal begins to confound any free-radical signal changes induced by treatment in the second hour after excision. In the present study the formation of this signal is attributable to the artifical aging caused by wounding; not to desiccation.

3. Continual exposure of the leaf to far-red (710nm) light results in the formation, within 1 hour, of a new EPR free-radical signal (Signal N_{710}), which has a g-value of 2.0054 and an approximate peak-to-peak line width of 8.5 gauss. The species giving rise to this signal may be the early electron acceptor a_1, but the evidence is not conclusive.

4. Kinetic studies of free-radical signal formation and decay during treatment are possible in species which have minimal Mn^{++} and Fe^{++} signals underlying the photosynthetic signals. Unfortunately, all grass species investigated revealed large Mn^{++} and Fe^{++} signals which also change with treatment, thus confounding kinetic tracking of the photosynthetic or other free-radical signal changes which occur with treatment.

5. When air is replaced by N_2 in the spectrometer cavity there is a minimal decrease in Signal I and Signal II_{u+s}, if the leaf is continually irradiated with 710nm light. However, if the leaf is held in darkness for a brief period under N_2, then, when the leaf is returned to 710nm light there is only a 40 per cent restoration of Signal I after 1 hour of exposure to 710nm light, thereby suggesting that Signal I is heterogeneous.

6. No spin adducts were revealed when attempts were made to incorporate spin traps into excised leaf pieces. This is attributable to a lack of success in the incorporation of the spin traps into the leaf pieces or to a lack of new free radical formation in the 1 hour period during which excised leaf pieces can be validly studied.

7. Leaves of plants grown in intense sunlight reveal an unreported free-radical signal (Signal N_{pI}), which has a g-value of 2.0056 and a peak-to-peak line width of 9 gauss.

This signal is not light-dependent as identical signals are revealed when the leaves are held in darkness, under 710nm light or broad-band white light. In most leaves Signal N_{PI} is eliminated upon exposure of the leaf to microwave radiation in the cavity for 15 minutes. The identity of the species represented by Signal N_{PI} is unknown.

8. Once Signal N_{PI} is eliminated by exposure of the leaf to microwave radiation, the leaf may reveal; a. the typical photosynthetic signals from undamaged plants; b. a white light-induced Signal I indicative of damage to Photosystem II or; c. no induction of Signal I upon irradiation with far-red light, indicative of damage to Photosystem I.

9. Leaves fumigated with low levels of ozone (up to 80ppb) do not reveal free-radical signal changes during fumigation time periods of up to 8 hours.

10. After 3 hours of fumigation, leaves exposed to intermediate levels of ozone (80-250ppb) reveal the formation of a new free-radical signal (Signal N_{O1}) having a g-value of 2.0041 and a peak-to-peak line width of 10 gauss. Concomitant to the formation of Signal N_{O1} is the disappearance of all of Signal I and a decrease in Signal II_{u+s} intensity. These changes are reversible as Signal N_{O1} decays and Signal I is reformed within 20 minutes of the termination of fumigation. Signal

II_{u+s} is partially restored within 16 hours of the end of fumigation.

11. Leaves fumigated with high levels of ozone (exceeding 250ppb) reveal the formation of a different new free-radical signal (Signal N_{O2}) in darkness within 1.5 hours of fumigation. This signal has a g-value of 2.0055 and a peak-to-peak line width of 7-8 gauss.

12. Leaves fumigated with high levels of sulphur dioxide (10-500ppm) reveal a large Signal I upon exposure to 650nm or broad-band white light. This indicates a blockage of electron transport from PSII to PSI, possibly by perturbation of QB, similar to that caused by the addition of DCMU to chloroplast preparations. This blockage is dependent upon total external dose as both SO_2 concentration level and length of exposure affect the intensity of the signal and the time lag prior to its formation.

13. High levels of sulphur dioxide also perturb the oxidizing side of Photosystem II, as shown by the gradual disappearance of Signal II_{u+s} and concomitant increase in the Mn^{++} signal during fumigation. The exact site of SO_2 damage is unknown, as the precise roles of the Mn^{++} detectable by EPR spectroscopy and D, represented by Signal II_{u+s}, have yet to be clarified, but it likely involves at least peripheral damage to

the oxygen-evolving complex of PSII.

14. Leaves fumigated with low levels of sulphur dioxide (60-200pphm) reveal the decay of Signal I in 710nm light after 3 hours of fumigation. This is indicative of PSI damage as the light-oxidation of the chlorophyll a of the reaction centre of PSI needed for the formation of Signal I is no longer occurring.

15. These leaves also reveal the formation of a new free-radical signal (Signal N_{S1}) under broad-band white light. Signal N_{S1} has a g-value of 2.0032 and a peak-to-peak line width of 8.0 gauss, which are similar to the parameters of the signal attributed to the SO_3^- free-radical. If fumigation with SO_2 is continued, an unidentified new free-radical signal (Signal N_{S2}) is formed under 710nm and white light.

16. Upon extended fumigation with either ozone or sulphur dioxide, a free-radical signal (Signal N_{Sox}) with parameters identical to the superoxide anion free radical signal, is formed in plant leaves irradiated with broad-band white or 710nm light. The timing of the formation of this signal, after the formation of Signals N_{O1} and N_{O2} in the ozone studies and Signals N_{S1} and N_{S2} in the sulphur dioxide studies, suggests that it is formed as a result of stress and premature aging of the leaf caused by the pollutants - not as a direct result of exposure to the pollutants.

8.0 LITERATURE CITED

Allen, H. and O. Hill. 1978. The superoxide ion and the toxicity of molecular oxygen. pp. 173-208 In New Trends in Bioorganic Chemistry. J.P. Williams and J.R.R.F. DaSilva (Eds.) Academic Press: London-New York-San Francisco.

Amesz, J. 1983. The role of manganese in photosynthetic oxygen evolution. Biochim. Biophys. Acta 726:1-12.

Andersson, B. and J.M. Anderson. 1980. Lateral heterogeneity in the distribution of chlorophyll-protein complexes of the thylakoid membranes of spinach chloroplasts. Biochim. Biophys. Acta 593:427-440.

Andreyeva, A.S., A.I. Tikhonov and E.K. Ruuge. 1979. Influence of pre-history of illumination on course of the redox conversions of P700 in bean leaves. Biophys. 24:568-570.

Asada, K., M. Urano and M. Takahashi. 1973. Subcellular location of superoxide dismutase in spinach leaves and preparation and properties of crystalline spinach superoxide dismutase. Eur. J. Biochem. 36:257-266.

Asada, K., K. Yoshikawa, M.A. Takahashi, Y. Maeda and K. Enmanji. 1975. Superoxide dismutases from a blue-green alga, Plectonema boryanum. J. Biol. Chem. 250:2801-2807.

Asada, K., M. Takahashi and Y. Kona. 1976. Superoxide dismutases in photosynthetic organisms. pp. 551-564 In Advances in Experimental Medicine and Biology. Vol. 74. Iron and Copper Proteins. K. Yasunobu, H.F. Mower, and O. Hayaishi (Eds.) Plenum Press, New York.

Asada, K., M. Takahashi, K. Tanaka and Y. Nakano. 1977. Formation of active oxygen and its fate in chloroplasts. pp. 45-63 In Biochemical and Medical Aspects of Active Oxygen. O. Hayaishi and K. Asada (Eds.) University Park Press, Baltimore.

Ashenden, T.W. and T.A. Mansfield. 1977. Influence of wind speed on the sensitivity of ryegrass to SO_2. J. Exp. Bot. 28:729-735.

Ayazloo, M., S.G. Garsed and J.N.B. Bell. 1982. Studies on the tolerance to sulphur dioxide of grass populations in polluted areas. II. Morphological and physiological investigations. New Phytol. 90:109-126.

Babcock, G.T. and K. Sauer. 1973a. Electron paramagnetic resonance Signal II in spinach chloroplasts. I. Kinetic analysis for untreated chloroplasts. Biochim. Biophys. Acta 325:483-503.

Babcock, G.T. and K. Sauer. 1973b. Electron paramagnetic resonance Signal II in spinach chloroplasts. II. Alternative spectral forms and inhibitor effects on kinetics of Signal II in flashing light. Biochim. Biophys. Acta 325:504-519.

Babcock, G.T. and K. Sauer. 1975a. A rapid, light-induced transient in electron paramagnetic resonance Signal II activated upon inhibition of photosynthetic oxygen evolution. Biochim. Biophys. Acta 376:315-328.

Babcock, G.T. and K. Sauer. 1975b. The rapid component of electron paramagnetic resonance Signal II: A candidate for the physiological donor to Photosystem II in spinach chloroplasts. Biochim. Biophys. Acta 376:329-344.

Babcock, G.T., R.E. Blankenship and K. Sauer. 1976. Reaction kinetics for positive charge accumulation on the water side of chloroplast photosystem II. FEBS Lett. 61:286-289.

Baker, N.R., East, T.M. and Long, S.P. 1983. Chilling damage to photosynthesis in young Zea mays. J. Exp. Bot. 34:189-197.

Ballou, D., G. Palmer and V. Massey. 1969. Direct demonstration of superoxide anion production during the oxidation of reduced flavin and of its catalytic decomposition by erythrocuprein. Biochem. Biophys. Res. Commun. 36:898-904.

Baltimore, B.G. and R. Malkin. 1980. Spectral characterization of the intermediate electron acceptor (A_1) of photosystem I. FEBS Lett. 110:50-52.

Baum, J.A. and J.G. Scandalios. 1981. Isolation and characterization of the cytosolic and mitochondrial superoxide dismutases of maize. Arch. Biochem. Biophys. 206:249-264.

Bearden, A.J. and R. Malkin. 1972a. The bound ferredoxin of chloroplasts: a role as the primary electron acceptor of photosystem I. Biochem. Biophys. Res. Commun. 46:1299-1305.

Bearden, A.J. and R. Malkin. 1972b. Quantitative EPR studies of the primary reaction of photosystem I in chloroplasts. Biochim. Biophys. Acta 283:456-468.

Behar, D. and R.W. Fessenden. 1972. Electron spin resonance studies of inorganic radicals in irradiated aqueous solutions. I. Direct observation. J. Phys. Chem. 76:1706-1709.

Beinert, H., B. Kok and G. Hoch. 1962. The light induced electron paramagnetic resonance signal of photocatalyst P700*. Biochem. Biophys. Res. Commun. 3:209-213.

Belay, A. 1981. An experimental investigation of inhibition of phytoplankton photosynthesis at lake surfaces. New Phytol. 89:61-74.

Belay, A. and G.E. Fogg. 1978. Photoinhibition of photosynthesis in Asterionella formosa (Bacillariophycae). J. Phycol. 14:341-347.

Bell, J.N.B. and W.S. Clough. 1972. Depression of yield in ryegrass exposed to sulphur dioxide. Nature. 241:47-49.

Bendall, D.S. 1982. Photosynthetic cytochromes of oxygenic organisms. Biochim. Biophys. Acta 638:119-151.

Bengis, C. and N. Nelson. 1977. Subunit structure of chloroplast Photosystem I reaction centre. J. Biol. Chem. 252:4564-4569.

Bergstrom, J. 1985. The EPR spectrum and orientation of cytochrome b-563 in the chloroplast thylakoid membrane. FEBS Lett. 183:87-90.

Bisessar, S. and K.T. Palmer. 1984. Ozone, antioxidant spray and Meloidogyne hapla effects on tobacco. Atmos. Environ. 5:1025-1027.

Bjorkman, O. 1968. Further studies on differentiation of photosynthetic properties in sun and shade ecotypes of Solidago virgaurea. Physiol. Plant. 21:84-99.

Bjorkman, O. 1973. Comparative studies on photosynthesis in higher plants. Curr. Top. Photobiol. Photochem. Photophysiol. 8:1-63.

Bjorkman, O. 1981. Responses to different quantum flux densities. pp. 57-107 In Encyclopedia of Plant Physiology, New Ser. Vol. 12A Physiological Plant Ecology I. O.L. Lange, P.S. Nobel, C.B. Osmond, H. Ziegler, (Eds.) Berlin/Heidelberg: Springer-Verlag.

Bjorkman, O. and P. Holmgren. 1963. Adaptability of the photosynthetic apparatus to light intensity in ecotypes from exposed and shaded habitats. Physiol. Plant. 16:889-914.

Black, V.J. and M.H. Unsworth. 1979. Resistance analysis of sulphur dioxide fluxes to Vicia faba. Nature 282:68-69.

Black, V.J. and M.H. Unsworth. 1980. Effects of low concentrations of sulfur dioxide on net photosynthesis and dark respiration. J. Exp. Bot. 30:473-484.

Black, V.J., D.P. Ormrod and M.H. Unsworth. 1982. Effects of low concentration of ozone, singly and in combination with sulphur dioxide on net photosynthesis rates of Vicia faba L. J. Exp. Bot. 33:1302-1311.

Blankenship, R. E. and K. Sauer. 1974. Manganese in photosynthetic oxygen evolution. I. Electron paramagnetic resonance study of the environment of manganese in Tris-washed chloroplasts. Biochim. Biophys. Acta 357:252-266.

Blankenship, R.E., G.T. Babcock, J.T. Warden and K. Sauer. 1975a. Observation of a new EPR transient in chloroplasts that may reflect the electron donor to Photosystem II at room temperature. FEBS Lett. 51:287-293.

Blankenship, R.E., A. McGuire and K. Sauer. 1975b. Chemically induced dynamic electron polarization in chloroplasts at room temperature: Evidence for triplet state participation in photosynthesis. Proc. Natl. Acad. Sci. USA 72:4943-4947.

Blumenfeld, L.A., M.G. Goldfeld, A.I. Tzapin and V.S. Hangulov. 1974. Electron spin resonance Signal I in leaves of higher plants: behaviour under simultaneous and separate illumination with red and far red light. Photosynthetica 8:168-175.

Bonnerjea, J. and M.C.W. Evans. 1982. Identification of multiple components in the intermediary electron carrier complex of photosystem I. FEBS Lett. 148:313-316.

Bouges-Bocquet, B. 1977. Cytochrome f and plastocyanin kinetics in Chlorella pyrenoidosa. I. Oxidation kinetics after a flash. Biochim. Biophys. Acta 462:362-370.

Boussac, A., and A.L. Etienne. 1982a. Oxido-reduction kinetics of signal II slow in tris-washed chloroplasts. Biochem. Biophys. Res. Commun. 109:1200-1205.

Boussac, A., and A.L. Etienne. 1982b. Spectral and kinetic pH-dependence of fast and slow signal II in tris-washed chloroplasts. FEBS Lett. 148:113-116.

Bowes, J. M. and A. Crofts. 1980. Binary oscillations in the rate of reoxidation of the primary acceptor of Photosystem II. Biochim. Biophys. Acta 590:373-384.

Bray, R.C., G. Palmer and H. Beinert. 1964. Direct studies on the electron transfer sequence in xanthine oxidase by electron paramagnetic resonance spectroscopy. II. Kinetic studies employing rapid freezing. J. Biol. Chem. 239:2667-2676.

Bridges, S.M. and M.L. Salin. 1981. Distribution of iron-containing superoxide dismutase in vascular plants. Plant Physiol. 68:275-278.

Broadhurst, R.W., A.J. Hoff and P.J. Hore. 1986. Interpretation of the polarized electron paramagnetic resonance signal of plant Photosystem I. Biochim. Biophys. Acta 852:106-111.

Buchvarov, P. and T. Gantcheff. 1984. Influence of accelerated and natural aging on free radical levels in soybean seeds. Physiol. Plant. 60:53-56.

Bunce, J.A., D.I. Patterson and M.M. Peet. 1977. Light acclimation during and after leaf expansion in soybean. Plant Physiol. 60:255-258.

Caldwell, M.M. 1981. Plant response to solar ultraviolet radiation. pp. 170-197 In Encyclopedia of Plant Physiology, New Ser. Vol. 12A Physiological Plant Ecology I. O.L. Lange, P.S. Nobel, C.B. Osmond, H. Ziegler, (Eds.) Berlin/Heidelberg: Springer-Verlag.

Cammack, R. and M.C.W. Evans. 1975. EPR spectra of iron-sulphur proteins in dimethylsulfoxide solutions: evidence that chloroplast photosystem I particles contain 4Fe-4S centers. Biochem. Biophys. Res. Commun. 67:544-549.

Carlson, R.W. 1979. Reduction in the photosynthetic rate of Acer, Quercus and Fraxinus species caused by sulfur dioxide and ozone. Environ. Pollut. 18:159-170.

Carlson, R.W. 1983a. The effect of SO_2 on photosynthesis and leaf resistance at varying concentrations of CO_2. Environ. Pollut. 30:309-321.

Carlson, R.W. 1983b. Interaction between SO_2 and NO_2 and their effects on photosynthetic properties of soybean Glycine max. Environ. Pollut. 32:11-38.

Carnahan, J.E., E.L. Jenner and E.K.W. Wat. 1978. Prevention of ozone injury by a new protectant chemical. Phytopath. 68:1225-1229.

Casey, J. and K. Sauer. 1984a. Cryogenic photogeneration of an intermediate in photosynthetic oxygen evolution observed by EPR. Biophys. J. 45:217a.

Casey, J. and K. Sauer. 1984b. EPR detection of a cryogenically photogenerated intermediate in photosynthetic O_2 evolution. Biochim. Biophys. Acta 767:21-28.

Chanway, C.P. and V.C. Runeckles. 1984a. The role of superoxide dismutase in the susceptibility of bean leaves to ozone injury. Can. J. Bot. 62:236-240.

Chanway, C.P. and V.C. Runeckles. 1984b. Effect of ethylene diurea (EDU) on ozone tolerance and superoxide dismutase activity in bush bean. Environ. Pol. 35:49-56.

Cheniae, G.M. and I.F. Martin. 1970. Sites of function of manganese within Photosystem II. Roles in O_2 evolution and system II. Biochim. Biophys. Acta 227:219-239.

Chetverikov, A.G., L. Ya. Silkin and A.F. Banin. 1967. Investigation by the E.P.R. method of necrosis induced in leaves by salting the soil. Biophys. 12:159-161.

Chetverikov, A.G., I.S. Drozdova and N.P. Voskresenskaya. 1983. Patterns of change in the E.S.R. signals in the leaves of higher plants during seedling development. Biophys. 28:158-160.

Chetverikov, A.G., S.A. Stanko and G.V. Novikova. 1984. Change in the E.S.R. Signals I and II during development of the photosynthetic apparatus of wheat seedlings in light of different spectral composition. Biophys. 29:722-728.

Chia, L.S., J.E. Thompson and E.B. Dumbroff. 1981. Simulation of the effects of leaf senescence on membranes by treatment with paraquat. Pl. Physiol. 67:415-420.

Chia, L.S., D.G. McRae and J.E. Thompson. 1982. Light-dependence of paraquat-initiated membrane deterioration in bean plants. Evidence for the involvement of superoxide. Physiol. Plant. 82:80-87

Cleland, R.E. and C. Critchley. 1985. Studies on the mechanism of photoinhibition in higher plants. II. Inactivation by high light of photosystem II reaction center function in isolated spinach thylakoids and O_2 evolving particles. Photobiochem. Photobiophys. 10:83-92.

Commoner, B., J.J. Heise and J. Townsend. 1956. Light-induced paramagnetism in chloroplasts. Proc. Natl. Acad. Sci. USA 42:710-718.

Commoner, B., J.J. Heise, B.B. Lippincott, R.E. Norberg, J.V. Passonneau and J. Townsend. 1957. Biological activity of free radicals. Science 126:57-63.

Costonis, A.C. 1970. Acute foliar injury of eastern white pine induced by sulfur dioxide and ozone. Phytopath. 60:994-999.

Coulson, C.L. and R.L. Heath. 1974. Inhibition of the photosynthetic capacity of isolated chloroplasts by ozone. Plant Physiol. 53:32-38.

Covello, P.S. and J.E. Thompson. 1985. Spin trapping evidence for formation of the sulfite radical anion during chloroplast-mediated oxidation of bisulfite ion. Biochim. Biophys. Acta 843:150-154.

Cramer, W.A. and J. Whitmarsh. 1977. Photosynthetic cytochromes. Ann. Rev. Plant Physiol. 28:133-172.

Critchley, C. 1981. Studies on the mechanism of photoinhibition in higher plants. I. Effects of high light intensity on chloroplast activities in cucumber adapted to low light. Plant Physiol. 67:1161-1165.

Critchley, C. 1985. The role of chloride in Photosystem II. Biochim. Biophys. Acta 811:33-46.

Crofts, A.R. and C. Wraight. 1983. The electrochemical domain of photosynthesis. Biochim. Biophys. Acta 726:149-185.

Daniell, H. and G. Sarojini. 1981. On the possible site of sulphite action in the photosynthetic electron transport chain and the light modulation of enzyme activity. Photochem. Photobiophys. 2:61-68.

Delepelaire, P. and N.H. Chua. 1979. Lithium dodecyl sulfate/polyacrylamide gel electrophoresis of thylakoid membranes at 4^{o}C: Characterization of two additional chlorophyll a-protein complexes. Proc. Natl. Acad. Sci. USA 76:111-115.

Den Haan, G.A., J.T. Warden and L.M.N. Duysens. 1973. Kinetics of the fluorescence yield of chlorophyll a_2 in spinach chloroplasts at liquid nitrogen temperature during and following a 16us flash. Biochim. Biophys. Acta 325:120-125.

De Paula, J.C. and G.W. Brudwig. 1985. Magnetic properties of manganese in the photosynthetic O_2-evolving center. Biophys. J. 47:167a.

Dismukes, G.C. 1986. The metal centers of the photosynthetic oxygen-evolving complex. Photochem. Photobiol. 43:99-115.

Dismukes, G.C. and Y. Siderer. 1981. Intermediates of a polynuclear manganese centre involved in photosynthetic oxidation of water. Pro. Nat. Acad. Sci. USA 78:274-278.

Dismukes, G.C., A. McGuire, R.E. Blankenship and K.Sauer. 1978. Electron spin polarization in photosynthesis and the mechanism of electron transfer in photosystem I. Experimental observations. Biophys. J. 21:239-256.

Dupont, J., and P.A. Siegenthaler. 1986. A parallel study of pigment bleaching and cytochrome breakdown during aging of thylakoid membranes. Plant Cell Physiol. 27:473-484.

Eckert, H.J. and G. Renger. 1980. Photochemistry of the reaction centers of system II under repetitive flash group excitation in isolated chloroplasts. Photochem. Photobiol. 31:501-511.

Elstner, E.F. 1979. Oxygen activation and superoxide dismutase in chloroplasts. pp. 411-415 In Encyclopedia of Plant Physiology. Vol. 6. Photosynthesis 11: Carbon Metabolism and Related Processes. M. Gibbs and E. Latzko (Eds.) Springer-Verlag, New York.

Emerson, R. 1936. The effect of intense light on the assimilatory mechanism of green plants, and its bearing on the carbon dioxide factor. Cold Spring Harbor Symp. Quant. Biol. 3:128-137.

Ershov, B.G., A.I. Mustafaev and A.K. Pikaev. 1971. Electron paramagnetic resonance spectra of irradiated frozen aqueous solutions of sulphuric and phosphoric acids at 77K and their properties. Int. J. Radiat. Phys. Chem. 3:71-84.

Esser, A.F. 1974a. Electron paramagnetic resonance Signal II in spinach chloroplasts - I. High resolution spectra and morphological location. Photochem. Photobiol. 20:167-172.

Esser, A.F. 1974b. Electron paramagnetic resonance Signal II in spinach chloroplasts - II. Influence of phosphorylation and electron-transport inhibitors. Photochem. Photobiol. 20:173-181.

Evans, M.C.W., A. Telfer and A.V. Lord. 1972. Evidence for the role of a bound ferredoxin as the primary electron acceptor of photosystem I in spinach chloroplasts. Biochim. Biophys. Acta 267:530-537.

Evans, M.C.W., S.G. Reeves and R. Cammack. 1974. Determination of the oxidation-reduction potential of the bound iron-sulfur proteins of the primary electron acceptor complex of photosystem I in spinach chloroplasts. FEBS Lett. 49:111-114.

Evans, M.C.W., C.K. Sihra, J.R. Bolton and R. Cammack. 1975. Primary electron acceptor complex of photosystem I in spinach chloroplasts. Nature 256:668-670.

Ewald, D. and D. Schlee. 1983. Biochemical effects of sulphur dioxide on proline metabolism in the alga Trebouxia sp. New Phytol. 94:235-240.

Flagler, R.B. and V.B. Youngner. 1982a. Ozone and sulfur dioxide effects on tall fescue: I. Growth and yield responses. J. Environ. Qual. 11(3):386-389.

Flagler, R.B. and V.B. Youngner. 1982b. Ozone and sulfur dioxide effects on three tall fescue cultivars. J. Environ. Qual. 11(3):413-416.

Flockhart,B.D., K.J. Ivin, R.C. Pink and B.D. Sharma. 1971. The nature of the radical intermediates in the reactions between hydroperoxides and sulphur dioxide and their reaction with alkene derivatives: electron spin resonance study. Chem. Commun. 339-340.

Ford, R. and J. Barber. 1980. The use of diphenylhexatriene to monitor the fluidity of the thylakoid membrane. Photobiochem. Photobiophys. 1:263-270.

Fork, D.C., G. Oquist and S.B. Powles. 1980. Photoinhibition in bean: a fluorescence analysis. Carnegie Inst. Washington Yearb. 81:52-57.

Forster, V., Y.Q. Hong and W. Junge. 1981. Electron transfer and proton pumping under excitation of dark-adapted chloroplasts with flashes of light. Biochim. Biophys. Acta 638:141-152.

Foster, J.G. and G.E. Edwards. 1980. Localization of superoxide dismutase in leaves of C_3 and C_4 plants. Plant and Cell Physiol. 21:895-906.

Foster, J.G. and J.L. Hess. 1982. Oxygen effects on maize leaf superoxide dismutase and glutathione reductase. Phytochem. 21:1527-1532.

Frank, H.A., M. McLean and K. Sauer. 1979a. Triplet states in photosystem I of spinach chloroplasts and subchloroplast particles. Proc. Natl. Acad. Sci. USA 76:5124-5128.

Frank, H.A., J.D. Bolt, S. M. de B. Costa and K. Sauer. 1979b. Electron paramagnetic resonance detection of carotenoid triplet states. J. Am. Chem. Soc. 102:4893-4898.

Frederick, P.E. and R.L. Heath. 1974. Ozone-induced fatty acid and viability changes in Chlorella. Plant Physiol. 55:15-19.

Frenkel, C. 1978. Role of hydroperoxides in the onset of senescence process in plant tissues. pp. 443-448 In Postharvest Biology and Biotechnology H.O. Hultin and M. Milner (Eds.) Food and Nutrition Press, Westport.

Fridovich, I. 1976a. Superoxide dismutases: studies in structure and function. pp. 530-539 In Advances in Experimental Medicine and Biology. Vol. 74. Iron and Copper Proteins. K. Yasunobu, H.F. Mover and O. Hayaise (Eds.) Plenum Press, New York.

Fridovich, I. 1976b. Superoxide and superoxide dismutases. pp. 67-90 In Advances in Inorganic Biochemistry. Vol. 1. G.L. Eichorn and L.G. Marzilli (Eds.) Elsevier/North Holland, New York.

Fridovich, I. 1978. The biology of oxygen radicals. Science 201:875-880.

Fridovich, I. 1981. Superoxide radical and superoxide dismutases. pp. 250-272 In Oxygen and Living Processes An Interdisciplinary Approach. D.L. Gilbert (Ed.) Springer-Verlag. New York-Heidelberg-Berlin.

Gast, P. and A.J. Hoff. 1979. Transfer of light-induced electron spin polarization from the intermediary acceptor to the prereduced primary acceptor in the reaction centre of photosynthetic bacteria. Biochim. Biophys. Acta 548:520-535.

Gast, P., T. Swarthoff, F.C.R. Ebskamp and A.J. Hoff. 1983. Evidence for a new early acceptor in Photosystem I of plants. An ESR investigation of reaction center triplet yield and of the reduced intermediate acceptors. Biochim. Biophys. Acta 722:163-175.

Gauhl, E. 1979. Sun and shade ecotypes of Solanum dulcamara L.: Photosynthetic light dependence characteristics in relation to mild water stress. Oecologia 39:61-70.

Giannopolitis, C.N. and S.K. Ries. 1977. Superoxide dismutases. 1. Occurence in higher plants. Plant Physiol. 59:309-314.

Glidewell, S. and J.A. Raven. 1975. Measurement of simultaneous oxygen evolution and uptake in Hydrodictyon africanum. J. Exp. Bot. 26:479-488.

Golbeck, J.H. and J.T. Warden. 1982. Electron spin resonance studies of the bound iron-sulphur centers in Photosystem I. Photoreduction of Center A occurs in the absence of center B. Biochim. Biophys. Acta 681:77-84.

Goldberg, B. and A. Stern. 1976. Superoxide anion as a mediator of drug-induced oxidative hemolysis. J. Biol. Chem. 251:6468-6470.

Goldfeld, M.G. and L.A. Blumenfeld. 1979. Light-dependent paramagnetic centers in the photosynthesis of higher plants. Bull. Mag. Res. 1:66-112.

Govindjee, T. Kambara and W. Coleman. 1985. The electron donor side of photosystem II: The oxygen evolving complex. Photochem. Photobiol. 42:187-210.

Haehnel, W. 1984. Photosynthetic electron transport in plants. Ann. Rev. Plant Physiol. 35:659-693.

Hales, B.J. and E.E. Case. 1981. Immobilized radicals IV. Biological semiquinone anions and neutral semiquinones. Biochim. Biophys. Acta 637:291-302.

Hales, B.J. and A. Das Gupta. 1981. Supposition of the origin of Signal II from random and oriented chloroplasts. Biochim. Biophys. Acta 637:291-302.

Halliwell, B. 1981. Free radicals, oxygen toxicity and aging. pp. 2-28 In Age Pigments. R.S. Sohal (Ed.) Elsevier/North Holland Biomedical Press.

Harbour, J.R. and J.R. Bolton. 1975. Superoxide formation in spinach chloroplasts: ESR detection by spin trapping. Biochem. Biophys. Res. Commun. 64:803-807.

Harbour, J.R. and J.R. Bolton. 1978. The involvement of the hydroxyl radical in the destructive photooxidation of chlorophylls in vivo and in vitro. Photochem. Photobiol. 28:231-234.

Hauska, G., E. Hurt, N. Gabellini and W. Lockau. 1983. Comparative aspects of quinol-cytochrome c/plastocyanin oxidoreductases. Biochim. Biophys. Acta 726:97-133.

Heath, R.L. 1975. Ozone. pp. 23-55 In Responses of Plants to Air Pollutants. J.B. Mudd and T.T. Kozlowski (Eds.) Academic Press, New York.

Heathcote, P. and M.C.W. Evans. 1980. Properties of the EPR spectrum of the intermediate electron acceptor (A_1) in several different photosystem particle preparations. FEBS Lett. 111:381-385.

Heck, W.W., and J.A. Dunning. 1967. The effects of ozone on tobacco and pinto bean as conditioned by several ecological factors. J. Air Pollut. Control Assoc. 17:112-114.

Hill, R. and F. Bendall. 1960. Function of the two cytochrome components in chloroplasts: A working hypothesis. Nature 186:136-1137.

Hoff, A.J. 1984. Electron spin polarization of photosynthetic reactants. Quart. Rev. Biophys. 17:153-282.

Hunziker, D., D.A. Abramowicz, R. Damoder and G.C. Dismukes. 1987. Evidence for an association between a 33kDa extrinsic membrane protein, manganese and photosynthetic oxygen evolution. I. Correlation with the S_2 multiline EPR signal. Biochim. Biophys. Acta 890:6-14.

Jansson, C., H.E. Akerlund and B. Andersson. 1983. Isolation and characterization of a 23kDa protein essential for photosynthetic oxygen evolution. Photosynth. Res. 4:271-279.

Joliot, P., G. Barbieri and R. Chabad. 1969. Un nouveau modele des centres photochimiques du systeme II. Photochem. Photobiol. 10:309-329.

Ke, B., R.E. Hansen and H. Beinert. 1973. Oxidation-reduction potentials of bound iron-sulfur proteins of photosystem I. Proc. Natl. Acad. Sci. USA 70:2941-2945.

Kellogg III, E.W. and I. Fridovich. 1975. Superoxide, hydrogen peroxide, and singlet oxygen in lipid peroxidation by a xanthine oxidase system. J. Biol. Chem. 250:8812-8817.

Kellogg III, E.W. and I. Fridovich. 1977. Liposome oxidation and erythrocyte lysis by enzymatically generated superoxide and hydrogen peroxide. J. Biol. Chem. 252:6721-6728.

Khangulov, S.V. and M.G. Gol'dfel'd. 1977. Two types of processes of reduction of the reaction centres of P^+700 in the leaves of higher plants. Biophys. 22:278-282.

Kharitonenkov, I.G. and G.S. Kalichava. 1966. Nature of the free radical states of plant tissues-I*. Biophys. 11:708-710.

Klimov, V.V., S.I. Allakhverdiev, V.A. Shuvalov and A.A. Krasnovsky. 1982. Effect of extraction and re-addition of manganese on light reactions of photosystem-II preparations. FEBS Lett. 148:307-312.

Knowles, P.F., J.F. Gibson, F.M. Pick and R.C. Bray 1969. Electron spin resonance evidence for enzymic reduction of oxygen to a free radical, the superoxide ion. Biochem. J. 111:53-58.

Kohl, D.H. and P.M. Wood. 1969. On the molecular identity of ESR Signal II observed in photosynthetic systems: The effect of heptane extraction and reconstitution with plastoquinone and deuterated plastoquionone. Plant Physiol. 44:1439-1445.

Kohl, D.H., J.R. Wright and M. Weissman. 1969. Electron spin resonance studies of free radicals derived from plastoquinone, - and -tocopherol and their relation to free radicals observed in photosynthetic materials. Biochim. Biophys. Acta 180:536-544.

Koike, H. and S. Katoh. 1982. Spectral features of the bound electron acceptor A_2 of photosystem I. Photochem. Photobiol. 35:5127-531.

Kok, B. 1956. On the inhibition of photosynthesis by intense light. Biochim. Biophys. Acta 21:234-244.

Kok, B., E.B. Gassner and H.J. Rurainski. 1965. Photoinhibition of chloroplast reactions. Photochem. Photobiol. 4:215-217.

Kok, B., B. Forbush and M. McGloin. 1970. Cooperation of charges in photosynthetic O_2 evolution-I. A linear fourstep mechanism. Photochem. Photobiol. 11:457-475.

Kono, Y. and I. Fridovich. 1982. Superoxide radical inhibits catalase. J. Biol. Chem. 257:5751-5754.

Kono, Y., M. Takahashi and K. Asada. 1979. Superoxide dismutases from kidney bean leaves. Plant and Cell Physiol. 20:1229-1235.

Koziol, M.J. and C.F. Jordan. 1978. Changes in carbohydrate levels in red kidney bean (Phaseolus vulgaris L.) exposed to sulphur dioxide. J. Exp. Bot. 29:1037-1043.

Kuthan, H., V. Ullrich and R.W. Estabrook. 1982. A quantitative test for superoxide radicals produced in biological systems. Biochem. J. 203:551-558.

Kuwabara, T. and N. Murata. 1982. An improved purification method and a further characterization of the 33 kilodalton protein in spinach chloroplasts. Biochim. Biophys. Acta 680:210-215.

Kuwabara, T. and N. Murata. 1983. Quantitative analysis of the inactivation of photosynthetic oxygen evolution and the release of polypeptides and manganese in the photosystem II particles of spinach chloroplasts. Plant Cell Physiol. 24:741-747.

Kyle, D.J., C.J. Arntzen and I. Ohad. 1983. The herbicide-binding 32 KD polypeptide is the primary site of photoinhibition damage. Plant Physiol. Suppl. 72:52.

Lamoreaux, R.J. and W.R. Chaney. 1978. Photosynthesis and transpiration of excised silver maple leaves exposed to cadmium and sulphur dioxide. Environ. Pollut. 17:259-268.

Lavelle, F., A.M. Michelson and L. Dimitrejevic. 1973. Biological protection by superoxide dismutase. Biochem. Biophys. Res. Commun. 55:350-357.

Le Sueur-Brymer, N.M. and D.P. Ormrod. 1984. Carbon dioxide exchange rates of fruiting soybean plants exposed to ozone and sulphur dioxide singly or in combination. Can. J. Pl. Sci. 64:69-75.

Lee, E.H. and J.H. Bennett. 1982. Superoxide dismutase. A possible protective enzyme against ozone injury in snap beans (Phaseolus vulgaris L.). Plant Physiol. 69:1444-1449.

Legassicke, B.C. and D.P. Ormrod. 1981. Suppression of ozone-injury on tomatoes by ethylene diurea in controlled environments and in the field. Hort Sci. 16:183-184.

Leshem, Y.Y. 1981. Oxy free radicals and plant senescence. What's New in Plant Physiol. 12:1-4.

Leshem, Y.Y., Y. Liftman, S. Grossman and A.A. Frimer. 1981. Free radicals and pea foliage senescence: Increase of lipoxygenase and ESR signals and cytokinin-induced changes. pp. 676-678 In Oxygen and Oxy-radicals in Chemistry and Biology. E.L. Powers and M.A.J. Rodgers (Eds.) Academic Press, New York.

Levitt, J. 1980. Man-made stresses. pp. 507-530 In Responses of Plants to Environmental Stresses. Vol. II. Academic Press, New York.

Louwerse, W. and W.V.D. Zweerde. 1977. Photosynthesis, transpiration and leaf morphology of Phaseolus vulgaris and Zea mays grown at different irradiances in artificial and sunlight. Photosynthetica. 11:11-21.

Lozier, R.H. and W.L. Butler. 1973. Effects of photosystem II inhibitors on electron paramagnetic resonance Signal II of spinach chloroplasts. Photochem. Photobiol. 17:133-137.

Lozier, R.H. and W.L. Butler. 1974. Redox titrations of the primary electron acceptor of Photosystem I in spinach chloroplasts. Biochim. Biophys. Acta. 333:460-464.

Ludlow, M.M. and O. Bjorkman. 1983. Paraheliotropic leaf movement as a protective mechanism against drought-induced damage to primary photosynthetic reactions. Carnegie Inst. Washington Yearb. 82:73-78.

Majernik, O. 1971. A physiological study of the effects of SO_2 pollution, phenylmercuric acetate sprays, and parasitic infection on stomatal behavior and aging in barley. Phytopath Z. 72:255-268.

Majernik, O. and T.A. Mansfield. 1971. Effects of SO_2 pollution on stomatal movements in Vicia faba. Phytopath Z. 71:123-128.

Majernik, O. and T.A. Mansfield. 1972. Stomatal responses to raised atmospheric CO_2 concentrations during exposure of plants to SO_2 pollution. Environ. Pollut. 3:1-7.

Malhotra, S.S. and D. Hocking. 1976. Biochemical and cytological effects of sulphur dioxide on plant metabolism. New Phytol. 76:227-237.

Malhotra, S.S. and S.K. Sarkar. 1979. Effects of sulfur dioxide on sugar and free amino acid content of pine seedlings. Plant Physiol. 47:223-228.

Malkin, R. 1982. Redox properties and functional aspects of electron carriers in chloroplast photosynthesis. pp. 1-47 In Topics in Photosynthesis. J. Barber (Ed.). Elsevier Biomedical Press. Amsterdam/New York/Oxford.

Malkin, R. and A.J. Bearden. 1971. Primary reactions of photosynthesis: photoreduction of a bound chloroplast ferredoxin at low temperature as detected by EPR spectroscopy. Proc. Natl. Acad. Sci. USA 68:16-19.

Malkin, R. and A.J. Bearden. 1974. On the reversibility of the primary reaction of chloroplast photosystem I at low temperatures. Abstract No. 378. Fed. Proc. 33:1289.

Malkin, R. and A.J. Bearden. 1978. Membrane-bound iron-sulfur centers in photosynthetic systems. Biochim. Biophys. Acta 505:147-181.

Malkin, R. and T. Vanngard. 1980. An EPR study of cytochromes from spinach chloroplsts. FEBS Lett. 111:228-231.

McCain, D.C., T.C. Selig, Govindjee and J.L. Markley. 1984. Some plant leaves have orientation-dependent EPR and NMR spectra. Proc. Natl. Acad. Sci. USA 81:748-752.

McIntosh, A.R. and J.R. Bolton. 1976. Electron spin resonance spectrum of species "X" which may function as the primary electron acceptor in photosystem I of green plant photosynthesis. Biochim. Biophys. Acta. 430:555-559.

McIntosh, A.R. and J.R. Bolton. 1979. CIDEP in the photosystems of green plant photosynthesis. Rev. chem. Interm. 3:121-129.

McKersie, B.D., W.D. Beversdorf and P. Hucul. 1982. The relationship between ozone insensitivity, lipid-soluble antioxidants, and superoxide dismutase in Phaseolus vulgaris. Can. J. Bot. 60:2686-2691.

McLaughlin, S.B. and R.K. McConathy. 1983. Effects of SO_2 and O_3 on allocation of ^{14}C-labelled photosynthate in Phaseolus vulgaris. Plant Physiol. 73:630-351.

McRae, D.G. and J.E. Thompson. 1983. Senescence-dependent changes in superoxide anion production by illuminated chloroplasts from bean leaves. Planta. 158:185-193.

Mehler, A.H. 1951. Studies on reactions of illuminated chloroplasts. I. Mechanism of the reduction of oxygen and other Hill reagents. Arch. Biochem. Biophys. 33:65-77.

Michelson, A.M. and M.E. Buckingham. 1974. Effects of superoxide radicals on myoblast growth and differentiation. Biochem. Biophys. Res. Commun. 58:1079-1086.

Milchunas, D.G., W.K. Lauenroth, J.L. Dodd and T.J. McNary. 1981. Effects of SO_2 exposure with nitrogen and sulphur fertilization on the growth of Agropyron smithii. J. App. Ecol. 18:291-302.

Miller, R.W. and MacDowell, F.D.H. 1975. The Tiron free radical as a sensitive indicator of chloroplastic photooxidation. Biochim. Biophys. Acta 387:176-187.

Mishra, S.D., I.C. Dave, B.B. Singh and B.K. Gaur. 1971. Electron spin resonance (ESR) study of developing and aging betel leaves. Proc. Natl. Acad. Sci. India (B) 74:102-105.

Mitchell, P. 1961. Coupling of phosphorylation to electron and hydrogen transfer by a chemi-osmotic type of mechanism. Nature 191:144-148.

Moller, B.L., J.H.A. Nugent and M.C.W. Evans. 1981. Electron paramagnetic resonance spectrometry of photosystem I mutants in barley. Carlsberg Res. Commun. 46:373-382.

Mottley, C., R.P. Mason, C.F. Chignell, K. Sivarajah and T.E. Eling. 1982a. The formation of sulfur trioxide radical anion during the prostaglandin hydroperoxidase-catalyzed oxidation of bisulfite (Hydrated sulfur dioxide). J. Biol. Chem. 257:5050-5055.

Mottley, C., T.B. Trice and R.P. Mason. 1982b. Direct detection of the sulfur trioxide radical anion during the horseradish peroxidase-hydrogen peroxide oxidation of sulfite (Aqueous sulfur dioxide). Mol. Pharmacol. 22:732-737.

Mudd, J.B., R. Leavitt, A. Ongun and T.T. McManus. 1969. Reaction of ozone with amino acids and protein. Atmos. Environ. 3:669-682.

Mudd, J.B., T.T. McManus, A. Ongun and T.E. McCullogh. 1971. Inhibition of glycolipid biosynthesis in chloroplasts by ozone and sulfhydryl reagents. Plant Physiol. 48:335-339.

Mudd, J.B. 1973. Biochemical effects of some air pollutants on plants. pp. 31-47 In Air Pollution Damage to Plants. Adv. Chem. Ser. Vol. 122. J.A. Naegele (Ed.) Am. Chem. Soc., Washington D.C.

Mudd, J.B., F. Leh and T.T. McManus. 1974. Reaction of ozone with nicotinamide and its derivatives. Arch. Biochem. Biophys. 161:408-419.

Mudd, J.B. 1982. Effects of oxidants on metabolic function. pp. 189-203 In Effects of Gaseous Air Pollution in Agriculture and Horticulture. M.H. Unsworth and D.P. Ormrod (Eds.) Butterworth Scientific, Toronto.

Myers, J. and G.O. Burr. 1940. Studies on photosynthesis: Some effects of high intensity light on chlorella. J. Gen. Physiol. 24:45-67.

Nelson, N., H. Nelson and E. Racker. 1972. Photoreaction of FMN-Tricine and its participation in photophosphorylation. Photochem. Photobiol. 16:481-489.

Nilsson, R. and D.R. Kearns. 1973. A remarkable deuterium effect on the rate of photosensitized oxidations of alcohol dehydrogenase and trypsin. Photochem. Photobiol. 17:65-68.

Norman, R.O.C. and P.M. Storey. 1971. Electron spin resonance studies. Part XXXI. The generation and some reactions of the radicals SO_3^-, $S_2O_3^-$ and SH in aqueous solution. J Chem. Soc. Sect. B 1009-1013.

Norris, J.R., R.A. Uphaus, H.L. Crespi and J.J. Katz. 1971. Electron spin resonance of chlorophyll and the origin of Signal I in photosynthesis. Proc. Natl. Acad. Sci. USA 68:625-628.

Nugent, J.H.A. and M.C.W. Evans. 1980. EPR signals of cytochromes in subchloroplast particles. FEBS Lett. 112:1-4.

Nugent, J.H.A., B.A. Diner and M.C.W. Evans. 1981a. Direct detection of the electron acceptor of photosystem II. Evidence that Q is an iron-quinone complex. FEBS Lett. 124:241-244.

Nugent, J.H.A., B.L. Moller and M.C.W. Evans. 1981b. Comparison of the EPR properties of photosystem I iron-sulphur centres A and B in spinach and barley. Biochim. Biophys. Acta 634:249-255.

Nugent, J.H.A., B.A. Diner and M.C.W. Evans. 1981c. Direct detection of the electron acceptor of photosystem II. FEBS Lett. 124:241-244.

O'Malley, P.J. and G.T. Babcock. 1984a. EPR properties of immobilized quinone cation radicals and the molecular origin of Signal II in spinach chloroplasts. Biochim. Biophys. Acta 765:370-379.

O'Malley, P.J. and G.T. Babcock. 1984b. Electron nuclear double resonance evidence supporting a monomeric nature for P700+ in spinach chloroplasts. Proc. Natl. Acad. Sci. USA 81:1098-1101.

Ormrod, D.P., V.J. Black and M.H. Unsworth. 1981. Depression of net photosynthesis in Vicia faba L. exposed to sulphur dioxide and ozone. Nature 291:585-586.

Oshima, R.J., J.P. Bennett and P.K. Braegelmann. 1978. Effect of ozone on growth and assimilate partitioning in parsley. J. Amer. Soc. Hort. Sci. 103:348-350.

Palmer, G., R.C. Bray and H. Beinert. 1964. Direct studies on the electron transfer sequence in xanthine oxidase by electron paramagnetic resonance spectroscopy. I. Techniques and description of spectra. J. Biol. Chem. 239:2657-2666.

Patton, S.E., G.M. Rosen and E.J. Rauckman. 1980. Superoxide production by purified hampster hepatic nuclei. Mol. Pharmacol. 18:588-593.

Pauls, K.P. and J.E. Thompson. 1981a. In vitro simulation of senescence-related membrane damage by ozone-induced lipid peroxidation. Nature 283:504-506.

Pauls, K.P. and J.E. Thompson. 1981b. Effects of in vitro treatment with ozone on the physical and chemical properties of membranes. Physiol. Plant. 53:255-262.

Peiser, G.D. and S.F. Yang. 1977. Chlorophyll destruction by the bisulphite-oxygen system. Plant Physiol. 60:277-281.

Powles, S.B. 1984. Photoinhibition of photosynthesis induced by visible light. Ann. Rev. Plant Physiol. 35:15-44.

Powles, S.B. and O. Bjorkman. 1983. Photoinhibition of photosynthesis: Effect on chlorophyll fluorescence at 77K in intact leaves and in chloroplast membranes of Nerium oleander. Planta. 156:97-107.

Powles, S.B. and C. Critchley. 1980. Effect of light intensity during growth on photoinhibition of intact attached bean leaflets. Plant Physiol. 65:1181-1187.

Powles, S.B., C.B. Osmond and S.W. Thorne. 1979. Photoinhibition of intact attached leaves of C_3 plants illuminated in the absence of both carbon dioxide and of photorespiration. Plant Physiol. 64:982-988.

Powles, S.B. and S.W. Thorne. 1981. Effect of high-light treatments in inducing photoinhibition of photosynthesis in intact leaves of low-light grown Phaseolus vulgaris and Lastreopsi microsora. Planta 152:471-477.

Prenzel, U. and H.K. Lichtenthaler. 1982. Localization of B-carotene in chlorophyll-a proteins and changes in its levels during short-term high light exposure of plants. pp. 565-572 In Biochemistry and Metabolism of Plant Lipids. J.F.G.M.W.Bioernar, P.J.C. Kuiper (Eds.). Elsevier Press. Amsterdam

Priestley, D.A., M.B. McBride and C. Leopold. 1980. Tocopherol and organic free radical levels in soybean seeds during natural and accelerated aging. Plant Physiol. 66:715-719

Pryor, W.A. 1976. The role of free radical reactions in biological systems. pp. 1-49 In Free Radicals in Biology. Vol 1. W.A. Pryor (Ed.) Academic Press, New York.

Puget, K. and A.M. Michelson. 1974. Isolation of a new copper-containing superoxide dismutase: bacteriocuprein. Biochem. Biophys. Res. Commun. 58:830-838.

Rabinowitch, E.J. 1945. Photosynthesis and Related Processes. Vol. 1. New York: Interscience.

Rabinowitch, H.D. and I. Fridovich. 1983. Superoxide radicals, superoxide dismutases and oxygen toxicity in plants. Photochem. Photobiol. 37:679-690.

Rabinowitch, H.D. and D. Sklan. 1980. A possible protective agent against sunscald in tomatoes (Lycopersicon esculentum Mill.). Planta 148:162-167.

Rabinowitch, H.D. and D. Sklan. 1981. Superoxide dismutase activity in ripening cucumber and pepper fruit. Physiol. Plant. 52:380-384.

Reed, G.H. and M. Cohn. 1970. Electron paramagnetic resonance spectra of manganese (II)-protein complexes. Manganese (II)-concanavalin a. J. Biol. Chem. 245:662-667.

Reed, G.H. and W.J. Ray. 1971. Electron paramagnetic resonance studies of manganese (II) coordination in the phosphoglucomutase system. Biochem. J. 10:3190-3197.

Reed, G.H., J.S. Leigh Jr. and J.E. Pearson. 1971. Electron paramagnetic relaxation and EPR line shapes of manganous ion complexes in aqueous solutions. Frequency and ligand dependence. J. Chem. Phys. 55:3311-3316.

Rich, P.R. and W.D. Bonner. 1978. The sites of superoxide anion generation in higher plant mitochondria. Arch. Biochem. Biophys. 188:206-213.

Roberts, B.D. 1976. The response of field-grown white pine seedlings to different sulphur dioxide environments. Environ. Pollut. 11:175-180.

Robinson, D.C. and A.R. Wellburn. 1983. Light-induced changes in the quenching of 9-amino-acridine fluorescence by photosynthetic membranes due to atmospheric pollutants and their products. Environ. Pollut. 32:109-120.

Rowlands, J.R., E.M. Gause, C.F. Rodriguez and H.C. McKee. 1970. Electron spin resonance studies of vegetation damage. Final report SwRI Project No. 05-2622-01. Prepared for National Air Pollution Control Administration Division of Economic Effects Research North Carolina State University. 67pp.

Runeckles, V.C. 1974. Dosage of air pollutants and damage to vegetation. Environ. Conserv. 1:305-308.

Runeckles, V.C. and H.M. Resh. 1975. Effects of cytokinins on responses of bean leaves to chronic ozone treatment. Atmos. Environ. 9:749-753.

Rupp, H., A. De la Torre and D.O. Hall. 1979. The electron spin relaxation of the electron acceptors of photosystem I reaction centers studied by microwave power saturation. Biochim. Biophys. Acta 548:552-564.

Rutherford, A.W. 1985. Orientation of EPR signals arising from components in Photosystem II membranes. Biochim. Biophys. Acta 807:189-201.

Rutherford, A.W. and J.E. Mullet. 1981. Reaction centre triplet states in photosystem I and photosystem II. Biochim. Biophys. Acta 635:225-235.

Rutherford, A.W., D.R. Paterson and J.E. Mullet. 1981. A light-induced spin-polarized triplet detected by EPR in photosystem II reaction centres. Biochim. Biophys. Acta 635:205-214.

Rutherford, A.W., J.L. Zimmermann and P. Mathis. 1984a. The effect of herbicides on components of the PSII reaction centre measured by EPR. FEBS Lett. 165:156-162.

Rutherford, A.W., G. Renger, H. Koike and Y. Inoue. 1984b. Thermoluminescence as a probe of PS-II: the redox and protonation states of the secondary acceptor quinone and the O_2-evolving enzyme. Biochim. Biophys. Acta 767:548-556.

Ruuge, E.K. and A.N. Tikhonov. 1972. Investigation of the electron transport in photosynthetic systems of higher plants by the EPR method - III. Adaptational phenomena at different intensities of light. Biophys. 22:273-277.

Sakaki, T. and N. Kondo. 1983. Inhibition of photosynthesis by sulphite in mesophyll protoplasts isolated from Vicia faba L. in relation to intracellular sulphite accumulation. Plant Cell Physiol. 26:1045-1055.

Sakaki, T., N. Kondo and K. Sugahara. 1983. Breakdown of photosynthetic pigments and lipids in spinach leaves with ozone fumigation: Role of active oxygen. Physiol. Plant. 59:28-34.

Samuel, D. and F. Steckel. 1974. The physico-chemical properties of molecular oxygen. pp. 1-27 In Molecular Oxygen In Biology. O. Hayaishi (Ed.) Elsevier/North Holland: New York, Amsterdam, Oxford.

Satoh, K. 1970a. Mechanism of photoinactivation in photosynthetic systems. I. The dark reaction in photoinactivation. Plant Cell Physiol. 11:15-27.

Satoh, K. 1970b. Mechanism of photoinactivation in photosynthetic systems. II. The occurance and properties of two different types of photoinactivation. Plant Cell Physiol. 11:29-38.

Satoh, K. 1970c. Mechanism of photoinactivation in photosynthetic systems. III. Site and mode of photoinactivation in photosystem I. Plant Cell Physiol. 11:187-197.

Satoh, K., H. Koike and Y. Inoue. 1983. Properties of EPR Signal II in purified Photosystem II reaction center complex. Photobiochem. Photobiophys. 6:267-277.

Shimazaki, K. and K. Sugahara. 1979. Specific inhibition of photosystem II activity in chloroplasts by fumigation of spinach leaves with SO_2. Plant & Cell Physiol. 20:947-955.

Shimazaki, K. and K. Sugahara. 1980. Inhibition site of the electron transport system in lettuce chloroplasts by fumigation of leaves with SO_2. Plant & Cell Physiol. 21:125-135.

Shimazaki, K., T. Sakaki, N. Kondo and K. Sugahara. 1980. Active oxygen participation in chlorophyll destruction and lipid peroxidation in SO_2-fumigated leaves of spinach. Plant & Cell Physiol. 21:1193-1204.

Shimazaki, K., K. Nakamachi, N. Kondo and K. Sugahara. 1984a. Sulfite inhibition of photosystem II in illuminated spinach leaves. Plant & Cell Physiol. 25:337-341

Shimazaki, K., K. Ito, N. Kondo and K. Sugahara. 1984b. Reversible inhibition of photosynthetic water-splitting enzyme system by SO_2-fumigation assayed by chlorophyll fluorescence and EPR signal *in vivo*. Plant & Cell Physiol. 25:795-803.

Shuvalov, V.A., E Dolan and B. Ke. 1979. Spectral and kinetic evidence for two early electron acceptors in photosystem I. Proc. Natl. Acad. Sci. USA 76:770-773.

Singer, S.J. and G.L. Nicholson. 1972. The fluid mosaic model of the structure of cell membranes. Cell membranes are viewed as two-dimensional solutions of oriented globular proteins and lipids. Science 175:720-731.

Sironval, C.C. and O. Kandler. 1958. Photooxidation processes in normal green *Chlorella* cells. I. The bleaching process. Biochim. Biophys. Acta 29:359-368.

Sisson, W.B., J.A. Booth and G.O. Throneberry. 1981. Absorption of SO_2 by pecan (*Carya illinoensis* (Wang) K. Koch) and alfalfa (*Medicago sativa* L.) and its effect on net photosynthesis. J. Exp. Bot. 32:523-534.

Styring, S., M. Miyao and A.W. Rutherford. 1987. Formation and flash-dependent oscillation of the S_2-state multiline EPR signal in an oxygen-evolving Photosystem-II preparation lacking the three extrinsic proteins in the oxygen-evolving system. Biochim. Biophys. Acta 890:32-38.

Takemoto, B.K. and R.D. Noble. 1982. The effects of short-term SO_2 fumigation of photosynthesis and respiration in soybean *Glycine max*. Environ. Pollut. 28:67-74.

Tanaka, K. and K. Sugahara. 1980. Role of superoxide dismutase in the defence against SO_2 toxicity and increase in superoxide dismutase activity with SO_2 fumigation. Plant & Cell Physiol. 21:601-611.

Taylor, G.E. and D.T. Tingey. 1981. Physiology of ecotypic plant response to sulphur dioxide in *Geranium carolinianum* L. Oecologia. 49:76-82.

Theg, S.M. and R.T. Sayre. 1979. Characterization of chloroplasts manganese by electron paramagnetic resonance spectroscopy. Plant Sci. Lett. 15:319-326.

Thomas, M.D. and G.R. Hill. 1937. Relation of sulphur dioxide in the atmosphere to photosynthesis and respiration of alfalfa. Plant Physiol. 12:309-383.

Thompson, J.E., R.E. Legge and R.F. Barber. 1987. The role of free radicals in senescence and wounding. New Phytol. 105:317-344.

Tikhonov, A.N. and E.K. Ruuge. 1975a. Investigation of electron transport in the photosynthetic systems of higher plants by the EPR method - I. Influence of the pre-history of illumination on the kinetics of the photo-induced redox conversions of P700. Biophys. 20:1069-1974.

Tikhonov, A.N. and E.K. Ruuge. 1975b. Investigation of electron transport in the photosynthetic systems of higher plants by the EPR method - II. Influence of temperature on the course of photo-induced redox conversions of P700. Biophys. 20:1075-1079.

Tingey, D.T. 1974. Ozone-induced alterations in the metabolite pools and enzyme activities of plants. pp. 40-57 In Air Pollution Effects on Plant Growth. M. Dugger (Ed.) Am. Chem. Soc., Washington D.C.

Tomlinson, H. and S. Rich. 1970. Lipid peroxidation as a result of injury in bean leaves exposed to ozone. Phytopath. 60:1531-1532.

Treharne, R.W. and H.C. Eyster. 1962. Electron spin resonance study of manganese and iron in Chlorella pyrenoidosa. Biochem. Biophys. Res. Comm. 8477-480.

Treharne, R.W., C.W. Melton and R.M. Roppel. 1964. Electron spin resonance signals and cell structure of Chlorella pyrenoidosa grown under different light intensities. J. Mol. Biol. 10:57-62.

Van Ginkel, G. and J.K. Raison. 1980. Light-induced formation of O_2^- oxygen radicals in systems containing chlorophyll. Photochem. Photobiol. 32:793-798.

Van Gorkum, H.J., R.F. Meiburg and R.J. Van Dorssen. 1983. The effects of an electrical field on the primary reactions of photosystem 2. p. 204 Abstr. 6th Int. Congr. Photosynth., Brussels.

Velthuys, B.R. and J. Amesz. 1974. Charge accumulation at the reducing side of system 2 of photosynthesis. Biochim. Biophys. Acta 333:85-94.

Visser, J.W.M., J. Amesz and F. Van Gelder. 1974. EPR signals of oxidized plastocyanin in intact algae. Biochim. Biophys. Acta 333:279-287.

Warden, J.T. and J.R. Bolton. 1974a. The relation of the ESR Signal II to electron transport in Photosystem II of spinach chloroplasts. Photochem. Photobiol. 20:245-250.

Warden, J.T. and J.R. Bolton. 1974b. Flash photolysis-electron spin resonance studies of the dynamics of photosystem I in green-plant photosynthesis - II. Intact and broken spinach chloroplasts. Photochem. Photobiol. 20:263-269.

Warden, J.T., R.E. Blankenship and K. Sauer. 1976. A flash photolysis ESR study of photosystem II Signal II_{vf}, the physiological donor to $P\text{-}680^{+}$. Biochim. Biophys. Acta 423:462-478.

Warden, J.T. and J.H. Golbeck. 1987. Electron-spin resonance studies of the bound iron-sulfur centers in Photosystem I. II. Correlation of P-700 triplet production with urea/ferricyanide inactivation of the iron-sulfur clusters. Biochim. Biophys. Acta 891:286-292.

Warner, C.W. and Caldwell, M.M. 1983. Influence of photon flux density in the 400-700 nm waveband on inhibition of photosynthesis by UV-B (280-320 nm) irradiation in soybean leaves: Separation of indirect and immediate effects. Photochem. Photobiol. 37:

Wasielewski, M.R., J.R. Norris, L.L. Shipman, C. Lin, and W. Svec. 1981. Monomeric chlorophyll a enol: Evidence for its possible role as the primary electron donor in photosystem I of plant photosynthesis. Proc. Natl. Acad. Sci. USA 78:2957-2961.

Weaver, E.C. 1962. Possible interpretation of the slow-decaying ESR signal in algal solutions. Arch. Biochim. Biophys. 99:193-196.

Weaver, E.C. 1968. EPR studies of free radicals in photosynthetic systems. Ann. Rev. Plant Physiol. 19:283-294.

Weiss, J. 1935. Investigation on the radical HO_2 in solution. Trans. Faraday Soc. 31:668-681.

Wellburn, A.R., C. Higginson, D. Robinson and C. Walmsley. 1981. Biochemical explanations of more than additive inhibitory effects of low atmospheric levels of sulphur dioxide plus nitrogen dioxide upon plants. New Phytol. 88:223-237.

Whitelam, G.C. and G.A. Codd. 1983. Photoinhibition of photosynthesis in the cyanobacterium Microcystis acruginosa. Planta 157:561-566.

Wilton, A.C., J.J. Murray, H.E. Heggestad and F.V. Juska. 1972. Tolerance and susceptibility of Kentucky bluegrass (Poa pratensis L.) cultivars to air pollution, in the field and in an ozone chamber. J. Environ. Qual. 1:112-114.

Winner, W.E. and H.A. Mooney. 1980. Ecology of SO_2 resistance: II. Photosynthetic changes of shrubs in relation to SO_2 absorption and stomatal behaviour. Oecologia. 44:296-302.

Wydrzynski, T. and K. Sauer. 1980. Periodic changes in the oxidation state of manganese in photosynthetic oxygen evolution upon illumination with flashes. Biochim. Biophys. Acta 589:56-70.

Yamamoto, Y., M. Doi, N. Tamura and M. Nishimura. 1981. Release of polypeptides from highly active O_2 evolving photosystem 2 preparation by Tris treatment. FEBS Lett. 133:265-268.

Yamamoto, Y., S. Shimada and M. Nishimura. 1983. Purification and molecular properties of 3 polypeptides released from a highly active O_2 evolving photosystem-II preparation by Tris-treatment. FEBS Lett. 151:49-53.

Yocum, C.F. and G.T. Babcock. 1981. Amine-induced inhibition of photosynthetic oxygen evolution. FEBS Lett. 130:99-102.

Yocum, C.F., C.T. Yerkes, R.E. Blankenship, R.R. Sharp and G.T. Babcock. 1981. Stoichiometry, inhibitor sensitivity, and organization of manganese associated with photosynthetic oxygen evolution. Proc. Natl. Acad. Sci. USA 78:7507-7511.

Zimmermann, J.L. and A.W. Rutherford. 1984. EPR studies on the O_2-evolving enzyme of Photosystem II. Biochim. Biophys. Acta 767:160-167.

Zimmermann, J.L. and A.W. Rutherford. 1986. Photoreductant-induced oxidation of Fe^{2+} in the electron-acceptor complex of Photosystem II. Biochim. Biophys. Acta 851:416-423.

APPENDIX A

The use of electron paramagnetic resonance (EPR) spectroscopy enables the investigator to study the formation of free radicals in the electron transport chain of photosynthesis. EPR is a form of absorbance spectroscopy discovered by a Russian physicist (Zavoisky, 1945). EPR is similar to other forms of absorbance spectroscopy in that it relies upon a transition in the energy level of molecules upon absorption of radiation. In this case the transition energies in magnetic resonance caused by microwave radiation correspond to the interaction of unpaired electrons with a magnetic field. As the technique is dependent upon the detection of unpaired electrons it is quite specific. It is only applicable to the study of free radicals and metallocomplexes which have paramagnetic metal components.

In biological systems, copper, iron and manganese are the most prevalent paramagnetic metals but molybdenum, cobalt, vanadium and tungsten also show EPR signals in some of their valence states. In EPR spectrometry the magnetic resonance absorption is displayed as its first derivative; i.e. maximum absorption occurs at the field strength at which the spectral line crosses the baseline. EPR signals are primarily identified by their g-values, line widths and hyperfine splittings. The

g-value is a dimensionless constant determined experimentally from the first derivative signal as the value at the point of the maximum downward slope of the curve, i.e. the field strength for maximum absorption. It is defined as:

$$h\nu = gBH$$

where h is Planck's constant, v is the radiation frequency, B is the Bohr magneton (natural unit of electron magnetic moment) and H is the magnetic field as measured in gauss (1 gauss = 9.35×10^{-5}cm).

In addition to the use of the above equation, g-values can be obtained by comparison to a standard such as DPPH (diphenyl-picrylhydrazyl) for which the g-value (2.0037) is known. The unknown g-value, g_X, is calculated from the equation:

$$g_X = g_S\left[1 + \frac{(H_S - H_X)}{H_S}\right]$$

where g_S is the g-value of the standard and H_S and H_X are the magnetic fields for the standard and unknown, respectively.

Organic free radicals have a g-value of approximately 2.0023, with deviations only occurring at the third decimal place, thereby making identification based only upon the g-value difficult, and also causing an overlap of signals in many cases. The hyperfine splittings associated with EPR signals are caused by the interaction of the unpaired electrons with neighbouring nuclei - usually protons or nitrogen atoms. These splittings are frequently resolvable in simple biological

systems but are exceedingly complex in whole tissue. Other aids in identification of EPR signals include line shape, peak-to-peak line width and line amplitude (Knowles et al. 1976).

In many cases the positions and splittings of the lines, as specified by the g-values and hyperfine constants, are dependent upon the direction of the magnetic field relative to the molecular axes. This spectral anisotrophy is not encountered in systems where the free electron is extensively delocalized. In such systems the anisotrophy is small and the rapid random rotation of the radicals in free solution averages out the remaining small anisotrophic splittings and shifts. However, in systems where the free electron is not delocalized, such as crystalline systems, the anisotrophy is normally completely specified by the three g-values and hyperfine constants obtained parallel to the principle axes. The g-values are usually cited as g_z, g_x and g_y. In cases where the molecular system is axially symmetrical, the principal g-values are designated as $g_{parallel}$ ($g_{||}$) and $g_{perpendicular}$ ($g_{\perp}$) (Knowles et al. 1976).

Optimal signal strength with minimum noise is obtained through experimentation with varying the scan time and the time constant. A long time constant will improve the signal-to-noise ratio but if the scan time is limited, the limiting response of

the time constant will cause distortions in the lineshape. Thus, the settings chosen are a compromise between the time taken to scan the spectrum and the the extent to which noise is filtered out. The choice of modulation amplitude is also a compromise, between the modulation required to detect a strong signal and lineshape distortion, known as modulation broadening, which occurs as a result of excessively high modulation amplitudes. Settings are optimized by varying the time constant, scan time and modulation amplitude until no further change is produced in the lineshape.

Spin trapping is a technique whereby short-lived reactive free radicals may be transformed into persistent paramagnetic species. Consequently, EPR techniques can be used to detect radicals at concentrations below the normal detection limits (Finkelstein et al. 1980). The technique is dependent upon the incorporation of a diamagnetic substance, called the spin trap, which has a high affinity for a reactive radical, to the reaction system containing the radical. The product of this combination, called the spin adduct, must be a persistent free radical whose concentration will build to readily detectable levels (Perkins, 1980). Useful spin traps include DMPO (5,5-dimethyl-pyrroline-N-oxide), which forms spin adducts with characteristic EPR signals from different free radicals such as the superoxide, hydroxyl and sulphur trioxide free radicals, and Tiron ((1,2-dihydroxybenzene-3,5-disulphonate), which is very

specific, as it forms a spin adduct with superoxide and does not combine with hydroxyl or singlet oxygen (Miller and MacDowell, 1975). However, the intensity of spin adduct signals obtained with DMPO as the spin trap is influenced by the presence of iron (Buettner et al. 1978), while their half-life varies, depending upon pH (Buettner and Oberley, 1978). Also, the specificity of Tiron to the superoxide free radical is not universally accepted as Van Ginkel and Raison (1980) state that Tiron scavenges the hydroxyl free radical, not the superoxide free radical.

LITERATURE CITED

Buettner, G.R. and L.W. Oberley. 1978. Considerations in the spin trapping of superoxide and hydroxyl radical in aqueous systems using 5,5-dimethyl-1-pyrroline-1-oxide. Biochem. Biophys. Res. Commun. 83:69-74.

Buettner, G.R., L.W. Oberley and S.W.H. Chan Leuthauser. 1978. The effect of iron on the distribution of superoxide and hydroxyl radicals as seen by spin trapping and on the superoxide dismutase assay. Photochem. Photobiol. 28:693-695.

Finkelstein, E., G.M. Rosen and E.J. Rauckman. 1980. Spin trapping of superoxide and hydroxyl radical: practical aspects. Arch. Biochem. Biophys. 200:1-16.

Knowles, P.F., D. Marsh and H.W.E. Rattle. 1976. Magnetic Resonance of Biomolecules. John Wiley and Sons. London, New York, Sydney, Toronto. 343pp.

Miller, R.W. and F.D.H. MacDowell. 1975. The Tiron free radical as a sensitive indicator of chloroplastic photooxidation. Biochim Biophys. Acta 387:176-187.

Perkins, M.J. 1980. Spin trapping. pp. 1-64 In Advances in Physical Organic Chemistry. Vol. 17. V. Gold and D. Bethell (Eds.). Academic Press (London Ltd.

Van Ginkel, G. and J.K. Raison. 1980. Light-induced formation of O_2^- oxygen radicals in systems containing chlorophyll. Photochem. Photobiol. 32:793-798.

Zavoisky, E. 1945. Paramagnetic relaxation of liquid solutions for perpendicular fields. J. Phys. USSR 9:211-216.

APPENDIX B

Established EPR Signals Relevant to This Study

Photosynthetic Signals

Name	g-value	Width	Function of Free Radical
Signal I	2.0025	7.5-9.0g	Primary donor to Photosystem I
Signal II (u+s)	2.0046	18-20g	Unidentified secondary donor to Photosystem II
a_1	2.0054	10.8g	Unidentified early acceptor of Photosystem I
a_0	2.0017	11.5g	Unidentified early acceptor of Photosystem I

Other Signals

Name	g-value	Width	Other Relevant Information
DPPH	2.0037	4g	Used as a marker to establish g-values of other free radicals
O_2^-	2.001	10g	Present in superoxide-forming enzyme systems; asymmetrical
SO_3^-	2.0030-2.0033	--	Present in SO_3^--forming enzyme systems
'Organic' Free Radical	2.00	9-11g	Present in aged plant material

APPENDIX B (Continued)

Previously Unreported Signals Revealed in This Study

Name	g-value	Width	Other Characteristics
N_{710}	2.0054	8.5g	Occurs in plant leaves within 1 hour of exposure to 710nm light
N_{PI}	2.0056	9.0g	Present in leaves exposed to high photon flux density
N_{O1}	2.0041	10.0g	Occurs in leaves exposed to more than 2 hours of intermediate levels of ozone (80-250ppb)
N_{O2}	2.0055	7-8.0g	Occurs in darkness in leaves exposed to high levels of ozone
N_{Sox}	2.001 + 2.08	10.0g	Asymmetrical; similar to superoxide anion radical signal; occurs in leaves subjected to prolonged fumigation with SO_2 or O_3
N_{S1}	2.0032	8.0g	Occurs under broad-band white light in leaves fumigated with low levels of SO_2
N_{S2}	2.0042	11.0g	Occurs under white or 710nm light in leaves fumigated with SO_2 for more than 3 hours

APPENDIX C

In addition to the photosynthetic signals centered around the 2.000 g-value, plant leaves also reveal a six peak Mn^{++} signal, and a broad Fe^{++} signal which slopes down from low to high field. The magnitude of these signals varies from species to species and with the age of the leaf, but in most cases, these metal signals are much larger than the photosynthetic signals. Photosynthetic Signals I and II, and other free-radical signals which have a g-value close to 2.000, are shown as a split in the 4th manganese signal peak from the low field end of the broad spectrum (Figure 1a).

In short-term studies the metal signals can be eliminated by signal subtraction since they change more slowly than the photosynthetic signals upon leaf exposure to gaseous air pollutants. However, if signals in the region of interest (g=approximately 2.000) are presented as revealed prior to subtraction, the presence of the metal signals suggests a sloping baseline. The direction and degree of this slope is a function of the size of the Mn^{++} and Fe^{++} signals. If the Mn^{++} signal is large the baseline of the photosynthetic signals will appear to slope upward from low field to high field (Figure 1b) because the photosynthetic signals begin and end on the fourth Mn^{++} peak (Figure 1a). In contrast, if the Mn^{++}

signal is small, but the Fe^{++} signal is large, the baseline in the region of interest will appear to slope down from low to high field.

The sloping baseline attributable to the Fe^{++} signal can usually be corrected for through the use of the baseline adjustment in the Varian software package but the larger upward slope caused by the Mn^{++} peak is difficult to correct. In most leaves the receiver gain required to successfully characterize small signals around the 2.000 g-value is such that the larger Mn^{++} signal can not be recorded in its entirety, thus prohibiting estimation of the degree of correction necessary to create an accurate non-sloping baseline. Consequently, the baseline was not adjusted on these signals.

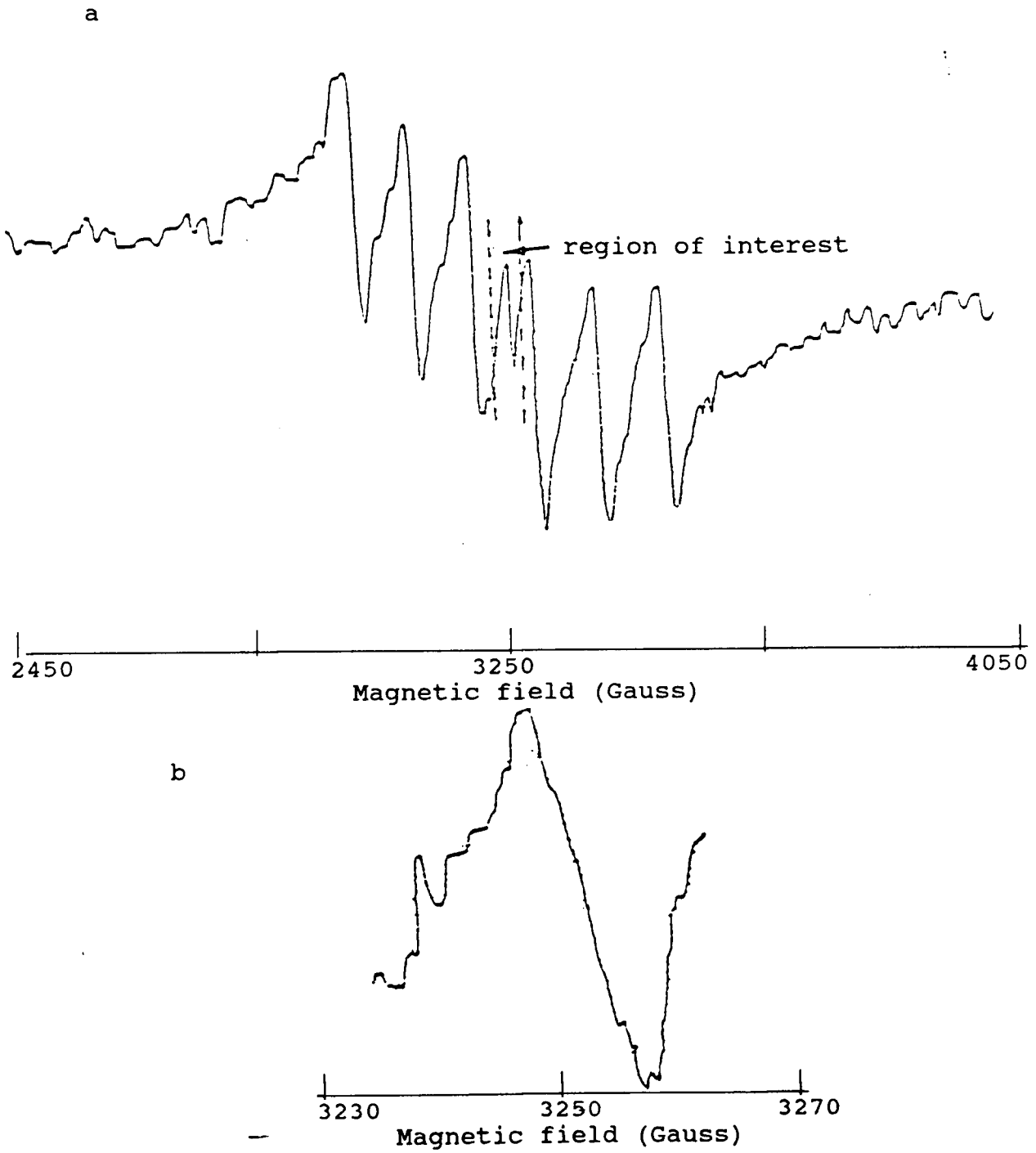

Figure 1. White-light induced signal from an unfumigated perennial ryegrass leaf. a. Broad signal over 1600 gauss; b. Signal in region of interest. Microwave frequency - 9.188.